Performance Analysis and Optimization of Next Generation Wireless Networks

Emmanouil Skondras

Three-member advisory committee

Assoc. Prof. Dimitrios D. Vergados *(Supervisor)*

Prof. Angelos Michalas

Prof. Christos Douligeris

Department of Informatics

School of Information and Communication Technologies

University of Piraeus

This dissertation is submitted for the degree of

Doctor of Philosophy

University of Piraeus April 2019

Performance Analysis and Optimization of Next Generation Wireless Networks

PhD Thesis of Emmanouil Skondras
(Submitted at University of Piraeus, School of Information and Communication Technologies, Department of Informatics, April 2019)

Seven-member PhD evaluation committee

1. Dimitrios D. Vergados, Associate Professor, University of Piraeus
2. Angelos Michalas, Professor, Technological Education Institution of Western Macedonia
3. Christos Douligeris, Professor, University of Piraeus
4. George Tsihrintzis, Professor, University of Piraeus
5. Konstantinos Oikonomou, Associate Professor, Ionian University
6. Ioannis Anagnostopoulos, Associate Professor, University of Thessaly
7. Stavros Kotsopoulos, Professor, University of Patras

April 22, 2019

I would like to thank Assoc. Prof. Dimitrios D. Vergados for his supervision, knowledge, support and persistent encouragement during my PhD at Department of Informatics, School of Information and Communication Technologies, University of Piraeus. I could not have imagined having a better mentor for my PhD study. Also, I would like to thank my advisor Prof. Angelos Michalas for his guidance and expertise. His discussion, ideas and feedback have been invaluable and this work would not have been possible without his input.

Furthermore, I would like to express my sincere gratitude to my advisor Prof. Christos Douligeris for the continuous support of my PhD study and the related research. His guidance helped me in all the time of research and writing of this thesis. I would also like to thank my family for their constant support and encouragement over the years. They have been there for me and I am thankful for everything they helped me achieve. A special note of appreciation to my fiancée Eirini Zoumi. I would like to express my gratitude for putting her faith in me and supporting me in every possible way.

Acknowledgements

The publications made in the context of this PhD thesis have been partly supported by the University of Piraeus Research Center (UPRC) and the Technological Educational Institute of Western Macedonia.

Abstract

The Fifth Generation (5G) networks, including the 5G Vehicular Cloud Computing (5G-VCC) systems, have evolved rapidly offering multiple services to users. The operating principles of vehicular networks, Cloud Computing (CC), Fog Computing (FC), Mobile Edge Computing (MEC) and Software Defined Networks (SDN) are applied to 5G infrastructures. In a 5G-VCC system, the vehicles are equipped with On-Board Units (OBUs) which communicate with each other as well as with Road Side Units (RSUs). Each RSU interacts with a Cloud infrastructure which offers vehicular services with strict Quality of Service (QoS) requirements, including Driver Assistance (DA), Passengers Entertainment and Information (PEnI) and Medical (MED) services. Dense deployments of 5G access networks are also implemented, called Ultra Dense Networks (UDNs), aiming to support high data rates produced by an increased number of vehicular users. In this environment, heterogeneous technologies are used to transfer the network services to vehicles. Optimal manipulation of the communication resources is required, while at the same time vehicular users should always obtain connectivity to the most appropriate network access technology, in order the constraints of the vehicular services to be satisfied. In this thesis, existing schemes for resource allocation as well as for mobility management are studied, while novel solutions are proposed for each topic.

Initially, the theoretical background of the 5G wireless networks and 5G-VCC systems is described. Subsequently, the available delivery models for providing cloud services in 5G infrastructures are mentioned, while the available 5G-VCC architectures and the communication models are presented.

Regarding the topic of the manipulation of the available network resources in 5G-VCC systems, the available Medium Access Control schemes (MAC schemes) are studied, while at the same time resource scheduling algorithms implemented at the MAC layer of 5G-VCC systems are described. Subsequently, two novel solutions are proposed to optimize the resource allocation process in modern networks. The first one is called FLS Advanced (FLSA) and optimizes the resource allocation for real-time services. Additionally, the second one is called FLS Advanced - Cross Carrier (FLSA-CC) and is specialized for LTE-Advanced (LTE-A) access networks where carrier aggregation is applied in order to provide widened bandwidth to the

users. The evaluation of the proposed algorithms is performed through extended experiments. Simulation results show that the proposed algorithms outperform existing solutions.

The mobility management requirements arising at the 5G-VCC systems are also studied. As a result of this study, initially three methods for calculating the significance of the criteria affecting the mobility management are proposed, namely the Trapezoidal Fuzzy Analytical Network Process (TF-ANP), the Trapezoidal Fuzzy Adaptive Analytical Network Process (TF-AANP) and the Pentagonal Fuzzy Analytical Network Process (PF-ANP). Subsequently, three network selection algorithms are proposed, namely the Trapezoidal Fuzzy TOPSIS (TFT), the Trapezoidal Fuzzy TOPSIS with Adaptive Criteria Weights (TFT-ACW) and the Pentagonal Fuzzy TOPSIS (PFT). Following this study and regarding the research results of the implemented algorithms, a mobility management scheme is proposed. This scheme takes into consideration the Signal to Noise plus Interference (SINR) parameters as well as the velocity of the vehicular users to evaluate the necessity of performing a handover. Then, it applies the PFT algorithm to select the most appropriate network for the user. Experimental results showed that the proposed scheme outperforms the existing solutions described in the research literature.

Περίληψη

Η μελέτη της διατριβής εντάσσεται στην ερευνητική περιοχή των ασύρματων τηλεπικοινωνιακών συστημάτων και ειδικότερα των δικτύων Πέμπτης Γενιάς (Fifth Generation -5G). Τα δίκτυα 5G, συμπεριλαμβανομένων των συστημάτων 5G Vehicular Cloud Computing (5G-VCC) , έχουν εξελιχθεί με ταχείς ρυθμούς προσφέροντας πολλαπλές σύγχρονες υπηρεσίες στους χρήστες. Σε μία υποδομή 5G, συνηθίζεται να εφαρμόζονται οι αρχές λειτουργίας που διέπουν τα οχηματικά δίκτυα, το Cloud Computing (CC) , το Fog Computing (FC) , το Mobile Edge Computing (MEC) και τα Software Defined Networks (SDN) . Επιπρόσθετα, σε ένα σύστημα 5G-VCC, τα οχήματα είναι εξοπλισμένα με υπολογιστικές μονάδες επί του οχήματος (On Board Units - OBU) οι οποίες επικοινωνούν μεταξύ τους καθώς και με υπολογιστικές μονάδες εγκατεστημένες δίπλα στο οδικό δίκτυο (Road Side Units - RSU). Κάθε μονάδα RSU αλληλεπιδρά με μία υποδομή Cloud, η οποία προσφέρει υπηρεσίες με αυστηρές απαιτήσεις ως προς την Ποιότητας της Υπηρεσίας (Quality of Service - QoS). Ενδεικτικά, υπηρεσίες υποστήριξης του οδηγού (Driver Assistance - DA) , υπηρεσίες ψυχαγωγίας και ενημέρωσης των επιβατών (Passengers Entertainment and Information - PEnI) , καθώς και ιατρικές υπηρεσίες (Medical - MED) συνηθίζεται να παρέχονται στα οχήματα από την προαναφερθείσα υποδομή Cloud. Επίσης, σε μία αρχιτεκτονική 5G, συνηθίζεται η ανάπτυξη πυκνών υποδομών πρόσβασης στο δίκτυο, οι οποίες αναφέρονται ως Ultra Dense Networks (UDN) . Ένα UDN αναπτύσσεται με στόχο την υποστήριξη των υψηλών ρυθμών δεδομένων που παράγονται από τον αυξημένο αριθμό οχηματικών χρηστών. Στο εν λόγω περιβάλλον ασύρματης πρόσβασης χρησιμοποιούνται ετερογενείς τεχνολογίες για τη μεταφορά των δικτυακών υπηρεσιών από το Cloud στα οχήματα.

Όπως γίνεται σαφές, απαιτείται βέλτιστος χειρισμός των τηλεπικοινωνιακών πόρων, ενώ ταυτόχρονα οι χρήστες των οχημάτων θα πρέπει πάντα να αποκτούν συνδεσιμότητα με την καταλληλότερη τεχνολογία πρόσβασης στο δίκτυο, προκειμένου να ικανοποιούνται οι περιορισμοί των υπηρεσιών που χρησιμοποιούν.

Στο πλαίσιο της παρούσας διδακτορικής διατριβής μελετώνται τα μοντέλα κατανομής πόρων, καθώς και τα μοντέλα διαχείρισης της κινητικότητας των χρηστών, που έχουν προταθεί από την ερευνητική κοινότητα, ενώ νέες βελτιστοποιημένες λύσεις προτείνονται για κάθε ένα από τα εν λόγω ζητήματα. Συγκεκριμένα, αρχικά αναλύεται το θεωρητικό υ-

πόβαθρο στο οποίο βασίζεται η διατριβή. Περιγράφονται οι βασικές αρχές που διέπουν τα συστήματα 5G, και πραγματοποιείται μνεία στα συστήματα 5G Vehicular Cloud Computing (5G-VCC). Πραγματοποιείται επίσης μία επισκόπηση των διαθέσιμων μοντέλων παροχής υπηρεσιών υπολογιστικού νέφους, καθώς και κατηγοριοποίησή τους. Ακολούθως, πραγματοποιείται εκτενής επισκόπηση των ασύρματων δικτύων 5G, με έμφαση στα συστήματα 5G-VCC που έχουν προταθεί στην ερευνητική βιβλιογραφία, όπου αναλύονται οι αρχιτεκτονικές τους, τα μοντέλα επικοινωνίας μεταξύ των συστατικών τους, καθώς και οι αρχές που εφαρμόζονται για την διάθεση των υπηρεσιών που αυτά προσφέρουν.

Στη συνέχεια, εξετάζεται ο τομέας της διαχείρισης των δικτυακών πόρων των ασύρματων δικτύων επόμενης γενιάς, συμπεριλαμβανομένων των δικτύων 5G και των συστημάτων 5G-VCC. Στο πλαίσιο της μελέτης αυτής, προτείνονται δύο νέοι αλγόριθμου χρονοπρογραμματισμού για ασύρματα δίκτυα 5G. Συγκεκριμένα, αρχικά προτείνεται ο αλγόριθμος χρονοπρογραμματισμού FLS Advanced (FLSA) , ο οποίος βελτιστοποιεί την εξυπηρέτηση υπηρεσιών πραγματικού χρόνου. Στη συνέχεια προτείνεται ο αλγόριθμος χρονοπρογραμματισμού FLS Advanced - Cross Carrier (FLSA-CC) ο οποίος αποτελεί εξέλιξη του αλγορίθμου FLSA του οποίου η εφαρμογή εξειδικεύεται για δίκτυα LTE-Advanced (LTE-A) όπου πραγματοποιείται συνένωση πολλαπλών φερουσών συχνοτήτων (carrier aggregation) με σκοπό τη διεύρυνση του διαθέσιμου εύρους ζώνης.

Εξετάζεται επίσης ο τομέας της διαχείρισης της κινητικότητας των χρηστών ασύρματων δικτύων επόμενης γενιάς. Αρχικά, πραγματοποιείται μελέτη των απαιτήσεων που υπάρχουν στα ασύρματα δίκτυα 5G, με έμφαση στα συστήματα 5G-VCC, ως προς τη διαχείριση της κινητικότητας των χρηστών. Ακολούθως, προτείνεται ένα σύνολο μεθόδων για τον υπολογισμό της σημαντικότητας των κριτηρίων που μπορεί να ληφθούν υπόψη κατά τη διάρκεια της διαχείρισης της κινητικότητας των χρηστών. Οι εν λόγω μέθοδοι αναφέρονται ως Trapezoidal Fuzzy Analytic Network Process (TF-ANP), Trapezoidal Fuzzy Adaptive Analytic Network Process (TF-AANP) και Pentagonal Fuzzy Analytic Network Process (PF-ANP) . Επίσης, προτείνεται ένα σύνολο αλγορίθμων που αφορούν την επιλογή του καταλληλότερου δικτύου πρόσβασης για τον εκάστοτε χρήστη, οι οποίοι αναφέρονται ως Trapezoidal Fuzzy TOPSIS (TFT), Trapezoidal Fuzzy TOPSIS with Adaptive Criteria Weights (TFT-ACW) και Pentagonal Fuzzy TOPSIS (PFT). Ως αποτέλεσμα της εν λόγω έρευνας, προτείνεται ένα νέο μοντέλο, το οποίο εξειδικεύεται στη διαχείριση της κινητικότητας των χρηστών που αλληλοεπιδρούν με συστήματα 5G-VCC. Το μοντέλο αυτό, λαμβάνει υπόψη το Signal to Noise plus Interference (SINR) καθώς και την ταχύτητα κίνησης του χρήστη, ώστε να αξιολογήσει την ανάγκη πραγματοποίησης διαπομπής, ενώ στη συνέχεια εφαρμόζει τον αλγόριθμο PFT για την επιλογή του καταλληλότερου δικτύου για τον χρήστη. Το μοντέλο αξιολογείται ενδελεχώς μέσω προσομοιώσεων, μέσω των οποίων αποδεικνύεται ότι

βελτιστοποιεί τη διαχείριση της κινητικότητας των χρηστών ξεπερνώντας τις υπάρχουσες λύσεις που περιγράφονται στη βιβλιογραφία.

Contents

List of Figures

List of Tables

Chapter 1

Introduction

In a Fifth Generation Vehicular Cloud Computing (5G-VCC) system the operating principles of vehicular networks, Cloud Computing (CC) [1] and Software Defined Networks (SDN) [2], considered as the key enabling technologies for the 5G networks, are combined. In a typical VCC system, vehicles are equipped with On-Board Units (OBUs) with computational, storage and communication resources. Vehicles communicate with each other as well as with Road Side Units (RSUs). Also, each RSU interacts with a Cloud infrastructure which offers a variety of modern services with strict Quality of Service (QoS) requirements. Vehicles such as cars, motorcycles, buses and trains provide a wide variety of cloud services to their passengers. Each vehicle could serve many passengers with different services and various requirements. Such services may include Driver Assistance (DA), Passenger Entertainment and Information (PEnI), and Medical (MED) services. The DA services include Navigation Assistance (NAV) [3] and Parking Assistance (PRK) [4] services. The PEnI services include Conversational Video (CV) [5], Voice over IP (VoIP) [6], Buffered Streaming (BS) [7] and Web Browsing (WB) [8] services. Moreover, the MED services include Live Healthcare Video (LHVideo) [9], Medical Images (MedImages) [10], Health Monitoring (HMonitoring) [11] and Clinical Data Transmission (CData) [12] services.

To support the communication needs of the vehicles, dense deployments of 5G networks are implemented, called Ultra Dense Networks (UDNs) [13]. UDNs aim to support the high data rates produced by the increased number of vehicular users. Heterogeneous network access technologies, such as the 3GPP Long Term Evolution Advanced (LTE-A) [14], the IEEE 802.16 Worldwide Interoperability for Microwave Access (WiMAX) [15] or the IEEE 802.11p Wireless Access for Vehicular Environment (WAVE) [16] RSUs are used to provide network services to vehicles. In addition, a large number of small cells, such as Femtocells, is deployed inside the network coverage area in order to increase the overall capacity of the network [17][18]. Network operators use the Anything as a Service (ANYaaS) [19] delivery

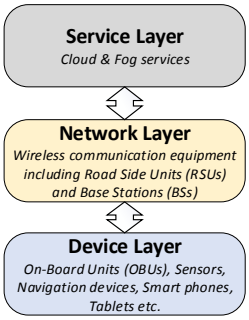

Figure 1.1 The Three-Layer Stack of the 5G-VCC Systems.

model in order to deploy and orchestrate network management algorithms and services using the Cloud infrastructure. Specifically, the Mobility Management as a Service (MMaaS) [20] [21] subcategory of ANYaaS, could be applied to accomplish mobility management operations by the Cloud infrastructure. The MMaaS model allows for each vehicular user the creation of a Mobility Instance (MI) at the Cloud, offering mobility management services and manipulating the user's mobility. In this way, the user equipment resources will experience a decreased workload and will consume less energy during the mobility management. The 5G architecture could be improved by applying the operating principles of Fog or Mobile Edge Computing (MEC) [22–26]. Specifically, WAVE RSUs, as well as LTE and WiMAX Base Stations (BSs) are equipped with additional computational and storage resources and thus they are called as micro-datacenter RSUs (md-RSUs) and micro-datacenter BSs (md-BSs), respectively. Vehicular services are provided directly from the access network. Thus, the durability and the response latency of the services are improved, compared with the traditional centralized cloud server approach.

5G-VCC systems could be described considering the three-layer stack [27][28] presented in Figure 1.1, where the Service, the Network and the Device layers are defined. The Device layer contains the end-user equipment such as On-Board Units (OBUs), smart phones, tablets, navigation devices and sensors. The Network layer contains the communication equipment, such as Macrocell/Femtocell Base Stations (BSs) or Road-Side Units (RSUs), as well as in-vehicle network devices. The Service layer contains Cloud or Fog infrastructures that offer vehicular services.

The vehicular users should always obtain connectivity to the most appropriate network access technology, according to the requirements of their services. In general, the mobility management process consists of three subprocesses, namely the VHO initiation, the network selection and the VHO execution. The VHO initiation decides when a handover must be performed. Subsequently, the network selection deals with the selection of the most appropriate network for the vehicle to handover. Finally, during the VHO execution two general techniques

are considered. The first one is called Soft Handover or "Connect before Break". It defines that the OBU is firstly connected to the new network and then it is disconnected from its previous network. The second technique is called Hard Handover or "Break before Connect". In this case, the OBU is firstly disconnected from its previous network and then it is connected to the next network.

1.1 Delivery Models for Cloud Services

The delivery models refer to the way in which the service is delivered to the users. The main cloud computing delivery models are the Software as a Service (SaaS), the Platform as a Service (PaaS) and the Infrastructure as a Service (IaaS). As presented in Figure 1.2, each one of the main delivery models contains a variety of delivery models. These delivery models are described in the following subsections.

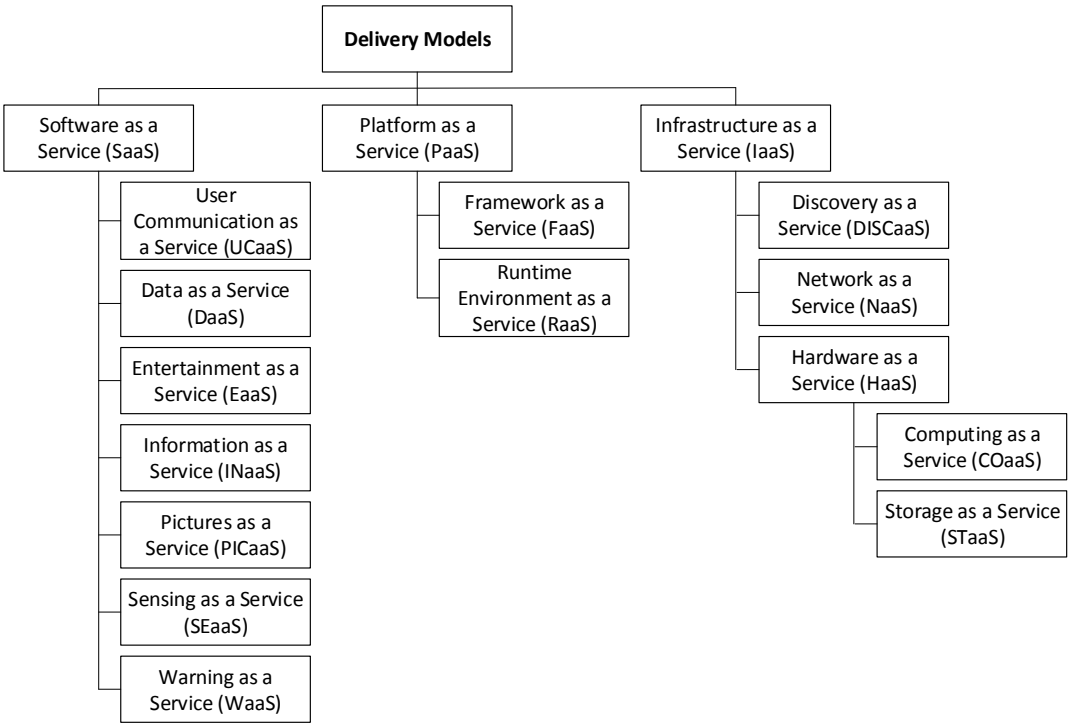

Figure 1.2 Classification of Delivery Models for Cloud Services.

1.1.1 Software as a Service (SaaS) based Delivery Models

Software as a Service (SaaS) provides cloud services to the end-users, while at the same time it prevents them from configuring the services' source code or controlling the underlying cloud infrastructure. The SaaS delivery model includes the following subcategories:

- *User Communication as a Service (UCaaS):* This delivery model [29] provides the necessary applications to the users, in order to be able to communicate with each other, by making voice or video calls, sending emails, using chat boxes etc.
- *Data as a Service (DaaS):* In a 5G network architecture, data sourcing and data manipulation could be performed in the cloud infrastructure using the appropriate applications. DaaS allows users to retrieve data from the cloud, in order to avoid the permanent storage of big data sets on their devices [30].
- *Entertainment as a Service (EaaS):* Modern 5G network infrastructures offer media services such as video, music or advertisements to users. EaaS defines that the provided media services are hosted in the cloud and broadcasted to users or offered to them on-demand [31].
- *Information as a Service (INaaS):* Users often need information related to events, points of interest (POIs) or emergency situations. The INaaS delivery model provides that information to the users. Indicatively, in [32] users share information about their location with other users as well as with a cloud infrastructure. Then, if a user needs information about a specific location, he/she interacts with the cloud and subscribes to the INaaS in order to receive it.
- *Pictures as a Service (PICaaS):* According to the PICaaS operating principles described in [33], users are registered to a centralized cloud manager and they periodically share their geographical coordinates. A customer user requests multimedia material about a specific geographic area. Thus, some users are selected according to their positions, to take photos or videos of the given area using their cameras. Finally, such multimedia material is sent to the consumer user.
- *Sensing as a Service (SEaaS):* Sensors are distributed to the countryside to collect data about the respective environment. The sensor data are collected in the cloud and, subsequently, they are broadcasted to the SEaaS users [34].
- *Warning as a Service (WaaS):* The cloud infrastructure collects information about emergency situations or disasters. Subsequently, warning messages are transmitted to users depending on their locations [35].

1.1.2 Platform as a Service (PaaS) based Delivery Models

In the Platform as a Service (PaaS) model, the users are considered as application developers. Specifically, PaaS provides computational and storage resources to the users by hiding the underlying hardware infrastructure from them [36]. Also, PaaS offers the necessary platform (e.g. the underlying Operation System - OS) to users for the deployment of their applications. The users are able to remotely develop and deploy their applications. These applications should be compatible with the provided cloud platform. The following delivery models could be considered as PaaS subcategories [37]:

- *Framework as a Service (FaaS):* FaaS provides a framework for the implementation of user applications.
- *Runtime Environment as a Service (RaaS):* RaaS provides a deployment and execution environment for the user applications.

1.1.3 Infrastructure as a Service (IaaS) based Delivery Models

Infrastructure as a Service (IaaS) refers to the provision of infrastructure from the cloud to the users in order to be able to set up a specific platform (e.g. an OS) to deploy their applications. The IaaS delivery model provides resources to users. Furthermore, the IaaS model includes the following subcategories:

- *Discovery as a Service (DISCaaS):* This delivery model allows users to discover cloud recourses with specific characteristics [38].
- *Network as a Service (NaaS):* In NaaS the users with internet access can offer this facility to the users that do not have any access [39].
- *Hardware as a Service (HaaS):* In HaaS the user devices or the cloud with plenty computational resources can offer these to the users that need more resources [40]. The HaaS model contains two subcategories, the Computing as a Service (COaaS) [36] and the Storage as a Service (STaaS) [41]. COaaS provides computational resources, such as Central Processing Unit (CPU) cores to users, in order to develop and run their applications. STaaS provides storage space to users to deploy their applications.

1.1.4 Comparison of the Delivery Models

The determination of the advantages and the disadvantages of each of the main delivery models is necessary, in order to provide a complete view of their functionalities. SaaS is the most

cost effective delivery model, due to the fact that the user leases only the software that he uses and not the resources that host it. In addition, the SaaS services are easy in use and they can be rapidly provided on-demand, because they are already deployed on the cloud by their provider. Also, the user does not have to worry about the services management, as this is the provider's responsibility. On the other hand, the user has no control neither over the application implementation and parameterization, nor on the data processing functionalities. Also, the user has limited control over the application deployment and upgrade processes, while integration with other user's software or systems is difficult, considering the fact that the integration must be presupported by the service provider.

PaaS is less cost effective in comparison to SaaS, while at the same time it is more cost effective than IaaS, as the user is leasing only the software platform (e.g. an Operating System installation) and not the entire infrastructure that hosts the platform. Unlike SaaS, a user can deploy his own applications to run on the aforementioned platform and, thus, he has full control over the software that he runs. Therefore, the user has also full control over the rights of the users accessing his software as well as over the data processing functionalities of his applications. Furthermore, the integration between user applications and external systems can be done at the application level, since the user has full control over the source code of his applications. Another PaaS advantage is the minimal Virtual Machine (VM) management that is required, since such processes are handled by the infrastructure provider. However, the lack of control over the VM could create security risks in terms of application data privacy. Also, the provided platform is usually a shared platform and other users could be running their applications at the same time over it, creating even more privacy risks as well as overloading the underlying infrastructure with additional workflows.

In IaaS, the user has full control over his VM, while he can deploy and run anything he wants inside it. Furthermore, the user has full control of data processing functionalities inside the entire VM and not only inside his applications as it happens in PaaS. As a consequence, IaaS simplifies ever more the integration with other systems compared with PaaS. In addition, it is considered as the most privacy aware cloud service due to the fact that the user can deploy, run and control his own virtual infrastructure with full control to his VMs. However, IaaS is more expensive than SaaS and PaaS, since the user is leasing physical resources, such as CPU cores, RAM and storage space. Also, unlike SaaS or PaaS, in IaaS the user is responsible for the entire VM manipulation processes, which may lead to additional tasks for him. Table 1 summarizes the main delivery models' advantages and disadvantages.

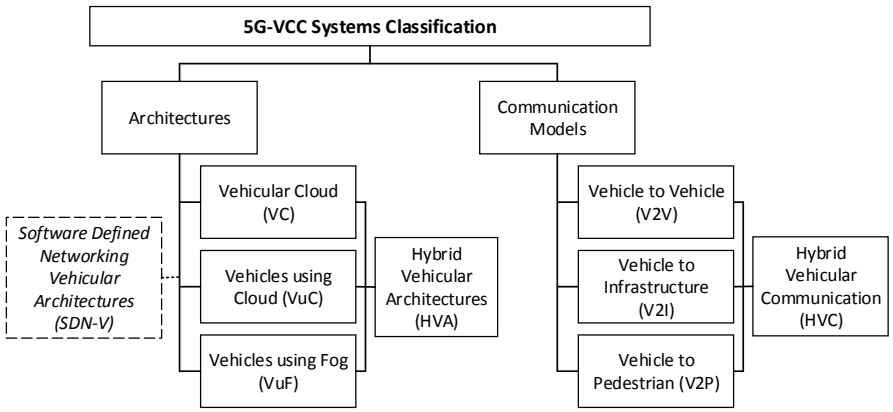

Figure 1.3 Classification of 5G-VCC systems.

1.2 5G Vehicular Cloud Computing Systems (5G-VCC)

1.2.1 5G-VCC Architectures

Three main 5G-VCC architectures are derived in the research literature, namely the Vehicular Cloud (VC), the Vehicles using Cloud (VuC) and the Vehicles using Fog (VuF). Moreover, Software Defined Vehicular (SDN-V) architectures, improving the management of the network, have been proposed. Finally, Hybrid Vehicular Architectures (HVA) combining the operating principles of multiple 5G-VCC architectures are suggested. The following paragraphs describe each one of the available architectures (Figure 1.3).

1.2.1.1 Vehicular Cloud (VC)

According to the VC architecture [38, 41–46], the cloud is consisted of vehicles with computing resources (Figure 1.4). Vehicles directly interact with each other, while data forwarding is supported by proprietary protocols such as the 802.11s [47].

Vehicles' resources [48] remain idle for a long period of time in vehicles parked for many hours each day, or even for many days in some cases, as well as in vehicles that remain stuck due to congested traffic roads. The resources of such vehicles could be used for constructing a cloud infrastructure [49][50]. In such cases, additional resource manipulation factors are arising, since the constructed cloud is based on an ever-changing architecture where vehicular VMs (VVMs) [51] are continuously added or removed. Thus, in order to assure service continuity, multiple instances of each service should be distributed simultaneously in several VVMs [52]. Furthermore, the authorization of each vehicle's owner is required [53], for the vehicles' resources to be provided to the VC architecture.

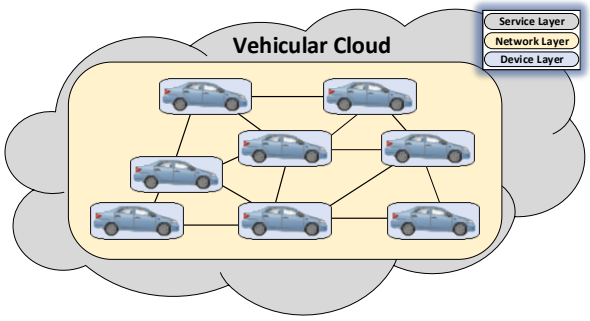

Figure 1.4 The Vehicular Cloud (VC) architecture.

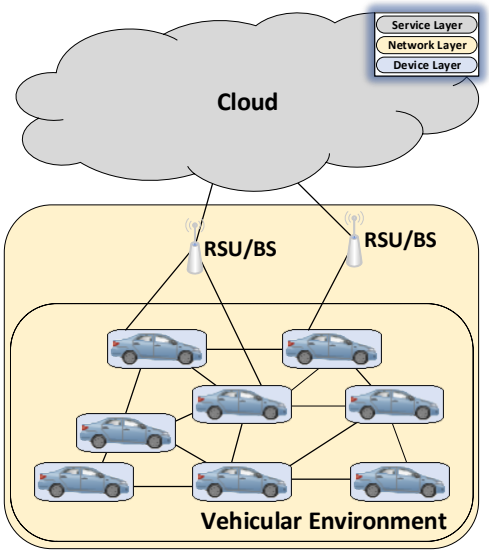

Figure 1.5 The Vehicles using Cloud (VuC) architecture.

1.2.1.2 Vehicles using Cloud (VuC)

According to the VuC architecture [27, 28, 35, 54–60], the vehicles interact with a Cloud infrastructure through Macrocell/Femtocell BSs or RSUs, as presented in Figure 1.5. Compared to the VC architecture, in a VuC architecture the vehicles are considered as the end users.

1.2.1.3 Vehicles using Fog (VuF)

The VuF architecture [61] presented in Figure 1.6, could be considered as an evolution of the aforementioned VuC architecture, where the operating principles of Fog computing [22–26] are applied. Specifically, the VuF architecture defines that the BSs or RSUs are equipped with additional computational and storage resources, while they are also referred as micro-datacenter BSs (md-BSs) and micro-datacenter RSUs (md-RSUs), respectively. In this case, the vehicles

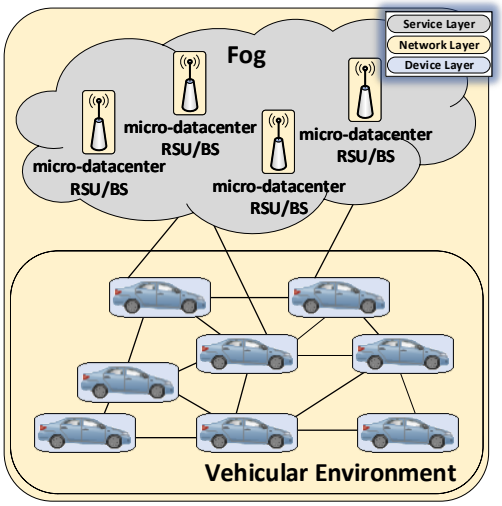

Figure 1.6 The Vehicles using Fog (VuF) architecture.

interact with computing and storage resources characterized by proximity, low latency and high bandwidth.

1.2.1.4 Software Defined Vehicular Architectures (SDN-V)

Each VCC architecture could be enhanced with advanced manipulation functionalities using the Software Defined Networks (SDN) technology [62]. More specifically, the SDN technology simplifies the network management procedures, while at the same time it reduces the network equipment cost. Its operating principles include:

- The network control plane and the data plane are decoupled.
- The network orchestration and management is performed by SDN controllers.
- The interaction with network equipment from different vendors is achieved by proving Open Application Programming Interfaces (Open APIs).

SDN control could be implemented either at the Cloud or the Fog infrastructure. The SDN components could be virtualized [63], considering the operating principles of Network Functions Virtualization (NFV) [64][65], in order to reduce the required SDN hardware as well as to improve the overall system sustainability. In particular, concerning the Cloud-based SDN control, in [66], [67] and [68] the SDN controller is implemented at the Cloud infrastructure, by one or more Virtual Machines (VM). On the other hand, in [69] and [70] a Fog infrastructure implementing the SDN control is described. Specifically, an md-RSU contains a computing device and an OpenFlow (OF) Switch. The computing device include

a VM and a lightweight hypervisor. The hypervisor is a middleware which enables VMs to share resources to their hosted services [71]. Furthermore, some md-RSUs contain additional software, such as OF Controllers, Cloud Controllers and RSU Cloud Resource Managers (RSU CRMs). The OF Controllers control the OF Switch rules via the control plane, while the Cloud Controllers control the hypervisors and the VMs resources. Accordingly, each RSU CRM communicates with both OF and Cloud controllers via the data plane and disseminates information about services and data flows changes. Furthermore, in [72], the authors describe a Software Defined VCC architecture, where an SDN controller exists between the RSUs and the Cloud infrastructure, providing centralized resource manipulation functionalities for the entire architecture.

1.2.1.5 Hybrid Vehicular Architectures (HVA)

The previous main models are combined in hybrid 5G-VCC architectures. Indicatively, in [73] a hybrid 5G-VCC architecture combining both the VuC and VuF models, is discussed. Services are offered by both Cloud and Fog infrastructures, while the Cognitive Radio Networks (CRN) [74] communication principles are adopted. More specifically, the traffic flows generated by the Clouds are considered as primary flows, while the ones generated by the Fog are considered as secondary flows. Also, vehicles are separated into two groups, the primary vehicles which use the Cloud services and the secondary vehicles which use the Fog services. Primary vehicles have higher priority on the spectrum usage, while secondary vehicles connecting to the Fog use the remaining time and frequency holes. Additionally, in [75] and [31] an HVA architecture (Figure 1.7) is introduced, combining the design characteristics of VC, VuC and VuF architectures. Its main advantage is that the entire computation and storage resources are virtualized. The complete virtualization provides enhanced system flexibility as well as resources sustainability. Also, in [76] a HVA architecture which combines both VC and VuC architectures is described. More specifically, a VC provides vehicle cooperation functionalities such as Internet access via multihop traffic routing (mesh networking). Also, the VC collects information about its vehicles, such as fuel consumption, GPS coordinates, CO_2 emissions and traffic data. The VC evaluates this information and extracts traffic related conclusions about its area. Subsequently, the conclusions are sent to the central cloud. Thus, vehicles that does not belong to the VC can obtain the traffic related information concerning the VC area. Furthermore, the extended version of this architecture includes multiple VCs could. Each VC evaluates traffic related information of its geographic area. The central cloud collects the traffic related results from all VCs and extracts conclusions for the whole area.

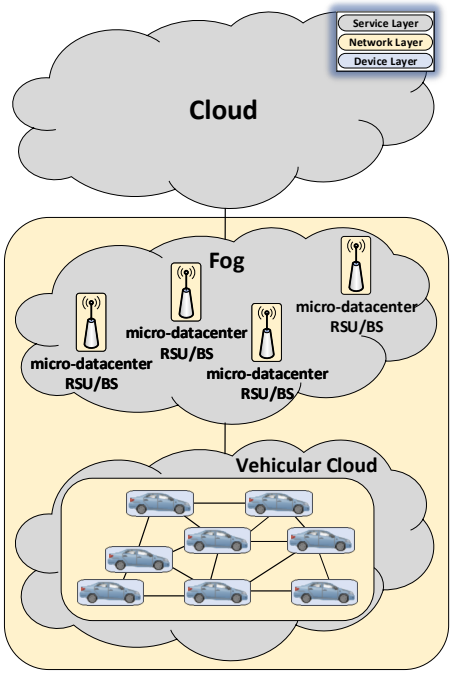

Figure 1.7 A hybrid architecture which combines the design characteristics of both VC, VuC and VuF architectures.

1.2.2 Communication Models for 5G-VCC Systems

Communication models determine which entities communicate with each other in a VCC architecture. In general, they are referred as Vehicle to Everything or V2X, where V stands for vehicle and X determines the entity which communicates with the vehicle. More specifically, the X parameter represents another vehicle in a Vehicle to Vehicle (V2V) communication, a network infrastructure in a Vehicle to Infrastructure (V2I) communication or a pedestrian in a Vehicle to Pedestrian (V2P) communication (Figure 1.3).

1.2.2.1 Vehicle to Vehicle (V2V)

V2V communications [77–83] comprises a wireless network where vehicles exchange information each other. Such information could include vehicle location, speed, direction, braking, stability loss as well as any other information including traffic or multimedia. V2V could applied in a mesh network, meaning that every vehicle could receive and forward messages from/to other vehicles. The first V2V implementations warned the driver about traffic conditions but not took control of the vehicle, while later implementations improve the braking or steering capabilities of the vehicles.

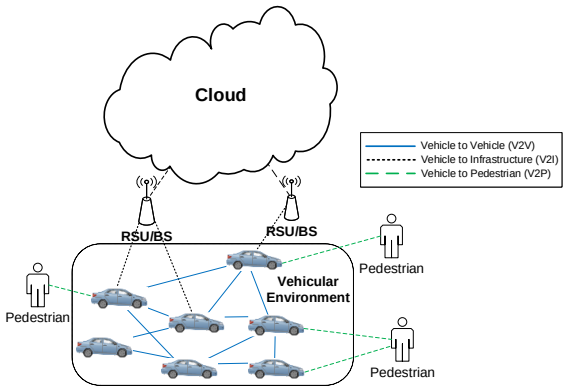

Figure 1.8 The available communication models.

1.2.2.2 Vehicle to Infrastructure (V2I)

V2I communication [84–90] is performed through the RSUs, while the information gathered by the infrastructure could include traffic or road conditions and Points of Interest (PoI). Indicatively, the vehicles velocities and accelerations as well as the inter-vehicle distances could be suggested by the infrastructure considering the traffic conditions and optimizing the traffic manipulation, the fuel consumption and the driver safety.

1.2.2.3 Vehicle to Pedestrian (V2P)

In a V2P communication [91–97] information between vehicles and pedestrians is exchanged. The pedestrians could exchange road safety information with vehicles using their mobile devices in order to avoid accidents.

1.2.2.4 Hybrid Vehicular Communication (HVC)

In a 5G-VCC architecture, multiple communication models could also be used together [98–104] (Figure 1.8).

1.3 Thesis Structure

In the first chapter the fundamental operating principles of the Fifth Generation (5G) wireless networks and 5G Vehicle Cloud Computing (5G-VCC) systems are introduced. Additionally, the three-layer stack used to design and analyze the 5G-VCC systems is described. Subsequently, the theoretical background of the thesis is analyzed. Specifically, the available delivery models for cloud services are mentioned and existing 5g-VCC architectures are presented. Finally, the main communication models are described.

The second chapter, which deals with the management of network resources in 5G-VCC systems, firstly describes the available Medium Access Control schemes (MAC schemes). Subsequently, existing resource scheduling algorithms implemented at the MAC layer of 5G-VCC systems are described, while two novel solutions are proposed to optimize the resource allocation process.

In the third chapter, the requirements of the 5G-VCC systems for the management of mobility of vehicular users are described. Three methods for calculating the significance of the criteria affecting the mobility management are proposed. Furthermore, three network selection algorithms are proposed. Subsequently, the proposed algorithms are evaluated.

The fourth chapter describes a proposed scheme for performing mobility management in 5G wireless networks. The scheme takes into consideration the Signal to Noise plus Interference (SINR) while at the same time it performs optimized supervision of the user's velocity, in order to evaluate the necessity of performing a handover. Subsequently, it selects the most appropriate network for the user. Experimental results showed that the proposed model outperforms the existing solutions described in the research literature.

Finally, in the fifth chapter a brief review of the thesis is made. The conclusions extracted from the performed research are mentioned, while guidance for future work is given.

1.4 Thesis Novelty

The novelty of this thesis is found in the following points:

- Medium Access Control (MAC) schemes for 5G Wireless Networks
  - Study, classification and evaluation of the most used medium access mechanisms for 5G wireless networks and specifically for 5G-VCC systems.
- 5G Wireless Network Architectures
  - Study, classification and evaluation of the 5G wireless network architectures and in particular of 5G-VCC systems, considering the applied network topologies and communication models proposed in the research literature.
- Delivery Models for Cloud Services in 5G Wireless Networks
  - Study, classification and evaluation of the most used cloud delivery models that can be applied to 5G network architectures.
- Resource Allocation (scheduling) in 5G Wireless Networks

  - Two novel resource allocation (scheduling) algorithms that can be applied to 5G Wireless Networks, including 5G-VCC systems, are proposed. The experimental results showed that they optimize the allocation of network resources in order the constraints of real-time services to be optimally satisfied.

- Mobility Management in 5G Wireless Networks

  - Three novel methods for calculating the weights of mobility management criteria are proposed. Experimental results showed that the proposed methods optimize the calculation of the significance of each mobility management criterion.
  - Three novel network selection algorithms for 5G wireless network, including 5G-VCC systems, are proposed. The experimental results showed that these algorithms select the optimal network considering the requirements of both users and network operators.
  - An integrated mobility management scheme for 5G wireless networks, including 5G-VCC systems, is proposed. Extensive experimental results demonstrated that it optimizes the mobility management process by minimizing the number of required handovers, while at the same time it ensures that the user is connected to the optimal access network considering both his requirements as well as network operators constraints.

Chapter 2

Resource Allocation - Scheduling

2.1 Medium Access Control (MAC) Schemes for 5G-VCC systems

This section describes MAC schemes that can be applied in 5G-VCC systems. The schemes are organized considering their underlying multiple access mechanism. Since the vehicular environment often changes due to the high mobility of vehicles, while at the same time both V2V and V2I communications must be supported, sometimes in an ad-hoc manner, the most common multiple access mechanisms considered in vehicular MAC schemes include the TDMA and the CSMA/CA. Hybrid schemes have also been proposed in the literature combining more than one multiple access mechanism. Figure 2.1 presents the schemes that will be discussed in the following subsections.

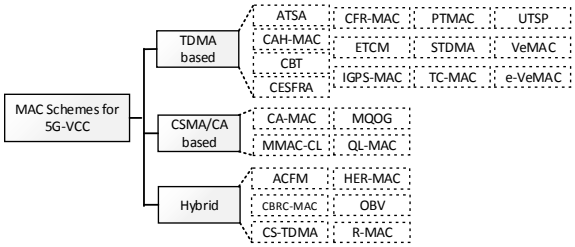

Figure 2.1 MAC Schemes for 5G-VCC Systems.

2.1.1 Time Division Multiple Access (TDMA) based MAC Schemes

TDMA-based MAC schemes share the medium in the field of time. In the Adaptive TDMA Slot Assignment (ATSA) [105] scheme, for example, each vehicle selects a frame length, which

is reduced to improve channel utilization when the vehicle density becomes low, or increased when the vehicle density becomes high to ensure that each vehicle can access the medium. Time slots are divided in two sets, namely the Left and the Right set. A slot management mechanism based on a binary tree model is used. The vehicles on the left sub-tree can compete for the Left time slots, while the vehicles on the right sub-tree can compete for the Right time slots. When a vehicle receives slot allocation information from its neighbors, it discovers which slots are in use. Thus, the remaining slots are available to compete for.

The Cluster Based TDMA (CBT) [106] scheme provides a mechanism for intra-cluster and inter-cluster communication to minimize the packet collisions that could occur when two clusters are moving close to each other. In each cluster, the vehicles are synchronized in time using their GPS devices, while one vehicle is elected as the Cluster Head (CH). A TDMA related technique is used where each frame consists of N time slots. The CH maintains a Slot Allocation Map (SAM) allocating time slots to vehicles. Moreover, the CH periodically broadcasts its SAM and a beacon frame to its cluster's vehicles. The cluster remains in the intra-cluster communication state if the beacon frames from the CHs of the other clusters are not received. However, if a beacon frame comes from an external CH, the two neighboring clusters' CHs exchange their SAMs in order to prevent inter-cluster interference. The CH that successfully sends first its SAM is considered as the Winner, while the other is considered as the Loser. The Loser must reschedule its own SAM.

Another TDMA-based MAC scheme is the Cross-layer Extended Sliding Frame Reservation Aloha (CESFRA) [107]. In CESFRA safety information is disseminated up to the third hop neighboring vehicles without any routing scheme. This scheme divides each frame into N time slots. All the vehicles are considered to be synchronized in time using their Geographical Positioning System (GPS) devices. When a vehicle has packets to transmit, it senses the medium in order to find an idle time slot. Once an idle time slot is found, the vehicle starts transmitting its packets. The time slot is also reserved by the vehicle in the subsequent frames in order to transmit the remaining packets.

The Collision Free Reservation MAC (CFR-MAC) [108] is another mechanism that provides TDMA based medium access. It considers the vehicles' traffic flows as well as their velocities. As in the ATSA, the time slots are divided into two sets, the Left and the Right set. The Left set is assigned to vehicles that are moving to the one direction, while the Right set is assigned to vehicles moving to the opposite. In general, when multiple vehicles are moving on the same street with different velocities the interference levels on the wireless environment are constantly changing leading on unpredictable changes in the medium quality. CFR-MAC addresses this problem by dividing each slot's set into three subsets. Each subset is associated to a specific

velocity, namely the High, the Medium and the Low velocity. In this way the interference levels inside each subset become less variable and the medium quality more resistant.

The Vehicular MAC (VeMAC) [109] supports broadcast services. Similar to the CBT and CFR-MAC schemes, the two vehicles' moving directions are considered, namely the Left and the Right direction. A set of time slots is assigned to vehicles that move in the Left direction and the Right direction, respectively. Using these time slots, the vehicles of each direction communicate with each other, while the vehicles' time synchronization is performed using their GPS devices. Although VeMAC supports reliable transmission, it is not fully applicable in vehicular networks with parallel transmissions. In [110] an enhanced version of VeMAC scheme, the e-VeMAC, is proposed. The e-VeMAC scheme is based on the insight of the one-hop neighboring vehicles in order to improve the performance of the VeMAC scheme when parallel transmission occurs.

The Enhanced TDMA Cluster-based MAC (ETCM) [111], the Prediction-based TDMA MAC (PTMAC) [112] and the Unified TDMA-Based Scheduling Protocol (UTSP) [113] schemes also implement TDMA based multiple access. The ETCM scheme defines that the vehicles are organized into clusters, while a vehicle of each cluster is defined as the CH. Subsequently, the CH applies a TDMA based method to assign time slots to the cluster's vehicles.

The main operating principle of PTMAC is the packet collision prediction. PTMAC consists of three parts, namely the collision prediction part, the collision detection part and the collision elimination part. According to the collision prediction part, data traffic and vehicles mobility information is used in order to predict potential future collisions. Furthermore, the collision detection uses time slot information to detect collisions that occurred in cases where two vehicles transmit data using the same time slot. Finally, the collision elimination part reschedules the slots considering the information obtained from both the collision prediction and the collision detection parts, in order to eliminate the packet collisions.

The UTSP scheme implements a centralized resource allocation mechanism for V2I communication. Initially, the RSU collects information about the channel state, the vehicles' velocities and the priorities of the vehicles' services. Then, it uses a weighted function to compute a score for each vehicle. Finally, the RSU assigns TDMA time slots to each vehicle according to its score, where the amount of time slots assigned to each vehicle is proportional to the corresponding vehicle's score.

Similar to the aforementioned MAC schemes, other TDMA-based schemes are the Cooperative ADHOC MAC (CAH-MAC) [114], the Improved Generalized Prime Sequence Based MAC (IGPS-MAC) [115], the Self-organizing Time Division Multiple Access (STDMA) [116], and the TDMA Cluster-based MAC (TC-MAC) [117].

2.1.2 Carrier Sense Multiple Access with Collision Avoidance (CSMA/CA) based MAC Schemes

The schemes of this category share the medium by applying the CSMA/CA operating principles.

The Context Aware MAC (CA-MAC) [118] considers the network load status in order to improve the medium access performance of 802.11p MAC. More specifically, CA-MAC consists of two parts, the Reasoning part and the Self-adaption part. Initially, the Reasoning part obtains the network load based on context information. Thus, the network is characterized as congested, idle or normal. Subsequently, the Self-adaption part considers the network load and dynamically adjusts the 802.11p Contention Window [119] size, which is used for channel reservation by the vehicles. Accordingly, if a high network load is observed, the CW is incremented to reduce the collisions probability. On the contrary, if a low network load is observed the CW is decreased to avoid unnecessary medium access delays. More specifically, if the Reasoning part indicates that the network is congested, the CW will be increased by 1, while if the Reasoning part indicates that the network status is idle, the value of CW will be halved. The CW will remain unchanged, if the Reasoning part indicates that the network status is normal.

Another CSMA/CA-based scheme called Multichannel MAC - Cross Layer (MMAC-CL) [120] aims to reduce the interference between vehicles at both the MAC and the Network layers considering two multichannel radio interfaces per vehicle. The MMAC-CL maximizes the average Signal to Interference Ratio (SIR) between the source and the destination. Transmission channels are selected considering a SIR evaluation, in order to minimize the cochannel interference observed by the vehicles.

The Multichannel QoS Cognitive MAC (MQOG) [121] is a multichannel scheme using a dedicated Control Channel (CCH) for control information exchange and multiple Service Channels (SCHs) for data transmission. Each vehicle assesses the interference level in each channel and acquires the best one for transmission. Subsequently, each vehicle tracks its neighbors' communications using a Channel Neighbor State Table (CNST). The vehicles obtain information from the CCH in order to update their CNST tables and select the appropriate SCHs for their data transmission.

The Q-Learning MAC (QL-MAC) [122] provides a delay tolerant medium access, where neighboring vehicles exchange positioning information. A Contention Window (CW) is defined, while the best CW size is evaluated using a Q-Learning algorithm, in order to improve the contention efficiency. A positive reward is awarded to each vehicle when a data frame is successfully transferred. On the contrary, a negative reward is given when a data frame transmission is failed. The dynamic CW size adjustment reduces the packet collisions, while at the same time it achieves a low medium access delay. When the payload size is larger than a

predefined threshold, the RTS/CTS mechanism is applied in order to avoid the hidden terminal and the exposed terminal problems, otherwise the position information is utilized in order to decide whether to start the transmission.

2.1.3 Hybrid MAC Schemes

This category includes MAC schemes that use the operating principles of more than one of the aforementioned multiple access mechanisms. The Adaptive Collision Free MAC (ACFM) [123] scheme combines both TDMA and FDMA. ACFM implements a time slot reservation mechanism located at each RSU. Each frame operates in a specific frequency and contains 36 time slots that can be used for data transmission and 1 slot that is called RSU Slot (RS). Furthermore, each RSU maintains a Slot Assignment Cycle (SAC) for the next 100ms, while each cycle can contain from 1 and up to 5 frames according to the vehicles density. Specifically, if the vehicle density is low, the RSU uses a few frames in order to avoid situations where a lot of slots remain unused. On the contrary, if the vehicle density is high, the RSU uses more frames in order to support the increased needs for resources.

Similar to the ACFM scheme, the Cluster Based RSU Centric MAC (CBRC-MAC) [124] combines both TDMA and FDMA for providing multiple access to vehicles. Firstly, the available spectrum is divided into a set of subfrequencies using FDMA and, subsequently, each subfrequency is divided into a set of time slots. Thus, Resource Blocks (RBs) are created including a specific subfrequency in the frequency domain and a specific slot in the time domain. RSUs assign RBs to vehicles considering their communication needs.

Some schemes combine TDMA with CSMA/CA to accomplish the multiple access. In the Hybrid Efficient and Reliable MAC (HER-MAC) [125] scheme, vehicles are synchronized using their GPS devices. When a vehicle needs to transmit data, it uses the CSMA/CA to perform a 3-way handshake in Wireless Access for Vehicular Environment (WAVE) [16] called Wireless Service Announcement/Request for Service (WSA/RFS). During this handshake, the transmitter vehicle broadcasts a WSA message in order to reserve TDMA time slots for data transmission. When the slot reservation is complete, the transmitter vehicle sends a RFS message to the recipient vehicle. Subsequently, the recipient vehicle responds with an acknowledgment message (ACK) and, then, the transmitter vehicle can start the data transmission.

The Risk-Aware MAC (R-MAC) [126] scheme divides each frame into two segments, namely the RSU segment and the vehicle segment. RSUs broadcast control messages using the RSU segment, while the vehicle segment is further divided into two sub-segments, namely the CSMA/CA sub-segment and the TDMA sub-segment. The CSMA/CA sub-segment is used for

warning messages transmission (e.g. in case of an accident) while the TDMA sub-segment is used for non-safety data transmission.

It should also be noted that in some hybrid mechanisms, the TDMA or CSMA/CA are combined with the Space Division Multiple Access (SDMA) that considers the geographic position of each vehicle. For example, the CSMA-based Self-Organizing TDMA (CS-TDMA) [127] combines TDMA, CSMA/CA and SDMA to support both safety and non-safety applications. A CCH channel is used for the data transmissions of the safety applications, while a SCH channel is used for the non-safety applications. The ratio between the CCH and SCH lengths is adjusted taking into consideration the vehicle density in each location. If the vehicles density is high, the CCH length is increased and the SCH length is decreased in order to guarantee a maximum delay for safety applications. On the contrary, if the vehicles density is low, the CCH length is decreased and the SCH length is increased in order to improve the throughput for non-safety applications.

Finally, in the OFDMA-based MAC scheme for VANETs (OBV) [128] the CSMA/CA is combined with the OFDMA mechanism. During a resource negotiation phase, vehicles allocate resources using CSMA/CA. Thereafter, the data transmissions are performed using OFDMA, while at the same time the vehicles are synchronized using their GPS receivers in order to guarantee the orthogonality between the OFDMA subcarriers.

2.1.4 Discussion on MAC Schemes for 5G-VCC Systems

Although most of the available MAC schemes have been designed for vehicular systems and not necessarily for 5G-VCC systems, they could be easily applied to the vehicular part of a 5G-VCC architecture. The study of these schemes reveals the fact that various approaches have been proposed to the literature.

As mentioned in the previous sections, a main factor of the discussed schemes is the underlying multiple access protocol. The most common multiple access protocols used include TDMA and CSMA/CA. Additionally, some schemes apply hybrid solutions by combining more than one multiple access protocols. These schemes combine FDMA with TDMA (e.g. ACFM and CBRC-MAC), CSMA/CA with TDMA (e.g. HER-MAC and R-MAC), OFDMA with CSMA/CA (e.g. OBV) and so on. Furthermore, some schemes organize the vehicles into clusters (e.g. CBRC-MAC, CBT, ETCM, IGPS-MAC, R-MAC and TC-MAC), while the rest do not consider clusters of vehicles. In general, clustering could be considered as a useful methodology which offers an improved use of the available spectrum. A positioning system is also required in some cases in order to monitor the vehicles positions. The existence of a positioning system enables the vehicles to be synchronized in time with each other using their GPS receivers.

Another important factor is the control type applied in each scheme. Some schemes apply distributed control, while other schemes apply centralized control. Although the distributed control distributes the resource manipulation workload, the centralized control could be considered as more appropriate in some cases, since it simplifies the manipulation of the communication resources. In 5G-VCC architectures where a centralized Software Defined Network (SDN) [129] controller supervises the manipulation of the entire system, centralized MAC schemes could be easily configured considering the complete view of the system's resources. Distributed schemes could also be configured in 5G-VCC systems considering the operating principles of Fog computing [130].

Cognitive Radio Networking (CRN) [74] is another factor that is proposed in 5G-VCC systems to organize the vehicles into two groups, namely the Primary and the Secondary vehicles. Primary vehicles obtain immediate access to network resources as determined in their Service Level Agreements (SLAs) [131]. However, sometimes Primary vehicles do not need the entire network resources provided according to their SLAs. In such cases, Secondary vehicles could use the free network resources, which are also called White Spaces. Furthermore, whenever a Primary vehicle requires the resources defined in its SLA, it immediately reserves them, while the Secondary vehicles should obtain access to other free network resources. Considering the CRN operating principles, some MAC schemes (e.g. MQOG) take advantage of the free white spaces into the available spectrum in order to serve more vehicles. Finally, the communication type (V2V or V2I) that each scheme supports is considered. Table 4.2 presents the characteristics of the discussed MAC schemes considering the aforementioned factors.

2.2 Overview of Downlink Packet Schedulers

Several downlink packet schedulers have been proposed in the literature. They can be classified into two groups, namely non-QoS and QoS aware, respectively. A non-QoS aware scheduler does not take into account parameters that affect the service quality, while a QoS aware distributes resources considering the specific constraints of each service. This section makes a brief overview of the available scheduling strategies for LTE systems, since LTE is considered as one of the most important network access technologies for the 5G architectures.

2.2.1 Non-QoS Aware Schedulers

In [132] the non-QoS aware schedulers Maximum Throughput (MT), Proportional Fair (PF) and Throughput to Average (TTA) are evaluated in terms of the throughput and the fairness index. The MT scheduler aims at the maximization of the overall system throughput and

Table 2.1 The Characteristics of the discussed MAC Schemes.

MAC Scheme	Multiple Access	Cluster based	Positioning System Required	Centralized /Distributed control	CRN Support	Communication
ACFM [123]	FDMA, TDMA	No	No	Centralized	No	V2I
ATSA [105]	TDMA	No	No	Distributed	No	V2V
CAH-MAC [114]	TDMA	No	Yes	Distributed	No	V2V
CA-MAC [118]	CSMA/CA	No	No	Distributed	No	V2V, V2I
CBRC-MAC [124]	FDMA, TDMA	Yes	No	Centralized	No	V2I
CBT [106]	TDMA	Yes	Yes	Centralized	No	V2V
CESFRA [107]	TDMA	No	Yes	Distributed	No	V2V
CFR-MAC [108]	TDMA	No	Yes	Distributed	No	V2V
CS-TDMA [127]	CSMA/CA, SDMA, TDMA	No	Yes	Distributed	No	V2V
ETCM [111]	TDMA	Yes	Yes	Centralized	No	V2V
HER-MAC [125]	CSMA/CA, TDMA	No	Yes	Distributed	No	V2V
IGPS-MAC [115]	TDMA	Yes	Yes	Centralized	No	V2V
MMAC-CL [120]	CSMA/CA	No	Optional	Distributed	No	V2V, V2I
MQOG [121]	CSMA/CA	No	No	Distributed	Yes	V2V, V2I
OBV [128]	CSMA/CA, OFDMA	No	Yes	Distributed	No	V2V, V2I
PTMAC [112]	TDMA	No	Yes	Distributed	No	V2V
QL-MAC [122]	CSMA/CA	No	Yes	Distributed	No	V2V
R-MAC [126]	CSMA/CA, TDMA	Yes	Yes	Centralized	No	V2V, V2I
STDMA [116]	TDMA	No	Yes	Distributed	No	V2V
TC-MAC [117]	TDMA	Yes	Yes	Centralized	No	V2V
UTSP [113]	TDMA	No	Yes	Centralized	No	V2I
VeMAC [109]	TDMA	No	Yes	Distributed	No	V2V
e-VeMAC [110]	TDMA	No	Yes	Distributed	No	V2V

allocates resources using the metric calculated by formula 2.1, where $d_k^i(t)$ represents the available throughput in the k^{th} RB of the i^{th} Transmission Time Interval (TTI). The PF aims at fair distribution of network resources to users. Its metric is estimated using formula 2.2, where $\bar{R}^i(t-1)$ denotes the past average throughput. Finally, the TTA metric is calculated using formula 2.3 where $d^i(t)$ represents the available throughput in the i^{th} TTI. Simulation results in [132], [133] showed that the MT achieves higher throughput, the TTA has better performance in terms of the fairness index while the PF provides satisfactory throughput and fairness.

$$m_{i,k}^{MT} = d_k^i(t) \tag{2.1}$$

$$m_{i,k}^{PF} = \frac{d_k^i(t)}{\bar{R}^i(t-1)} \tag{2.2}$$

$$m_{i,k}^{TTA} = \frac{d_k^i(t)}{d^i(t)} \tag{2.3}$$

The Blind Equal Throughput (BET) non-QoS aware scheduler described in [134] distributes equally the throughput to the users using formula 2.4. The authors of [135] compare the MT,

the PF and the BET schedulers using TCP traffic in a vehicular environment. Numerical results showed that the MT and the PF schedulers achieve similar throughputs, while their performance is better than the one achieved by the BET algorithm.

$$m_{i,k}^{BET} = \frac{1}{\bar{R}^i(t-1)} \tag{2.4}$$

Moreover, the authors of [136] evaluate the performance of video streaming using the MT, the PF and the Round Robin (RR) which allocates resources sequentially to users. Simulation results showed that the PF algorithm achieves a higher Mean Opinion Score (MOS) and throughput for a large number of users, while the MT performs better in terms of the Freezing Delay Ratio (FDR).

2.2.2 QoS Aware Schedulers

In [137] a QoS aware downlink scheduler is proposed which considers requirements of Guaranteed Bit Rate (GBR) and non - Guaranteed Bit Rate (non-GBR) bearers as well as channel conditions for resource allocation. Scheduling is performed in two phases. At the time domain (TD) phase a list of GBR and a list of non-GBR users requiring transmission are created and their priorities are defined. At the frequency domain (FD) phase the allocation of users to RBs is performed. Evaluation results showed that the suggested scheduler can handle effectively VoIP, Video, HTTP and FTP traffic.

The authors of [138] propose a scheduling algorithm in wireless networks which uses a utility function to perform resource allocation for both QoS aware and Best Effort (BE) traffic. Numerical results showed that the proposed solution satisfies users with various QoS requirements while it provides fairness to BE users.

The Modified Largest Weighted Delay First (M-LWDF) and the Exponential/PF (EXP/PF) QoS aware schedulers are described in [139] and [140], respectively. Both algorithms extend the PF metric by taking into consideration network factors such as delays and packet losses that affect the service quality. Specifically, the M-LWDF metric is estimated using formula 2.5, while the EXP/PF metric is calculated by formula 2.6. The $D_{HOL,i}$ parameter represents the head of line delay. Additionally, the α_i value is determined by formula 2.7, where δ_i is the target packet loss ratio and τ_i is the delay constraint. Finally, the X value is calculated by formula 2.8, where N_{rt} is the number of active real time flows. Numerical results showed that the M-LWDF scheduler performs better when the network load is low, while the EXP/PF algorithm gives better results when the load increases.

$$m_{i,k}^{M-LWDF} = a_i \cdot D_{HOL,i} \cdot m_{i,k}^{PF} \tag{2.5}$$

$$m_{i,k}^{EXP/PF} = exp(\frac{a_i \cdot D_{HOL,i} - X}{1 - \sqrt{X}}) \cdot m_{i,k}^{PF} \tag{2.6}$$

$$\alpha_i = -\frac{log\delta_i}{\tau_i} \tag{2.7}$$

$$X = \frac{1}{N_{rt}} \cdot \sum_{i=1}^{N_{rt}} a_i \cdot D_{HOL,i} \tag{2.8}$$

The LOG RULE and the EXP RULE schedulers presented in [141] take into account the head of line packet delay and the channel quality reported by UEs, to support delay sensitive flows. The LOG RULE metric is estimated using formula 2.9, where Γ_k^i is the spectral efficiency for the i^{th} user on the k^{th} subchannel. The EXP RULE metric is estimated using formula 2.10, where b_i and c are configurable parameters. Simulation results showed that both LOG RULE and EXP RULE could guarantee delay constraints by configuring scheduler parameters according to the users' target delays.

$$m_{i,k}^{LOGRULE} = b_i \cdot log(c + a_i \cdot D_{HOL,i}) \cdot \Gamma_k^i \tag{2.9}$$

$$m_{i,k}^{EXPRULE} = b_i \cdot exp(\frac{a_i \cdot D_{HOL,i}}{c + \sqrt{(1/N_{rt}) \sum_j D_{HOL,j}}}) \cdot \Gamma_k^i \tag{2.10}$$

The FLS scheduler described in [142] implements a two level QoS aware strategy. The upper level uses formula 2.11 to estimate the $u_i(k)$ quota of data that the i^{th} real time flow must transmit at the k^{th} frame to satisfy its QoS constraints. In this formula, $q_i(k)$ represents the queue length in the k^{th} frame, M_i the number of coefficients used and $c_i(n)$ the n^{th} coefficient value. Coefficients are used in order to guarantee the required delay constraints for real time flows. The number M_i of coefficients is estimated using formula 2.12, where τ_i represents the target delay. Additionally, the coefficient value $c_i(n)$ is determined by formula 2.13. The lower level uses the PF metric to allocate network resources to real time flows for transmitting their quota of data, whereas the remaining resources are allocated to best effort flows. Simulation results showed that the proposed model improves the performance of real time flows compared to the EXP RULE and LOG RULE schedulers.

$$\begin{aligned} u_i(k) = q_i(k) + \sum_{n=2}^{M_i} [q_i \cdot (k-n+1) \\ - q_i \cdot (k-n+2) - u_i \cdot (k-n+1)] \cdot c_i(n) \end{aligned} \tag{2.11}$$

$$\tau_i = (M_i + 1) \cdot T_f \tag{2.12}$$

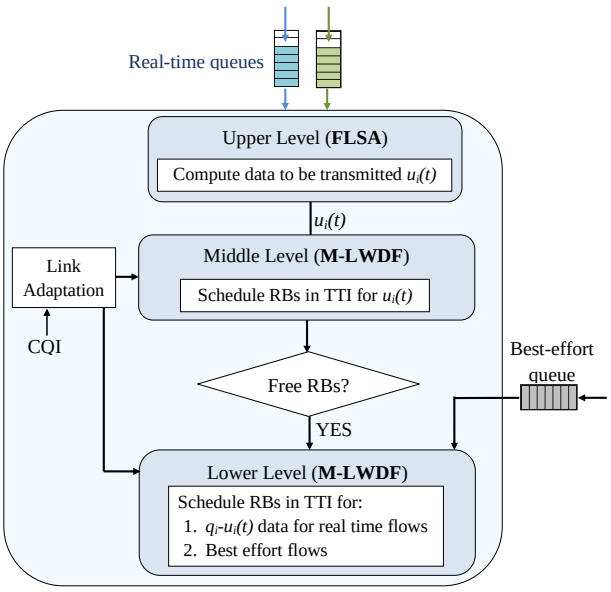

Figure 2.2 The Three-Level Scheduler.

$$c_i(n) = \begin{cases} 0 \text{ , when } n = 0 \\ 1 \text{ , when } n = 1 \\ c_i(n-1)/2 \text{ , when } n \geq 2 \end{cases} \tag{2.13}$$

The work described in [133] classifies the LTE downlink schedulers into five categories namely the channel-unaware, the channel-aware/QOS-unaware, the channel-aware/QoS-aware, the semi-persistent for VoIP support and finally the energy aware scheduling algorithms. Simulations that performed for the channel-aware/QoS-aware category showed that the FLS scheduler outperforms the M-LWDF, the EXP/PF, the EXP RULE and the LOG RULE in terms of packet losses and packet delays as the number of video flows increases.

2.3 The Proposed FLS Advanced (FLSA) Scheduler

This section describes the proposed FLSA scheduler which aims at the optimization of real time flows in the LTE downlink. It has been built on three distinct levels as presented in Figure 2.2. The three levels cooperate to dynamically assign radio resources to users in each TTI. The real time flows receive a higher priority than the best effort ones because of their strict service constraints.

2.3.1 The Upper Level of the Scheduler

The upper level of FLSA uses formula 2.11 of FLS to estimate the quota $u_i(k)$ of data that the i^{th} real time flow should transmit in each k^{th} TTI, to satisfy its QoS constraints. In other words, $u_i(k)$ quota is estimated in each k^{th} TTI of a frame, whereas in FLS it is estimated once at the beginning of each k^{th} frame. Performance improvement has been observed due to the fact that in FLS, when a real time flow transmits its $u_i(k)$ quota of data, it loses the opportunity to continue the transmission until the beginning of the next frame. By recalculating the formula 2.11 in each TTI (instead of estimating it only at the beginning of each frame), the FLSA provides more resources to real time flows that have remaining data for transmission.

2.3.2 The Middle Level of the Scheduler

In every TTI, the middle level uses the M-LWDF scheduler to allocate resource blocks (RBs) to real time flows for transmitting their $u_i(t)$ quota of data obtained from the upper level. Parameters such as the signal to interference plus noise ratio (SINR), the throughput, the head of line delay, the target delay, the target packet loss ratio and the queue length, are considered according to formula 2.5. Moreover, the use of the QoS aware M-LWDF scheduler realizes an improved resource distribution among the real time flows in comparison with the FLS scheduler which at the second level uses the non-QoS aware PF algorithm.

2.3.3 The Lower Level of the Scheduler

The third level has been added to allocate the remaining RBs of each TTI to both real time and best effort flows using the M-LWDF algorithm, in a way similar to [143]. The RBs are allocated to real time flows for transmitting their $q_i - u_i(t)$ data, where q_i denotes the queue length for the flow i, as well as to best effort flows, considering the fact that the latter have no specific service constraints. In comparison with the FLS scheduler, which allocates the remaining RBs only to best effort flows using the PF scheduler, this level of FLSA further improves the resource distribution in a QoS aware manner.

2.3.4 Performance Evaluation of the FLSA

The performance of the FLSA was evaluated against the PF, M-LWDF, EXP/PF, FLS, EXP-RULE and LOG-RULE schedulers. For the EXP-RULE metric the used parameter set is $a_i \in [5/(0.99 \cdot \tau_i), 10/(0.99 \cdot \tau_i)]$, $b_i = 1/E[\Gamma^i]$ and $c = 1$ as proposed in [144] for best performance. Table 2.5 summarizes the factors considered by each scheduler for resource allocation, demonstrating that the FLSA is the most complete strategy, since it considers the entire factors.

Table 2.2 The Parameters considered in each Scheduler in comparison with the ones considered by the FLSA.

Scheduler	SINR	Throughput	HOL Delay	Max. Delay	Max. PLR	Queue Length
PF	x	x				
M-LWDF	x	x	x	x	x	
EXP/PF	x	x	x	x	x	
FLS	x	x		x		x
FLSA	x	x	x	x	x	x
EXP RULE	x	x	x	x		
LOG RULE	x	x	x	x		

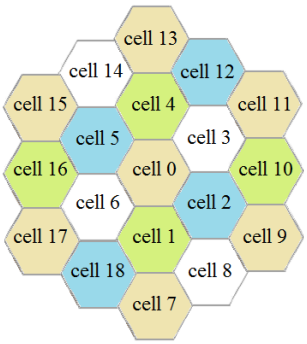

Figure 2.3 The Topology Simulated for the Evaluation of the FLSA Scheduler.

In the simulations, an LTE network topology composed of 19 cells is considered. Each cell contains 1 eNB with 43 dBm transmission power and 10 MHz downlink bandwidth providing 50 RBs available for allocation per TTI. The system sub-frequencies have been distributed to cells using a reuse factor equal to 2 as presented in Figure 2.3, to avoid interference between neighbor cells. A full bandwidth periodic Channel Quality Indication (CQI) reporting scheme is applied and each user equipment (UE) reports its downlink Signal to Interference plus Noise Ratio (SINR) to eNB, in every TTI. The eNB quantizes the reported SINR value and calculates the CQI as described in [145], Then, it uses the CQI to guarantee a maximum block error rate (BLER) less than 10% regardless of the scheduling strategy applied. A number of users, between the range [10, 40], is moving inside the borders of each eNB according to the random way-point mobility model. Each user receives two real time flows, including an H264 video with bitrate equal to 440 kbps and a voice over IP (VoIP) using the G.729 codec. Furthermore, one best effort flow is added as background traffic. Table 2.6 summarizes the simulation parameters.

In general, QoS aware schedulers increase the packet loss ratio (PLR) as they try to maintain the required target delay. This strategy is based on the assumption that real time services such as VoIP and video have no advantages of receiving expired packets. Thus, since the delay constraint is satisfied, the algorithms are evaluated in terms of PLR, so as to have a

Table 2.3 The Simulation Parameters for the Evaluation of the FLSA Scheduler.

Parameter	**Value**
Simulation time	100 seconds
Downlink bandwidth	10 MHz
Modulation	QPSK, QAM-16 and QAM-64
Number of cells	19
Cell radius	0.5 km
Number of users	up to 40 users per cell
Users mobility	Random way point
Traffic models	Real time traffics: H264 video at 440 kbps, VoIP using G.729 codec Best effort traffic: Web

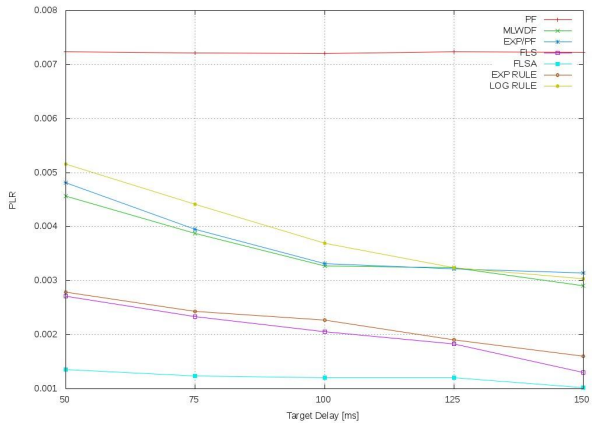

Figure 2.4 Evaluation of the FLSA Scheduler in terms of VoIP Packet Loss Ratio using Different Target Delays.

comprehensive view about the performance improvements. Figures 2.4 and 2.5 illustrate the impact of the target delay parameter in the PLR for VoIP and video flows, respectively, for the case of having 20 users per cell. While the target delay increases from 50ms to 150ms, the PLR decreases. Additionally, it may be observed that FLSA compared with FLS exhibits a lower PLR by up to 7%.

In Figures 2.6 and 2.7, the PLR for the VOIP and video flows is presented as the number of cell users varies from 10 to 40. The considered target delays are set to 100ms and 150ms for VoIP and video flows respectively, as determined by the LTE QoS class specifications for these service types [146]. As shown, FLSA results in a lower PLR than the rest of the algorithms. FLSA shows a marginal decrease of its PLR compared to FLS for VoIP flows. Also, its PLR is 10% lower than that of FLS for video flows.

The analysis of the throughput provides an important insight on the performance of the FLSA in comparison with the other schedulers. As presented in Figures 2.8 and 2.9 the FLSA outperforms the rest of the schedulers, independently of the number of users for VoIP and video

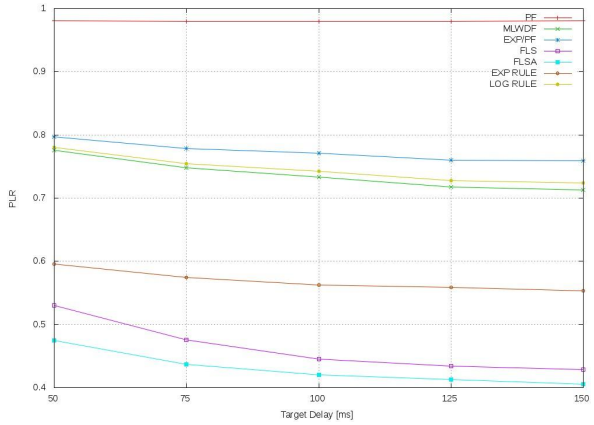

Figure 2.5 Evaluation of the FLSA Scheduler in terms of Video Packet Loss Ratio using Different Target Delays.

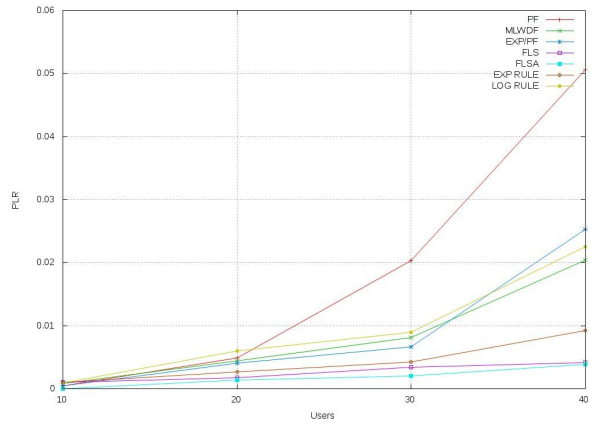

Figure 2.6 Evaluation of the FLSA Scheduler in terms of VoIP Packet Loss Ratio.

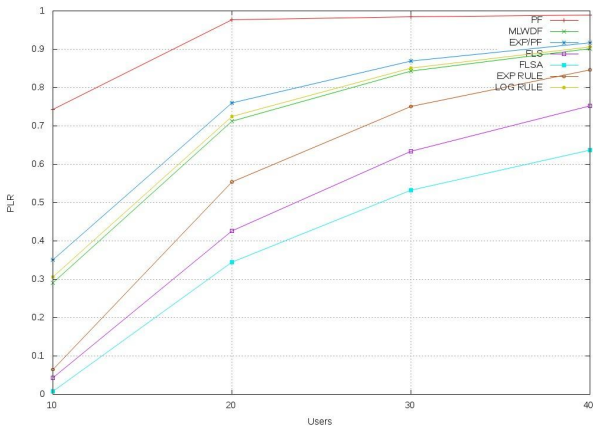

Figure 2.7 Evaluation of the FLSA Scheduler in terms of Video Packet Loss Ratio.

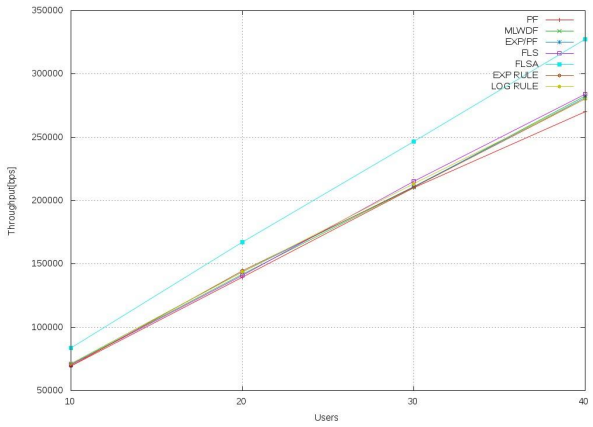

Figure 2.8 Evaluation of the FLSA Scheduler in terms of VoIP Throughput.

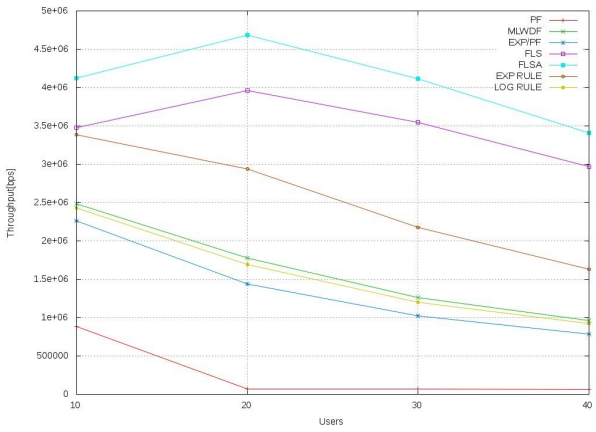

Figure 2.9 Evaluation of the FLSA Scheduler in terms of Video Throughput.

flows, respectively. This is expected due to the recalculation of formula 2.11 in each TTI by the upper level of FLSA as well as the inclusion of the lower level in the scheduler. The FLSA achieves higher throughputs than the rest of the algorithms providing rates of up to 330kbps for VoIP and up to 4.7 Mbps for video services.

The proposed scheduler is also evaluated in terms of the Jain fairness index, which is estimated using formula 2.14 where n is the number of the service flows and x_i is the throughput of the i^{th} flow.

$$Jain\_Fairness = \frac{(\sum_{i=1}^{n} x_i)^2}{n \cdot \sum_{i=1}^{n} x_i^2} \tag{2.14}$$

Flows with the same service constraints must receive similar QoS to avoid the situation of having a set of satisfied users against a set of dissatisfied ones of the same service type. The maximum value of fairness is 1 while the more a scheduler accomplishes a value close to 1, the more the resource allocation is fair. As presented in Figure 2.10 the fairness for VoIP flows is

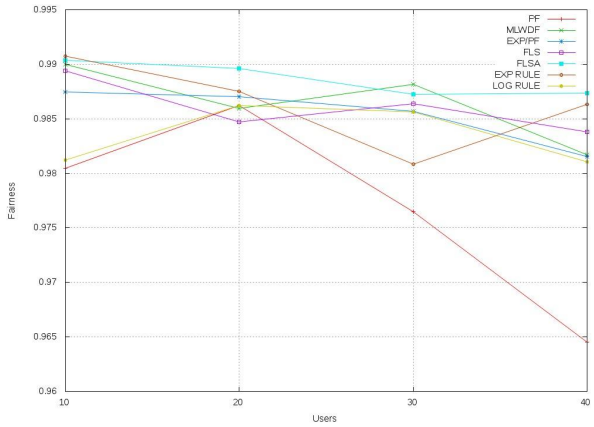

Figure 2.10 Evaluation of the FLSA Scheduler in terms of VoIP Fairness Index.

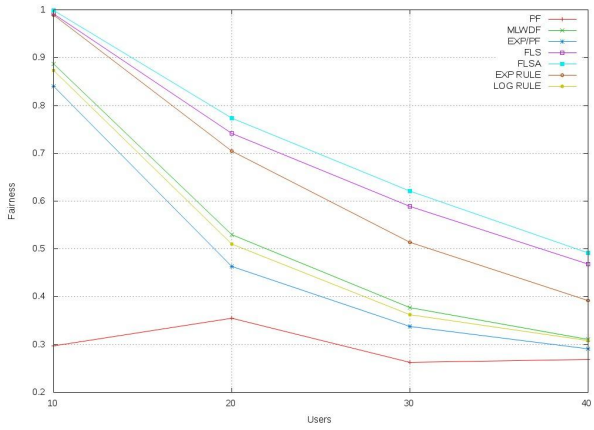

Figure 2.11 Evaluation of the FLSA Scheduler in terms of Video Fairness Index.

very close to 1. Additionally, Figure 2.11 demonstrates that the FLSA scheduler improves the fairness for the video flows compared with the rest of the schedulers.

2.4 The Proposed FLS Advanced - Cross Carrier (FLSA-CC) Scheduler

This section describes the proposed FLSA-CC scheduler (Fig. 2.12) which aims at the optimization of system performance using carrier aggregation in the LTE downlink. The FLSA-CC improves the FLSA scheduler in a cross carrier manner adapting the resource allocation process at different channel conditions of the aggregated component carriers. Furthermore, due to the fact that in the Cross Carrier Scheduling (CCS) methodology adopted by this scheduler, only the PCC uses the PDCCH channel for transmission of scheduling information, an interference decrement is observed resulting in better channel conditions in terms of SINR, thus increasing the overall system capacity. The FLSA-CC has been built upon three distinct levels, which cooperate with each other for dynamically assigning radio resources to users in each TTI.

The upper level of FLSA-CC uses the formula (2.11) of the FLS [142] to estimate the $u_i(x)$ quota of data that the i^{th} real time flow should transmit in each x^{th} TTI, in order to satisfy its QoS constraints. In other words, $u_i(x)$ quota is estimated in each x^{th} TTI of a frame, whereas in FLS it is estimated once, at the beginning of each frame. The FLSA-CC estimates the coefficient value $c_i(n)$ using formula (2.15), where N represents the number of component carriers. A performance improvement has been observed due to the fact that in FLS, when a real time flow transmits its $u_i(x)$ quota of data, it loses the opportunity to continue the transmission until the beginning of the next frame. By recalculating the formula (2.11) in each TTI (instead of estimating it only at the beginning of each frame), the FLSA-CC provides more resources to real time flows that have remaining data for transmission.

$$c_i(n) = \begin{cases} n \text{ , when } 0 \leq n \leq 1 \\ c_i(n-1)/(2 \cdot N) \text{ , when } n \geq 2 \end{cases} \tag{2.15}$$

In each TTI, the middle level uses a cross carrier version of the MLWDF scheduler, called MLWDF-CC, to allocate RBs to real time flows for transmitting their $u_i(x)$ quota of data which have been calculated by the upper level. This scheduler extends the PF-CC metric [147] [148] $m_{i,k}^{PF-CC}$ given in formula (2.16). The MLWDF-CC metric is evaluated by formula (2.17) where the α_i value is determined by formula (2.7). The use of the cross carrier QoS aware MLWDF-CC scheduler achieves an improved resource distribution among the real time flows in comparison with the FLS scheduler which at the second level uses the non-cross carrier principle as well as the non-QoS aware PF algorithm.

The third level has been added to allocate the remaining RBs of each TTI to best effort flows using formula (2.16) of the PF-CC algorithm.

$$m_{i,k}^{PF-CC} = \frac{d_k^i(t)}{\sum_{j=1}^{N} \bar{R}^{i,j}(t-1)} \tag{2.16}$$

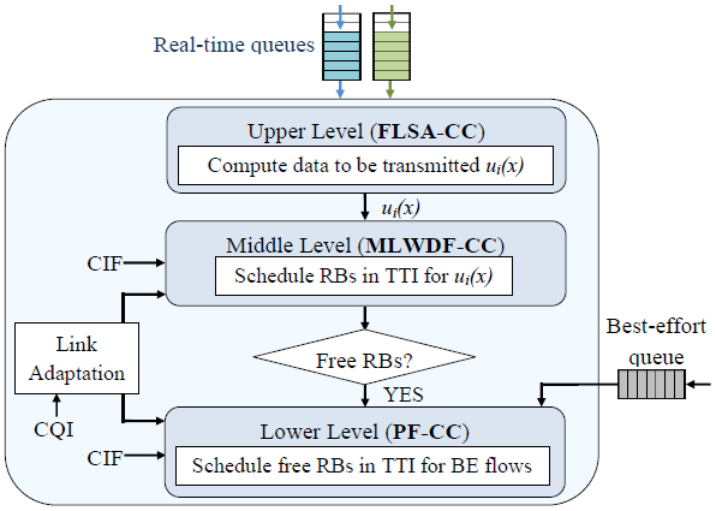

Figure 2.12 The FLSA-CC Scheduler Design.

$$m_{i,k}^{MLWDF-CC} = a_i \cdot D_{HOL,i} \cdot m_{i,k}^{PF-CC} \tag{2.17}$$

2.4.1 Simulation Environment for the FLSA-CC Evaluation

The simulation environment is implemented using an extended version of the Lte-Sim [145] simulator. More specifically, the iCanCloud [149] and the OpenFlow [150] modules of the Omnet++ [151] simulator have been configured and embedded to the Lte-Sim enabling the ability to include a cloud infrastructure and SDN controllers to the simulated LTE topologies.

The simulation environment consists of an LTE Evolved UMTS Terrestrial Radio Access Network (E-UTRAN) and a Cloud infrastructure. The E-UTRAN includes 7 DeNBs and 28 RNs (4 per DeNB). The transmission radius is equal to 1 kilometer for each DeNB and 100 meters for each RN. Each RN is positioned at 90% of the transmission radius of its DeNB. Furthermore, Type-1 Outband Relaying is applied and thus two link types are defined, namely the access link and the backhaul link. The access link is used for communication between a UE and an RN or a DeNB using a frequency f_1, while the backhaul link is used for communication between an RN and a DeNB using a frequency $f_2 \neq f_1$.

Inter-band Carrier Aggregation (CA) is applied in each DeNB and RN. According to this CA configuration, two component carriers, which belong to different frequency bands, are aggregated. Each component carrier bandwidth is equal to 20MHz and contains 100 resource blocks. Thus, a 40MHz bandwidth is assigned to each cell (RN or DeNB) and a total of 200 RBs are available for scheduling in each TTI. Table 2.4 presents the system sub-frequencies assigned to each cell.

Table 2.4 The Sub-Frequencies that are assigned to each Cell.

Cell	Aggregated Component Carriers
DeNB0	PCC: 1805 MHz – 1825 MHz *(band 3)* SCC: 760 MHz – 780 MHz *(band 28)*
DeNB1,3,5	PCC: 1825 MHz – 1845 MHz *(band 3)* SCC: 870 MHz – 890 MHz *(band 5)*
DeNB2,4,6	PCC: 2110 MHz – 2130 MHz *(band 1)* SCC: 940 MHz – 960 MHz *(band 8)*
Relay nodes	*Case 1* { PCC: 2620 MHz – 2640 MHz *(band 7)*; SCC: 780 MHz – 800 MHz *(band 28)* } *Case 2* { PCC: 2640 MHz – 2660 MHz *(band 7)*; SCC: 800 MHz – 820 MHz *(band 20)* }

The 3GPP urban channel model [152] [153] is used. Since the channel between DeNB or RN and UE encounters non-line-of-sight (NLOS) transmission, its propagation loss is estimated using formula (2.18) and (2.19), for DeNB-UE and RN-UE communication respectively, where d represents the distance among the nodes and f_c the carrier frequency. Also, since the channel between a DeNB and an RN encounters line-of-sight (LOS) transmission, its propagation loss is estimated using formula (2.20).

$$PL^{NLOS}_{DeNB\rightarrow UE} = 37.6 \cdot log_{10}(d) + 58.94 + 21 \cdot log_{10}(f_c) \tag{2.18}$$

$$PL^{NLOS}_{RN\rightarrow UE} = 36.7 \cdot log_{10}(d) + 22.7 + 26 \cdot log_{10}(f_c) \tag{2.19}$$

$$PL^{LOS}_{DeNB\rightarrow RN} = 22 \cdot log_{10}(d) + 28 + 20 \cdot log_{10}(f_c) \tag{2.20}$$

The Cloud contains a set of virtual machines (VMs) and implements the functionalities of the LTE Evolved Packet Core (EPC). Additional VMs with user applications are created. Specifically, one VM is created for each UE running three applications namely one VoIP, one video and one best effort.

Flow forwarding as well as resource scheduling in each DeNB and RN are performed using a centralized global controller placed into the Service Gateway (SGW) having a wide view of the entire system. The simulated topology is presented in Figure 2.13.

2.4.2 Performance Evaluation of the FLSA-CC Algorithm

The performance of the FLSA-CC was evaluated against the PF, MLWDF, EXP/PF, FLS, FLSA, EXP-RULE and LOG-RULE schedulers. For the EXP-RULE metric the used parameter set is $a_i \in [5/(0.99 \cdot \tau_i), 10/(0.99 \cdot \tau_i)]$, $b_i = 1/E[\Gamma^i]$ and $c = 1$ as proposed in [144] for best performance. Table 2.5 summarizes the factors considered by each scheduler for resource allocation, demonstrating that the FLSA-CC is the most complete strategy. Furthermore, the full band periodic Channel Quality Indication (CQI) reporting scheme is applied. Thus, each UE reports its downlink SINR to RN for each component carrier in every TTI. The RN quantizes

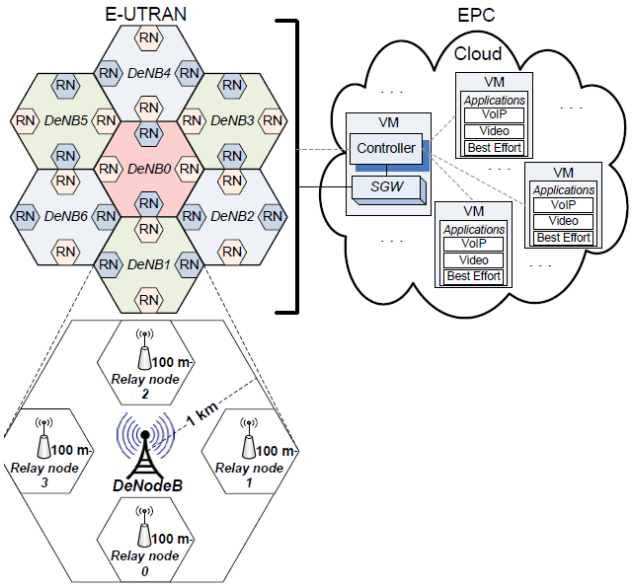

Figure 2.13 The Topology Simulated for the Evaluation of the FLSA-CC Scheduler.

the reported SINR value and calculates the CQI as described in [145]. Then, it uses the CQI to guarantee a maximum BLER less than 10% regardless of the scheduling strategy applied.

Table 2.5 The Parameters considered in each Scheduler in comparison with the ones considered by the FLSA-CC.

Scheduler	SINR	Throughput	HOL Delay	Max. Delay	Max. PLR	Queue Length	CCS
PF	✓	✓					
MLWDF	✓	✓	✓	✓	✓		
EXP/PF	✓	✓	✓	✓	✓		
FLS	✓	✓		✓		✓	
FLSA	✓	✓	✓	✓	✓	✓	
FLSA-CC	✓	✓	✓	✓	✓	✓	✓
EXP RULE	✓	✓	✓	✓			
LOG RULE	✓	✓	✓	✓			

A number of users move inside the borders of each RN according to the random way-point mobility model. Each user receives two real time flows, an H264 video with bitrate equal to 440 kbps and a Voice over IP (VoIP) using the G.729 codec. Furthermore, one best effort flow is added as background traffic. Table 2.6 summarizes the simulation parameters.

2.4.2.1 Real Time Services Results

Due to the fact that the simulation environment includes an LTE topology with RNs, a two hop target delay for real time flows $\tau_i = \tau_{i,DeNB \rightarrow RN} + \tau_{i,RN \rightarrow UE}$ is considered, where $\tau_{i,DeNB \rightarrow RN}$

Table 2.6 The Simulation Parameters for the Evaluation of the Proposed Algorithm.

Parameter	**Value**
Simulation time	100 seconds
Downlink bandwidth	2*20 = 40 MHz
Modulation	QPSK, QAM-16 and QAM-64
DeNBs number / radius	7 / 1 km
Relay nodes number / radius	4 per DeNB / 100 m
Number of users	up to 100 users per relay node
Users mobility	Random way point
Traffic models	Real time: { H264 video at 440 kbps; VoIP using G.729 codec } Best effort: Web

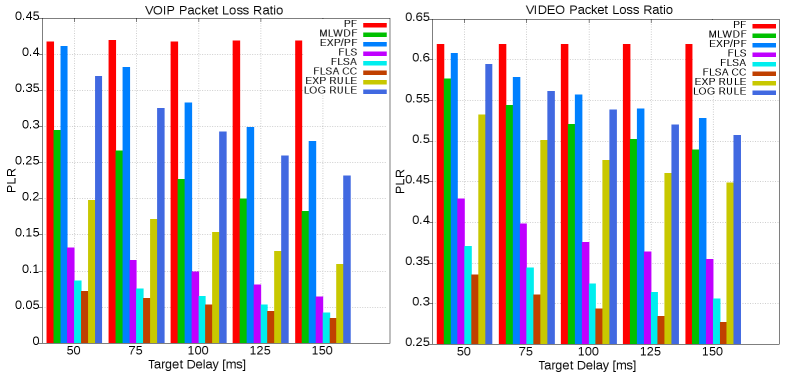

Figure 2.14 The FLSA-CC Scheduler Evaluation in terms of the Packet Loss Ratio of the Real Time Flows using Different Target Delays.

represents the target delay between a DeNB and an RN, and $\tau_{i,RN\rightarrow UE}$ represents the target delay between an RN and a UE. We consider $\tau_{i,DeNB\rightarrow RN} = \tau_{i,RN\rightarrow UE}$. In general, QoS aware schedulers increase the packet loss ratio (PLR) to guarantee the required τ_i. This strategy is based on the assumption that real time services such as VoIP and Video can not use expired packets. Thus, since the delay constraint is satisfied, the algorithms are evaluated in terms of PLR, so as to have a comprehensive view about the performance improvements. Figure 2.14 illustrates the impact of the target delay parameter τ_i in the PLR for VoIP and video flows, for the case of having 100 users per RN. As the target delay increases from 50ms to 150ms, the PLR decreases. Additionally it may be observed that FLSA-CC compared with FLSA exhibits lower PLR independently of the target delay parameter.

In Figure 2.15, the PLR for VOIP and video flows is presented while the number of cell RN users varies from 20 to 100. In this case, the considered target delays are set to 100ms and 150ms for VoIP and video flows respectively, as determined by the LTE QoS class specifications for these service types. As shown, FLSA-CC results in a lower PLR than the rest

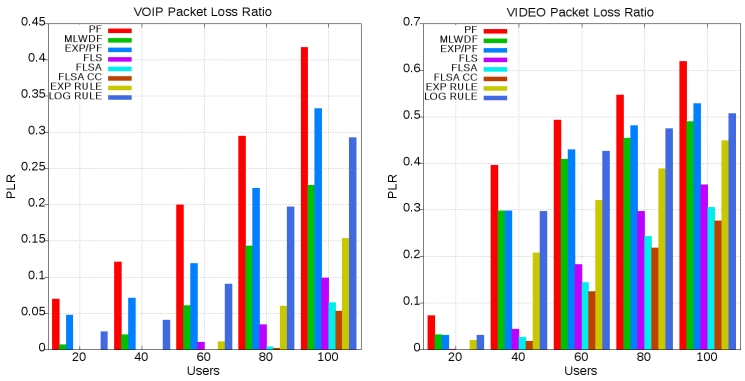

Figure 2.15 The FLSA-CC Scheduler Evaluation in terms of the Packet Loss Ratio of the Real Time Flows.

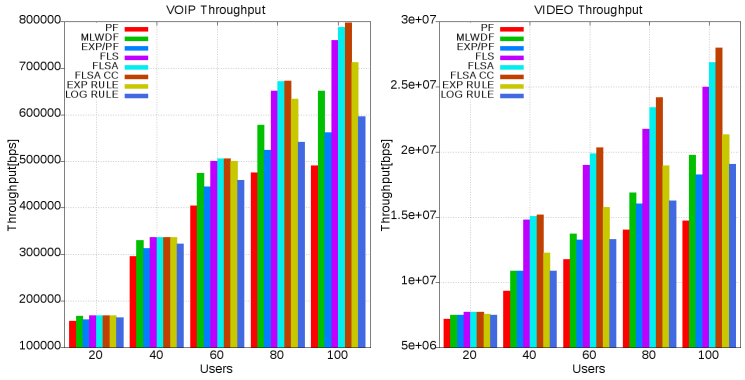

Figure 2.16 The FLSA-CC Scheduler Evaluation in terms of the Throughput of the Real Time Flows.

of the algorithms. Specifically, FLSA shows a marginal decrease of its PLR for VoIP flows as well as up to a 3% lower PLR for video flows compared to FLSA.

The analysis of the throughput offered to real time services provides an important insight on the performance of the FLSA-CC in comparison with the other schedulers. As presented in Figure 2.16 the FLSA-CC outperforms the rest of the schedulers, independently of the number of users for VoIP and video flows. This is expected due to the cross carrier scheduling operating principle applied as well as due to the recalculation of formula (2.11) in each TTI by the upper level of the FLSA-CC. More specifically, the FLSA-CC achieves higher throughputs than the rest of the algorithms providing rates of up to 800kbps for VoIP and up to 28Mbps for video services.

The proposed scheduler is also evaluated in terms of Jain fairness index, which is estimated using formula 2.14. Figure 2.17 demonstrates that the FLSA-CC scheduler improves the fairness for both VoIP and video flows.

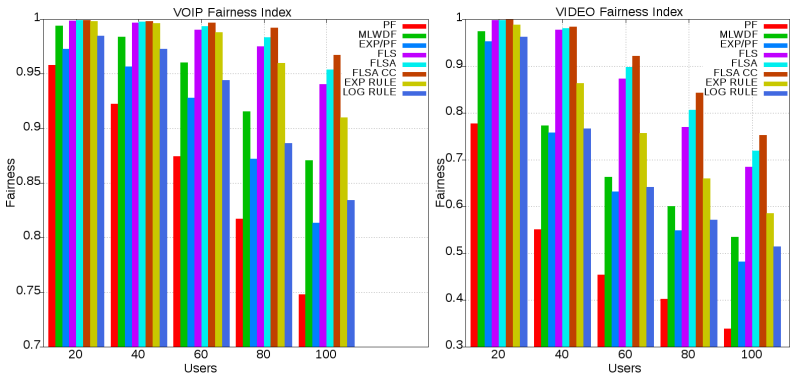

Figure 2.17 The FLSA-CC Scheduler Evaluation in terms of the Fairness Index of the Real Time Flows.

2.4.2.2 Best Effort Services Results

In this subsection tne FLSA-CC, FLSA and FLS schedulers, which accomplish better performance for real time services are evaluated for best effort flows in terms of the throughput and the fairness index. As presented in Figure 2.18, the FLSA-CC outperforms the other two schedulers and provides a throughput up to 1.5Mbps for best effort flows even when the number of users increases, while the FLSA accomplishes only a 100kbps throughput. Additionally, the FLSA-CC scheduler significantly improves the fairness index of the best effort flows.

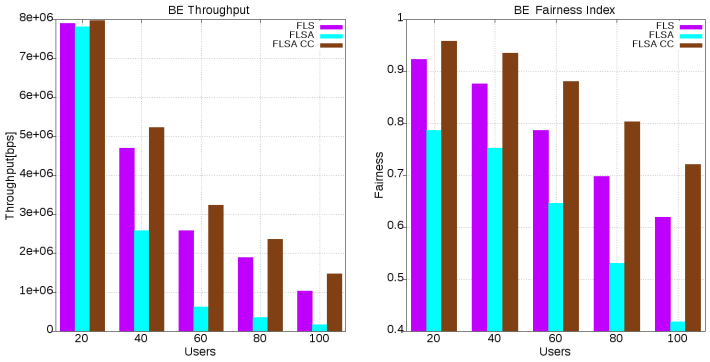

Figure 2.18 The FLSA-CC Scheduler Evaluation in terms of the Throughput and the Fairness Index of the Best Effort Flows.

Chapter 3

Mobility Management

3.1 Related Methodologies

3.1.1 Fuzzy Logic

3.1.1.1 The Interval-Valued Trapezoidal Fuzzy Numbers (IVTFN)

The concept of fuzzy logic was introduced by Zadeh [154] and is used to make a decision from indeterminate and approximate information. A fuzzy number is represented by a set of real values representing an uncertain quantity and a convex normalized continuous function which estimates the degree of membership for each value in the subset. Triangular or trapezoidal fuzzy numbers are frequently used to represent uncertain information. A trapezoidal fuzzy number can be defined as a vector $x = (x_1, x_2, x_3, x_4, v_{\hat{A}})$ with a membership function $\mu(x)$:

$$\mu(x) = \begin{cases} \frac{x-x_1}{x_2-x_1}, & \text{if } x_1 \leq x < x_2; \\ v_{\hat{A}}, & \text{if } x_2 \leq x \leq x_3; \\ \frac{x-x_4}{x_3-x_4}, & \text{if } x_3 < x \leq x_4; \\ 0, & \text{otherwise.} \end{cases} \tag{3.1}$$

where $x_1 < x_2 < x_3 < x_4$ and $v_{\hat{A}} \in [0,1]$.

An Interval-valued fuzzy number (IVFN) was introduced by Sambuc [155]. An IVFN is defined as $A = [A^L, A^U]$ consisting of the lower A^L and the upper A^U fuzzy numbers. IVFNs replace the crisp membership values by intervals in $[0,1]$. They were proposed due to the fact that fuzzy information can be better expressed by intervals than by single values. Liu and Jin [156] and Cornelis et al. [157] suggest that IVFNs are useful in multiple criteria decision making (MCDM) problems and particularly in cases where attribute values are in the form of linguistic expressions. Therefore, Ashtiani et al. [158] propose an extension of the fuzzy TOPSIS method using interval-valued triangular fuzzy numbers. Moreover, Liu and Jin [156] propose a decision making method using weighted geometric aggregation operators on attribute values expressed in the form of interval-valued trapezoidal fuzzy numbers. According to the

definition in [158], an IVFS A is defined as follows:

$$A = \{(x, [\mu_A^L(x), \mu_A^U(x)])\} \tag{3.2}$$

$$\mu_A^L(x), \mu_A^U(x) : X \to [0,1] \forall x \in X, \mu_A^L(x) < \mu_A^U(x) \tag{3.3}$$

$$\hat{\mu}_A(x) = [\mu_A^L(x), \mu_A^U(x)] \tag{3.4}$$

$$A = \{(x, \hat{\mu}_A(x))\}, x \in (-\infty, \infty) \tag{3.5}$$

In particular, the interval-valued trapezoidal fuzzy number defined in [159], is a general form of fuzzy number (Figure 3.1). This number can be represented as: $A = [A^L, A^U] = [(x_1^L, x_2^L, x_3^L, x_4^L, v_{A^L}), (x_1^U, x_2^U, x_3^U, x_4^U, v_{A^U}))]$ where: $0 \leq x_1^L \leq x_2^L \leq x_3^L \leq x_4^L \leq 1$, $0 \leq x_1^U \leq x_2^U \leq x_3^U \leq x_4^U \leq 1$, $0 \leq v_{A^L} \leq v_{A^U} \leq 1$ and $A^L \subset A^U$. The operational rules of the interval-valued trapezoidal fuzzy numbers are defined in [159].

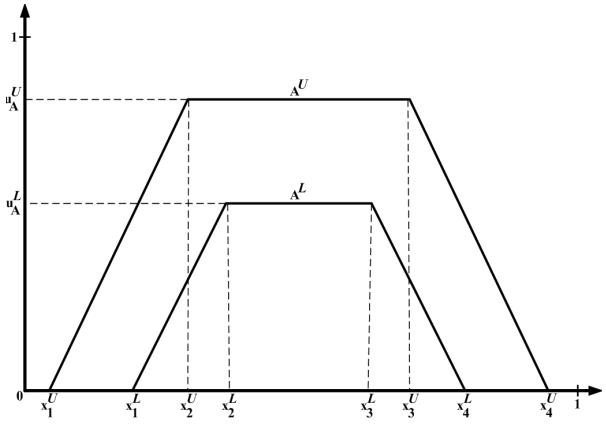

Figure 3.1 The Interval-Valued Trapezoidal Fuzzy Numbers.

3.1.1.2 The Interval-Valued Pentagonal Fuzzy Numbers (IVPFN)

A pentagonal fuzzy number can be defined as a vector $x = (x_1, x_2, x_3, x_4, x_5, v_{\hat{A}}, v_{\hat{A}1}, v_{\hat{A}2})$ with membership function:

$$\mu(x) = \begin{cases} v_{\hat{A}1} \cdot \frac{x - x_1}{x_2 - x_1}, & \text{if } x_1 \leqslant x < x_2; \\ v_{\hat{A}} - (v_{\hat{A}} - v_{\hat{A}1}) \cdot \frac{x - x_2}{x_3 - x_2}, & \text{if } x_2 \leqslant x < x_3; \\ v_{\hat{A}}, & \text{if } x = x_3; \\ v_{\hat{A}} - (v_{\hat{A}} - v_{\hat{A}2}) \cdot \frac{x - x_3}{x_4 - x_3}, & \text{if } x_3 < x \leqslant x_4; \\ v_{\hat{A}2} \cdot \frac{x - x_5}{x_4 - x_5}, & \text{if } x_4 < x \leqslant x_5; \\ 0, & \text{otherwise.} \end{cases} \tag{3.6}$$

where $x_1 \leqslant x_2 \leqslant x_3 \leqslant x_4 \leqslant x_5$ and $v_{\hat{A}}, v_{\hat{A}1}, v_{\hat{A}2} \in [0,1]$.

The interval-valued pentagonal fuzzy number is a general IVFN case (Figure 3.2) defined as: $A = [A^L, A^U] = [(x_1^L, x_2^L, x_3^L, x_4^L, x_5^L, v_A^L, v_{A1}^L, v_{A2}^L), (x_1^U, x_2^U, x_3^U, x_4^U, x_5^U, v_A^U, v_{A1}^U, v_{A2}^U))]$ where: $A^L \subset A^U$, $0 \leqslant x_1^L \leqslant x_2^L \leqslant x_3^L \leqslant x_4^L \leqslant x_5^L \leqslant 1$, $0 \leqslant x_1^U \leqslant x_2^U \leqslant x_3^U \leqslant x_4^U \leqslant x_5^U \leqslant 1$, $v_A^L \leqslant v_A^U$, $v_{A1}^L \leqslant v_{A2}^L \leqslant v_A^L$, $v_{A1}^U \leqslant v_{A2}^U \leqslant v_A^U$ and $v_A^L, v_{A1}^L, v_{A2}^L, v_A^U, v_{A1}^U, v_{A2}^U \in [0,1]$. The operational rules of the interval-valued pentagonal fuzzy numbers are defined in [160].

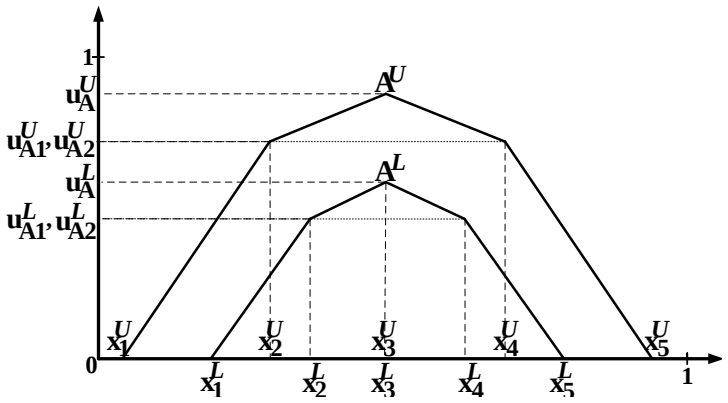

Figure 3.2 The Interval-Valued Pentagonal Fuzzy Numbers.

3.1.1.3 Creating Fuzzy Numbers: The Equalized Universe Method (EUM)

The Equalized Universe Method (EUM) [161] [162] creates IVFNs with their centroids equally spaced along a predefined domain of values. The values of the i^{th} IVPFN are calculated using formula 3.7, where U_{min} and U_{max} are the minimum and maximum value of the domain and c represents the number of the IVPFNs created. The v_{A1}^L, v_{A1}^U, v_{A2}^L and v_{A2}^U are defined by the user.

$$IVPFN_i = \begin{cases} x_{i,1}^U = x_{i,2}^U - \frac{U_{max}-U_{min}}{4\cdot(c-1)}, x_{i,1}^L = x_{i,1}^U \cdot (v_{A1}^L / v_{A1}^U) \\ x_{i,2}^U = x_{i,3}^U - \frac{U_{max}-U_{min}}{2\cdot(c-1)}, x_{i,2}^L = x_{i,2}^U \cdot (v_{A1}^L / v_{A1}^U) \\ x_{i,3}^{U,L} = U_{min} + \frac{U_{max}-U_{min}}{c-1} \cdot (i-1) \\ x_{i,4}^U = x_{i,3}^U + \frac{U_{max}-U_{min}}{2\cdot(c-1)}, x_{i,4}^L = x_{i,4}^U \cdot (v_{A2}^L / v_{A2}^U) \\ x_{i,5}^U = x_{i,4}^U + \frac{U_{max}-U_{min}}{4\cdot(c-1)}, x_{i,5}^L = x_{i,5}^U \cdot (v_{A2}^L / v_{A2}^U) \end{cases} \tag{3.7}$$

3.1.1.4 The Mamdani Pentagonal Fuzzy Inference System (MPFIS)

Fuzzy Inference (FI) [163–165] involves the mapping of a given input to an output using fuzzy logic. The Mamdani Pentagonal Fuzzy Inference System (MPFIS) considers two inputs ($Input_1$ and $Input_2$) to estimate the value of the $Output$. Both $Input_1$ and $Input_2$ have normalized values within the range [0, 1]. Also, the MF_{Input_1}, MF_{Input_2}, MF_{Output} membership functions (MF) are defined, indicating the linguistic terms and the corresponding Interval Valued Pentagonal Fuzzy Numbers (IVPFN) for the fuzzy representation of the $Input_1$, $Input_2$ and $Output$, respectively.

Thus, for each crisp value, two membership degrees are determined in the corresponding MF, one for the upper pentagon and one for the lower pentagon. The MPFIS implements the following methods:

Step 1. *Membership Functions Definition:* The Membership Functions (MF) for $Input_1$, $Input_2$ and $Output$ parameters are defined.

Step 2. *Fuzzy rule (or knowledge) base:* A set R of fuzzy rules is defined, where each rule $r \in R$ is a simple if-then statement with a condition and a conclusion. The rule's condition consists of MF_{Input_1} and MF_{Input_2} membership functions, while its conclusion indicates an MF_{Output} membership function.

Step 3. *Fuzzification:* The $Input_1$ and $Input_2$ crisp values are converted to degrees of membership indicated as $Input'_1$ and $Input'_2$ by a lookup in MF_{Input_1} and MF_{Input_2} membership functions respectively.

Step 4. *Combination of the fuzzified inputs (Fuzzy Operations):* A Z'_r degree is calculated considering the rule's condition, that indicates the strength of the r rule. Furthermore, in case that a rule's condition has multiple parts, the fuzzy operators 'AND' and 'OR' may be used to combine more than one conditions. The 'Algebraic product' and the 'Algebraic sum' are applied for the 'AND' and the 'OR' operators respectively. In our study, the 'Algebraic product' is calculated using formula 3.8, while the 'Algebraic sum' is calculated using formula 3.9.

$$Z'_{u,i,r} = Input'_1 \hat{} Input'_2 = Input'_1 \cdot Input'_2 \tag{3.8}$$

$$Z'_{u,i,r} = (Input'_1 + Input'_2) - (Input'_1 \cdot Input'_2) \tag{3.9}$$

Step 5. *Implication method:* The implication method estimates the consequence $MF_{Output^c_r}$ of the rule conclusion, considering both the rule conclusion MF_{Output_r} and the rule strength Z'_r. The MF_{Output_r} height is trimmed with respect to the Z'_r degree, using formula 3.10, which applies the Min method.

$$MF_{Output^c_{r_{Height}}} = min\{MF_{Output_{r_{Height}}}, Z'_r\} \tag{3.10}$$

Step 6. *Aggregation method:* The aggregation method combines the R rules' consequences to calculate the $Output^A$ fuzzy set, using formula 3.11, which applies the Max method.

$$Output^A = MF_{Output^c_1} \cup MF_{Output^c_2} \cup \ldots \cup MF_{Output^c_R} \tag{3.11}$$

Step 7. *Defuzzification:* During the defuzzification, the $Output^A$ fuzzy set is transformed to the crisp value $Output$. Formula 3.31 that applies the Weighted Average method is used, where μ_r is the height and h_r is the centroid of each rule obtained from the $Output^A$. Also, symbols U and L represent the upper and the lower pentagon of each rule respectively .

$$Output = \frac{\sum_{r=1}^{R} (\mu_r^U \cdot h_r^U + \mu_r^L \cdot h_r^L)}{\sum_{r=1}^{R} (h_r^U + h_r^L)} \tag{3.12}$$

3.1.2 Estimating the Mobility Management Criteria Importance

3.1.2.1 The Analytic Network Process (ANP)

The Analytic Network Process (ANP) was introduced by Saaty [166] to deal with decision problems with criteria and alternatives that depend on each other. ANP is a generalization of the Analytic Hierarchy Process (AHP). A decision problem that is analyzed with the ANP can be designed either as a control-hierarchy or as a non-hierarchical network. The nodes of the network represent the components (or clusters) of the system while the arcs denote the interactions between them. All the interactions and the feedbacks within the clusters are called inner dependencies, while the interactions and the feedbacks between clusters are called outer dependencies. ANP is composed of four major steps [167]:

Step 1. *Model construction and problem structuring:* During this step the problem is analyzed and decomposed into a rational system, like a network.

Step 2. *Pairwise comparison matrices and priority vectors:* During this step, the pairwise comparison matrix is derived using Saaty's nine-point importance scale based (Table 3.1).

Table 3.1 The Saaty's Nine-Point Importance Scale.

Importance	Definition
1	Equal Importance
3	Moderate Importance
5	Strong Importance
7	Very Strong Importance
9	Extreme Importance
2, 4, 6, 8	Intermediate Values

Step 3. *Supermatrix formation:* During this step, the supermatrix of the ANP model is constructed to represent the inner and the outer dependencies of the network. This is a

partitioned matrix, where each matrix segment represents a relationship between two clusters in the network. To construct the supermatrix the local priority vectors obtained in Step 2 are grouped and placed in the appropriate positions in a supermatrix based on the flow of influence from one cluster to another, or from a cluster to itself, as in the loop. Then, the supermatrix is transformed to a stochastic one, the weighted supermatrix. Finally, the weighted supermatrix is raised to limiting powers until all the entries converge to calculate the overall priorities, and thus the cumulative influence of each element on every other element with which it interacts is obtained [168]. At this point, all the columns of the new matrix, the limit supermatrix, are the same and their values show the global priority of each element of the network.

For example, if we assume a network with n clusters, where each cluster $C_k, k = 1,2,\ldots,n$, and has m_n elements, denoted as $e_{k1}, e_{k2}, \ldots, e_{km_k}$, then the standard form, W, for a supermatrix can be expressed as:

$$
W = \begin{array}{cc}
 & \begin{array}{cccccc} C_1 & \ldots & C_k & \ldots & C_n \end{array} \\
 & \begin{array}{cccccc} e_{11}\ldots e_{1m_1} & \ldots & e_{k1}\ldots e_{km_k} & \ldots & e_{n1}\ldots e_{nm_n} \end{array} \\
\begin{array}{c} e_{11} \\ \vdots \\ C_1 \\ e_{1m_1} \\ \vdots \\ e_{k1} \\ \vdots \\ C_k \\ e_{km_k} \\ \vdots \\ e_{n1} \\ \vdots \\ C_n \\ e_{nm_n} \end{array} &
\begin{bmatrix}
 & & & & \\
W_{11} & \ldots & W_{1k} & \ldots & W_{1n} \\
\vdots & \vdots & \vdots & \vdots & \vdots \\
W_{k1} & \ldots & W_{kk} & \ldots & W_{kn} \\
\vdots & \vdots & \vdots & \vdots & \vdots \\
W_{n1} & \ldots & W_{nk} & \ldots & W_{nn}
\end{bmatrix}
\end{array}
\tag{3.13}
$$

Step 4. *Selection of the best alternatives:* If the supermatrix formed in Step 3 covers the whole network, then the priority weights of the alternatives can be found in the column of the alternatives in the normalized supermatrix. Otherwise, additional calculations are required in order to obtain the overall priorities of the alternatives. The alternative with the largest overall priority should be selected, as it is the best alternative as determined by the calculations made using matrix operations.

3.1.3 The Trapezoidal Fuzzy Analytic Network Process (TF-ANP)

A decision problem that is analyzed with the TF-ANP can be represented as a network of nodes. Each node represents a component (or cluster) of the system while arcs denote interactions between them. Interactions and feedbacks within clusters are called inner dependencies, while interactions and feedbacks between clusters are called outer dependencies. The TF-ANP is composed of five major steps:

Step 1. *Model Construction and Problem Structuring:* During this step the problem is analyzed and decomposed into a rational system, consisting of a network of nodes.

Step 2. *Pairwise comparison matrices and priority vectors:* In this step, initially the fuzzy pairwise comparison matrix $\tilde{A}$ is derived for each TF-ANP cluster using the linguistic terms presented in Table 3.2, which corresponds to the nine-point importance scale introduced in [166]. The standard form of the $\tilde{A}$ matrix is expressed as follows:

$$\tilde{A} = \begin{bmatrix} 1 & \dots & \tilde{a}_{1j} & \dots & \tilde{a}_{1n} \\ \vdots & & \vdots & & \vdots \\ 1/\tilde{a}_{1i} & \dots & 1 & \dots & \tilde{a}_{in} \\ \vdots & & \vdots & & \vdots \\ 1/\tilde{a}_{1n} & \dots & 1/\tilde{a}_{jn} & \dots & 1 \end{bmatrix} \tag{3.14}$$

where n denotes the number of the cluster elements. Subsequently, the geometric mean $r_{\tilde{A}_i}$ of each row i in $\tilde{A}$ is estimated according to formula 3.34, where $\otimes$ denotes the multiplication operator of two fuzzy numbers as defined in [169].

$$r_{\tilde{A}_i} = (\tilde{a}_{i1} \otimes \tilde{a}_{i2} \otimes \dots \otimes \tilde{a}_{in})^{\frac{1}{n}} \tag{3.15}$$

Then, the priority vector $\tilde{\Omega}_i$ of cluster elements is constructed as follows:

$$\tilde{\Omega}_i = [\ \tilde{\omega}_1 \quad \tilde{\omega}_2 \quad \dots \quad \tilde{\omega}_n\ ] \tag{3.16}$$

where each $\tilde{\omega}_i = \left[(\omega_1^U, \omega_2^U, \omega_3^U, \omega_4^U, v_i^U); (\omega_1^L, \omega_2^L, \omega_3^L, \omega_4^L, v_i^L)\right]$ is calculated using formula 3.36. The $\oplus$ indicates the addition operator of two fuzzy numbers as defined in [169].

$$\tilde{\omega}_i = r_{\tilde{A}_i} / (r_{\tilde{A}_1} \oplus r_{\tilde{A}_2} \oplus \dots \oplus r_{\tilde{A}_i} \oplus \dots \oplus r_{\tilde{A}_n}) \tag{3.17}$$

Step 3. *Construction of the Supermatrix:* In this step, the fuzzy supermatrix $\tilde{W}$ of the TF-ANP model is constructed. This matrix represents the inner and outer dependencies of the TF-ANP network. It is a partitioned matrix, with each matrix segment representing the relationship between two clusters of the network. To construct the supermatrix, the local priority vectors $\tilde{\Omega}$ are grouped and placed in the appropriate positions in the supermatrix

based on the flow of influence from one cluster to another, or from a cluster to itself, as in the loop. For example, if we assume a TF-ANP network of q clusters, C_k with $k = [1,2,\ldots,q]$ and that each cluster has n_q elements, denoted as $e_{k1}, e_{k2}, \ldots, e_{kn_k}$, then the supermatrix $\tilde{W}$ is expressed as:

$$\tilde{W} = \begin{array}{c} \\ \\ C_1 \\ \vdots \\ \\ C_k \\ \vdots \\ \\ C_q \\ \\ \end{array} \begin{array}{c} \\ \\ e_{11} \\ \vdots \\ e_{1n_1} \\ \vdots \\ e_{k1} \\ \vdots \\ e_{kn_k} \\ \vdots \\ e_{q1} \\ \vdots \\ e_{qn_q} \end{array} \begin{array}{c} \begin{array}{ccccccc} C_1 & & \ldots & C_k & & \ldots & C_q \\ e_{11}\ldots e_{1n_1} & & \ldots & e_{k1}\ldots e_{kn_k} & & \ldots & e_{q1}\ldots e_{qn_q} \end{array} \\ \begin{bmatrix} \tilde{W}_{11} & \ldots & \tilde{W}_{1j} & \ldots & \tilde{W}_{1q} \\ \vdots & \vdots & \vdots & \vdots & \vdots \\ \tilde{W}_{k1} & \ldots & \tilde{W}_{kj} & \ldots & \tilde{W}_{kq} \\ \vdots & \vdots & \vdots & \vdots & \vdots \\ \tilde{W}_{q1} & \ldots & \tilde{W}_{qj} & \ldots & \tilde{W}_{qq} \end{bmatrix} \end{array} \tag{3.18}$$

Step 4. *Construction of the Weighted Supermatrix:* During this step, the supermatrix is transformed to a stochastic one,the Weighted Supermatrix $\tilde{W}'$ using formula 3.19.

$$\tilde{W}'_{k,j} = \tilde{W}_{k,j}/q \tag{3.19}$$

Step 5. *Calculation of the Limited Supermatrix:* In this step, initially the deffuzified Weighted Supermatrix W is estimated using the Weighted Average method. According to this method formula 3.20 is used, where the parameters v and d represent the height and the centroid of each $\tilde{W}'_{k,j}$ trapezoid respectively. Subsequently, W is raised to limiting powers until all the entries converge. By this way, the overall priorities are calculated, and thus the cumulative influence of each element on every other interacting element is obtained [168]. At this point, all the columns of the produced Limit Supermatrix are the same and their values show the estimated weight for each element of the TF-ANP network.

$$W_{k,j} = \frac{v^U \cdot d^U + v^L \cdot d^L}{d^U + d^L} \tag{3.20}$$

3.1.3.1 The Trapezoidal Fuzzy Adaptive Analytic Network Process (TF-AANP)

A decision problem that is analyzed with the TF-AANP can be represented as a network of nodes. Each node represents a component (or cluster) of the system while arcs denote

interactions between them. Interactions and feedbacks within clusters are called inner dependencies, while interactions and feedbacks between clusters are called outer dependencies. The TF-AANP is composed of seven major steps:

Step 1. *Estimation of the importance of each service:* The fuzzy pairwise comparison matrix $\tilde{P}$ is derived for the services using the linguistic terms presented in Table 3.2, which correspond to the nine-point importance scale introduced in [166]. The standard form of the $\tilde{P}$ matrix is expressed as follows:

$$\tilde{P} = \begin{bmatrix} 1 & \dots & \tilde{p}_{1j} & \dots & \tilde{p}_{1S} \\ \vdots & & \vdots & & \vdots \\ 1/\tilde{p}_{1s} & \dots & 1 & \dots & \tilde{p}_{sS} \\ \vdots & & \vdots & & \vdots \\ 1/\tilde{p}_{1S} & \dots & 1/\tilde{p}_{jS} & \dots & 1 \end{bmatrix} \tag{3.21}$$

where S denotes the number of the services. Subsequently, the geometric mean $r_{\tilde{P}_s}$ of each service (row) s in $\tilde{P}$ is estimated according to formula 3.22, where $\otimes$ denotes the multiplication operator of two fuzzy numbers as defined in [169].

$$r_{\tilde{P}_s} = (\tilde{p}_{s1} \otimes \tilde{p}_{s2} \otimes \dots \otimes \tilde{p}_{sS})^{\frac{1}{S}} \tag{3.22}$$

Then, the priority vector $\tilde{\Omega}_{\tilde{P}_s}$ of services is constructed as follows:

$$\tilde{\Omega}_{\tilde{P}_s} = [\ \tilde{\omega}_{\tilde{p}1} \quad \tilde{\omega}_{\tilde{p}2} \quad \dots \quad \tilde{\omega}_{\tilde{p}S}\ ] \tag{3.23}$$

where each $\tilde{\omega}_{\tilde{p}s} = \left[(\omega^U_{\tilde{p}1}, \omega^U_{\tilde{p}2}, \omega^U_{\tilde{p}3}, \omega^U_{\tilde{p}4}, v^U_{ps}); (\omega^L_{\tilde{p}1}, \omega^L_{\tilde{p}2}, \omega^L_{\tilde{p}3}, \omega^L_{\tilde{p}4}, v^L_{ps})\right]$ is calculated using formula 3.24. The $\oplus$ indicates the addition operator of two fuzzy numbers as defined in [169].

$$\tilde{\omega}_{\tilde{p}s} = r_{\tilde{P}_s} / (r_{\tilde{P}_1} \oplus r_{\tilde{P}_2} \oplus \dots \oplus r_{\tilde{P}_s} \oplus \dots \oplus r_{\tilde{P}_S}) \tag{3.24}$$

Step 2. *Model Construction and Problem Structuring for each service:* During this step, for each service $s \in S$ the problem is analyzed and decomposed into a rational system, consisted of a network of nodes.

Step 3. *Pairwise comparison matrices and priority vectors:* In this step, for each service $s \in S$, the fuzzy pairwise comparison matrix $\tilde{A}_s$ is derived for each TF-AANP cluster using the linguistic terms presented in Table 3.2. The standard form of the $\tilde{A}$ matrix is expressed as follows:

$$\tilde{A}_s = \begin{bmatrix} 1 & \dots & \tilde{a}_{s1j} & \dots & \tilde{a}_{s1n} \\ \vdots & & \vdots & & \vdots \\ 1/\tilde{a}_{s1i} & \dots & 1 & \dots & \tilde{a}_{sin} \\ \vdots & & \vdots & & \vdots \\ 1/\tilde{a}_{1sn} & \dots & 1/\tilde{a}_{sjn} & \dots & 1 \end{bmatrix} \tag{3.25}$$

where n denotes the number of the cluster elements. Subsequently, the geometric mean $r_{\tilde{A}_{si}}$ of each row i in $\tilde{A}_s$ is estimated according to formula 3.26.

$$r_{\tilde{A}_s i} = (\tilde{a}_{si1} \otimes \tilde{a}_{si2} \otimes \ldots \otimes \tilde{a}_{sin})^{\frac{1}{n}} \tag{3.26}$$

Then, the priority vector $\tilde{\Omega}_{si}$ of the cluster elements is constructed as follows:

$$\tilde{\Omega}_{si} = [\ \tilde{\omega}_{s1} \quad \tilde{\omega}_{s2} \quad \ldots \quad \tilde{\omega}_{sn}\ ] \tag{3.27}$$

where each $\tilde{\omega}_{si} = \left[(\omega^U_{s1}, \omega^U_{s2}, \omega^U_{s3}, \omega^U_{s4}, v^U_{si}); (\omega^L_{s1}, \omega^L_{s2}, \omega^L_{s3}, \omega^L_{s4}, v^L_{si})\right]$ is calculated using formula 3.36. The $\oplus$ indicates the addition operator of two fuzzy numbers as defined in [169].

$$\tilde{\omega}_{si} = r_{\tilde{A}_{si}} / (r_{\tilde{A}_{s1}} \oplus r_{\tilde{A}_{s2}} \oplus \ldots \oplus r_{\tilde{A}_{si}} \oplus \ldots \oplus r_{\tilde{A}_{sn}}) \tag{3.28}$$

Step 4. *Construction of the Supermatrices:* In this step, the fuzzy supermatrix $\tilde{W}_s$ of the TF-AANP model is constructed for each service representing the inner and the outer dependencies of the TF-AANP network. It is a partitioned matrix, with each matrix segment representing the relationship between two clusters of the network. To construct the supermatrix, the local priority vectors $\tilde{\Omega}_s$ are grouped and placed in the appropriate positions in the supermatrix based on the flow of influence from one cluster to another, or from a cluster to itself, as in the loop. For example, if we assume that we have a TF-AANP network of q clusters, C_k, with $k = [1,2,\ldots,q]$ and that each cluster has n_q elements, denoted as $e_{k1}, e_{k2}, \ldots, e_{kn_k}$, then the supermatrix is expressed as:

$$\tilde{W}_s = \begin{array}{c} \\ \\ C_1 \\ \vdots \\ C_k \\ \vdots \\ C_q \end{array} \begin{array}{c} \begin{array}{cccccc} & C_1 & \ldots & C_k & \ldots & C_q \\ & e_{11}\ldots e_{1n_1} & \ldots & e_{k1}\ldots e_{kn_k} & \ldots & e_{q1}\ldots e_{qn_q} \end{array} \\ \begin{array}{c} e_{11} \\ \vdots \\ e_{1n_1} \\ \\ e_{k1} \\ \vdots \\ e_{kn_k} \\ \\ e_{q1} \\ \vdots \\ e_{qn_q} \end{array} \begin{bmatrix} \tilde{W}_{s11} & \ldots & \tilde{W}_{s1j} & \ldots & \tilde{W}_{s1q} \\ \vdots & \vdots & \vdots & \vdots & \vdots \\ \tilde{W}_{sk1} & \ldots & \tilde{W}_{skj} & \ldots & \tilde{W}_{skq} \\ \vdots & \vdots & \vdots & \vdots & \vdots \\ \tilde{W}_{sq1} & \ldots & \tilde{W}_{sqj} & \ldots & \tilde{W}_{sqq} \end{bmatrix} \end{array} \tag{3.29}$$

Step 5. *Construction of the Weighted Supermatrices:* During this step, the supermatrix of each service is transformed to a stochastic one,the Weighted Supermatrix $\tilde{W}'_s$ using formula

3.38.

$$\tilde{W}'_{s,k,j} = \tilde{W}_{s,k,j}/q \tag{3.30}$$

Step 6. *Calculation of the Limited Supermatrices:* In this step, initially the deffuzified Weighted Supermatrix W_s of each service is estimated by applying the Weighted Average method. According to this method formula 3.31 is used, where the parameters v_s and d_s represent the height and the centroid of each $\tilde{W}'_{s,k,j}$ trapezoid respectively. Subsequently, each W_s is raised to limiting powers until all the entries converge. By this way the overall priorities are calculated, and thus the cumulative influence of each element on every other interacting element is obtained [168]. At this point, all the columns of each produced Limit Supermatrix L_s, are the same and their values show the importance of each element e of the TF-AANP network for the corresponding service s.

$$W_{s,k,j} = \frac{v_s^U \cdot d_s^U + v_s^L \cdot d_s^L}{d_s^U + d_s^L} \tag{3.31}$$

Step 7. *Estimation of the Criteria Weights:* In this step, the weight w_e for each element e of the TF-AANP network is calculated using formula 3.32 where the importance $\tilde{\omega}_{\tilde{P}_S}$ of each service s is considered.

$$w_e = \sum_{s=1}^{S} \tilde{\omega}_{\tilde{P},s} * L_{s,e} \tag{3.32}$$

3.1.3.2 The Pentagonal Fuzzy Analytic Network Process (PF-ANP)

The Pentagonal Fuzzy Analytic Network Process (PF-ANP) method is the IVPFN version of the typical ANP [166] method, used for the calculation of the criteria weights. PF-ANP allows complex relationships within and among clusters of selection criteria using a network model of dependencies. A decision problem that is analyzed with the PF-ANP can be represented as a network of nodes. Each node represents a component (or cluster) of the system while the arcs denote the interactions between them. The interactions and the feedbacks within the clusters are called inner dependencies, while the interactions and the feedbacks between clusters are called outer dependencies. Indicatively, we could consider one cluster with network characteristics criteria such as throughput, delay, jitter and packet loss, as well as one cluster with operator policy criteria such as service reliability, security and price. In this situation, the PF-ANP will consider two clusters. The PF-ANP is composed of five major steps of selection criteria:

Step 1. *Model Construction and Problem Structuring:* During this step the problem is analyzed and decomposed into a rational system, consisting of a network of nodes.

Step 2. *Pairwise comparison matrices and priority vectors:* Initially the fuzzy pairwise comparison matrix $\tilde{A}$ is derived for each cluster using the linguistic terms presented in Table 3.2,

which are calculated using the EUM method and correspond to the nine-point importance scale introduced in [166]. The standard form of the $\tilde{A}$ matrix is expressed as follows:

$$\tilde{A} = \begin{bmatrix} 1 & \dots & \tilde{a}_{1j} & \dots & \tilde{a}_{1n} \\ \vdots & & \vdots & & \vdots \\ 1/\tilde{a}_{1i} & \dots & 1 & \dots & \tilde{a}_{in} \\ \vdots & & \vdots & & \vdots \\ 1/\tilde{a}_{1n} & \dots & 1/\tilde{a}_{jn} & \dots & 1 \end{bmatrix} \tag{3.33}$$

where n denotes the number of the cluster elements. Subsequently, the geometric mean

Table 3.2 The Linguistic Terms that are used for the Criteria Pairwise Comparisons.

Linguistic term	**Interval-valued pentagonal fuzzy number**
Equally Important (EI)	[(0.043, 0.062, 0.1, 0.137, 0.156, 0.8, 0.6, 0.6), (0.025, 0.05, 0.1, 0.15, 0.175, 1.0, 0.8, 0.8)]
More than Equally Important (MEI)	[(0.143, 0.162, 0.2, 0.237, 0.256, 0.8, 0.6, 0.6), (0.125, 0.15, 0.2, 0.25, 0.275, 1.0, 0.8, 0.8)]
Moderately More Important (MMI)	[(0.243, 0.262, 0.3, 0.337, 0.356, 0.8, 0.6, 0.6), (0.225, 0.25, 0.3, 0.35, 0.375, 1.0, 0.8, 0.8)]
More than Moderately More Important (MMMI)	[(0.343, 0.362, 0.4, 0.437, 0.456, 0.8, 0.6, 0.6), (0.325, 0.35, 0.4, 0.45, 0.475, 1.0, 0.8, 0.8)]
Strongly More Important (SMI)	[(0.443, 0.462, 0.5, 0.537, 0.556, 0.8, 0.6, 0.6), (0.425, 0.45, 0.5, 0.55, 0.575, 1.0, 0.8, 0.8)]
More than Strongly More Important (MSMI)	[(0.543, 0.562, 0.6, 0.637, 0.656, 0.8, 0.6, 0.6), (0.525, 0.55, 0.6, 0.65, 0.675, 1.0, 0.8, 0.8)]
Very Strongly More Important (VSMI)	[(0.643, 0.662, 0.7, 0.737, 0.756, 0.8, 0.6, 0.6), (0.625, 0.65, 0.7, 0.75, 0.775, 1.0, 0.8, 0.8)]
More than Very Strongly More Important (MVSMI)	[(0.743, 0.762, 0.8, 0.837, 0.856, 0.8, 0.6, 0.6), (0.725, 0.75, 0.8, 0.85, 0.875, 1.0, 0.8, 0.8)]
Extremely More Important (EMI)	[(0.843, 0.862, 0.9, 0.937, 0.956, 0.8, 0.6, 0.6), (0.825, 0.85, 0.9, 0.95, 0.975, 1.0, 0.8, 0.8)]

$r_{\tilde{A}_i}$ of each row i in $\tilde{A}$ is calculated according to formula 3.34, where $\otimes$ denotes the multiplication operator of two fuzzy numbers as defined in [169].

$$r_{\tilde{A}_i} = (\tilde{a}_{i1} \otimes \tilde{a}_{i2} \otimes \dots \otimes \tilde{a}_{in})^{\frac{1}{n}} \tag{3.34}$$

Then, the priority vector $\tilde{\Omega}_i$ of each cluster element is constructed as follows:

$$\tilde{\Omega}_i = [\ \tilde{\omega}_1 \quad \tilde{\omega}_2 \quad \dots \quad \tilde{\omega}_n\ ] \tag{3.35}$$

where each $\tilde{\omega}_i = [(\omega_1^U, \omega_2^U, \omega_3^U, \omega_4^U, \omega_5^U, v_i^U, v_{i1}^U, v_{i2}^U); (\omega_1^L, \omega_2^L, \omega_3^L, \omega_4^L, \omega_5^L, v_i^L, v_{i1}^L, v_{i2}^L)]$ is calculated using formula 3.36. The $\oplus$ indicates the addition operator of two fuzzy numbers as defined in [169].

$$\tilde{\omega}_i = r_{\tilde{A}_i} / (r_{\tilde{A}_1} \oplus r_{\tilde{A}_2} \oplus \dots \oplus r_{\tilde{A}_i} \oplus \dots \oplus r_{\tilde{A}_n}) \tag{3.36}$$

Step 3. *Construction of the Supermatrix:* In this step, the fuzzy supermatrix $\tilde{W}$ of the PF-ANP model is constructed representing the inner and outer dependencies of the PF-ANP network. This is a partitioned matrix, with each matrix segment representing the

relationship between two clusters of the network. To construst the supermatrix, the local priority vectors $\tilde{\Omega}$ are grouped and placed in the appropriate positions in the supermatrix based on the flow of influence from one cluster to another. For example if we assume a network of q clusters, where each cluster C_k, $k = [1,2,\ldots,q]$ has n_k elements, denoted as $e_{k1}, e_{k2}, \ldots, e_{kn_k}$, then the supermatrix is expressed as:

$$\tilde{W} = \begin{array}{c} \\ \\ C_1 \\ \\ \vdots \\ \\ C_k \\ \\ \vdots \\ \\ C_q \\ \\ \end{array} \begin{array}{c} \\ \\ e_{11} \\ \vdots \\ e_{1n_1} \\ \\ e_{k1} \\ \vdots \\ e_{kn_k} \\ \\ e_{q1} \\ \vdots \\ e_{qn_q} \end{array} \begin{array}{c} \begin{array}{ccccccc} C_1 & & \ldots & C_k & & \ldots & C_q \\ e_{11}\ldots e_{1n_1} & & \ldots & e_{k1}\ldots e_{kn_k} & & \ldots & e_{q1}\ldots e_{qn_q} \end{array} \\ \begin{bmatrix} \tilde{W}_{11} & \ldots & \tilde{W}_{1j} & \ldots & \tilde{W}_{1q} \\ \vdots & \vdots & \vdots & \vdots & \vdots \\ \tilde{W}_{k1} & \ldots & \tilde{W}_{kj} & \ldots & \tilde{W}_{kq} \\ \vdots & \vdots & \vdots & \vdots & \vdots \\ \tilde{W}_{q1} & \ldots & \tilde{W}_{qj} & \ldots & \tilde{W}_{qq} \end{bmatrix} \end{array} \tag{3.37}$$

Step 4. *Construction of the Weighted Supermatrix:* During this step, the supermatrix is transformed to a stochastic one,the Weighted Supermatrix $\tilde{W}'$ using formula 3.38.

$$\tilde{W}'_{k,j} = \tilde{W}_{k,j}/q \tag{3.38}$$

Step 5. *Calculation of the Limited Supermatrix:* In this step, initially the deffuzified Weighted Supermatrix W is estimated by applying the Weighted Average method using formula 3.39. The parameters v and d represent the height and the centroid of each $\tilde{W}'_{k,j}$ pentagon respectively. Subsequently, W is raised to limiting powers until all the entries converge. In this way the overall priorities are calculated, and thus the cumulative influence of each element on every other interacting element is obtained [168]. At this point, all the columns of the produced Limited Supermatrix, are the same and their values show the global priority of each element of the network.

$$W_{k,j} = \frac{v^U \cdot d^U + v^L \cdot d^L}{d^U + d^L} \tag{3.39}$$

3.1.4 Network Selection Methods

3.1.4.1 The Trapezoidal Interval-Valued Fuzzy TOPSIS (TFT)

TOPSIS, introduced by Hwang and Yoon [170], is based on the concept that the best alternative should have the shortest distance from the positive ideal solution and the longer distance from the negative ideal solution. In the present work, network selection is performed using a proposed fuzzy version of TOPSIS, namely the Trapezoidal interval-valued Fuzzy TOPSIS (TFT). This method assumes that the linguistic values of the criteria attributes are represented by interval-valued trapezoidal fuzzy numbers.

Suppose that $A = \{A_1, A_2, \ldots, A_n\}$ is the set of possible alternatives, $C = \{C_1, C_2, \ldots, C_n\}$ is the set of criteria and $w_1, w2, \ldots, w_m$ are the weights of each criterion. The steps of the method are as follows:

Step 1. *Construction of the decision matrix:* Each element x_{ij} of the $n \times m$ decision matrix D is an interval-valued trapezoidal fuzzy number which expresses the performance of alternative i for criterion j. Thus

$$D = \begin{array}{c|ccc} & C_1 & \ldots & C_m \\ \hline A_1 & x_{11} & \ldots & x_{1m} \\ \vdots & \vdots & \ddots & \vdots \\ A_n & x_{n1} & \ldots & x_{nm} \end{array} \tag{3.40}$$

where: $x_{ij} = \left[(x^L_{ij1}, x^L_{ij2}, x^L_{ij3}, x^L_{ij4}, v^L_{ij}), (x^U_{ij1}, x^U_{ij2}, x^U_{ij3}, x^U_{ij4}, v^U_{ij})\right]$

In case there are Q decision makers, the decision matrix and the criteria weights include the average of the performance values and of the weights of the decision makers, respectively. Hence, assuming that for the k-th decision maker x_{ijk} is the performance of alternative i for criterion j, and w_{jk} is the importance weight for criterion j, the average of the performance values and weights are given by

$$x_{ij} = \frac{1}{Q}\sum_{k=1}^{Q} x_{ijk} = \left[\left(\frac{1}{Q}\sum_{k=1}^{Q} x^L_{ijk1}, \frac{1}{Q}\sum_{k=1}^{Q} x^L_{ijk2}, \frac{1}{Q}\sum_{k=1}^{Q} x^L_{ijk3}, \frac{1}{Q}\sum_{k=1}^{Q} x^L_{ijk4}, v^L_{ijk}\right), \left(\frac{1}{Q}\sum_{k=1}^{Q} x^U_{ijk1}, \frac{1}{Q}\sum_{k=1}^{Q} x^U_{ijk2}, \frac{1}{Q}\sum_{k=1}^{Q} x^U_{ijk3}, \frac{1}{Q}\sum_{k=1}^{Q} x^U_{ijk4}, v^U_{ijk}\right)\right] \tag{3.41}$$

and

$$w_j = \frac{1}{Q}\sum_{k=1}^{Q} w_{jk}. \tag{3.42}$$

Step 2. *Normalization of the decision matrix:* Consider that Ω_b is the set of benefits attributes and Ω_c is the set of costs attributes. Then the elements of the normalized decision matrix are computed as:

a)

$$r_{ij} = \left[\left(\frac{x_{ij1}^L}{b_j}, \frac{x_{ij2}^L}{b_j}, \frac{x_{ij3}^L}{b_j}, \frac{x_{ij4}^L}{b_j}, v_{ij}^L \right), \left(\frac{x_{ij1}^U}{b_j}, \frac{x_{ij2}^U}{b_j}, \frac{x_{ij3}^U}{b_j}, \frac{x_{ij4}^U}{b_j}, v_{ij}^U \right) \right] \tag{3.43}$$

where $b_j = \max_i x_{ij4}^U$ for each $j \in \Omega_b$ and

b)

$$r_{ij} = \left[\left(\frac{c_j}{x_{ij4}^L}, \frac{c_j}{x_{ij3}^L}, \frac{c_j}{x_{ij2}^L}, \frac{c_j}{x_{ij1}^L}, v_{ij}^L \right), \left(\frac{c_j}{x_{ij4}^U}, \frac{c_j}{x_{ij3}^U}, \frac{c_j}{x_{ij2}^U}, \frac{c_j}{x_{ij1}^U}, v_{ij}^U \right) \right] \tag{3.44}$$

where $c_j = \min_i x_{ij4}^L$ for each $j \in \Omega_c$.

Step 3. *Construction of the weighted normalized decision matrix:* The weighted normalized decision matrix is constructed by multiplying each element of the normalized decision matrix r_{ij} with the respective weight w_j according to the formula

$$u_{ij} = \left[\left(r_{ij1}^L \cdot w_j, r_{ij2}^L \cdot w_j, r_{ij3}^L \cdot w_j, r_{ij4}^L \cdot w_j, v_{ij}^L \right), \left(r_{ij1}^U \cdot w_j, r_{ij2}^U \cdot w_j, r_{ij3}^U \cdot w_j, r_{ij4}^U \cdot w_j, v_{ij}^U \right) \right] \tag{3.45}$$

Step 4. *Determination of the positive and negative ideal solution:* The positive ideal solution X^+ is defined as follows:

$$\begin{aligned} X^+ = & \left[\left(x_{ij1}^{+L}, x_{ij2}^{+L}, x_{ij3}^{+L}, x_{ij4}^{+L}, v_{ij}^{+L} \right), \left(x_{ij1}^{+U}, x_{ij2}^{+U}, x_{ij3}^{+U}, x_{ij4}^{+U}, v_{ij}^{+U} \right) \right] = \\ & \left[\left(\bigwedge_i u_{ij1}^L, \bigwedge_i u_{ij2}^L, \bigwedge_i u_{ij3}^L, \bigwedge_i u_{ij4}^L, v_{ij}^L \right), \left(\bigwedge_i u_{ij1}^U, \bigwedge_i u_{ij2}^U, \bigwedge_i u_{ij3}^U, \bigwedge_i u_{ij4}^U, v_{ij}^U \right) \right] \end{aligned} \tag{3.46}$$

where $\bigwedge_i \equiv \max_i$ in case $j \in \Omega_b$ and $\bigwedge_i \equiv \min_i$ in case $j \in \Omega_c$.

The negative ideal solution X^- is defined as follows:

$$\begin{aligned} X^- &= \left[\left(x_{ij1}^{-L}, x_{ij2}^{-L}, x_{ij3}^{-L}, x_{ij4}^{-L}, v_{ij}^{-L} \right), \left(x_{ij1}^{-U}, x_{ij2}^{-U}, x_{ij3}^{-U}, x_{ij4}^{-U}, v_{ij}^{-U} \right) \right] \\ &= \left[\left(\bigvee_i u_{ij1}^L, \bigvee_i u_{ij2}^L, \bigvee_i u_{ij3}^L, \bigvee_i u_{ij4}^L, v_{ij}^L \right), \left(\bigvee_i u_{ij1}^U, \bigvee_i u_{ij2}^U, \bigvee_i u_{ij3}^U, \bigvee_i u_{ij4}^U, v_{ij}^U \right) \right] \end{aligned} \tag{3.47}$$

where $\bigvee_i \equiv \min_i$ in case $j \in \Omega_b$ and $\bigvee_i \equiv \max_i$ in case $j \in \Omega_c$.

Step 5. Measurement of the distance of each alternative from the ideal solutions: The distances d_{i1}^+ and d_{i2}^+ of each alternative from the positive ideal solution are evaluated as follows:

$$d_{i1}^+ = \sum_{j=1}^m \left\{ \frac{1}{4} \left[\left(u_{ij1}^L - x_{ij1}^{+L} \right)^2 + \left(u_{ij2}^L - x_{ij2}^{+L} \right)^2 + \left(u_{ij3}^L - x_{ij3}^{+L} \right)^2 + \left(u_{ij4}^L - x_{ij4}^{+L} \right)^2 \right] \right\}^{\frac{1}{2}} \tag{3.48}$$

$$d_{i2}^+ = \sum_{j=1}^m \left\{ \frac{1}{4} \left[\left(u_{ij1}^U - x_{ij1}^{+U} \right)^2 + \left(u_{ij2}^U - x_{ij2}^{+U} \right)^2 + \left(u_{ij3}^U - x_{ij3}^{+U} \right)^2 + \left(u_{ij4}^U - x_{ij4}^{+U} \right)^2 \right] \right\}^{\frac{1}{2}} \tag{3.49}$$

Likewise, the distances d_{i1}^{-} and d_{i2}^{-} of each alternative from the negative ideal solution are estimated as follows:

$$d_{i1}^{-} = \sum_{j=1}^{m} \left\{ \frac{1}{4} \left[\left(u_{ij1}^{L} - x_{ij1}^{-L} \right)^2 + \left(u_{ij2}^{L} - x_{ij2}^{-L} \right)^2 + \left(u_{ij3}^{L} - x_{ij3}^{-L} \right)^2 + \left(u_{ij4}^{L} - x_{ij4}^{-L} \right)^2 \right] \right\}^{\frac{1}{2}} \tag{3.50}$$

$$d_{i2}^{-} = \sum_{j=1}^{m} \left\{ \frac{1}{4} \left[\left(u_{ij1}^{U} - x_{ij1}^{-U} \right)^2 + \left(u_{ij2}^{U} - x_{ij2}^{-U} \right)^2 + \left(u_{ij3}^{U} - x_{ij3}^{-U} \right)^2 + \left(u_{ij4}^{U} - x_{ij4}^{-U} \right)^2 \right] \right\}^{\frac{1}{2}} \tag{3.51}$$

Consequently, similarly to [158] the distance of the alternatives from the positive and the negative ideal solutions are expressed by intervals such as $[d_{i1}^{+}, d_{i2}^{+}]$ and $[d_{i1}^{-}, d_{i2}^{-}]$, instead of single values. In this way less information is lost.

Step 6. *Calculation of the relative closeness:* The relative closeness of the distances from the ideal solutions are computed as:

$$RC_{i1} = \frac{d_{i1}^{-}}{d_{i1}^{+} + d_{i1}^{-}} \tag{3.52}$$

and

$$RC_{i2} = \frac{d_{i2}^{-}}{d_{i2}^{+} + d_{i2}^{-}} \tag{3.53}$$

The compound relative closeness RC_i is obtained from the average of the above values:

$$RC_i = \frac{RC_{i1} + RC_{i2}}{2} \tag{3.54}$$

Step 7. Alternatives ranking: The alternatives are ranked according to their RC_i values. The best alternative is the one with the higher RC_i value.

3.1.4.2 The Trapezoidal Fuzzy TOPSIS with Adaptive Criteria Weights (TFT-ACW)

The candidate networks are ranked using the TFT-ACW algorithm, which improves the TFT [171] by using the adaptive weights that estimated from the TF-AANP method. Thus, the importance of the opinion of each service (decision maker) is considered, since the opinions of some decision makers could have a higher importance than the ones of the other decision makers. In general, similar to TFT, the TFT-ACW method is based on the concept that the best alternative should have the shortest distance from the positive ideal solution and the longer distance from the negative ideal solution. Also, it assumes that the linguistic values of the criteria attributes are represented by interval-valued trapezoidal fuzzy numbers. More specifically, suppose that $AL = \{AL_1, AL_2, \ldots, AL_z\}$ is the set of possible alternatives, $CR = \{CR_1, CR_2, \ldots, CR_n\}$ is the set of criteria and $w_1, w_2, \ldots, w_n$ are the importance weights of the respective criteria obtained from the application of the TF-AANP algorithm. The steps of the method are as follows:

Step 1. *Construction of the decision matrix:* Each element $\tilde{g}_{ie}$ of the $z \times n$ decision matrix $\tilde{D}$ is an IVTFN number expressing the performance of alternative i for criterion e. Thus,

$$\tilde{D} = \begin{array}{c|ccc} & CR_1 & \dots & CR_n \\ \hline AL_1 & \tilde{g}_{11} & \dots & \tilde{g}_{1n} \\ \vdots & \vdots & \ddots & \vdots \\ AL_z & \tilde{g}_{z1} & \dots & \tilde{g}_{zn} \end{array} \tag{3.55}$$

where $\tilde{g}_{ie} = \left[(g^L_{ie1}, g^L_{ie2}, g^L_{ie3}, g^L_{ie4}, v^L_{ie}), (g^U_{ie1}, g^U_{ie2}, g^U_{ie3}, g^U_{ie4}, v^U_{ie})\right]$.

In the case that there are S services (decision makers) the decision matrix include the average of the performance values. Hence, assuming that for the s^{th} decision maker $\tilde{g}_{iex}$ is the performance of alternative i for criterion (element) e, the average of the performance values is given by formula 3.56.

$$\tilde{g}_{ie} = \sum_{s=1}^{S} (\tilde{g}_{ies} \cdot \tilde{\omega}_{\tilde{p}s}) \tag{3.56}$$

Step 2. *Normalization of the decision matrix:* Let Γ_b be the set of benefit attributes and Γ_c the set of cost attributes. Then, the elements of the normalized decision matrix are calculated using either formula 3.57 or 3.58, where $b_e = \max_i g^U_{ie4}$ for each $e \in \Gamma_b$ and $c_e = \min_i g^L_{ie4}$ for each $e \in \Gamma_c$.

$$\tilde{g}'_{ie} = \left[\left(\frac{g^L_{ie1}}{b_e}, \frac{g^L_{ie2}}{b_e}, \frac{g^L_{ie3}}{b_e}, \frac{g^L_{ie4}}{b_e}, v^L_{ie}\right), \left(\frac{g^U_{ie1}}{b_e}, \frac{g^U_{ie2}}{b_e}, \frac{g^U_{ie3}}{b_e}, \frac{g^U_{ie4}}{b_e}, v^U_{ie}\right)\right] \tag{3.57}$$

$$\tilde{g}'_{ie} = \left[\left(\frac{c_e}{g^L_{ie4}}, \frac{c_e}{g^L_{ie3}}, \frac{c_e}{g^L_{ie2}}, \frac{c_e}{g^L_{ie1}}, v^L_{ie}\right), \left(\frac{c_e}{g^U_{ie4}}, \frac{c_e}{g^U_{ie3}}, \frac{c_e}{g^U_{ie2}}, \frac{c_e}{g^U_{ie1}}, v^U_{ie}\right)\right] \tag{3.58}$$

Step 3. *Construction of the weighted normalized decision matrix:* The weighted normalized decision matrix is constructed by multiplying each element of the normalized decision matrix $\tilde{g}'_{ie}$ with the respective weight w_e according to the formula 3.59.

$$\begin{aligned} \tilde{u}_{ie} = \Big[&\left(g'^L_{ie1} \cdot w_e, g'^L_{ie2} \cdot w_e, g'^L_{ie3} \cdot w_e, g'^L_{ie4} \cdot w_e, v'^L_{ie}\right), \\ &\left(g'^U_{ie1} \cdot w_e, g'^U_{ie2} \cdot w_e, g'^U_{ie3} \cdot w_e, g'^U_{ie4} \cdot w_e, v^U_{ie}\right)\Big] \end{aligned} \tag{3.59}$$

Step 4. *Determination of the positive and negative ideal solution:* The positive ideal solution is defined in formula 3.60, where $\bigwedge_i \equiv \max_i$ in case $e \in \Gamma_b$ and $\bigwedge_i \equiv \min_i$ in case $e \in \Gamma_c$. Correspondingly, the negative ideal solution is defined in formula 3.61, where $\bigvee_i \equiv \min_i$

in case $e \in \Gamma_b$ and $\bigvee_i \equiv \max_i$ in case $e \in \Gamma_c$.

$$\begin{aligned}\tilde{G}^{+} &= \left[\left(g_{ie1}^{+L}, g_{ie2}^{+L}, g_{ie3}^{+L}, g_{ie4}^{+L}, v_{ie}^{+L}\right), \left(g_{ie1}^{+U}, g_{ie2}^{+U}, g_{ie3}^{+U}, g_{ie4}^{+U}, v_{ie}^{+U}\right)\right] \\ &= \left[\left(\bigwedge_i u_{ie1}^{L}, \bigwedge_i u_{ie2}^{L}, \bigwedge_i u_{ie3}^{L}, \bigwedge_i u_{ie4}^{L}, v_{ie}^{L}\right),\right. \\ &\quad \left.\left(\bigwedge_i u_{ie1}^{U}, \bigwedge_i u_{ie2}^{U}, \bigwedge_i u_{ie3}^{U}, \bigwedge_i u_{ie4}^{U}, v_{ie}^{U}\right)\right]\end{aligned} \tag{3.60}$$

$$\begin{aligned}\tilde{G}^{-} &= \left[\left(g_{ie1}^{-L}, g_{ie2}^{-L}, g_{ie3}^{-L}, g_{ie4}^{-L}, v_{ie}^{-L}\right), \left(g_{ie1}^{-U}, g_{ie2}^{-U}, g_{ie3}^{-U}, g_{ie4}^{-U}, v_{ie}^{-U}\right)\right] \\ &= \left[\left(\bigvee_i u_{ie1}^{L}, \bigvee_i u_{ie2}^{L}, \bigvee_i u_{ie3}^{L}, \bigvee_i u_{ie4}^{L}, v_{ie}^{L}\right),\right. \\ &\quad \left.\left(\bigvee_i u_{ie1}^{U}, \bigvee_i u_{ie2}^{U}, \bigvee_i u_{ie3}^{U}, \bigvee_i u_{ie4}^{U}, v_{ie}^{U}\right)\right]\end{aligned} \tag{3.61}$$

Step 5. *Measurement of the distance of each alternative from the ideal solutions:* The distances of each alternative from the positive ideal solution are evaluated using formulas 3.62 and 3.63.

$$p_{i1}^{+} = \sum_{e=1}^{n} \left\{ \frac{1}{4} \left[\left(u_{ie1}^{L} - g_{ie1}^{+L}\right)^2 + \left(u_{ie2}^{L} - g_{ie2}^{+L}\right)^2 + \left(u_{ie3}^{L} - g_{ie3}^{+L}\right)^2 + \left(u_{ie4}^{L} - g_{ie4}^{+L}\right)^2 \right] \right\}^{\frac{1}{2}} \tag{3.62}$$

$$p_{i2}^{+} = \sum_{e=1}^{n} \left\{ \frac{1}{4} \left[\left(u_{ie1}^{U} - g_{ie1}^{+U}\right)^2 + \left(u_{ie2}^{U} - g_{ie2}^{+U}\right)^2 + \left(u_{ie3}^{U} - g_{ie3}^{+U}\right)^2 + \left(u_{ie4}^{U} - g_{ie4}^{+U}\right)^2 \right] \right\}^{\frac{1}{2}} \tag{3.63}$$

Likewise, the distances of each alternative from the negative ideal solution are estimated using formulas 3.64 and 3.65.

$$p_{i1}^{-} = \sum_{e=1}^{n} \left\{ \frac{1}{4} \left[\left(u_{ie1}^{L} - g_{ie1}^{-L}\right)^2 + \left(u_{ie2}^{L} - g_{ie2}^{-L}\right)^2 + \left(u_{ie3}^{L} - g_{ie3}^{-L}\right)^2 + \left(u_{ie4}^{L} - g_{ie4}^{-L}\right)^2 \right] \right\}^{\frac{1}{2}} \tag{3.64}$$

$$p_{i2}^{-} = \sum_{e=1}^{n} \left\{ \frac{1}{4} \left[\left(u_{ie1}^{U} - g_{ie1}^{-U}\right)^2 + \left(u_{ie2}^{U} - g_{ie2}^{-U}\right)^2 + \left(u_{ie3}^{U} - g_{ie3}^{-U}\right)^2 + \left(u_{ie4}^{U} - g_{ie4}^{-U}\right)^2 \right] \right\}^{\frac{1}{2}} \tag{3.65}$$

Consequently, the alternative distance from the positive and from the negative ideal solutions are expressed by intervals such as $[p_{i1}^{+}, p_{i2}^{+}]$ and $[p_{i1}^{-}, p_{i2}^{-}]$, instead of single values, thus less information is lost.

Step 6. *Calculation of the relative closeness:* The relative closeness of the distances from the ideal solutions are calculated using formula 3.66 and 3.67.

$$RC_{i1} = \frac{p_{i1}^{-}}{p_{i1}^{+} + p_{i1}^{-}} \tag{3.66}$$

$$RC_{i2} = \frac{p_{i2}^{-}}{p_{i2}^{+} + p_{i2}^{-}} \tag{3.67}$$

Subsequently, the compound relative closeness is obtained using formula 3.68

$$RC_i = \frac{RC_{i1} + RC_{i2}}{2} \tag{3.68}$$

Step 7. *Alternative networks ranking:* The alternative networks are ranked according to their RC_i values. The best alternative is that with the higher RC_i value.

3.1.4.3 The Pentagonal Fuzzy TOPSIS (PFT)

The Pentagonal Fuzzy TOPSIS (PFT) algorithm is an improved version of the TOPSIS using interval-valued pentagonal fuzzy numbers. PFT assumes that the linguistic values of the criteria attributes are represented by IVPFN numbers.

Suppose that $A = \{A_1, A_2, ..., A_n\}$ is the set of possible alternatives, $C = \{C_1, C_2, \ldots, C_m\}$ is the set of criteria and $w_1, w2, \ldots, w_m$ are the weights of each criterion. The steps of the method are as follows:

Step 1. *Construction of the decision matrix:* Each element x_{ij} of the $n \times m$ decision matrix D is an interval-valued pentagonal fuzzy number which expresses the performance of alternative i for criterion j. Thus

$$D = \begin{array}{c|ccc} & C_1 & \ldots & C_m \\ \hline A_1 & x_{11} & \ldots & x_{1m} \\ \vdots & \vdots & \ddots & \vdots \\ A_n & x_{n1} & \ldots & x_{nm} \end{array} \tag{3.69}$$

where: $x_{ij} = [(x^L_{ij1}, x^L_{ij2}, x^L_{ij3}, x^L_{ij4}, x^L_{ij5}, v^L_{ij}, v^L_{ij1}, v^L_{ij2}), (x^U_{ij1}, x^U_{ij2}, x^U_{ij3}, x^U_{ij4}, x^U_{ij5}, v^U_{ij}, v^U_{ij1}, v^U_{ij2})]$. In case there are Q decision makers the decision matrix and the criteria weights include the average of the performance values and of the weights respectively, of the decision makers. Hence, assuming that for the k-th decision maker x_{ijk} is the performance of alternative i for criterion j, and w_{jk} is the importance weight for criterion j, the average of the performance values and weights are given by:

$$x_{ij} = \frac{1}{Q} \sum_{k=1}^{Q} x_{ijk} \tag{3.70}$$

and

$$w_j = \frac{1}{Q} \sum_{k=1}^{Q} w_{jk}. \tag{3.71}$$

Step 2. *Normalization of the decision matrix:* Consider that Ω_b is the set of benefit attributes and Ω_c is the set of cost attributes. Then, the elements of the normalized decision matrix are

computed as:

$$r_{ij} = [(\frac{x_{ij1}^L}{b_j}, \frac{x_{ij2}^L}{b_j}, \frac{x_{ij3}^L}{b_j}, \frac{x_{ij4}^L}{b_j}, \frac{x_{ij5}^L}{b_j}, v_{ij}^L, v_{ij1}^L, v_{ij2}^L), (\frac{x_{ij1}^U}{b_j}, \frac{x_{ij2}^U}{b_j}, \frac{x_{ij3}^U}{b_j}, \frac{x_{ij4}^U}{b_j}, \frac{x_{ij5}^U}{b_j}, v_{ij}^U, v_{ij1}^U, v_{ij2}^U)] \tag{3.72}$$

where $b_j = \max_i x_{ij4}^U$ for each $j \in \Omega_b$, or

$$r_{ij} = [(\frac{c_j}{x_{ij5}^L}, \frac{c_j}{x_{ij4}^L}, \frac{c_j}{x_{ij3}^L}, \frac{c_j}{x_{ij2}^L}, \frac{c_j}{x_{ij1}^L}, v_{ij}^L, v_{ij2}^L, v_{ij1}^L), (\frac{c_j}{x_{ij5}^U}, \frac{c_j}{x_{ij4}^U}, \frac{c_j}{x_{ij3}^U}, \frac{c_j}{x_{ij2}^U}, \frac{c_j}{x_{ij1}^U}, v_{ij}^U, v_{ij2}^U, v_{ij1}^U)] \tag{3.73}$$

where $c_j = \min_i x_{ij4}^L$ for each $j \in \Omega_c$.

Step 3. *Construction of the weighted normalized decision matrix:* The weighted normalized decision matrix is constructed by multiplying each element of the normalized decision matrix r_{ij} with the respective weight w_j according to:

$$u_{ij} = [(r_{ij1}^L \cdot w_j, r_{ij2}^L \cdot w_j, r_{ij3}^L \cdot w_j, r_{ij4}^L \cdot w_j, r_{ij5}^L \cdot w_j, v_{ij}^L, v_{ij1}^L, v_{ij2}^L), (r_{ij1}^U \cdot w_j, r_{ij2}^U \cdot w_j, r_{ij3}^U \cdot w_j, r_{ij4}^U \cdot w_j, r_{ij5}^U \cdot w_j, v_{ij}^U, v_{ij1}^U, v_{ij2}^U)] \tag{3.74}$$

Step 4. *Determination of the positive and negative ideal solutions:* The positive ideal solution is given by:

$$X^+ = [(x_{ij1}^{+L}, x_{ij2}^{+L}, x_{ij3}^{+L}, x_{ij4}^{+L}, x_{ij5}^{+L}, v_{ij}^{+L}, v_{ij1}^{+L}, v_{ij2}^{+L}), (x_{ij1}^{+U}, x_{ij2}^{+U}, x_{ij3}^{+U}, x_{ij4}^{+U}, x_{ij5}^{+U}, v_{ij}^{+U}, v_{ij1}^{+U}, v_{ij2}^{+U})] =$$
$$[(\bigwedge_i u_{ij1}^L, \bigwedge_i u_{ij2}^L, \bigwedge_i u_{ij3}^L, \bigwedge_i u_{ij4}^L, \bigwedge_i u_{ij5}^L, v_{ij}^L, v_{ij1}^L, v_{ij2}^L), (\bigwedge_i u_{ij1}^U, \bigwedge_i u_{ij2}^U, \bigwedge_i u_{ij3}^U, \bigwedge_i u_{ij4}^U, \bigwedge_i u_{ij5}^U, v_{ij}^U, v_{ij1}^U, v_{ij2}^U)] \tag{3.75}$$

where $\bigwedge_i \equiv \max_i$ in case $j \in \Omega_b$ and $\bigwedge_i \equiv \min_i$ in case $j \in \Omega_c$.

The negative ideal solutions is given by:

$$X^- = [(x_{ij1}^{-L}, x_{ij2}^{-L}, x_{ij3}^{-L}, x_{ij4}^{-L}, x_{ij5}^{-L}, v_{ij}^{-L}, v_{ij1}^{-L}, v_{ij2}^{-L}), (x_{ij1}^{-U}, x_{ij2}^{-U}, x_{ij3}^{-U}, x_{ij4}^{-U}, x_{ij5}^{-U}, v_{ij}^{-U}, v_{ij1}^{-U}, v_{ij2}^{-U})] =$$
$$[(\bigvee_i u_{ij1}^L, \bigvee_i u_{ij2}^L, \bigvee_i u_{ij3}^L, \bigvee_i u_{ij4}^L, \bigvee_i u_{ij5}^L, v_{ij}^L, v_{ij1}^L, v_{ij2}^L), (\bigvee_i u_{ij1}^U, \bigvee_i u_{ij2}^U, \bigvee_i u_{ij3}^U, \bigvee_i u_{ij4}^U, \bigvee_i u_{ij5}^U, v_{ij}^U, v_{ij1}^U, v_{ij2}^U)] \tag{3.76}$$

where $\bigvee_i \equiv \min_i$ in case $j \in \Omega_b$ and $\bigvee_i \equiv \max_i$ in case $j \in \Omega_c$.

Step 5. Measurement of the distance of each alternative from the ideal solutions: The distances of each alternative from the positive ideal solution are evaluated as follows:

$$d_{i1}^+ = \sum_{j=1}^m \{\frac{1}{5}[(u_{ij1}^L - x_{ij1}^{+L})^2 + (u_{ij2}^L - x_{ij2}^{+L})^2 + (u_{ij3}^L - x_{ij3}^{+L})^2 + (u_{ij4}^L - x_{ij4}^{+L})^2 + (u_{ij5}^L - x_{ij5}^{+L})^2]\}^{\frac{1}{2}} \tag{3.77}$$

$$d_{i2}^+ = \sum_{j=1}^m \{\frac{1}{5}[(u_{ij1}^U - x_{ij1}^{+U})^2 + (u_{ij2}^U - x_{ij2}^{+U})^2 + (u_{ij3}^U - x_{ij3}^{+U})^2 + (u_{ij4}^U - x_{ij4}^{+U})^2 + (u_{ij5}^U - x_{ij5}^{+U})^2]\}^{\frac{1}{2}} \tag{3.78}$$

Likewise the distances of each alternative from the negative ideal solution are estimated by:

$$d_{i1}^{-} = \sum_{j=1}^{m} \{15[(u_{ij1}^{L} - x_{ij1}^{-L})^2 + (u_{ij2}^{L} - x_{ij2}^{-L})^2 + (u_{ij3}^{L} - x_{ij3}^{-L})^2 + (u_{ij4}^{L} - x_{ij4}^{-L})^2 + (u_{ij5}^{L} - x_{ij5}^{-L})^2]\}^{\frac{1}{2}} \quad (3.79)$$

$$d_{i2}^{-} = \sum_{j=1}^{m} \{\frac{1}{5}[(u_{ij1}^{U} - x_{ij1}^{-U})^2 + (u_{ij2}^{U} - x_{ij2}^{-U})^2 + (u_{ij3}^{U} - x_{ij3}^{-U})^2 + (u_{ij4}^{U} - x_{ij4}^{-U})^2 + (u_{ij5}^{U} - x_{ij5}^{-U})^2]\}^{\frac{1}{2}} \quad (3.80)$$

Consequently, similarly to [158] the distance of the alternatives from the positive and negative ideal solutions are expressed by intervals such as $[d_{i1}^{+}, d_{i2}^{+}]$ and $[d_{i1}^{-}, d_{i2}^{-}]$, instead of single values. In this way less information is lost.

Step 6. *Calculation of the relative closeness:* The relative closeness RC_{i1} and RC_{i2} of the distances from the ideal solutions are computed as:

$$RC_{i1} = \frac{d_{i1}^{-}}{d_{i1}^{+} + d_{i1}^{-}} \quad (3.81)$$

and

$$RC_{i2} = \frac{d_{i2}^{-}}{d_{i2}^{+} + d_{i2}^{-}} \quad (3.82)$$

The compound relative closeness RC_i is obtained from the average of the above values

$$RC_i = \frac{RC_{i1} + RC_{i2}}{2} \quad (3.83)$$

Step 7. Alternatives ranking: The alternatives are ranked according to their RC_i values. The best alternative is that with the higher RC_i value.

3.1.5 Evaluation of the Proposed Methods

3.1.5.1 Network Selection using the ANP and the TFT Algorithms

3.1.5.1.1 Simulation Setup : In our experiments we consider a heterogeneous network environment consisting of a number of LTE, WiMAX and WiFi networks. Each network can provide at least one of the following five service types: VoIP, conversational video (CVideo), buffered streaming (BStreaming), real time gaming (RTGaming) and web browsing. In order to allow service continuity, QoS mapping among the QoS classes of the different access technologies is required. Table 3.3 shows this mapping relation among the different technologies.

Four SLAs are defined with SLA1 having the higher service priority and SLA 4 having the lower service priority. SLA1 supports all the service types and it provides the best values for the QoS and policy decision criteria. SLA2 supports a smaller number of service types, by it does not provide support for the VoIP and real time gaming services. Additionally, it provides

Table 3.3 QoS Class Mapping and SLAs.

LTE QCI (Type/ Priority)	WiMAX QoS class	IEEE 802.11e QoS class	Required Throughput	Required Packet loss	Required Delay	Required Jitter	Services
1 (GBR/ 2)	UGS/ ertPS (802.16e-802.16m)	AC_VO	200 Kbps	10^{-2}	100ms	50ms	VoIP, CVideo, BStreaming, RTGaming, Web
3 (GBR/ 3)	UGS	AC_VO	250 Kbps	10^{-3}	50ms	40ms	CVideo, BStreaming, RTGaming, Web
2 (GBR/ 4)	UGS	AC_VI	8 Mbps	10^{-3}	65ms	50ms	CVideo, BStreaming, Web
4 (GBR/ 5)	rtPS	AC_VI	8 Mbps	10^{-5}	65ms	60ms	CVideo, BStreaming, Web
6 (Non-GBR/ 6)	nrtPS	AC_BE	2.5 Mbps	10^{-5}	200ms	N/A	BStreaming, Web
7 (Non-GBR/ 7)	nrtPS	AC_BE	2 Mbps	10^{-5}	160ms	100ms	BStreaming, Web
8 (Non-GBR/ 8)	BE	AC_BE	1.5 Mbps	10^{-3}	300ms	N/A	Web
9 (Non-GBR/ 9)	BE	AC_BE	1.5 Mbps	10^{-5}	300ms	N/A	

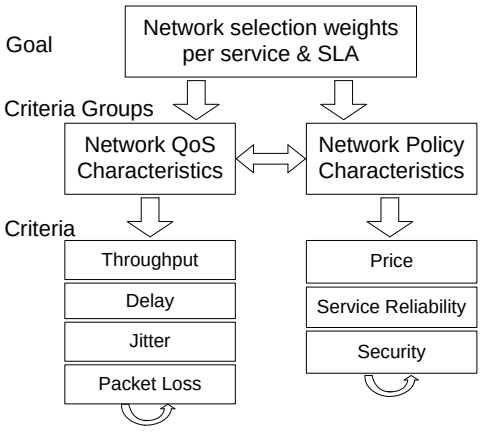

Figure 3.3 The ANP Network Model.

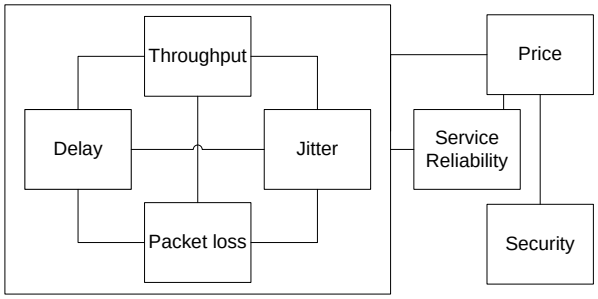

Figure 3.4 The Relations of the Criteria considered by the ANP Network Model.

slightly worse decision criteria values than those offered by SLA1. SLA3 supports only the buffered streaming and the web browsing services and satisfactory QoS characteristics and policies, whereas the low price SLA4 supports only the web browsing service while providing acceptable decision criteria values.

3.1.5.1.2 Performance Evaluation : The ANP method is applied in order to estimate the weights of network selection criteria per service type and SLA. Figure 3.3 depicts the ANP network model. The criteria are classified into two groups namely the QoS and the policy characteristics. The QoS characteristics group contains network performance related criteria including throughput, delay, jitter and packet loss while the policy characteristics group contains operator defined rules such as price, security and service reliability. Pairwise comparison decision matrices are created based on relations among the seven selection criteria depicted in Figure 3.4. Then, these pairwise comparison decision matrices are used to evaluate the priority vectors of criteria and form the supermatrix per service type and SLA. Subsequently, the weighted supermatrices and, finally, the limit supermatrices are obtained. Indicatively, for the SLA1 VoIP service, the initial, the weighted and the limit supermatrices are presented in Tables 3.4, 3.5 and 3.6 respectively.

Table 3.4 The ANP Supermatrix for the SLA1 VoIP Service.

	Throughput	**Delay**	**Jitter**	**Packet loss**	**Price**	**Reliability**	**Security**
Throughput	0.015625	0.015625	0.015625	0.015625	0.015625	0.015625	0.015625
Delay	0.328125	0.328125	0.328125	0.328125	0.328125	0.328125	0.328125
Jitter	0.328125	0.328125	0.328125	0.328125	0.328125	0.328125	0.328125
Packet loss	0.328125	0.328125	0.328125	0.328125	0.328125	0.328125	0.328125
Price	0.05	0.05	0.05	0.05	0.019607	0.05	0.0625
Reliability	0.95	0.95	0.95	0.95	0.759804	0.95	0
Security	0	0	0	0	0.220588	0	0.9375

Table 3.5 The ANP Weighted Supermatrix for the SLA1 VoIP Service.

	Throughput	**Delay**	**Jitter**	**Packet loss**	**Price**	**Reliability**	**Security**
Throughput	0.0078125	0.0078125	0.0078125	0.0078125	0.0078125	0.0078125	0.0078125
Delay	0.164062	0.164062	0.164062	0.164062	0.164062	0.164062	0.164062
Jitter	0.164062	0.164062	0.164062	0.164062	0.164062	0.164062	0.164062
Packet loss	0.164062	0.164062	0.164062	0.164062	0.164062	0.164062	0.164062
Price	0.025	0.025	0.025	0.025	0.00980392	0.025	0.03125
Reliability	0.475	0.475	0.475	0.475	0.379902	0.475	0
Security	0	0	0	0	0.110294	0	0.46875

The criteria weights per service and SLA obtained by the limit supermatrices are presented in Figures 3.5, 3.6, 3.7 and 3.8. As illustrated, the weights are proportional to the constraints of each service as well as to the agreements of each SLA. In particular, the weight of the price

Table 3.6 The ANP Limit Supermatrix for the SLA1 VoIP Service.

	Throughput	**Delay**	**Jitter**	**Packet loss**	**Price**	**Reliability**	**Security**
Throughput	0.0078125	0.0078125	0.0078125	0.0078125	0.0078125	0.0078125	0.0078125
Delay	0.164062	0.164062	0.164062	0.164062	0.164062	0.164062	0.164062
Jitter	0.164062	0.164062	0.164062	0.164062	0.164062	0.164062	0.164062
Packet loss	0.164062	0.164062	0.164062	0.164062	0.164062	0.164062	0.164062
Price	0.0246573	0.0246573	0.0246573	0.0246573	0.0246573	0.0246573	0.0246573
Reliability	0.470224	0.470224	0.470224	0.470224	0.470224	0.470224	0.470224
Security	0.0051191	0.0051191	0.0051191	0.0051191	0.0051191	0.0051191	0.0051191

criterion is low for SLA1, in which the service reliability and the network QoS characteristics are considered as the most important factors. In SLA2 the price criterion is more important than in SLA1, thus the respective weight is greater than that of SLA1. Consequently, the weights of the service reliability and QoS characteristics criteria in SLA2 are lower compared to the relative weights of SLA1. In SLA3 the weights of the price and the service reliability criteria are balanced as they are almost of equivalent importance. Finally, in SLA4 the price is the most important criterion resulting in a high estimated weight value.

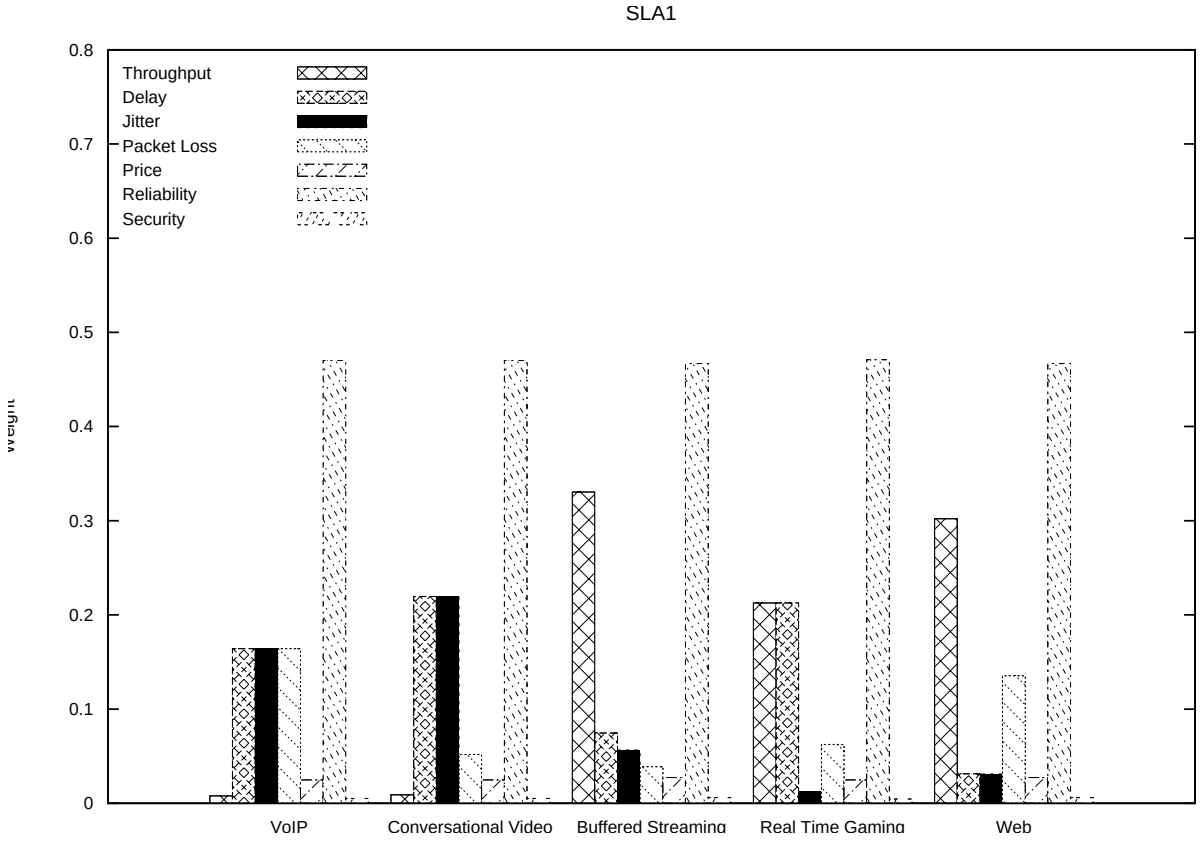

Figure 3.5 Criteria Weights for SLA1.

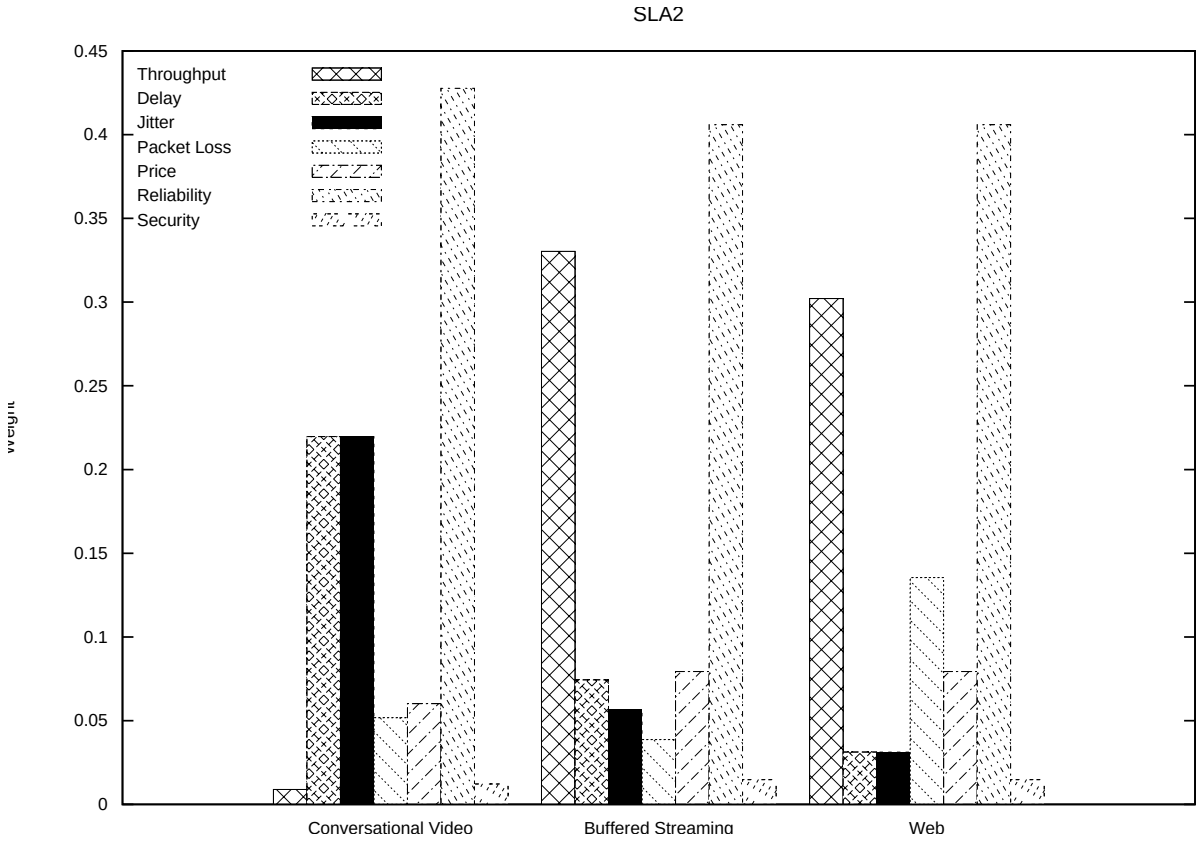

Figure 3.6 Criteria Weights for SLA2.

The ranking of the networks alternatives is performed using the TFT algorithm described in the subsection 3.1.4.1. The weights of the network selection criteria are obtained from Figures 3.5 - 3.8. The linguistic terms for the criteria attributes are represented by interval-valued trapezoidal fuzzy numbers as shown in Table 3.7. The network policy specifications are expressed directly using linguistic terms. Additionally, crisp values of network QoS characteristics are converted into linguistic terms which correspond to specific ranges of values per service type. Table 3.8 presents a relative example for the VoIP service, illustrating the correspondence between ranges of network QoS characteristics values and linguistic terms.

The available - candidate networks in our simulations at the time of network selection per service and SLA, as well as, their specifications expressed by linguistic terms are depicted in Tables 3.9 and 3.10.

The case of having several services of different QoS constraints running at the user site is being addressed by the TFT algorithm and network selection is performed in a way satisfying multiple groups of criteria per user. We consider the case where nine users need to select a network which satisfies the requirements of their services as presented in Table 3.11 and at the same time comply with their respective SLA agreements. To achieve this goal the proposed

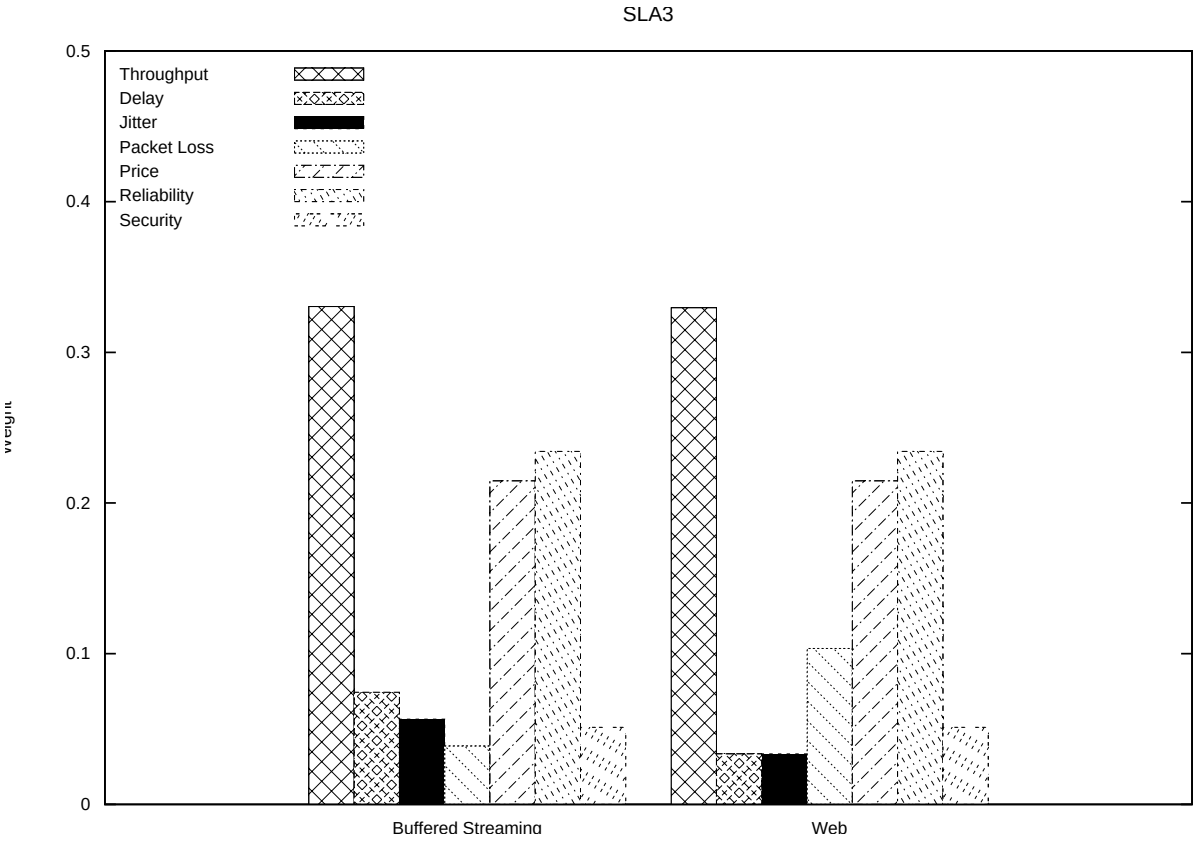

Figure 3.7 Criteria Weights for SLA3.

TFT algorithm is applied for each user and the available networks are ranked as shown in Figure 3.9. The positive and the negative ideal solutions are represented by unary and null trapezoidal fuzzy numbers respectively to eliminate the ranking abnormality problem.

From the obtained results it is clear that the ranking of the network alternatives is in accordance with the users expectations. For example, user 1 who requires increased QoS provisioning selects LTE 1 network which guarantees the best QoS characteristics and service reliability. As Figure 3.9 depicts, LTE 1 achieves higher ranking than the other networks, due to the high values of the QoS characteristics and service reliability factors bearing higher importance according to the relative ANP weights in SLA1. On the contrary, user 9 whose prior selection criterion is the price of the service, selects the WiFi 1 network which satisfies his requirements as expressed in his SLA agreement.

The performance of the TFT algorithm was evaluated against the original TOPSIS method, as well as, against the method presented in [172], the Fuzzy AHP - ELECTRE (FAE) method. The FAE method calculates the criteria weights using the Fuzzy AHP and performs the network selection by applying the ELECTRE algorithm. We consider the scenario of the nine users of Table 3.11. A critical weakness of TOPSIS and FAE is that they do not support users with

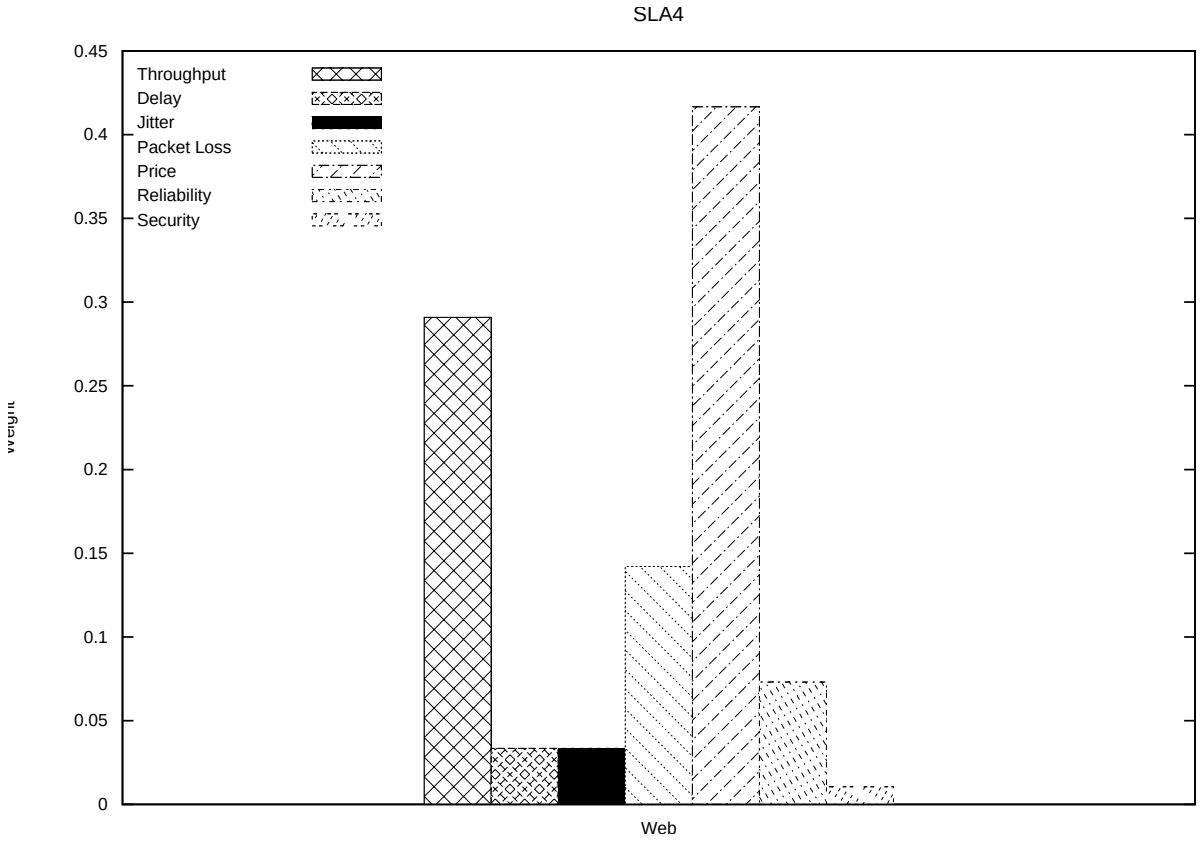

Figure 3.8 Criteria Weights for SLA4

more than one service. In these cases, the TOPSIS and FAE methods consider only the most demanding service of the user. Specifically, for users 2 and 3 they applied only considering the VoIP service and for user 7 are applied only considering the BStreaming service, whereas for the rest users the methods are applied respectively for each single user service defined in Table 3.11.

Table 3.12 presents the network classification performed by TFT, TOPSIS and FAE. From the analysis of the results we conclude that when a user has only one service, the methods usually provide similar results. However, when a user requires multiple services, TFT accomplishes more reliable results than TOPSIS and FAE, since it considers the weights of each service. For example, the results concerning user 1 using only the VoIP service, are similar for TFT and TOPSIS with the exception of the evaluation sequence of the WiFi 1 and WiFi 2 networks. Also, FAE accomplishes quite similar network rates with TFT and TOPSIS for this user. Nevertheless, TFT achieves more reliable results for user 4, compared with TOPSIS and FAE. In this case, only the RTGaming service is used and the most important criteria are service reliability, throughput and delay. TFT selects the WiMAX2 network which provides AG for service reliability, VG for throughput and AG for delay criterion. On the other hand,

Table 3.7 Linguistic Terms and the corresponding Interval-Valued Trapezoidal Fuzzy Numbers used for the Evaluation of the TFT algorithm.

Linguistic term	Interval-valued trapezoidal fuzzy number
Absolutely Poor (AP)	[(0.0, 0.0, 0.0, 0.0, 0.8), (0.0, 0.0, 0.0, 0.0, 1)]
Very Poor (VP)	[(0.01, 0.02, 0.03, 0.07, 0.8), (0.0, 0.01, 0.05, 0.08, 1)]
Poor (P)	[(0.04, 0.1, 0.18, 0.23, 0.8), (0.02, 0.08, 0.2, 0.25, 1)]
Medium Poor (MP)	[(0.17, 0.22, 0.36, 0.42, 0.8), (0.14, 0.18, 0.38, 0.45, 1)]
Medium (M)	[(0.32, 0.41, 0.58, 0.65, 0.8), (0.28, 0.38, 0.6, 0.7, 1)]
Medium Good (MG)	[(0.58, 0.63, 0.8, 0.86, 0.8), (0.5, 0.6, 0.9, 0.92, 1)]
Good (G)	[(0.72, 0.78, 0.92, 0.97, 0.8), (0.7, 0.75, 0.95, 0.98, 1)]
Very Good (VG)	[(0.93, 0.98, 1, 1, 0.8), (0.9, 0.95, 1, 1, 1)]
Absolutely Good (AG)	[(1, 1, 1, 1, 0.8), (1, 1, 1, 1, 1)]

Table 3.8 Relation of the Network QoS Characteristics and the Linguistic Terms for VoIP.

Linguistic term	Throughput range (Kbps)	Delay range (ms)	Jitter range (ms)	Packet loss range
AP	≤ 164	≥ 116	≥ 65	≥ 0.4
VP	165 - 174	111-115	55 - 64	≥ 0.2 - 0.4
P	175 - 184	106-110	45 - 54	$>10^{-1}$ - <0.2
MP	185 - 194	100 - 105	40 - 44	10^{-1}
M	195 - 204	95 - 99	35 - 49	10^{-2}
MG	205 - 214	86 - 94	30 - 34	10^{-3}
G	215 - 224	66 - 85	25 - 29	10^{-4}
VG	225 - 239	41 - 65	20 - 24	10^{-5}
AG	≥ 240	≤ 40	≤ 20	$\leq 10^{-6}$

TOPSIS selects the LTE1 network, which has similar values with the WiMAX2 for service reliability and delay criteria but worse performance for throughout by providing G instead of VG. Moreover, FAE does not provide a clear choice for user 4 and results to equal rankings for both WiMAX2 and LTE1 networks. Finally, the classification of the networks obtained by the three methods is quite different for user 7 who requests both BStreaming and web browsing services. In this case, the TFT accomplishes more reliable results by taking into account the weights of both services.

3.1.5.1.3 Sensitivity Analysis : In this subsection, the sensitivity of TFT is evaluated when the number of the available access networks changes frequently. We consider three different network configuration scenarios for the users defined in Table 3.11. In the first scenario all the networks defined in Tables 3.9 and 3.10 are available. In the second and third scenarios the LTE 1 and the WiFi 2 networks respectively are not reachable. The graphs of Figures 3.10-3.18 include three column types of different patern indicating the ranking of network alternatives in each case. In the first case, user 1 selects the LTE 1 network. In the second case, the remaining networks improve their ranking order, thus user 1 selects the WiMAX 2 network. Furthermore, in the third case only the last rated WiFi 3 network increases its rank, since the WiFi 2 network preceded WiFi 3 in the other two cases. Similar behavior is observed in the ranking of the

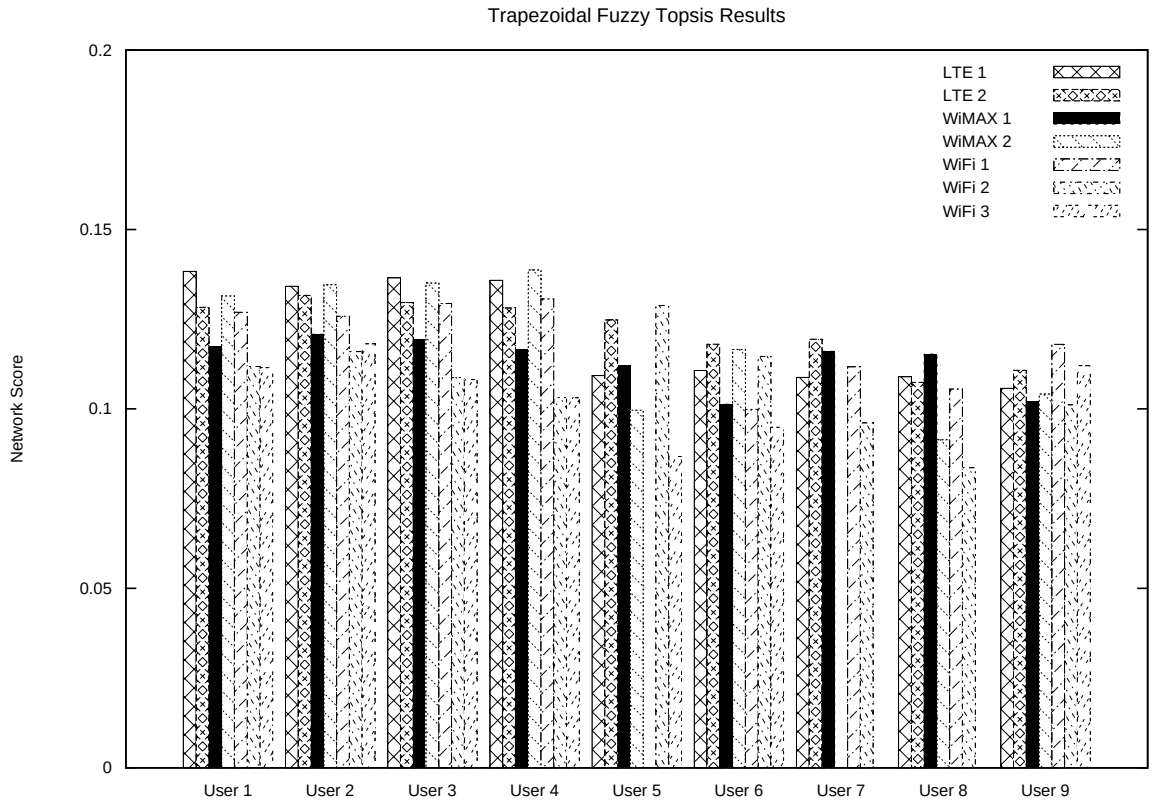

Figure 3.9 The TFT Results.

network alternatives for the other users. From the aforementioned analysis we conclude that the ranking results of the proposed method are normally adjusted with respect to the heterogeneous network environment changes, highlighting thus the method's sensitivity.

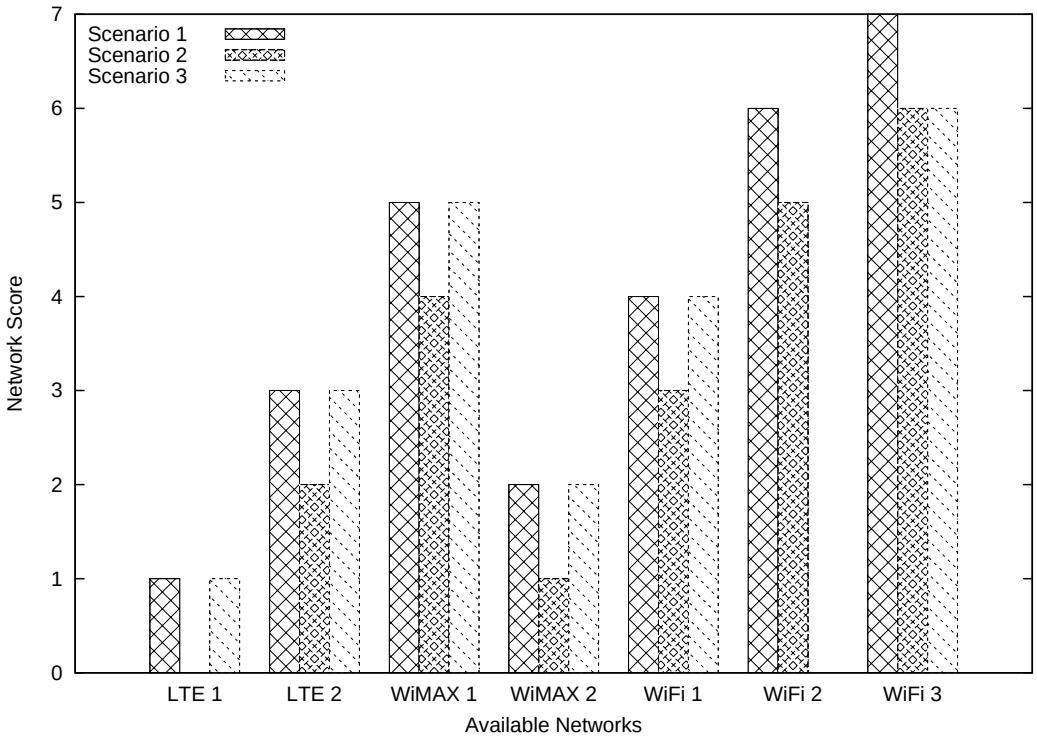

Figure 3.10 The TFT's Network Ranking for User 1 in case of Network Environment Changes.

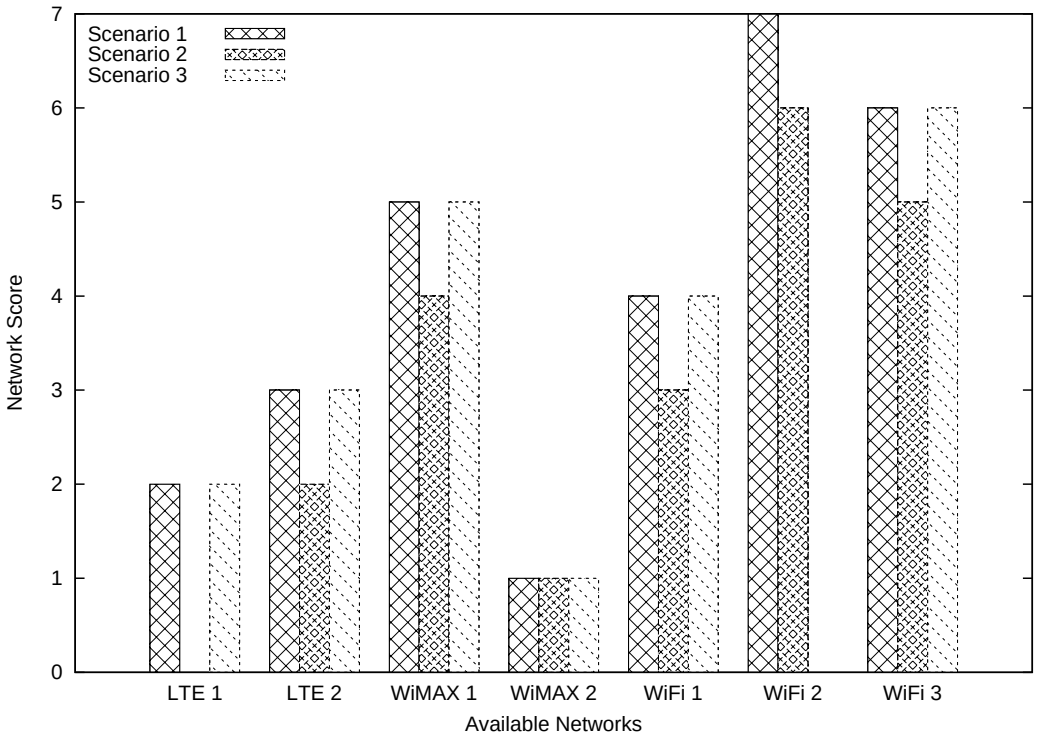

Figure 3.11 The TFT's Network Ranking for User 2 in case of Network Environment Changes.

Table 3.9 The Available Networks of SLA1 and SLA2.

SLA	Service	Network	Throughput	Delay	Jitter	Packet Loss	Price	Service Reliability	Security
SLA1	VoIP	LTE 1	MG	AG	VG	VG	VP	AG	VG
		LTE 2	AG	MG	AG	MG	VP	VG	AG
		WiMAX 1	M	M	MP	AG	P	VG	AG
		WiMAX 2	G	G	G	G	P	AG	VG
		WiFi 1	VG	VG	MG	AG	MP	G	G
		WiFi 2	MG	M	MG	VG	MP	MG	MG
		WiFi 3	M	MP	M	AG	MP	G	G
	CVideo	LTE 1	MP	MG	VG	G	AP	AG	VG
		LTE 2	AG	AG	AG	VG	AP	VG	AG
		WiMAX 1	MP	M	MG	AG	AP	VG	AG
		WiMAX 2	MG	MG	G	AG	VP	AG	VG
		WiFi 1	M	MG	M	VG	P	G	G
		WiFi 2	VG	VG	VG	AG	P	MG	MG
		WiFi 3	G	G	M	VG	P	G	G
	BStreaming	LTE 1	M	G	VG	VG	AP	AG	VG
		LTE 2	VG	VG	AG	AG	AP	VG	AG
		WiMAX 1	M	MG	MG	VG	VP	VG	AG
		WiMAX 2	MG	G	MG	G	P	AG	VG
		WiFi 1	VG	G	M	AG	P	G	G
		WiFi 2	AG	AG	G	VG	P	MG	MG
		WiFi 3	G	VG	VG	AG	MP	G	G
	RTGaming	LTE 1	G	AG	AG	VG	VP	AG	VG
		LTE 2	G	MG	VG	AG	VP	VG	AG
		WiMAX 1	MP	MG	G	AG	P	VG	AG
		WiMAX 2	VG	AG	AG	VG	VP	AG	VG
		WiFi 1	AG	VG	VG	VG	VP	G	G
		WiFi 2	M	M	MG	AG	MP	MG	MG
		WiFi 3	P	M	M	AG	MP	G	G
	Web	LTE 1	AG	AG	AG	AG	VP	AG	VG
		LTE 2	MG	M	G	VG	MP	VG	AG
		WiMAX 1	G	M	G	AG	P	VG	AG
		WiMAX 2	VG	G	VG	AG	P	AG	VG
		WiFi 1	MG	MP	MG	VG	MP	G	G
		WiFi 2	VG	G	M	VG	MP	MG	MG
		WiFi 3	AG	VG	AG	AG	MP	G	G
SLA2	CVideo	LTE 1	MG	G	VG	AG	MP	G	G
		LTE 2	MP	M	MG	VG	M	G	G
		WiMAX 1	M	MG	G	AG	MP	MG	MG
		WiMAX 2	MP	M	M	AG	M	MG	MG
		WiFi 2	G	VG	VG	AG	MG	G	M
		WiFi 3	MP	G	M	VG	MG	P	M
	BStreaming	LTE 1	M	G	G	VG	MP	G	G
		LTE 2	MG	MG	AG	G	MP	G	G
		WiMAX 1	M	MG	MP	AG	MP	MG	MG
		WiMAX 2	G	G	MG	VG	MP	MG	MG
		WiFi 1	G	VG	MG	AG	MP	MP	MP
		WiFi 2	AG	AG	VG	VG	MP	M	M
		WiFi 3	MG	VG	VG	AG	M	P	M
	Web	LTE 2	M	MP	MG	VG	M	G	G
		WiMAX 1	MG	M	G	AG	MG	MG	MG
		WiMAX 2	VG	G	AG	AG	M	MG	MG
		WiFi 1	MG	MP	M	VG	MG	MP	MP
		WiFi 2	MG	M	G	VG	MG	M	M
		WiFi 3	VG	VG	AG	AG	MG	P	M

Table 3.10 The Available Networks of SLA3 and SLA4.

SLA	Service	Network	Throughput	Delay	Jitter	Packet Loss	Price	Service Reliability	Security
SLA3	BStreaming	LTE 1	M	MG	G	VG	MG	MP	MP
		LTE 2	G	G	M	AG	MG	M	M
		WiMAX 1	M	G	MP	VG	MG	M	M
		WiFi 1	G	G	MG	AG	G	VP	P
		WiFi 2	G	AG	G	VG	MG	VP	P
		WiFi 3	MG	VG	MG	AG	G	VP	P
	Web	LTE 1	MG	MP	M	G	G	MP	MP
		LTE 2	M	M	G	VG	G	M	M
		WiMAX 1	MG	M	M	AG	G	M	M
		WiMAX 2	VP	M	AG	AG	VG	P	MP
		WiFi 1	MG	MP	M	AG	G	VP	P
		WiFi 2	AP	AP	VP	G	VG	VP	P
SLA4	Web	LTE 1	MP	M	M	VG	VG	P	P
		LTE 2	M	M	G	MG	VG	P	MP
		WiMAX 1	VP	P	M	AG	AG	VP	VP
		WiMAX 2	P	MP	MP	G	VG	VP	P
		WiFi 1	MG	G	M	G	AG	AP	AP
		WiFi 2	AP	AP	VP	G	AG	AP	VP
		WiFi 3	AP	VP	P	AG	AG	AP	VP

Table 3.11 The Required Services per User.

User	SLA	Required services
1	SLA1	-VoIP
2	SLA1	-VoIP,-RTGaming, -BStreaming, -Web
3	SLA1	-VoIP, -RTGaming
4	SLA1	-RTGaming
5	SLA2	-CVideo
6	SLA2	-BStreaming
7	SLA3	-BStreaming, -Web
8	SLA3	-Web
9	SLA4	-Web

Table 3.12 Networks' Classification in respect of TFT, TOPSIS (T) and FAE Results.

	User 1			**User 2**			**User 3**			**User 4**			**User 5**			**User 6**			**User 7**			**User 8**			**User 9**		
Method / Networks	TFT	T	FAE	TFT	T	FAE	TFT	T	FAE	TFT	T	FAE	TFT	T	FAE	TFT	T	FAE	TFT	T	FAE	TFT	T	FAE	TFT	T	FAE
LTE 1	**1**	**1**	**1**	2	**1**	**1**	**1**	**1**	**1**	2	**1**	**1**	4	2	2	4	2	5	4	2	5	2	**1**	4	4	6	4
LTE 2	3	3	3	3	3	3	3	3	3	4	4	2	2	3	6	**1**	**1**	4	**1**	3	**1**	3	2	5	3	3	4
WiMAX 1	5	5	5	5	5	5	5	5	5	5	5	4	3	4	3	5	4	7	2	**1**	4	**1**	3	**1**	6	7	3
WiMAX 2	2	2	4	**1**	2	4	2	2	4	**1**	2	**1**	5	5	4	2	3	2	-	-	-	5	5	3	5	5	4
WiFi 1	4	6	2	4	6	2	4	6	2	3	3	3	-	-	-	6	6	3	3	5	3	4	4	2	**1**	**1**	**1**
WiFi 2	6	4	6	7	4	6	6	4	6	6	7	5	**1**	**1**	**1**	3	5	**1**	5	4	2	6	6	6	7	4	4
WiFi 3	7	7	6	6	7	6	7	7	6	7	6	6	6	6	5	7	7	6	-	-	-	-	-	-	2	2	2

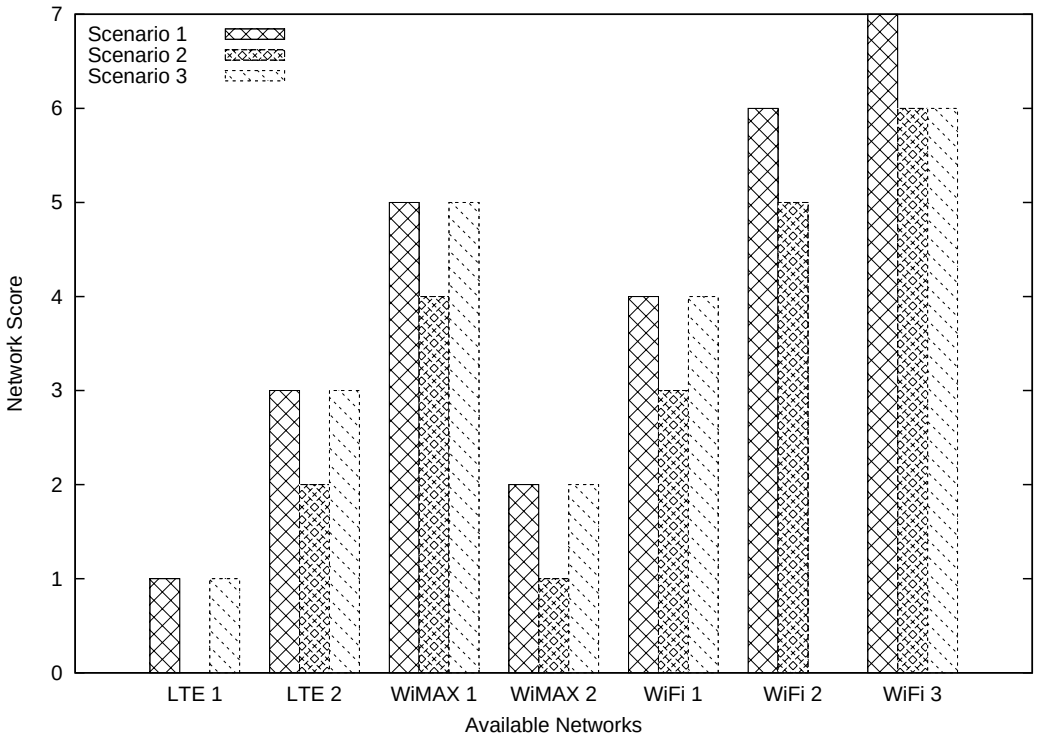

Figure 3.12 The TFT's Network Ranking for User 3 in case of Network Environment Changes.

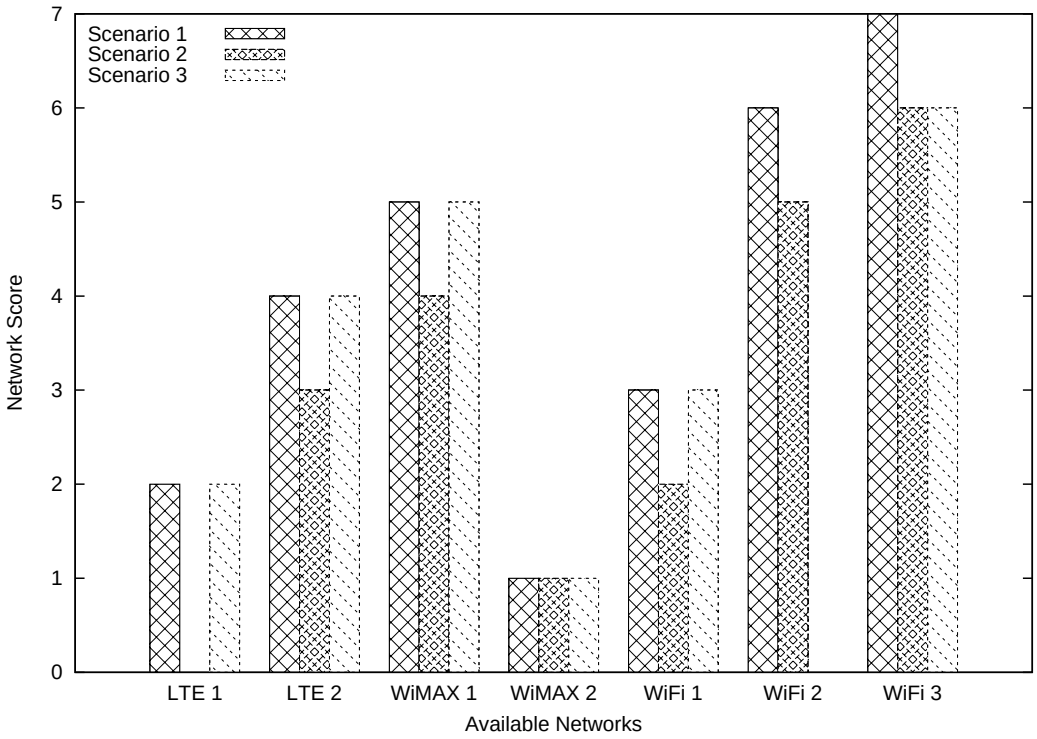

Figure 3.13 The TFT's Network Ranking for User 4 in case of Network Environment Changes.

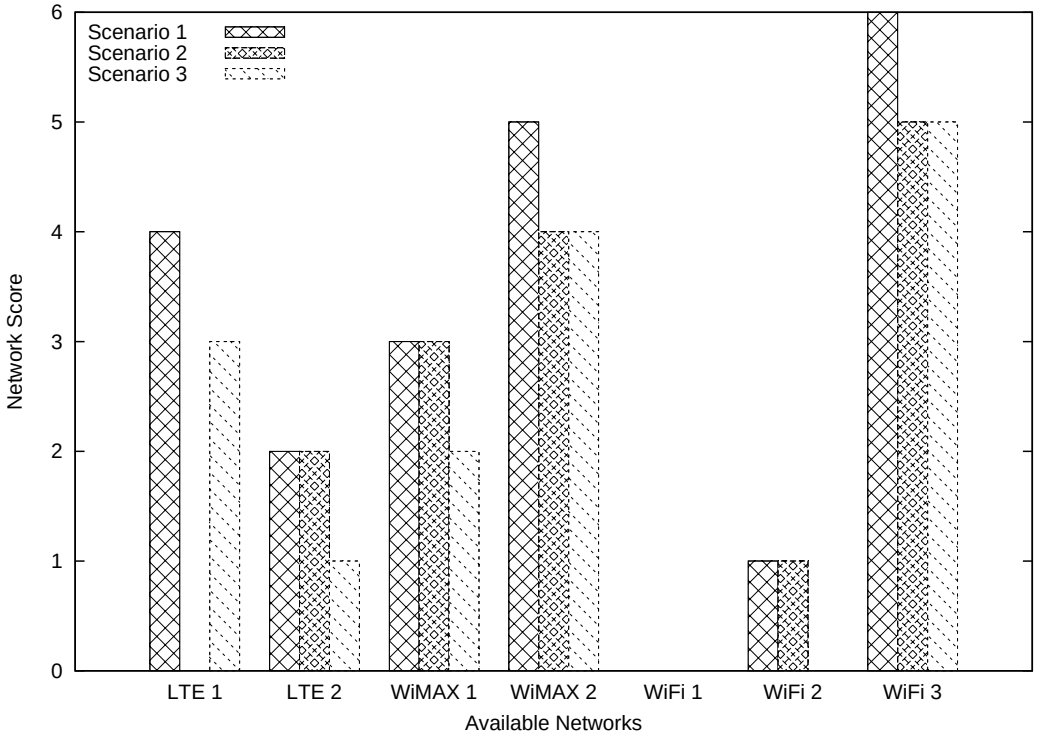

Figure 3.14 The TFT's Network Ranking for User 5 in case of Network Environment Changes.

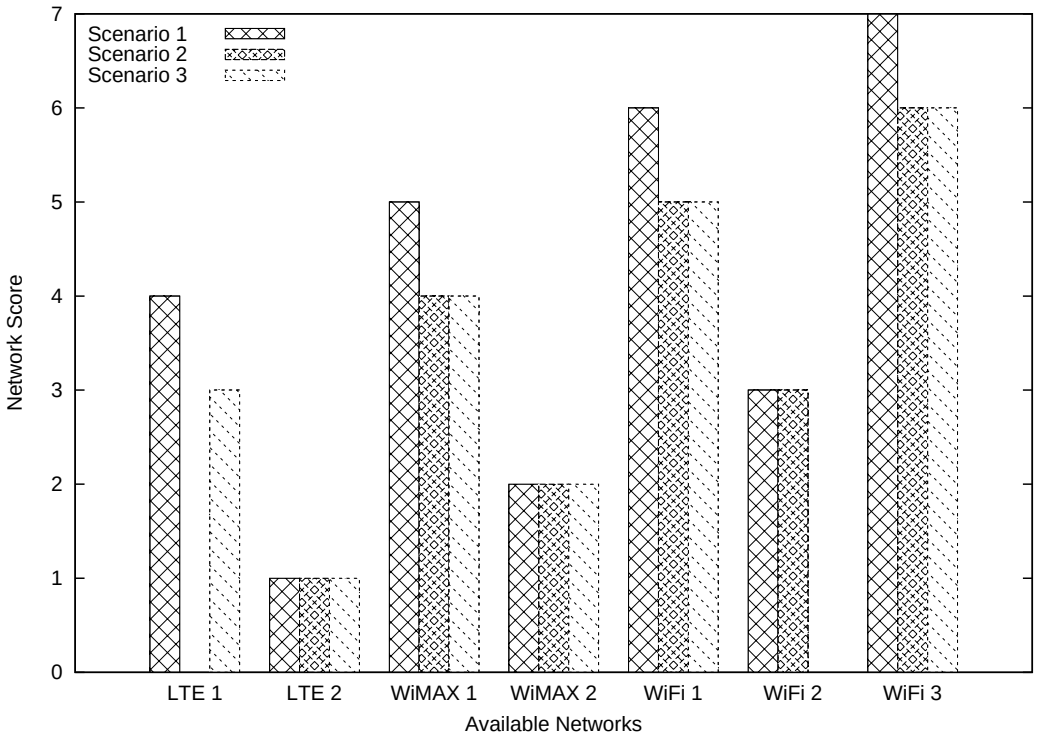

Figure 3.15 The TFT's Network Ranking for User 6 in case of Network Environment Changes.

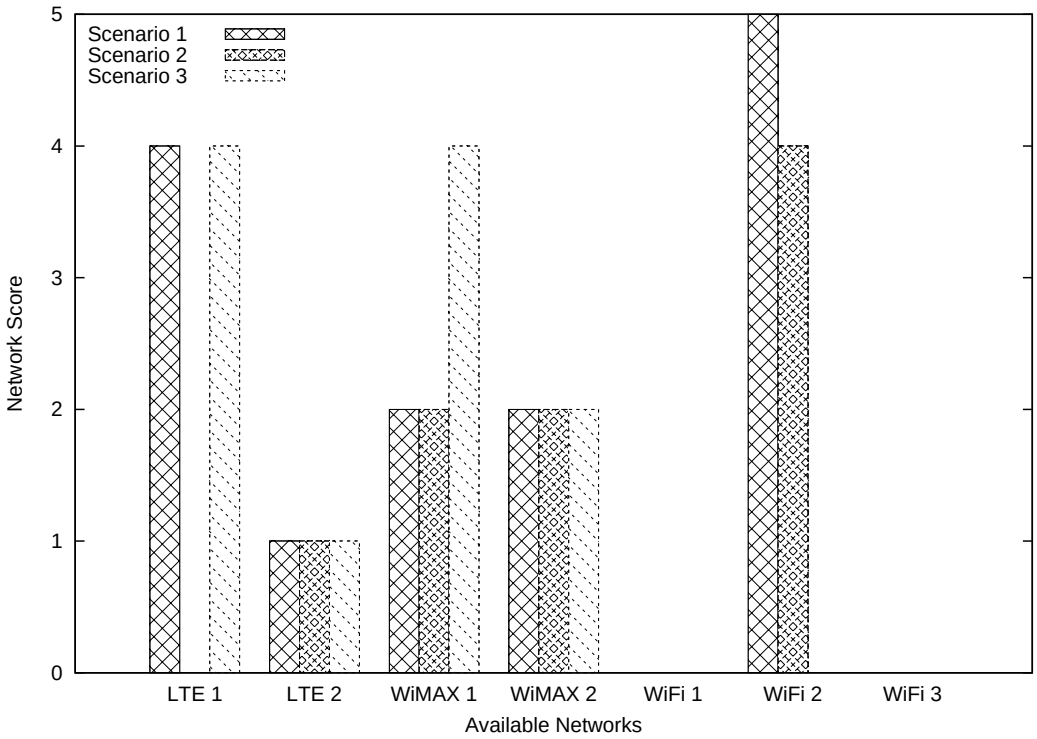

Figure 3.16 The TFT's Network Ranking for User 7 in case of Network Environment Changes.

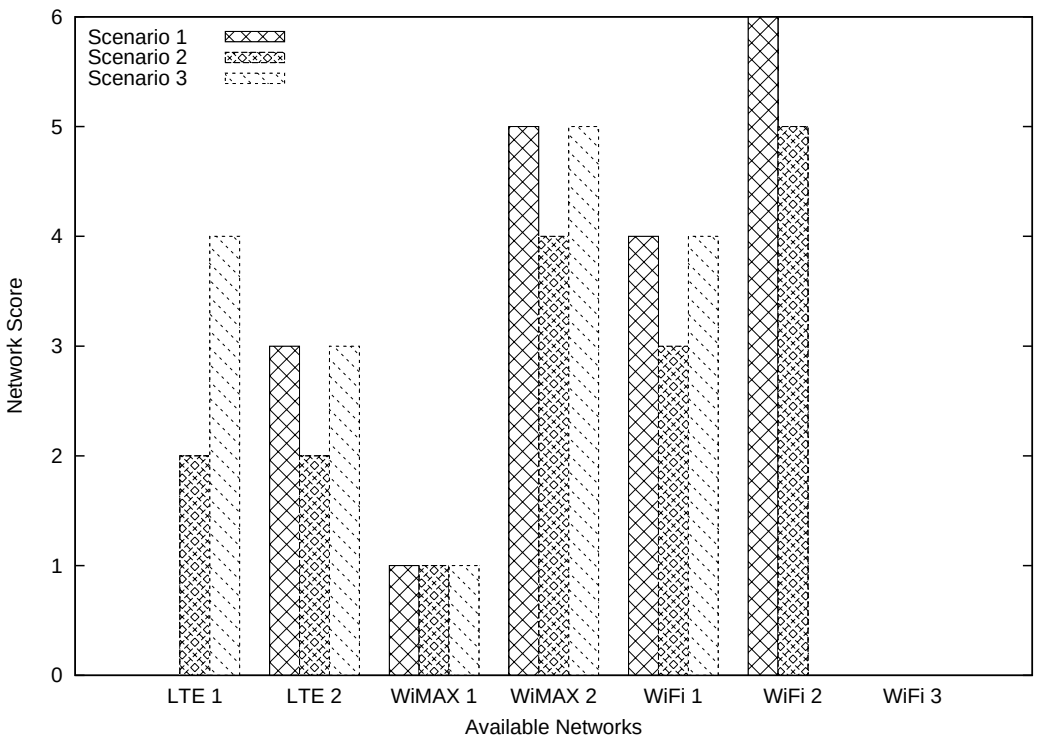

Figure 3.17 The TFT's Network Ranking for User 8 in case of Network Environment Changes.

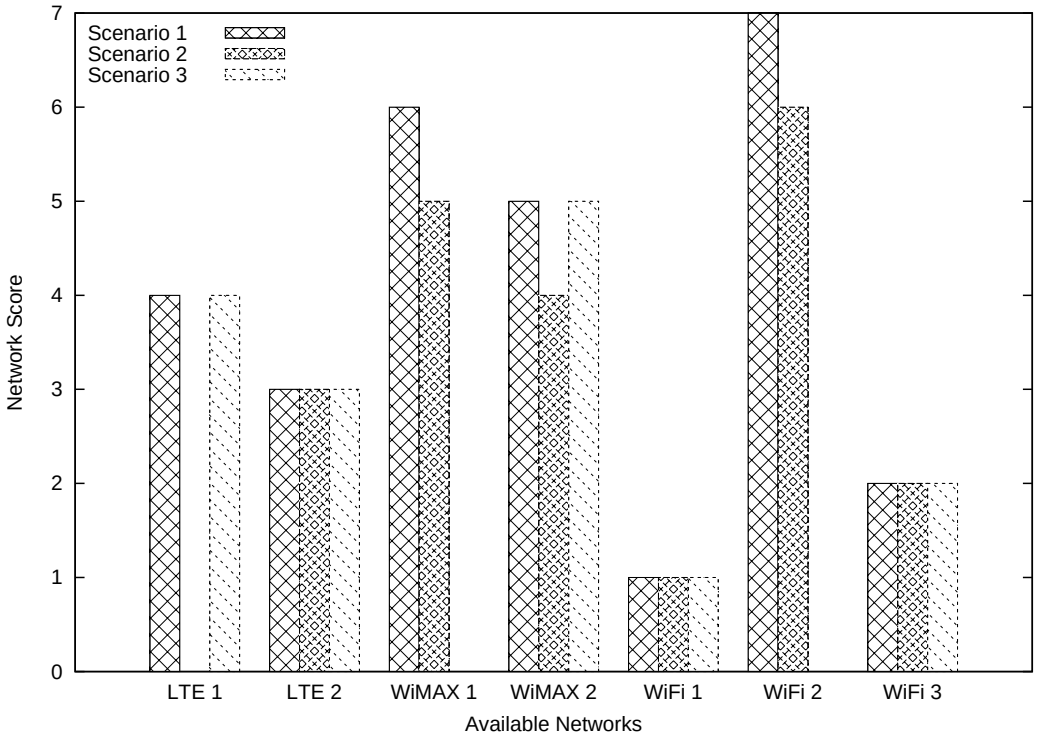

Figure 3.18 The TFT's Network Ranking for User 9 in case of Network Environment Changes.

3.1.5.2 Network Selection using the TF-ANP and the TFT Algorithms for supporting Medical Services

3.1.5.2.1 Simulation Setup : We consider an heterogeneous network environment consisting of a number of LTE, WAVE and WiMAX networks. Each network supports at least one of the following medical service types: Live Video, Medical Data, Sensor Data and Clinical Data. Also, we consider the case where 10 vehicles with patients are moving inside the network environment and need to be connected to a network which satisfies the requirements of their services and at the same time complies with their patient health status. The health status of each patient is evaluated using the Manchester Triage System (MTS) [173] healthcare classification system, which defines 5 health statuses, called Non-Urgent, Standard, Urgent, Very-Urgent and Immediate. The Non-Urgent status has the lower risk about patient's life, while the Immediate status has the higher one.

3.1.5.2.2 Performance Evaluation : During the network selection process the TF-ANP method is applied initially, in order to estimate the decision weights per service type and patient health status, considering the ANP network model proposed in [171]. The criteria used include throughput, delay, jitter, packet loss, service reliability, security and price. Pairwise comparison decision matrices are created to evaluate the priority vectors of criteria and to form the fuzzy Supermatrix per service type and patient health status. Subsequently, the fuzzy Weighted Supermatrix and, finally, the Limit Supermatrix are obtained. Indicatively, when the patient health status is evaluated as Non-Urgent, for the Sensor Data service the initial, the weighted and the limit supermatrices are presented in Tables 3.4, 3.5 and 3.6 respectively. For each health status, the criteria weights per healthcare service obtained by the corresponding Limit Supermatrix are presented in Figure 3.19. As illustrated, the weights are proportional to the constraints of each service as well as to the health status of each patient. In particular, the weight of the price criterion is low for Immediate health status, resulting in a weight value which is very close to 0. Accordingly, when the health status is evaluated as Non-Urgent, the medical risk for the patient is very low and the price criterion becomes more important.

The ranking of the networks alternatives is performed using the TFT algorithm using the weights of the network selection criteria obtained using the TF-ANP method. The linguistic terms for the criteria attributes are represented by IVTFNs as shown in Table 4.1. Furthermore, the available-candidate networks in our simulations at the time of network selection per service as well as their specifications expressed by linguistic terms are depicted in Table 3.14.

The case of having several medical services of different QoS constraints running at the vehicle site is also addressed. The network selection is performed in a way that satisfies multiple groups of criteria per vehicle. The vehicles need to select a network which satisfies

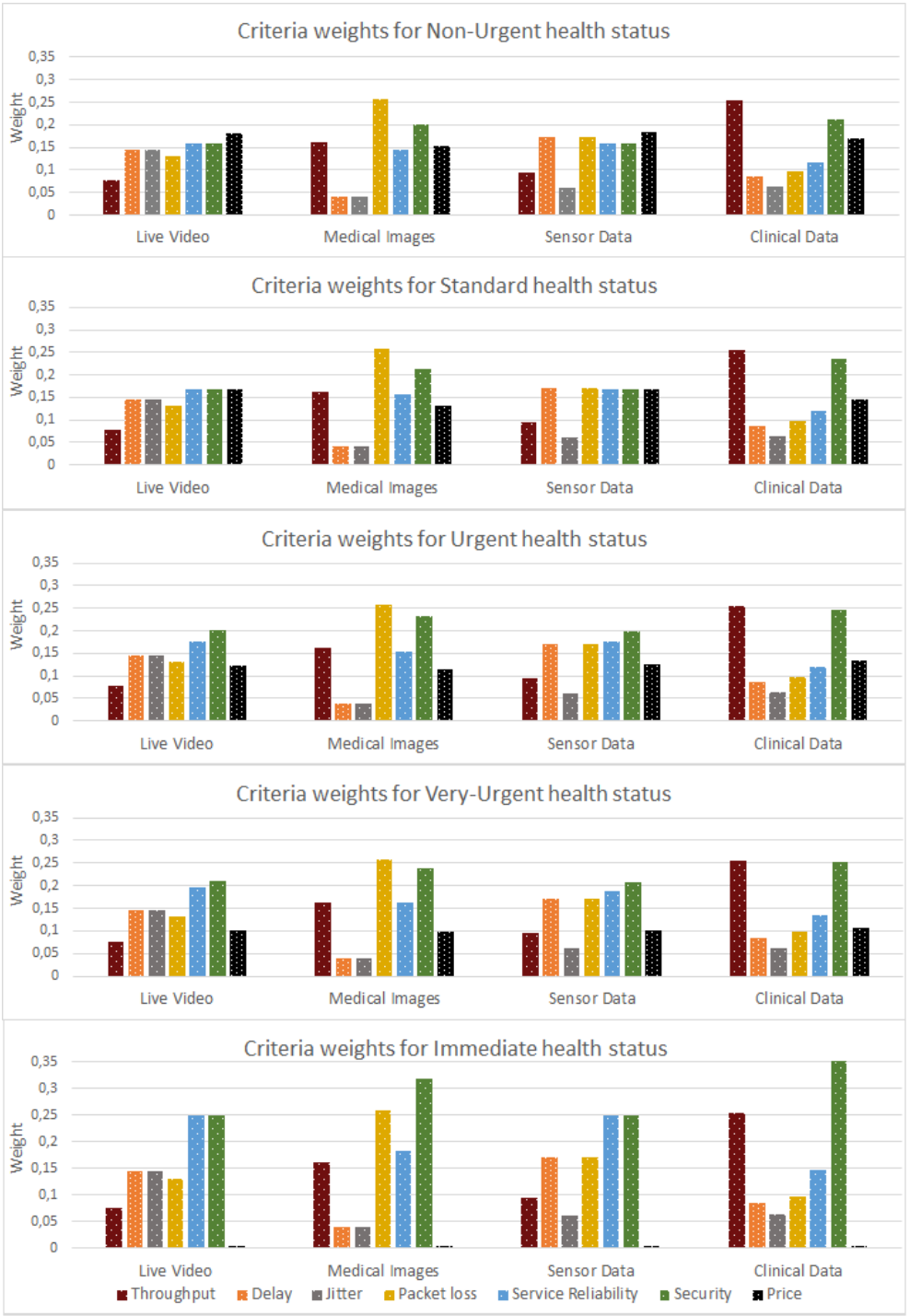

Figure 3.19 The TF-ANP Weights per Service and Patient Health Status.

Table 3.13 Linguistic Terms and the Corresponding Interval-Valued Trapezoidal Fuzzy Numbers used for the Criteria Attributes for the Evaluation of the TFT Algorithm in cases where Medical Services are used.

Linguistic term	**Interval-valued trapezoidal fuzzy number**
Absolutely Poor (AP)	[(0.0, 0.0, 0.0, 0.0, 0.9), (0.0, 0.0, 0.0, 0.0, 1.0)]
Very Poor (VP)	[(0.01, 0.02, 0.03, 0.07, 0.9), (0.0, 0.01, 0.05, 0.08, 1.0)]
Poor (P)	[(0.04, 0.1, 0.18, 0.23, 0.9), (0.02, 0.08, 0.2, 0.25, 1.0)]
Medium Poor (MP)	[(0.17, 0.22, 0.36, 0.42, 0.9), (0.14, 0.18, 0.38, 0.45, 1.0)]
Medium (M)	[(0.32, 0.41, 0.58, 0.65, 0.9), (0.28, 0.38, 0.6, 0.7, 1.0)]
Medium Good (MG)	[(0.58, 0.63, 0.8, 0.86, 0.9), (0.5, 0.6, 0.9, 0.92, 1.0)]
Good (G)	[(0.72, 0.78, 0.92, 0.97, 0.9), (0.7, 0.75, 0.95, 0.98, 1.0)]
Very Good (VG)	[(0.93, 0.98, 1.0, 1.0, 0.9), (0.9, 0.95, 1.0, 1.0, 1.0)]
Absolutely Good (AG)	[(1.0, 1.0, 1.0, 1.0, 0.9), (1.0, 1.0, 1.0, 1.0, 1.0)]

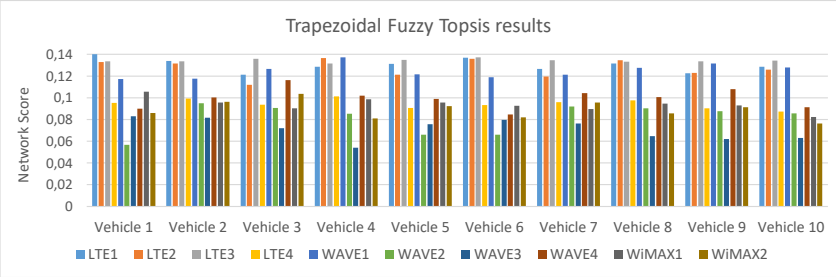

Figure 3.20 The TFT Results for each Vehicle.

the requirements of their healthcare services as presented in Table 4.8 considering the health status of each patient. To achieve this goal the proposed TFT algorithm is applied for each vehicle. The available networks are ranked as shown in Figure 3.20.

From the obtained results it is clear that the ranking of the network alternatives is in accordance with the vehicles expectations. For example, vehicle 1 requiring increased QoS provisioning selects the LTE 1 network which guarantees the best QoS characteristics and service reliability. In particular, LTE 1 achieves higher ranking than the other networks, due to the high values of the QoS characteristics and the service reliability factors bearing higher importance according to the relative ANP weights for the Live Video service. On the contrary, vehicle 4 whose prior selection criterion is the throughput of the service, selects the WAVE 1 network which satisfies his requirements considering the Clinical Data service constraints and the Non-Urgent health status of its patient.

The performance of TFT, was evaluated against the ANST [174] and the FAS [175] methods. A critical weakness of ANST is that it considers only the throughput criterion, while a weakness of FAS is that it does not support vehicles with more than one service. Therefore, in the case of FAS only the most demanding service of the vehicle is considered when more than one service is required. Specifically, for vehicles 5, 7, 9 and 10 FAS is applied only for the Sensor Data

Table 3.14 The Available Wide Coverage Networks for each Service.

Medical Service	Network	Throughput	Delay	Jitter	Packet Loss	Service Reliability	Security	Price
Live Video	LTE1	VG	AG	AG	VG	AG	VG	P
	LTE2	G	MG	VG	AG	VG	AG	AP
	LTE3	AG	AG	MG	VG	AG	AG	VG
	LTE4	MP	P	VG	G	M	P	MG
	WAVE1	MG	MG	G	VG	MG	MG	AG
	WAVE2	AP	AP	G	VP	AP	AG	M
	WAVE3	MP	M	MG	G	AG	G	AG
	WAVE4	M	M	VG	MG	MG	MG	G
	WiMAX1	VG	AG	VG	G	AG	VG	MG
	WiMAX2	MG	M	MP	VG	MG	MG	M
Medical Images	LTE1	MG	MG	VG	AG	AG	VG	P
	LTE2	AG	AG	AG	MG	VG	AG	AP
	LTE3	AG	VG	G	G	AG	VG	VG
	LTE4	M	VG	G	M	VG	P	MG
	WAVE1	MG	MG	AG	MG	MG	G	AG
	WAVE2	G	G	VG	VG	AG	AG	M
	WAVE3	MG	MG	AG	VG	MP	G	AG
	WAVE4	G	G	VG	VG	MG	G	G
	WiMAX1	MG	VP	AG	G	VG	AG	MG
	WiMAX2	VG	AG	AG	VG	MP	G	M
Sensor Data	LTE1	MP	P	P	VP	VG	G	P
	LTE2	M	G	MG	MP	MG	G	AP
	LTE3	G	G	VG	VG	M	G	VG
	LTE4	MG	MP	M	MG	M	AG	MG
	WAVE1	MP	MG	VG	MG	AG	VG	AG
	WAVE2	AG	AG	AG	VG	VG	AG	M
	WAVE3	G	VG	AG	AG	VG	G	AG
	WAVE4	MG	AG	G	MG	MG	VG	G
	WiMAX1	MG	MP	VG	G	MG	MG	MG
	WiMAX2	G	G	AG	MG	MG	VG	M
Clinical Data	LTE1	G	M	VG	VG	AG	VG	P
	LTE2	VG	AG	VG	AG	MG	AG	AP
	LTE3	G	G	VG	AG	VG	G	VG
	LTE4	AG	VP	P	VG	AP	VP	MG
	WAVE1	VG	VG	AG	AG	VG	AG	AG
	WAVE2	G	G	VG	VG	M	G	M
	WAVE3	MP	P	P	P	M	VG	AG
	WAVE4	G	VG	G	AG	MG	AG	G
	WiMAX1	AG	VG	AP	VG	G	AG	MG
	WiMAX2	MP	MG	AG	MP	MG	G	M

service. Additionally, for vehicle 6 it is applied only for the Live Video service, whereas for vehicle 8 it is applied only for the Medical Images service.

Table 3.20 presents the network classification performed by the proposed TFT, the ANST and the FAS algorithms, respectively. From the analysis of the results we conclude that the proposed method achieves better performance for the entire vehicles. Indicatively, the TFT results concerning vehicle 2 are better than the ones obtained from both ANST and FAS, due to the fact that TFT selects the LTE 1 network which offers AG packet loss, while the ANST selects the LTE 3 and the FAS select the WAVE that offer G and VG packet loss respectively. Additionally, TFT provides more reliable results for vehicle 10 by taking into account the criteria importance for the Medical Images, the Sensor Data and the Clinical Data services as

Table 3.15 The Simulated Vehicles for the Evaluation of the TFT Algorithm.

Vehicle	Medical Services	Patient Health Status
1	Live Video	Very urgent
2	Medical Images	Urgent
3	Sensor Data	Standard
4	Clinical Data	Non urgent
5	Live Video & Sensor Data	Very urgent
6	Live Video & Medical Images	Immediate
7	Medical Images & Sensor Data	Very urgent
8	Medical Images & Clinical Data	Urgent
9	Sensor Data & Clinical Data	Standard
10	Medical Images & Sensor Data & Clinical Data	Immediate

Table 3.16 Networks' Classification in respect of TFT, ANST and FAS Results.

	Vehicle 1			Vehicle 2			Vehicle 3			Vehicle 4			Vehicle 5			Vehicle 6			Vehicle 7			Vehicle 8			Vehicle 9			Vehicle 10		
Method / Networks	TFT	ANST	FAS	TFT	ANST	FAS	TFT	ANST	FAS	TFT	ANST	FAS	TFT	ANST	FAS	TFT	ANST	FAS	TFT	ANST	FAS	TFT	ANST	FAS	TFT	ANST	FAS	TFT	ANST	FAS
LTE 1	**1**	2	**1**	**1**	8	3	3	9	7	4	8	9	2	3	7	2	3	**1**	2	8	7	3	8	3	4	8	7	2	8	7
LTE 2	3	4	2	3	2	10	5	7	5	2	4	4	4	7	5	3	2	2	4	5	5	**1**	2	10	3	2	5	4	2	5
LTE 3	2	**1**	4	2	**1**	9	**1**	2	**1**	3	5	**1**	**1**	**1**	**1**	**1**	**1**	4	**1**	**1**	**1**	2	**1**	9	**1**	4	**1**	**1**	**1**	**1**
LTE 4	6	9	7	6	10	2	7	4	10	6	**1**	6	8	9	10	5	8	7	6	10	10	6	10	2	8	**1**	10	6	10	10
WAVE 1	4	6	5	4	9	7	2	8	3	**1**	3	3	3	6	3	4	5	5	3	9	3	4	7	7	2	6	3	3	7	3
WAVE 2	10	10	10	9	5	6	8	**1**	4	8	6	8	10	10	4	10	9	10	8	4	4	8	5	6	9	3	4	7	4	4
WAVE 3	9	8	9	10	6	4	10	3	9	10	10	7	9	8	9	9	7	9	10	6	9	10	9	4	10	10	9	10	9	9
WAVE 4	7	7	6	5	4	**1**	4	6	2	5	7	2	5	4	2	7	6	6	5	2	2	5	4	**1**	5	5	2	5	5	2
WiMAX 1	5	3	3	8	7	5	9	5	8	7	2	10	6	2	8	6	3	3	9	7	8	7	6	5	6	7	8	8	6	8
WiMAX 2	8	5	8	7	3	8	6	3	6	9	9	5	7	5	6	8	4	8	7	3	6	9	3	8	7	9	6	9	3	6

well as the entire set of criteria, while ANST considers only the throughput criterion and FAS takes into account only the Sensor Data service.

3.1.5.3 Network Selection using the TF-AANP and the TFT-ACW Algorithms for supporting Medical Services

3.1.5.3.1 Simulation Setup : In our experiments, the 5G-VCC topology presented in Figure 3.21 is simulated. A mobility trace indicating the map of the Syntagma square in Athens along with road traffic data has been created using the Open Street Map (OSM) software [176]. Then, the mobility trace has been used as input in the Simulator of Urban Mobility (SUMO) simulator [177] allowing the production of a realistic mobility pattern for the simulated vehicles. Furthermore, the network topology is being built upon the map, using the Network Simulator 3 (NS3) simulator [178]. The network topology includes a heterogeneous access network environment and a Cloud infrastructure. The access network environment includes 1 LTE Macrocell, 4 LTE Femtocells, 1 WiMAX Macrocell and 4 WAVE RSUs. The Cloud infrastructure includes a set of Virtual Machines (VMs) providing Driver Assistance (DA), Passengers Entertainment and Information (PeNI) and Medical (MED) services. The DA services include Navigation Assistance (NAV) and Parking Assistance (PRK) services. Accordingly, the PEnI services include Conversational Video (CV), Voice over IP (VoIP), Buffered Streaming (BS) and Web Browsing (WB) services. Finally, the MED services include

Live Healthcare Video (LHVideo) [9], Medical Images (MedImages) [10], Health Monitoring (HMonitoring) [11] and Clinical Data Transmission (CData) [12] services. Furthermore, a Software Defined Network (SDN) controller provides a centralized control of the entire system.

Table 3.17 Linguistic Terms and the corresponding Interval-Valued Trapezoidal Fuzzy Numbers used for the Criteria Attributes for the Evaluation of the TFT-ACW Algorithm.

Linguistic term	**Interval-valued trapezoidal fuzzy number**
Absolutely Poor (AP)	[(0.0, 0.0, 0.0, 0.0, 0.9), (0.0, 0.0, 0.0, 0.0, 1.0)]
Very Poor (VP)	[(0.01, 0.02, 0.03, 0.07, 0.9), (0.0, 0.01, 0.05, 0.08, 1.0)]
Poor (P)	[(0.04, 0.1, 0.18, 0.23, 0.9), (0.02, 0.08, 0.2, 0.25, 1.0)]
Medium Poor (MP)	[(0.17, 0.22, 0.36, 0.42, 0.9), (0.14, 0.18, 0.38, 0.45, 1.0)]
Medium (M)	[(0.32, 0.41, 0.58, 0.65, 0.9), (0.28, 0.38, 0.6, 0.7, 1.0)]
Medium Good (MG)	[(0.58, 0.63, 0.8, 0.86, 0.9), (0.5, 0.6, 0.9, 0.92, 1.0)]
Good (G)	[(0.72, 0.78, 0.92, 0.97, 0.9), (0.7, 0.75, 0.95, 0.98, 1.0)]
Very Good (VG)	[(0.93, 0.98, 1.0, 1.0, 0.9), (0.9, 0.95, 1.0, 1.0, 1.0)]
Absolutely Good (AG)	[(1.0, 1.0, 1.0, 1.0, 0.9), (1.0, 1.0, 1.0, 1.0, 1.0)]

Table 3.18 The Available Networks.

Service	SLA 1	SLA 2	SLA 3	Network	Throughput	Delay	Jitter	Packet Loss	Service Reliability	Security	Price
Navigation Assistance (NAV)	✓	✓	✓	LTE Macro	G	MG	VG	AG	VG	AG	VG
	✓	✓	✓	LTE Femto 1	VG	AG	VG	VG	AG	MG	P
	✓	✓		LTE Femto 2	AG	G	AG	G	VG	G	G
	✓			LTE Femto 3	G	MG	G	MG	G	AG	P
	✓			LTE Femto 4	AG	AG	MG	AG	G	G	AP
	✓	✓	✓	WiMAX Macro	G	AG	G	VG	AG	VG	VP
	✓	✓	✓	WAVE 1	VG	MG	VG	AG	VG	AG	G
	✓			WAVE 2	MG	MG	VG	VG	G	G	AP
	✓	✓	✓	WAVE 3	MG	MG	G	VG	MG	MG	M
	✓			WAVE 4	M	M	MG	VG	MG	MG	MP
Parking Assistance (PRK)	✓	✓	✓	LTE Macro	MG	M	G	VG	VG	AG	MP
	✓	✓	✓	LTE Femto 1	AG	AG	AG	AG	AG	VG	G
	✓	✓		LTE Femto 2	VG	AG	M	VG	AG	G	AG
	✓			LTE Femto 3	G	VG	MG	AG	VG	AG	MG
	✓			LTE Femto 4	MG	G	M	G	VG	G	G
	✓	✓	✓	WiMAX Macro	G	M	M	AG	MG	M	MP
	✓	✓	✓	WAVE 1	M	MP	MG	VG	G	G	VG
	✓			WAVE 2	MG	M	M	AG	M	M	M
	✓	✓	✓	WAVE 3	AG	G	G	AG	MG	MG	P
	✓			WAVE 4	G	M	AG	AG	MG	G	G
Conversation Video (CV)	✓	✓		LTE Macro	AG	AG	AG	VG	VG	AG	G
	✓	✓		LTE Femto 1	MP	MG	VG	AG	AG	VG	AP
	✓	✓		LTE Femto 2	G	G	MG	VG	AG	MG	M
	✓			LTE Femto 3	AG	VG	AG	G	VG	G	P
	✓			LTE Femto 4	G	VG	VG	AG	MG	AG	MG
	✓	✓		WiMAX Macro	MP	M	MG	G	G	G	MP
	✓	✓		WAVE 1	G	G	VG	VG	G	G	M
	✓			WAVE 2	MG	MG	AG	VG	G	MG	AG
	✓	✓		WAVE 3	MG	MG	G	AG	MG	VG	MP
	✓			WAVE 4	MP	MP	MG	AG	MG	G	P
Voice over IP (VoIP)	✓			LTE Macro	VG	VG	AG	AG	VG	AG	AP
	✓			LTE Femto 1	M	G	VG	VG	AG	VG	G
	✓			LTE Femto 2	G	VG	MG	AG	VG	G	MG
	✓			LTE Femto 3	MG	G	G	VG	G	MG	MP
	✓			LTE Femto 4	VG	AG	VG	AG	VG	VG	P
	✓			WiMAX Macro	M	G	MG	MG	G	G	M
	✓			WAVE 1	M	MG	AG	AG	G	G	VG
	✓			WAVE 2	MG	M	VG	AG	MG	M	M
	✓			WAVE 3	VG	AG	VG	AG	MG	VG	G
	✓			WAVE 4	G	VG	G	AG	MG	G	AG
Buffered Streaming (BS)	✓	✓		LTE Macro	G	MG	VG	AG	VG	AG	VG
	✓	✓		LTE Femto 1	VG	AG	AG	VG	AG	VG	P
	✓	✓		LTE Femto 2	AG	VG	VG	MG	MG	AG	G
	✓			LTE Femto 3	G	MG	VG	G	VG	G	M
	✓			LTE Femto 4	AG	AG	AG	VG	G	G	P
	✓	✓		WiMAX Macro	G	AG	G	VG	AG	VG	VP
	✓	✓		WAVE 1	VG	MG	VG	AG	VG	AG	G
	✓			WAVE 2	MG	MG	VG	VG	G	G	AP
	✓	✓		WAVE 3	MG	MG	G	VG	MG	MG	M
	✓			WAVE 4	M	M	MG	VG	MG	MG	MP
Web Browsing (WB)	✓	✓	✓	LTE Macro	MG	M	G	VG	VG	AG	MP
	✓	✓	✓	LTE Femto 1	AG	AG	AG	AG	AG	VG	G
	✓	✓		LTE Femto 2	G	G	M	G	G	VG	G
	✓			LTE Femto 3	AG	AG	MG	AG	VG	MG	M
	✓			LTE Femto 4	VG	G	G	VG	MG	G	MG
	✓	✓	✓	WiMAX Macro	G	VG	MG	G	M	VG	M
	✓	✓	✓	WAVE 1	M	MP	MG	VG	G	G	VG
	✓			WAVE 2	MG	M	M	AG	M	M	M
	✓	✓	✓	WAVE 3	AG	G	G	AG	MG	MG	AP
	✓			WAVE 4	G	M	AG	AG	MG	G	G
Live Healthcare Video (LHVideo)	✓	✓	✓	LTE Macro	MG	MG	G	VG	MG	VG	MP
	✓	✓	✓	LTE Femto 1	MP	MG	VG	AG	AG	VG	AP
	✓	✓		LTE Femto 2	G	VG	AG	AG	VG	G	G
	✓			LTE Femto 3	VG	AG	G	AG	G	MG	M
	✓			LTE Femto 4	MG	G	VG	G	AG	AG	G
	✓	✓	✓	WiMAX Macro	MP	M	MG	G	G	G	MP
	✓	✓	✓	WAVE 1	G	G	VG	VG	G	G	M
	✓			WAVE 2	MG	MG	AG	VG	G	MG	AG
	✓	✓	✓	WAVE 3	AG	AG	AG	AG	VG	AG	G
	✓			WAVE 4	MP	MP	MG	AG	MG	G	P
Medical Images (MedImages)	✓	✓	✓	LTE Macro	M	MG	AG	AG	G	AG	VG
	✓	✓	✓	LTE Femto 1	M	G	VG	VG	AG	VG	G
	✓	✓		LTE Femto 2	AG	AG	VG	AG	VG	AG	P
	✓			LTE Femto 3	VG	MG	G	MG	G	MG	MP
	✓			LTE Femto 4	G	G	VG	G	AG	G	MP
	✓	✓	✓	WiMAX Macro	M	G	MG	VG	G	G	M
	✓	✓	✓	WAVE 1	VG	VG	AG	AG	VG	AG	AP
	✓			WAVE 2	MG	M	VG	AG	MG	M	M
	✓	✓	✓	WAVE 3	VG	AG	VG	AG	MG	VG	G
	✓			WAVE 4	G	VG	G	AG	MG	G	MP
Health Monitoring (HMonitoring)	✓	✓	✓	LTE Macro	G	MG	VG	AG	VG	AG	VG
	✓	✓	✓	LTE Femto 1	VG	AG	AG	VG	AG	VG	P
	✓	✓		LTE Femto 2	AG	G	G	G	MG	G	VG
	✓			LTE Femto 3	VG	AG	MG	AG	MG	VG	G
	✓			LTE Femto 4	G	VG	VG	G	G	G	VG
	✓	✓	✓	WiMAX Macro	G	AG	G	VG	AG	VG	VP
	✓	✓	✓	WAVE 1	VG	MG	VG	AG	VG	AG	G
	✓			WAVE 2	MG	MG	VG	VG	G	G	AP
	✓	✓	✓	WAVE 3	MG	MG	G	VG	MG	MG	M
	✓			WAVE 4	M	M	MG	VG	MG	MG	MP
Clinical Data Transmission (CData)	✓	✓	✓	LTE Macro	MG	M	G	VG	VG	AG	MP
	✓	✓	✓	LTE Femto 1	AG	AG	AG	AG	AG	VG	P
	✓	✓		LTE Femto 2	AG	VG	MG	VG	VG	G	M
	✓			LTE Femto 3	G	AG	M	G	G	MG	M
	✓			LTE Femto 4	VG	G	G	AG	VG	AG	G
	✓	✓	✓	WiMAX Macro	G	MG	VG	G	VG	MG	AG
	✓	✓	✓	WAVE 1	M	MP	MG	VG	G	G	AG
	✓			WAVE 2	MG	M	M	AG	M	M	M
	✓	✓	✓	WAVE 3	AG	G	G	AG	MG	MG	P
	✓			WAVE 4	G	M	AG	AG	MG	G	G

Table 3.19 The Simulated Vehicles for the Evaluation of the TFT-ACW Algorithm.

Vehicle	SLA	**Vehicular Services**	**Patient Health Status**
1	1	PRK, CV, BS, WB, LHVideo	Immediate
2	1	WB, MedImages, HMonitoring	Non-Urgent
3	1	NAV, VoIP, HMonitoring	Standard
4	1	NAV, WB, CData	Urgent
5	2	CV, LHVideo, MedImages	Non-Urgent
6	2	CV, WB, MedImages	Immediate
7	2	WB, HMonitoring	Very urgent
8	3	WB, MedImages, CData	Standard
9	3	NAV, HMonitoring, CData	Urgent
10	3	WB, MedImages, HMonitoring	Immediate

Table 3.20 The Classification of the Networks according to TFT-ACW, TFT and FSAW Results.

	Vehicle 1			**Vehicle 2**			**Vehicle 3**			**Vehicle 4**			**Vehicle 5**			**Vehicle 6**			**Vehicle 7**			**Vehicle 8**			**Vehicle 9**			**Vehicle 10**		
Method / Networks	TFT-ACW	TFT	FSAW	TFT-ACW	TFT	FSAW	TFT-ACW	TFT	FSAW	TFT-ACW	TFT	FSAW	TFT-ACW	TFT	FSAW	TFT-ACW	TFT	FSAW	TFT-ACW	TFT	FSAW	TFT-ACW	TFT	FSAW	TFT-ACW	TFT	FSAW	TFT-ACW	TFT	FSAW
LTE Macro	4	3	3	2	2	2	**1**	**1**	**1**	2	2	**1**	2	2	**1**	2	**1**	**1**	**1**	2	2	**1**	**1**	2	2	3	4	3	2	3
LTE Femto 1	3	2	**1**	**1**	**1**	**1**	-	-	-	-	-	-	-	-	-	-	-	-	-	-	-	-	-	-	3	**1**	**1**	2	**1**	**1**
LTE Femto 2	2	**1**	2	3	4	3	-	-	-	-	-	-	-	-	-	-	-	-	-	-	-	-	-	-	-	-	-	-	-	-
LTE Femto 3	-	-	-	-	-	-	-	-	-	-	-	-	-	-	-	-	-	-	-	-	-	-	-	-	-	-	-	-	-	-
LTE Femto 4	-	-	-	-	-	-	-	-	-	**1**	4	5	-	-	-	-	-	-	-	-	-	-	-	-	-	-	-	-	-	-
WiMAX Macro	7	7	8	6	7	7	3	3	2	4	5	3	4	4	4	4	4	4	3	3	3	3	3	3	4	2	3	4	5	5
WAVE 1	5	4	4	4	3	4	2	2	3	3	**1**	2	3	3	3	**1**	3	3	2	**1**	**1**	2	2	**1**	**1**	4	2	**1**	3	2
WAVE 2	6	6	7	8	8	8	5	5	5	6	7	7	-	-	-	-	-	-	-	-	-	-	-	-	-	-	-	-	-	-
WAVE 3	**1**	5	5	5	5	6	4	4	4	7	6	6	**1**	**1**	2	3	2	2	4	4	4	4	4	4	5	5	5	5	4	4
WAVE 4	8	8	6	7	6	5	6	6	6	5	3	4	-	-	-	-	-	-	-	-	-	-	-	-	-	-	-	-	-	-

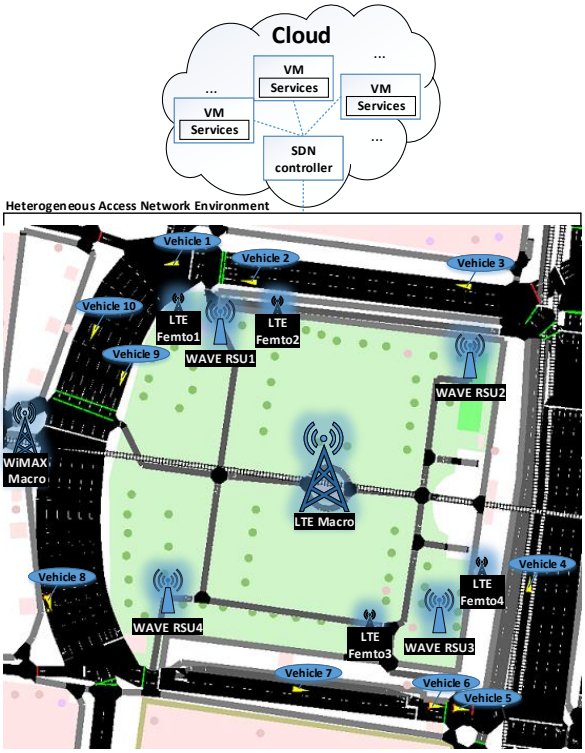

Figure 3.21 The Simulated Topology for the Evaluation of the TF-ANP and the TFT Algorithms.

Three Service Level Agreements (SLAs) are defined. Each SLA determines the available networks for each service type. SLA1 supports all the available networks while SLA3 supports only a small subset of the available networks.

Table 4.1 presents the lingustic terms and the corresponding interval-valued trapezoidal fuzzy numbers used for the criteria attributes of the available networks, while Table 3.18 presents the corresponding specifications per service and SLA of each network, in terms of throughput, delay, jitter, packet loss ratio, price, security and service reliability.

We consider the case where 10 vehicles with patients are moving inside the network environment and need to be connected to a network which satisfies the requirements of their services and at the same time complies with their patient health status, as well as with their respective SLA agreements. The health status of each patient is evaluated using the Manchester Triage System (MTS) [173] healthcare classification system, which defines 5 health statuses, called Non-Urgent, Standard, Urgent, Very-Urgent and Immediate. The Non-Urgent status has the lower risk about patient's life, while the Immediate status has the higher one.

3.1.5.3.2 Performance Evaluation : During the network selection process initially the relative importance $\tilde{\omega}_{\tilde{p}s}$ of each service is considered with respect to the patient health status. Figure 3.22 presents the importance of each service per patient health status, as it is obtained

using the TF-AANP method. As it can be observed, the importance of the MED services depends on the patient health status. Indicatively, when the patient health status becomes immediate, the MED services obtain higher importance than the DA and the PEnI services. Accordingly, when the patient health status becomes Non-Urgent, the relative importance of the services is quite similar. Subsequently, the TF-AANP estimates the decision weights w_e per service type and patient health status, using the ANP network model proposed in [171]. The criteria weights per SLA for the DA and the PEnI services are presented in Figures 3.23 and 3.24, respectively. Also, for each possible health status, the criteria weights per healthcare service for the MED services are presented in Figure 3.25. As illustrated the weights are proportional to the constraints of each service as well as to the health status of each patient. In particular, the weight of the price criterion is low for Immediate health status, resulting in a weight value which is very close to 0. Accordingly, when the health status is evaluated as Non-Urgent, the medical risk for the patient is very low and the price criterion becomes more important.

Considering the relative importance $\tilde{\omega}_{\tilde{p}s}$ of each service and the criteria weights w_e for the DA, PEnI and MED services, the final criteria weights are estimated for each vehicle with respect to the health status of onboard patients, as well as to the SLA of each vehicle (Figure 3.26).

The ranking of the network alternatives is performed using the TFT-ACW algorithm using the afforementioned criteria weights for each vehicle.

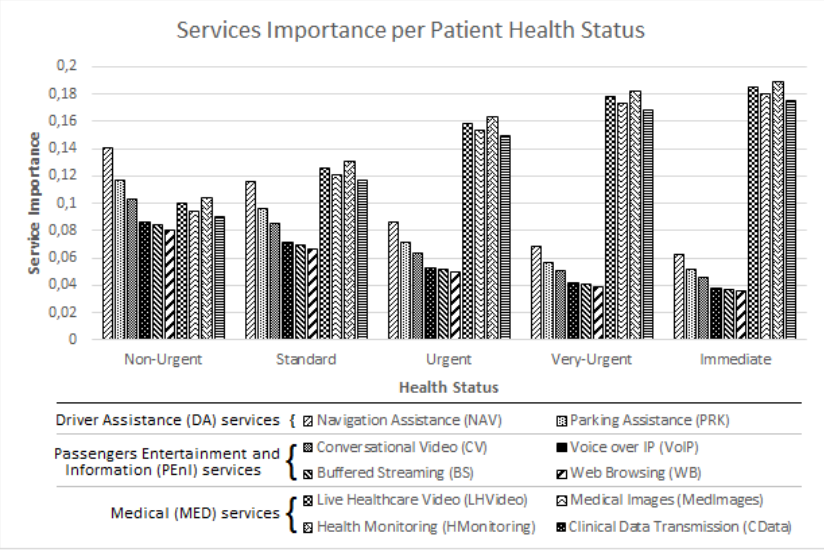

Figure 3.22 The Importance of each Service per Patient Health Status.

Subsequently, the experimental results of the TFT-ACW method are compared with the ones obtained using the TFT [171] and the FSAW [179] algorithms (Table 3.20). When the

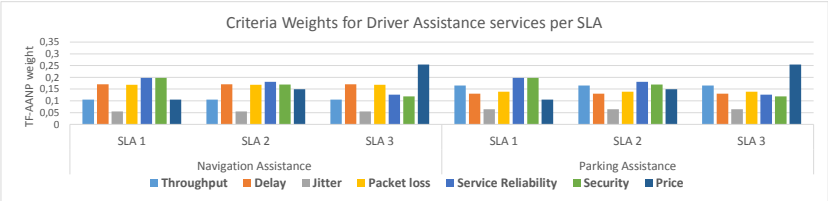

Figure 3.23 The TF-AANP Criteria Weights for the DA Services per SLA.

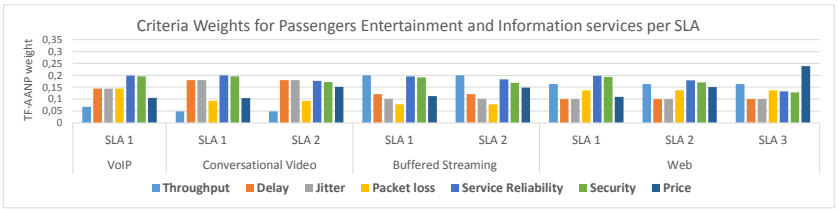

Figure 3.24 The TF-AANP Criteria Weights for the PeNI Services per SLA.

patient health status is Non-Urgent (vehicles 2 and 5) or Standard (vehicles 3 and 8) the results of TFT-ACW and TFT are similar, due to the similar relative importance considered by the TFT-ACW for each service. However, when the patient health status gets worse, the TFT-ACW assigns higher importance to the MED services and selects the most appropriate network to satisfy their strict constraints. Indicatively, in the case of vehicle 1, TFT-ACW selects the WAVE 3 network, which provides VG for service reliability, as well as AG for throughput, delay, jitter, packet loss and security, for the LHVideo medical service. On the contrary, the results of both TFT and FSAW are negatively affected by the existence of non medical services in the vehicle 1 ignoring the immediate health status of the patient. Specifically, TFT selects the LTE Femto 2 network, which provides worse specifications for the LHVideo service (e.g. G for throughput and VG for delay), while FSAW selects the LTE Femto 1 network, which also provides worse specifications for the aforementioned medical service (e.g. MP for throughput and MG for delay).

Figure 3.25 The TF-AANP Criteria Weights for the MED Services per SLA and Patient Health Status.

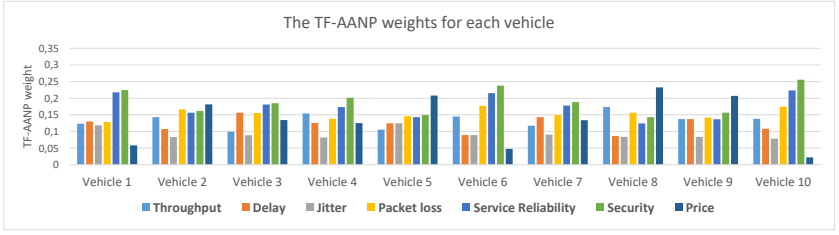

Figure 3.26 The TF-AANP Weights for each Vehicle.

3.2 Mobility Management Schemes for 5G Wireless Networks

3.2.1 Existing Mobility Management Schemes

In this section an overview of the existing mobility management schemes is presented. The mobility management process consists of the handover (HO) initiation, the network selection and the HO execution subprocesses. The consideration of the subprocesses that each scheme implements provides a useful view about each scheme's functionalities.

Some schemes implement only the HO initiation subprocess. These schemes aim at the evaluation of the necessity to perform a handover, by avoiding either unnecessary or delayed HOs, in order to ensure the continuity of vehicular services. Several parameters can be considered. The most common ones include signal quality factors, criteria that affect the vehicular services, the vehicle's velocity, the cells' coverage area and the operators' policies. Also, it should be noted that in these cases, the network selection and the HO execution must be performed using third party algorithms.

The Street Specific Handover for Vehicular Terminals (SSHVeT) [180] algorithm considers street aware parameters to evaluate the necessity of performing a handover. Parameters such as vehicle velocity, road direction, Reference Signals Received Power (RSRP) [181] and radio propagation characteristics are considered for the HO initiation. The algorithm adapts the corresponding handover thresholds considering the obtained parameter values for each street, in order the ping-pong effect to be minimized.

The Improved Inter-Network Handover (IINH) [182] estimates the necessity of performing a handover considering the cell size and the vehicle velocity, which affect the time that a vehicle will remain inside the coverage area of a cell. The vehicle makes the decision of performing a handover considering the aforementioned parameters. It should also be noted that the cell size is estimated considering the RSS, the path loss, the required transmission power from the vehicle to the base station, and the geographical terrain information. The scheme is implemented in the network layer using the functionalities offered by Mobile IP (MIP) to manipulate the vehicle mobility.

The Decision Process for Vertical Handover in Vehicular Networks (DPVHO) [183] algorithm estimates the necessity to perform a HO when the vehicle moves from an area covered by a network to an area covered by another network. It aims at reducing the HOs failure rate and the unnecessary HOs using a utility function based mechanism where parameters such as RSS, vehicle trajectory, cell radius and path loss exponent of each place are considered.

The Context Aware Handover Policy (CAHP) in [184] scheme considers an LTE network topology where both Macrocells and Femtocells exist. A load-aware algorithm is described, which determines two handover thresholds, namely the γ_{th}^{M} and the γ_{th}^{F}, for Macrocells and

Femtocells, respectively. Both of these thresholds are evaluated, considering the Reference Signal Received Power (RSRP) threshold defined in LTE [14], as well as network load information. When RSRP drops below the corresponding γ_{th} threshold, a Time-to-Trigger (TTT) timer is activated, which is initialized to a certain value T, considering parameters such as the cell transmission power, the distances between the available cells, the path loss, the carrier frequency, the network traffic load and the user velocity. During the countdown, if RSRP returns to values above the corresponding γ_{th} threshold, the timer is deactivated. Otherwise, when the timer becomes equal to zero, the handover is initiated and the user is transferred to the network with the highest RSRP.

The Context Aware Load Balancing (HO-CALB) [185] is another HO initiation scheme. It considers the scenario where both WiFi and WiMAX networks coexist. A network load aware algorithm distributes the traffic load to the WiFi and the WiMAX networks considering the available bandwidth of each network. Each user has a set of services with strict QoS constraints. If the observed QoS drops below a threshold, a handover policy instructs the users to perform a handover.

Several schemes implement only the network selection subprocess. These algorithms aim at the selection of the most appropriate access network for each vehicular user among a set of network alternatives. Similar to the HO initiation algorithms, several parameters can be considered, including Quality of Service (QoS) or Quality of Experience (QoE) factors, user preferences and operators' policies. In these cases, the HO initiation and the HO execution must be performed using third party algorithms.

The Mobility Aware Handover in Ultra Dense Vehicular Environment (MAH-UDVE) [186] scheme considers the direction of a vehicle's mobility to select the most appropriate network. The vehicle movement is statistically analyzed in order to create a set of possible next cells. Subsequently, four different approaches can be applied to select the most appropriate cell from the aforementioned set. The first approach selects the nearest cell, while the second approach selects the next cell that exists in the same street in the same direction with the direction of vehicle movement. The third approach selects the next cell that exists in the same street, but in the opposite direction of the vehicle's movement. Finally, the fourth approach selects the cell with the lowest load.

The Intelligent Network Selection (INS) [187] scheme implements the network selection process for supporting audio and video streaming vehicular services in heterogeneous network access environments. A utility function which considers the SNR, the channel capacity and the connection life time parameters is used. For the estimation of the connection lifetime parameter the vehicle's velocity and the cell radius are also considered. The candidate network which obtains the higher score from the proposed utility function is selected.

The Technique for Order Preference by Similarity to Ideal Solution (TOPSIS) [188][189] algorithm performs the selection of the best network access technology by considering contradictory selection criteria. The main concept of the TOPSIS algorithm is that the best alternative network should have the shortest distance from the positive ideal solution and the longest distance from the negative ideal solution. The criteria that could be considered include the network throughput, the delay, the jitter, the packet loss ratio, the network usage price, the security and the service reliability. Also, the importance of these criteria can be estimated either using the Analytic Hierarchy Process (AHP) [190] or the Analytic Network Process (ANP) [191] method.

The Simple Additive Weighting (SAW) [188] considers multiple criteria to perform the network selection. Firstly, the criteria weights are estimated using a method such as AHP or ANP. Subsequently, for each network alternative, the criteria values are normalized. Then, each value is multiplied with the corresponding weight in order the weighted criteria values to be calculated. Finally, the weighted criteria values are summarized in order to estimate the overall rating of the network alternative. The network with the highest rate is finally selected.

The Multiplicative Exponent Weighting (MEW) [188] method is similar to SAW. However, in MEW the weighted criteria values are multiplied with each other to estimate the overall rating of the network alternative.

The Gray Relational Analysis (GRA) [192] analyzes the relationship grade between the network alternatives and the ideal solution to perform the network selection. The ideal solution is calculated first. Subsequently, the similarity of each alternative network with the ideal solution is estimated using the Grey Relational Coefficient (GRC) [193]. The network with the highest similarity to the ideal solution is selected.

The concept of the Distance to Ideal Alternative (DIA)[188] algorithm is similar to the concept of TOPSIS. Firstly, DIA estimates the positive and the negative ideal solutions. Then, the Manhattan distance [194] of each network from the positive and from the negative solution is calculated. The network that has the shortest distance from the positive ideal solution and the longest distance from the negative ideal solution is selected.

The Weighted Product Method (WPM) [195] for each alternative network raises the normalized criteria values to the corresponding criteria weights values. Subsequently, the method calculates the product of the weighted values. The network with the highest product is finally selected.

In Quantum-inspired Immune Clonal Algorithm for Network Selection (QICA-NS) [196] two utility functions are used for network selection, one for the user and one for the network. The user utility function considers user related parameters, such as the user preferences, his moving velocity and his monetary budget. Accordingly, the network utility function considers

network related parameters, such as the network load, the price and the network QoS which is estimated using TOPSIS.

Sometimes many users have similar trajectories as they move. This situation becomes more frequent in the case of vehicular networks, since each vehicle usually serves multiple passengers. Consequently, many users with similar positions and requirements need to perform a network selection, usually considering the same network alternatives. In such cases, increased computational overhead arises from the decision process, since this process runs independently for each user. To address this issue, algorithms for performing group handover have been proposed in the research literature. An algorithm of this category groups users with similar trajectories in order to perform the network selection once for the entire user group, thus releasing usable system resources.

The Group Vertical Handover using Time Window (GVHO-TW) [197] distributes the MTs HO requests in a time sequence. Thus, each MT performs network selection using a utility function when its turn comes, considering the decision of all the previous MTs in order to select the most appropriate network not only to satisfy its requirements, but also to achieve a satisfactory load distribution to the available access networks.

Although GVHO-TW avoids the calculation of simultaneous decisions of multiple MTs, additional handover delays occur since each MT waits for its turn in order to perform the network selection. To address this issue, the Group Vertical Handover with Probability Distribution (GVHO-PD) [197] scheme uses a probability distribution vector instead of a time window. This vector contains a value for each available network, which determines the probability of the network to be selected from the MTs, considering its performance. Subsequently, each MT generates a random MT probability value and compares it with the values of the aforementioned probability vector. The network with the closest probability to the random MT probability value is selected. Thus, the MTs are distributed to the available networks.

Although the GVHO-PD scheme distributes probabilistic the workload to the available networks, it does not optimize the entire system performance. To address this issue the Network Assisted Group Vertical Handover (NA-GVHO) [197] scheme does not use a probability vector, but it collects information from both the networks and the MTs. Then, each MT performs the network selection using a Multi Attribute Decision Making (MADM) algorithm which considers both the MT's requirements and the current workload of each network, in order to distribute the workload to the available networks.

In general, there is a rate of uncertainty in characterizing performance measurements as well as rates of influence of performance metrics. Therefore, fuzzy MADM (FMADM) methods expressing uncertain quantities by fuzzy numbers have received the interest of many researchers in decision theory. In particular several FMADM network selection methods are suggested

utilizing linguistic variables, triangular fuzzy numbers, trapezoidal fuzzy numbers etc. to model network attributes and their respective weights. The use of fuzzy logic for network selection requires the definition of logic rules from specialists with thorough knowledge of the behavior of the available access networks in various conditions.

The Trapezoidal Fuzzy TOPSIS (TFT) [171] deals with the network selection process. It is a fuzzy version of the TOPSIS algorithm. TFT uses linguistic values for evaluating the criteria attributes, while each linguistic value is represented by an Interval Valued Trapezoidal Fuzzy Number (IVTFN) [198]. The criteria considered for the candidate networks ranking include throughput, delay, jitter, packet loss, price, security and service reliability. The Analytic Network Process (ANP) [191] is used for the estimation of the criteria weights indicating the importance of each criterion. The network that accomplishes the higher TFT rank is selected.

The Trapezoidal Fuzzy TOPSIS with Adaptive Criteria Weights (TFT-ACW) [66] is an improved version of the TFT algorithm. It deals with the satisfaction of the constraints of multiple vehicular services, in cases where MED services coexist with other service types in the vehicular environment. Specifically, DA services, PEnI services and MED services are considered that provided to vehicular users. The presence of MED services affects the importance of other services in situations where patients with immediate health status exist within the vehicle. The criteria used for network evaluation include throughput, delay, jitter, packet loss, service reliability, security and price. The Trapezoidal Fuzzy Adaptive Analytic Network Process (TF-AANP) is also proposed for the estimation of the services importance as well as of the corresponding criteria weights, which are adapted considering the health status of onboard patients and the Service Layer Agreement (SLA) of each vehicle.

In Intelligent Access Selection using Fuzzy Neural Network (IAS-FNN) [199] the concepts of fuzzy logic, neural networks and utility functions are combined to perform network selection. The proposed method makes use of a fuzzy neural network which obtains network, user and terminal related input criteria and evaluates the performance of each access network. The attributes of the criteria are defined through utility functions and processed through the fuzzification, interference and defuzzification layers of the neural network.

It should also be noted that some schemes implement only the HO execution. These algorithms determine the signaling that should be performed in order the HO to be successfully completed. A critical parameter that should be satisfied is the HO delay which is directly affected by the aforementioned signaling. Also, in the case of such algorithms, the HO initiation and the network selection must be performed using third party algorithms.

In Bulk Fast PMIPv6-based Network Mobilty (BFP-NEMO) [200], one or more RSUs are controlled by a Mobility Management Entity (MME) [201], which is called Mobile Access Gateway (MAG). The vehicles that are inserted in a MAG domain are grouped. Then, the

corresponding MAG pre-establishes a bidirectional tunnel between the vehicles' group and the candidate neighboring MAGs. Each neighboring MAG caches the data for each vehicle of the aforementioned group. Subsequently, when a vehicle of the group is connected to the next RSU, the corresponding MAG forwards the cached data to the vehicle.

The Enhanced Proxy Fast-handover Mobile IPv6 for Vehicular Networks (ePFMIPv6) [202] scheme implements a proactive Layer 3 handover mechanism. The concept of Mobile Access Gateway (MAG) is considered in this scheme as well. The issue of the simple PFMIPv6 protocol, where the next MAG waits to receive a Handover Acknowledge (HAck) [203] message from the serving MAG (although the vehicle has arrived to it) to start the data forwarding to vehicles, is resolved. Specifically, when the serving MAG services the vehicle, it also establishes a tunnel with each neighboring MAG which is considered as a candidate next MAG for the vehicle according to its RSS. When the vehicle arrives to its next MAG, its data are immediately forwarded to it through the aforementioned tunnel, without waiting for the HAcK message. Finally, when the HAcK message is received by the next MAG, the tunnel is abolished and the data which follows are forwarded to the vehicle by the next MAG without the tunnel. In this case, the "next MAG" which is now considered as the serving MAG establishes a tunnel with each neighboring candidate next MAG and so on.

Schemes that implement more than one mobility management subprocesses have also been proposed in the research literature. Many of these schemes implement both HO initiation and network selection.

The Predictive Handover Mechanism for Video Streaming in Cloud Based Urban VANET (PHMVV) [204] scheme defines a list of available networks is created for each vehicle considering its velocity, its distance from each network, as well as its moving direction. The assumption that the vehicle knows its geographical position, as well as the positions of the available networks, is made. Each vehicle monitors the link quality of the candidate networks, considering their Signal to Noise Ratio (SNR), Bit Error Rate (BER) and Packet Error Rate (PER) parameters. If a network alternative has higher link quality than the vehicle's current network, the vehicle performs a handover to this alternative.

Another scheme that implements both HO initiation and network selection is the Mobility Aware Handover for Smart Cities Environment (MAH-SCE) [205]. MAH-SCE uses traffic information that is gathered by sensors that are deployed in a Smart City [206] environment, to perform the HO initiation and the network selection. The scheme decides when to initiate a handover as a function of the aforementioned sensor data about the road traffic, as well as the perceived SNR. Subsequently, the vehicles with velocity up to 16 m/s consider both Macrocells and Femtocells as alternatives for performing a handover to them. In this case, if Femtocells exist inside the vehicle's area, the scheme selects the Femtocell which has the higher estimated

time that the vehicle will remain connected without a need to perform a handover to another cell. On the contrary, if the vehicle velocity is higher than 16 m/s only the Macrocells are considered as alternatives and the one that maximizes the time that the vehicle will remain connected to it, is selected.

The Speed-based Vertical Handover (S-VHO) [207] scheme also implements the HO initiation and the network selection subprocesses of the HO management. During the HO initiation, the algorithm considers the vehicle's velocity, the ingress time of the vehicle to the current cell and the geographical position of the vehicle (using its GPS) to calculate the cell crossing time. Subsequently, considering both the estimated cell crossing time and the observed throughput, the algorithm decides when a HO must be initiated. Afterwards, the alternative network that maximizes the throughput is selected and, then, the algorithm is deactivated for a time period T in order the ping-pong effect to be reduced. Finally, when the algorithm is reactivated it estimates when the next HO must be initiated.

The Media Independent Handover using Predictive Geographical Information (MIH-PGI) [208] defines a MIH-oriented HO mechanism for ensuring the continuity of the vehicular services and the minimal handover latency. During the HO initiation the vehicle estimates the appropriate time to perform a handover by predicting the behavior of its current network link quality based on the geographic information received from the Media Independent Information Services (MIIS) component of the MIH protocol, about the network access point position as well as the velocity of the vehicle. Subsequently, the vehicle lists the available candidate networks, while the next network is selected considering the estimated time duration that the vehicle will remail inside the coverage area of each candidate network. Thus, the network which maximizes this time is selected in order to minimize the number of future handovers.

The Cognitive Vertical Handover for Vehicular Communication (CVHO) [209] scheme considers multiple criteria to perform mobility management in a cognitive radio vehicular environment. The handover initiation considers parameters such as the RSS, the available bandwidth, the delay, the network load, the usage cost, the vehicle velocity and the service type, to evaluate the necessity of performing a VHO. Subsequently, the network selection is performed using the Analytic Hierarchy Process (AHP) [190] method using the aforementioned criteria. An Artificial Neural Network (ANN) [210] is used to train the scheme to adapt its handover threshold in order to take the reflex action to avoid either unnecessary handovers or link-down situations. The ANN is trained considering the success or the failure of all the previous handover initiation and network selection decisions.

The Auction Approach for Mobility Prediction (AAMP) [211] scheme defines a group based HO management mechanism which aims to maximize system throughput, while at the same time to minimize the network load when multiple vehicles perform simultaneous

handovers. It assumed that each vehicle is equipped with a GPS device. When a vehicle reaches the edge of its current network's coverage, it triggers a VHO, while at the same time it reports its position to a Vertical Handover Decision (VHD) controller, which could be considered as an SDN controller for HO functionalities implementation. When a VHD controller receives a HO request from a vehicle, it creates a list with the candidate networks for the vehicle considering the vehicle's position. Thus, considering the vehicle's velocity and position, the VHD controller predicts the entrance time and the exit time of the vehicle from each candidate network. When multiple vehicles of similar positions trigger a handover, the VHD controller groups them. Subsequently, an auction based [212] algorithm selects the most appropriate network for the aforementioned group of vehicles in order the total throughput of the group to be maximized. Thus, the network selection is performed once for the entire group of vehicles and not once per vehicle, thus minimizing the network load occurring from the decision process.

The Vertical Handover for Vehicular Cloud Computing Systems (VHO-VCC) [67] scheme takes into account the vehicle's velocity as well as its current connection type. A two step HO algorithm that reduces operation costs and optimizes mobility management is applied. Initially, a HO initiation process evaluates the necessity to perform handover using a Mamdani inference system [213] which evaluates the user satisfaction grade. When the user satisfaction drops below a predefined threshold, which depends on the vehicle's SLA, the network selection is performed using TFT in order to select the most appropriate network alternative considering both the vehicular service requirements and the operators' policies.

The Geolocation-based Multi ACcess network Handover algorithm for vehicUlar environments (GEO-MACHU) [214] algorithm implements three tasks, namely the Networking, the Neighborhooding and the Decision Making task. The Networking task performs the HO initiation considering context-aware information about the current network provided by the Media Independent Event Service (MIES) and by the Media Independent Command Service (MICS) [215] of the IEEE 802.21 MIH protocol (e.g. information about link-down events). The Neighborhooding task collects information about the available networks in the vehicle's location using the Media Independent Information Service (MIIS) [216] of the MIH protocol . The gathered information is considered by the Decision Making task, which performs the network selection using the TOPSIS algorithm.

The Hybrid Communication Approach (HCA) [217] scheme defines two network interface types, namely the IEEE 802.11p network access technology which is considered as the primary interface, while the 3GPP LTE is considered as the secondary. By default, a vehicle is connected to the primary interface. A QoS aware HO initiation algorithm is applied, which instructs the vehicle to perform handover to the secondary interface when the observed packet loss of the provided services exceeds a maximum acceptable threshold. Thereafter, a timer is activated

specifying the time interval that the user remains connected to a secondary interface. When the timer expires and the estimated packet loss ratio of the primary interface is lower than the maximum acceptable threshold, the vehicle performs a handover back to the primary interface.

The Velocity Aware Handover (VAH) [218] HO management scheme defines two network tiers, namely the tier-1 consisting of Macrocells and the tier-2 consisting of Femtocells. Four vertical handover strategies are considered, namely the Best Connected (BC), the Femto Skipping (FS), the Femto Disregard (FD) and the Macro Skipping (MS). The BC strategy is applied to static users and to users with Low mobility, while both Macrocells and Femtocells are considered as alternatives. The user connects to a Macrocell if $P_1 \cdot B_1 \cdot R_1^{-\eta} > P_2 \cdot B_2 \cdot R_2^{-\eta}$ is satisfied, or to the nearest Femtocell if $P_1 \cdot B_1 \cdot R_1^{-\eta} < P_2 \cdot B_2 \cdot R_2^{-\eta}$ is satisfied, where P is the transmission power, B is the bias factor, R is the user distance and η is the pathloss exponent for each tier. The FS strategy considers users with Medium mobility. The Femtocells alternatives are skipped to reduce the handover rate, when $P_1 \cdot B_1 \cdot R_1^{-\eta} < P_2 \cdot B_2 \cdot R_2^{-\eta}$. In the FD strategy, which is applied to users with High mobility, the user always skips the available Femtocells and connects only to the available Macrocells. Finally, in the MS strategy, for users with extremely High mobility, the user skips the entire set of Femtocells as well as some of the Macrocells.

Similarly to the FMADM network selection algorithms, some schemes that perform both HO initiation and network selection apply the operating principles of fuzzy logic. In these cases, as the number of selection criteria and the available networks increases, the rules become more complex, struggling to define effective policies either for evaluating the necessity to perform a handover or for selective the most appropriate network for the user. Accordingly, the use of fuzzy logic based solutions is limited to handover decision schemes with a reduced number of selection criteria and networks.

In the Fuzzy Logic Based Vertical Handover (FLB-VHO) [219] scheme, the RSS-based handover initiation mechanism is applied initially. Then, during the second phase, a triangular fuzzy MADM algorithm that considers parameters such as the RSS, the delay, the network load and the battery utilization is used.

In Fuzzy MADM for Vertical Handover (FMVHO) [220], an heterogeneous network environment that consists of LTE and WiMAX networks is considered. Firstly, the simple RSS based method is used for the network initiation. Thereafter, a triangular fuzzy version of the TOPSIS method is proposed for the network selection. Network parameters such as the offered data rate and the delay are considered during the network selection process.

Several schemes implement both the network selection and the HO execution. The Intermediate Mobile Access Gateway Inter-Domain Handover (iMAG-IDH) [221] scheme deals with the network selection and the HO execution parts of the HO management procedure, considering the operating principles of Proxy Mobile IPv6 (PMIPv6). Concerning the network

selection process, a location tracking mechanism is used in order to estimate the vehicle's moving direction. Thus, the most probable next RSU that the vehicle will pass through its coverage area is selected. Subsequently, the scheme proactively performs a Layer 3 handover where the appropriate signaling is exchanged in order to start the forwarding of the next data packets. Afterwards, a Layer 2 handover is performed where the vehicle is attached to the selected RSU.

The Hidden Markov Model - Kalman Filter (HMM-KF) [222] scheme deals with the network selection and the HO execution subprocesses of the mobility management. The mobility of the vehicles is modeled by tracking their movement considering information from their GPS devices. Also, each network maintains a Hidden Markov Model (HMM) indicating the possibilities that each vehicle connected to the network has to handover to each neighboring network, which are estimated using the Kalman Filter (KF). Subsequently, considering the HMM each vehicle selects its next network. Afterwards, the appropriate signaling is exchanged between the vehicle and the selected network in order the handover to be performed. Finally, the HMM probabilities of the previous and the new vehicle's network are updated.

The QoS Aware Handover for Session Initiation Protocol services in Vehicular Networks (QAH-SIP) [223] scheme is implemented in the Application Layer of the OSI stack. QAH-SIP defines a HO execution process for supporting vehicular SIP services. Initially, the vehicle performs the network selection considering QoS aware information (such as the maximum acceptable delay and the packet loss, as well as the minimum required RSS) required to satisfy the SIP service constraints. Then, it performs a pre-registration to the selected RSU where the vehicle also sends information about its position and velocity. Then, the selected RSU reserves the required resources in order to be available to serve the incoming vehicle. Subsequently, the SIP signaling process [224] is performed in order the HO to be completed.

It should also be noted that some schemes implement the entire mobility management subprocesses, including the HO initiation, network selection and HO execution.

The Vertical Handover for VANET using Multiple Parameters (VHOMP) [225] algorithm considers multiple criteria to perform the mobility management. During the HO initiation the Received Signal Strength (RSS) parameter is turned into account. When it becomes lower than a predefined threshold the HO is initiated. Subsequently, the network selection is performed considering the network bandwidth and the vehicle's velocity. Finally, the HO is executed using the appropriate signaling in order the vehicle to be connected to the selected network.

The Navigation Assisted Seamless Handover (NASH) [226] uses a HO initiation algorithm which considers the vehicle velocity, as well as RSRP information, to evaluate the necessity to perform a handover. The navigation information about the vehicle is used in order the most probable trajectory to be estimated, while the next cell that exists in this trajectory is selected.

Finally, considering an LTE-A network infrastructure the scheme proposes the appropriate signaling that should be performed between the current RSU/BS, the next RSU/BS the MME and the SGW, in order seamless handover to be operated ensuring the continuity of the vehicle's services.

The Robust Handover in Vehicular Networks (RHVN) [227] scheme defines that in Layer 2 the HO initiation is performed when the RSS drops below a predefined threshold. Subsequently, the vehicle selects the RSU with the higher RSS and performs the HO execution. In Layer 3 the handover occurs when a Layer 2 handover is completed. In this case, the vehicle uses its Original Care of Address (OCoA) [228] for fast IP connectivity and then its data are forwarded from its new RSU by applying an improved version of MIPv6 protocol, which considers the permanent vehicle's OCoA.

The Intelligent Handover for Vehicular Networks (IHVN) [229] scheme aims at the satisfaction of the real-time services' constraints during the vehicle's movement across different networks. The FMIPv6 mobility management protocol is considered, while the use of 802.21 MIH ensures the interoperability between different network access technologies. During the HO initiation process, when the link quality drops below a predefined threshold, a *MIH_Link_Going_Down* message is transmitted to the vehicle. This message triggers the vehicle to perform a VHO. Subsequently, a list of existing nearby networks is obtained, while link quality information (e.g. bandwidth) is obtained from each candidate network using *MIH_MN/N2N_HO_Candidate_Query* messages. Then, the link quality parameter is considered in order the network with the higher link quality to be selected. Finally, during the HO execution the appropriate signaling is exchanged between the vehicle and the selected network, while the HO is completed using a *MIH_Link_Up* message indicating that now the vehicle has been connected to the selected network.

In the VANET Backup Communication (VANBA) [230] scheme, the concept of the Communication Mediator (CM) is introduced. A CM is a vehicle that provides access to vehicular services through V2V communication. However, in a 5G-VCC systems, the CM could also be a RSU/BS or a pedestrian, that provides access to the services through V2I or V2P communication, respectively. Two processes for accomplishing the mobility management are defined, namely the Link Monitoring and the HO process. The Link Monitoring process, implemented at OSI Layers 6 and 7, monitors which CMs in the vehicle's area are available for providing access to vehicular applications (e.g. considering the coordinates of their positions). The HO process, implemented at OSI Layer 3, monitors the IP reachability to the services' providers. When the reachability is lost or the link quality drops below a predefined QoS threshold, a handover should be performed. Subsequently, the candidate CMs are sorted using a utility function where the bandwidth and the monetary cost parameters are considered. Then, the first

CM in the sorted list is selected and the HO is executed. If the HO execution fails (e.g. due to topology changes) then the next CM in the aforementioned list is selected and so on.

In Vehicular Fast Handover for Mobile IPv6 (VFMIPv6) [231] when the vehicle approaches the boundary of its current RSU (considering the RSS), it sends to the current RSU a request in order handover to be initiated. Along with the request, Handover Assist Information (HAI) is also sent from the vehicle to its current RSU, containing information about the candidate RSUs for the vehicle, considering the RSS of each RSU. The current RSU implements a utility function based mechanism where the HAI information is considered, in order to select the most appropriate next RSU for the vehicle, which is the one that minimizes the handover latency, the packet loss that occurs during the handover and the total communication overhead that is observed due to the handover latency and the corresponding packet loss. Thereafter, the appropriate signaling is exchanged between the current RSU, the selected next RSU, the Mobile IPv6 (MIP) Home Agent (HA) [232][233] and the MIP Correspondent Node (CN) [232] in order the vehicle to be connected to the selected next RSU. Table 3.21 summarizes the main functionalities of the discussed schemes.

Table 3.21 The Mobility Management Activities of each Scheme.

Scheme	VHO Initiation	Network Selection	VHO Execution
VHOMP [225]	✓	✓	✓
SSHVeT [180]	✓		
PHMVV [204]	✓	✓	
MAH-SCE [205]	✓	✓	
NASH [226]	✓	✓	✓
MAH-UDVE [186]		✓	
RHVN [227]	✓	✓	✓
S-VHO [207]	✓	✓	
BFP-NEMO [200]			✓
IINH [182]	✓		
IHVN [229]	✓	✓	✓
VANBA [230]	✓	✓	✓
iMAG-IDH [221]		✓	✓
VFMIPv6 [231]	✓	✓	✓
MIH-PGI [208]	✓	✓	
CVHO [209]	✓	✓	
DPVHO [183]	✓		
GVHO-TW [197]		✓	
GVHO-PD [197]		✓	
NA-GVHO [197]		✓	
ePFMIPv6 [202]			✓
AAMP [211]	✓	✓	
INS [187]		✓	
HMM-KF [222]		✓	✓
QAH-SIP [223]		✓	✓
CAHP [184]	✓		
HO-CALB [185]	✓		
TOPSIS [188][189]		✓	
TFT [171]		✓	
TFT-ACW [66]		✓	
VHO-VCC [67]	✓	✓	
GEO-MACHU [214]	✓	✓	
SAW [188]		✓	
MEW [188]		✓	
GRA [192]		✓	
DIA [188]		✓	
WPM [195]		✓	
QICA-NS [196]		✓	
IAS-FNN [199]		✓	
FLB-VHO [219]	✓	✓	
FMVHO [220]	✓	✓	
HCA [217]	✓	✓	
VAH [218]	✓	✓	

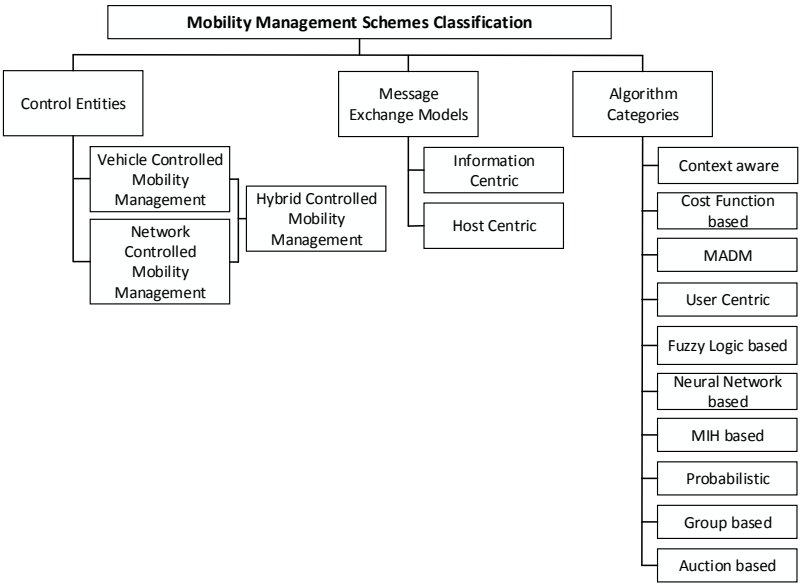

Figure 3.27 Classification of Mobility Management Schemes.

3.2.2 Taxonomy of Existing Mobility Management Schemes

In this section, the schemes described in Section III are classified. Firstly, the control entities that can implement each scheme are mentioned. Also, the OSI Layers with which each scheme is involved are considered. Thereafter, the supported message exchange models are described and, finally, the category of each scheme's algorithm is determined completing an in-depth study about each scheme's implementation.

3.2.2.1 Control Entities

Considering the entities that control the mobility management the entire process could be categorized as Vehicle Controlled or as Network Controlled. Furthermore, some solutions combine both Vehicle and Network control. In these cases, the mobility management process is called as Hybrid Controlled. The following paragraphs describe the available solutions, considering the aforementioned control entities.

3.2.2.1.1 Vehicle Controlled Mobility Management : In the vehicle controlled mobility management schemes the entire process is controlled by the vehicle (or user) equipment, namely the vehicle's OBU or the passengers' devices.

3.2.2.1.2 Network Controlled Mobility Management : In the network controlled solutions, the mobility management is performed by devices located in the network infrastructure.

Considering the underling network architecture, the mobility management task can be implemented from a Mobility Management Entity (MME) or an SDN controller installed in a Cloud or a Fog infrastructure. Alternatively, a Mobile Access Gateway (MAG) could be used, namely a BS or a RSU enhanced with mobility management capabilities. In general, the entity that performs the mobility management collects the necessary information for evaluating the necessity to perform a HO initiation. Also, after each HO initiation this entity selects the most appropriate network for the vehicle, using the methods that each mobility scheme implements for the network selection process. Subsequently, it orchestrates the HO execution through the appropriate signaling in order the vehicle to be connected to the selected network.

Compared to the vehicle controlled mobility management, the network controlled solutions succeed better performance since their functionalities are implemented to the network equipment. As a result, the mobility management workload is minimized for the vehicles, while at the same time their energy requirements are decreased.

3.2.2.1.3 Hybrid Controlled Mobility Management : Hybrid controlled solutions determine that the control of the mobility management task is distributed to both the vehicle and the network infrastructure side. Indicatively, in a hybrid controlled HO initiation algorithm, both vehicle and network infrastructure cooperate in order the necessity of performing a handover to be evaluated. Accordingly, in a hybrid controlled network selection algorithm the aforementioned cooperation is performed in order the most appropriate network to be selected. In both cases, several vehicle and network parameters can be considered. Indicatively, vehicles parameters can include the perceived QoS, the signal quality, the vehicular users' preferences or the used services. Also, regarding the network infrastructure side, network load or operator policy information obtained from the network infrastructure are indicative parameters that can be considered. Finally, in a hybrid controlled HO execution algorithm both vehicle's equipment and network infrastructure cooperate to accomplish the handover.

3.2.2.1.4 Discussion on Mobility Management Control Entities : As it could be observed in Table 3.22 some schemes support only vehicle controlled mobility management (SSHVeT [180], DPVHO [183], CAHP [184] and HO-CALB [185]), while some other schemes support both vehicle and network control (TFT-ACW [66], VHO-VCC [67], GVHO-TW [197], GVHO-PD [197], NA-GVHO [197] and AAMP [211]). It should also be noted that although some schemes have not been proposed for supporting network control, it could be performed by implementing some of their functionalities to 5G-VCC components such as a Cloud or a Fog infrastructure (e.g. TFT [171], VHOMP [225], PHMVV [204], MAH-SCE [205] etc.). The implementation of such algorithms in a Cloud or a Fog infrastructure eliminates the mobility

management workload that the vehicles OBUs undertake, while at the same time their energy requirements are decreased. Furthermore, in cases where an SDN controller is used, the results of these scheme can be improved since the controller supervises the manipulation of the entire system. Finally, the BFP-NEMO [200] scheme implements only network controlled mobility management.

Table 3.22 The Control Types that each Scheme supports.

Scheme	Vehicle Controlled	Network Controlled	Hybrid Controlled
VHOMP [225]	✓	*	*
SSHVeT [180]	✓		
PHMVV [204]	✓	*	*
MAH-SCE [205]	✓	*	*
NASH [226]	✓	*	*
MAH-UDVE [186]	✓	*	*
RHVN [227]	✓	*	*
S-VHO [207]	✓	*	*
BFP-NEMO [200]		✓	
IINH [182]	✓		
IHVN [229]	✓	*	*
VANBA [230]	✓	*	*
iMAG-IDH [221]	✓	*	*
VFMIPv6 [231]	✓	*	*
MIH-PGI [208]	✓	*	*
CVHO [209]	✓	*	*
DPVHO [183]	✓		
GVHO-TW [197]	✓	✓	✓
GVHO-PD [197]	✓	✓	✓
NA-GVHO [197]	✓	✓	✓
ePFMIPv6 [202]	✓	✓	✓
AAMP [211]	✓	✓	✓
INS [187]	✓	*	*
HMM-KF [222]	✓	*	*
QAH-SIP [223]	✓	*	*
CAHP [184]	✓		
HO-CALB [185]	✓		
TOPSIS [188][189]	✓	*	*
TFT [171]	✓	*	*
TFT-ACW [66]	✓	✓	✓
VHO-VCC [67]	✓	✓	✓
GEO-MACHU [214]	✓	*	*
SAW [188]	✓	*	*
MEW [188]	✓	*	*
GRA [192]	✓	*	*
DIA [188]	✓	*	*
WPM [195]	✓	*	*
QICA-NS [196]	✓	*	*
IAS-FNN [199]	✓	*	*
FLB-VHO [219]	✓	*	*
FMVHO [220]	✓	*	*
HCA [217]	✓	*	*
VAH [218]	✓	*	*
*✓: Directly supported , *: Could be supported to a 5G-VCC architecture*			

3.2.2.2 Message Exchange Models

Message exchange models determine how the entities communicate each other in a VCC architecture. Two models are available in VCC, the host centric and the information centric.

3.2.2.2.1 Information Centric : The information centric model proposes messages' delivery considering the content semantics. The information centric model is also called as publish-subscribe model. Considering its operating principles, two entities interact each other, the publisher and the subscriber. Firstly, the publisher publishes the set of items. Then, the subscriber expresses its interests for items through subscriptions. When an item that is contained into the subscriber's interests become available to the publisher, it is being sent to the subscriber. The use of the information centric model facilitates the vehicles of obtaining easily the required information, due to the fact that vehicles are usually interested for the information itself, ignoring its origin. The authors of [42] strengthen this opinion by describing two examples. In the first one, an autonomous vehicle travels in high speed on a highway. The vehicle must obtain contiguous information of surrounding vehicles that exist in short distance, in order to provide a safe course to its passengers. Using the information centric model, the vehicle regularly expresses its interests to the surrounding vehicles. Then, it periodically receives information about their position, speed and direction. Correspondingly, in the second example, the case of an accident ahead is considered. More specifically, the vehicle expresses the interest for retrieving information about the accident to the surrounding vehicles and RSUs. Vehicles or RSUs that become nearest to the accident provide the required information to the vehicle. Then, the vehicle's driver is immediately alerted in order to be able to manipulate efficiently the situation (e.g. by selecting an alternative route to avoid the accident area and save time). Furthermore, in [43] the authors show that the information centric model enables the development of routing methods with enhanced scalability characteristics. More specifically, they demonstrate that this model provides many advantages to the routing functionality, due to the fact that it enables the network architecture manipulation in terms of "information connectivity" considering the context semantics, instead of considering the physical nodes connectivity.

3.2.2.2.2 Host Centric : The host centric model is also called as request-response or client-server model [234–236], where a client machine requests to receive items offered from a host (or server) machine. Specifically, when a client machine needs an item that belongs to this set, it sends a request to the host machine. The host machine receives the clients request, retrieves the required item and sends it to the client. The communication is performed using the IP protocol, while in large scale network architectures, thousand connections could exist. Furthermore, as described in [237], the use of the term "host centric" was started when the "information-centric"

term was introduced. Specifically, since the "information centric" has been proposed as an alternative message exchange model, the "host centric" term is used to represent the existing model for messages exchange in current network infrastructures, in order the fundamental difference between Information Centric Networking (ICN) [238] and Host Centric Networking (HCN) [239] to be clearly identified. Specifically, in order to explain the difference between the two models, the authors of [240] refer that in the ICN model the information itself obtains a specific identifier (or address), while in the traditional HCN model each host machine has an IP address assigned. Indicatively, regarding the host centric model operating principle, the authors of [241] have proposed the implementation of a Service Oriented Architecture (SOA) [242] for providing both information and entertainment services for vehicular clients. Specifically, each client interacts with the implemented web services to obtain access to real time information (e.g. about road traffic conditions) as well as to multimedia content.

3.2.2.2.3 Discussion on compatibility of each Mobility Management scheme with the available Message Exchange Models : The rapid evolve of content distribution services has led to host centric solutions such as overlay networks to address the increased needs for network scalability. However, performance bottlenecks persist resulting to the network inability of controlling the huge traffic load. In addition, the communication sessions could be interrupted when the IP address of a client device changes. Consequently, the host centric model cannot manipulate efficiently the increased needs for information. On the contrary, in information centric model, network nodes are considered as content segments, rather than as IP addressed endpoints. Thus, information centric model improves the network scalability and enhances the mobility support as well as the multihoming functionalities.

Table 3.23 presents the applicability of each mobility management scheme to the available message exchange models. As it could be observed, since the message exchange is performed to Layer 3 (e.g. in IP-based host centric solutions), Layer 2 schemes (e.g. TFT [171], TFT-ACW [66], VHO-VCC [67], VHOMP [225] etc.) and Layer 7 schemes (QAH-SIP [223]) require the complementary use of a Layer 3 scheme (e.g. BFP-NEMO [200], IINH [182], VFMIPv6 [231] or ePFMIPv6 [202]) in order to support either the information centric or the host centric model. More specifically, only the Layer 3 schemes directly support the host centric model since it is based on the IP protocol of Layer 3. Also, in some cases the information centric model could not be directly supported, since some Layer 3 schemes support only IP based communication (e.g. RHVN [227], BFP-NEMO [200], IINH [182], IHVN [229] etc.), requiring an IP based architecture, while the information centric model does not use a such architecture. In such cases, the complementary use of an additional algorithm implemented to the upper layers is required for supporting the information centric model [243][244].

Table 3.23 The Applicability of each Scheme to the Available Message Exchange Models.

Scheme	**Information Centric**	**Host Centric**
VHOMP [225]	*	*
SSHVeT [180]	*	*
PHMVV [204]	*	*
MAH-SCE [205]	*	*
NASH [226]	*	*
MAH-UDVE [186]	*	*
RHVN [227]	+	✓
S-VHO [207]	*	*
BFP-NEMO [200]	+	✓
IINH [182]	+	✓
IHVN [229]	+	✓
VANBA [230]	+	✓
iMAG-IDH [221]	+	✓
VFMIPv6 [231]	+	✓
MIH-PGI [208]	*	✓
CVHO [209]	*	*
DPVHO [183]	*	*
GVHO-TW [197]	*	*
GVHO-PD [197]	*	*
NA-GVHO [197]	*	*
ePFMIPv6 [202]	+	✓
AAMP [211]	*	*
INS [187]	*	*
HMM-KF [222]	*	*
QAH-SIP [223]	+	*
CAHP [184]	*	*
HO-CALB [185]	*	*
TOPSIS [188][189]	*	*
TFT [171]	*	*
TFT-ACW [66]	*	*
VHO-VCC [67]	*	*
GEO-MACHU [214]	*	✓
SAW [188]	*	*
MEW [188]	*	*
GRA [192]	*	*
DIA [188]	*	*
WPM [195]	*	*
QICA-NS [196]	*	*
IAS-FNN [199]	*	*
FLB-VHO [219]	*	*
FMVHO [220]	*	*
HCA [217]	*	*
VAH [218]	*	*
** Supported using third party algorithm for Layer 3 mobility management*		
+ Supported using third party algorithm implemented to the Upper Layers		

3.2.2.3 Mobility Management Algorithm Categories

Several HO initiation and network selection approaches have been described considering network and user related parameters and can be classified into the following categories:

3.2.2.3.1 Context Aware : The decision is based on signal quality parameters. In this case, RSS, SNR or SINR are usually considered in order the signal quality of each network to be evaluated. Context aware HO initiation is performed when the signal quality of the current network drops below a threshold, while in case of context aware network selection the network with the best signal quality is selected. It should be noted that although several algorithms consider the signal quality to determine the set of network alternatives, in this category belong only the algorithms that make the final decision (e.g. the network ranking) considering such information.

3.2.2.3.2 Cost Function based : The cost of each network is estimated using a function. In the case of HO initiation, if the cost of the current network exceeds a maximum acceptable threshold, HO is initiated. Accordingly, in the case of a cost function network selection algorithm the cost of each candidate network is calculated and the network with the lowest cost is selected. The cost should refer to monetary cost, energy consumption aware cost, bandwidth etc. Each HO initiation or network selection algorithm could belong to more than one categories.

3.2.2.3.3 Multi Attribute Decision Making (MADM) : The decision is made considering multiple and conflicting network and user criteria. In the case of HO initiation, the current network is ranked, while HO is initiated when this rank drops below a predefined threshold. Also, in the case of a MADM network selection algorithm the entire network alternatives are ranked and the network with the higher rank is selected.

3.2.2.3.4 User Centric : The decision considers user preferences, which could be refer to parameters related to QoS, QoE, monetary costs and so on. In case of HO initiation the user satisfaction is evaluated considering his preferences. If the user satisfaction grade drops below a threshold the HO is initiated. Accordingly, in case of user centric network selection the utility of each network alternative is evaluated considering the user preferences and the network with the highest utility is selected. As it could be observed, this category can be considered as similar to the cost function based one. Specifically, the user centric schemes estimate the utility of each network alternative which is a positive parameter, while the cost based ones estimate

the cost of each alternative which is a negative parameter. Also, the schemes of this category are usually combined with MADM algorithms.

3.2.2.3.5 Fuzzy Logic based : They use fuzzy logic in order the decision uncertainty to be addressed, considering the related criteria to perform HO initiation or network selection. A fuzzy number is represented by a set of real values representing an uncertain quantity and a convex normalized continuous function which estimates the degree of membership for each value in the subset. Triangular, trapezoidal or pentagonal fuzzy numbers are frequently used to represent uncertain information. These algorithms are usually combined with MADM algorithms, while the HO initiation and the network selection are performed according to the MADM based networks ranking.

3.2.2.3.6 Neural Network based : A neural network is constructed determining a score for each candidate network. They are usually combined with MADM algorithms. Similar to the previous categories HO initiation and network selection are performed considering the score of each network.

3.2.2.3.7 MIH based : The algorithms of this category apply the operating principles of Media Indepentent Handover (MIH) []. In some cases, they are combined with algorithms of other categories, including context aware and MADM.

3.2.2.3.8 Probabilistic : They consider several probabilities to perform the mobility management, including probabilities about user trajectory or velocity. Indicatively, considering the most probable user trajectory, the distribution of the signal strength of each network can be predicted. Thus, in case of HO initiation the most appropriate time to perform a HO can be estimated, or in case of network selection the most appropriate network for the user is selected, considering the aforementioned prediction.

3.2.2.3.9 Group based : They consider the fact that sometimes many users with similar trajectories and requirements need to perform a HO simultaneously. Thus, increased computation requirements for performing the mobility management arise. In this case, the algorithms of this category group users with similar trajectories and perform the mobility management once for the entire group, decreasing the computational requirements of the entire process.

3.2.2.3.10 Auction based : The algorithms of this category perform the network selection using auctions. Each user makes an offer (e.g. according to his Service Level Agreement). Subsequently, users with higher offers obtain connectivity to better networks.

3.2.2.3.11 Discussion on Mobility Management Algorithm Categories : As presented in table 3.24 the algorithm that each mobility management schemes combine more than one algorithm types. Specifically, most of the schemes belong to the MADM type (e.g. TFT [171], TFT-ACW [66], VHO-VCC [67], VHOMP [225] etc.), as well as to the context aware type (e.g. VHO-VCC [67], VHOMP [225], SSHVeT [180], PHMVV [204] etc.). It could be explained since the MADM algorithm could consider several (sometimes contradictory) parameters. On the other hand, context information (e.g. signal strength) could be considered as the most fundamental information for a mobility management scheme, since it is necessary for determining the candidate networks for a vehicle. Furthermore, many schemes belong to the cost function based type (e.g. VFMIPv6 [231], DPVHO [183], GVHO-TW [197], INS [187] etc.). In addition, although user preferences could be considered as a useful factor for performing the mobility management, only two of the discussed schemes belong to the user centric type (VHO-VCC [67] and QICA-NS [196]),while at the same time some schemes also belong to the fuzzy logic type (TFT [171], TFT-ACW [66], VHO-VCC [67] and IAS-FNN [199]).Also, there are schemes that belong to the MIH based (GEO-MACHU [214], IHVN [229] and MIH-PGI [208]), to the probabilistic (e.g. NASH [226], MAH-UDVE [186], iMAG-IDH [221], DPVHO [183] etc.) or to the group based (BFP-NEMO [200], GVHO-TW [197], GVHO-PD [197], NA-GVHO [197] and AAMP [211]) types. Finally, a few schemes belong to the neural network based (CVHO [209] and IAS-FNN [199]) or to the auction based (AAMP [211]) type.

Table 3.24 The Type of Algorithms used in each Scheme.

Scheme	Cost Function based	User Centric	MADM	Fuzzy Logic based	Neural Network based	Context aware	MIH based	Probabilistic	Group based	Auction based
VHOMP [225]			✓			✓				
SSHVeT [180]			✓			✓				
PHMVV [204]			✓			✓				
MAH-SCE [205]			✓			✓				
NASH [226]						✓		✓		
MAH-UDVE [186]								✓		
RHVN [227]						✓				
S-VHO [207]			✓							
BFP-NEMO [200]									✓	
IINH [182]						✓				
IHVN [229]							✓			
VANBA [230]	✓									
iMAG-IDH [221]								✓		
VFMIPv6 [231]	✓					✓				
MIH-PGI [208]						✓	✓			
CVHO [209]			✓		✓	✓				
DPVHO [183]	✓					✓		✓		
GVHO-TW [197]	✓								✓	
GVHO-PD [197]								✓	✓	
NA-GVHO [197]			✓						✓	
ePFMIPv6 [202]						✓				
AAMP [211]									✓	✓
INS [187]	✓									
HMM-KF [222]								✓		
QAH-SIP [223]	✓					✓				
CAHP [184]						✓				
HO-CALB [185]						✓				
TOPSIS [188][189]			✓							
TFT [171]			✓	✓						
TFT-ACW [66]			✓	✓						
VHO-VCC [67]		✓	✓	✓		✓				
GEO-MACHU [214]			✓			✓	✓			
SAW [188]			✓							
MEW [188]			✓							
GRA [192]			✓							
DIA [188]			✓							
WPM [195]			✓							
QICA-NS [196]	✓	✓	✓							
IAS-FNN [199]	✓			✓	✓					
FLB-VHO [219]			✓			✓				
FMVHO [220]			✓			✓				
HCA [217]	✓									
VAH [218]						✓				

3.2.3 Mobility Management on 5G-VCC Systems

In this section, the 5G-VCC architectures as well as the communication models that each mobility management scheme supports are mentioned.

3.2.3.1 Mobility Management schemes for supporting 5G-VCC Architectures

The applicability and the performance of each mobility management scheme is affected of factors related to the implemented 5G-VCC architecture. Table 3.25 presents the factors that each 5G-VCC architecture satisfies, while table 3.26 presents the applicability of the discussed mobility management schemes to each 5G-VCC architecture.

The applicability of each scheme depends on the existence of a backbone network infrastructure. Specifically, the VC architecture as already mentioned has no backbone network infrastructure. It determines a complete ad-hoc topology, which consists of vehicles constructing the Cloud. Thus, only the VANBA [230] and the HCA [217] schemes can be applied to VC architectures, since in these cases the mobility management concerns the connectivity between the participating vehicles instead of the interaction between vehicles and a network infrastructure. This fact reinforces the need for further research since in some cases the VC architectures could support disaster management services [245] where the availability of access network infrastructures could be decreased. On the other hand, in the VuC, VuF, SDN-V and HVA architectures, a communication infrastructure providing access to cloud/fog resources, is implemented. Hence, the entire schemes can be applied to VuC, VuF, SDN-V and HVA architectures, since they have been designed to manipulate the user mobility in relation with an existing network infrastructure.

Furthermore, architectural factors such as the network control type applied (centralized or decentralized) and which architectural components are virtualized, affect the performance of each mobility management scheme.

Regarding the network control type applied, the discussed mobility management schemes could be adapted to perform either centralized or distributed control. Centralized control is optional in VC, SDN-V and HVA architectures. Such a configuration uses a central entity performing the mobility management, such as a single SDN controller or a central vehicle with increased responsibilities. Accordingly, decentralized control is performed when the network control process is distributed to more than one control entities. Decentralized control can be applied to the entire 5G-VCC architectures. Furthermore, both centralized and decentralized control can be combined. For instance, in some VC architectures clustering of vehicles is performed, where a vehicle is elected as the Cluster Head (CH) [246] implementing the

functionalities of a single SDN controller. In this case, centralized control is applied for intra-cluster communication, while distributed control is applied for inter-cluster communication.

Finally, the considered mobility management schemes can be deployed to several virtualized resources of a 5G-VCC architecture. Specifically, in a VC architecture virtualization of resources is performed by the end-user devices. Also, in a VuC architecture virtualization is applied in the Cloud, while in a VuF architecture virtualization is applied in the Fog. Network as a Service (NaaS) [247–249] enables the configuration of network resources in either the Cloud or the Fog. Furthermore, in HVA architectures, virtualization is simultaneously performed in two or more architectural components. Indicatively, in the architecture discussed in [73] virtualization is applied to both Cloud and Fog nodes. Also, a fully virtualized HVA architecture [31][75], optimizes the performance of mobility management schemes, since it provides increased system reliability, resource utilization and performance isolation.

Table 3.25 The Factors considered in each Architecture.

Architecture	**Virtualization**	**Centralization**	**Infrastructure requirements**
Vehicular Cloud (VC)	Yes	Optional	No
Vehicles using Cloud (VuC)	Yes	No	Yes
Vehicles using Fog (VuF)	Yes	No	Yes
Software Defined Vehicular Architectures (SDN-V)	Yes	Optional	Yes
Hybrid Vehicular Architectures (HVA)	Yes	Optional	Yes

Table 3.26 The Applicability of each Scheme to the Available 5G-VCC Architectures.

Scheme	Vehicular Cloud (VC)	Vehicles using Cloud (VuC)	Vehicles using Fog (VuF)	Software Defined Vehicular Architectures (SDN-V)	Hybrid Vehicular Architectures (HVA)
VHOMP [225]		✓	✓	✓	✓
SSHVeT [180]		✓	✓	✓	✓
PHMVV [204]		✓	✓	✓	✓
MAH-SCE [205]		✓	✓	✓	✓
NASH [226]		✓	✓	✓	✓
MAH-UDVE [186]		✓	✓	✓	✓
RHVN [227]		✓	✓	✓	✓
S-VHO [207]		✓	✓	✓	✓
BFP-NEMO [200]		✓	✓	✓	✓
IINH [182]		✓	✓	✓	✓
IHVN [229]		✓	✓	✓	✓
VANBA [230]	✓	✓	✓	✓	✓
iMAG-IDH [221]		✓	✓	✓	✓
VFMIPv6 [231]		✓	✓	✓	✓
MIH-PGI [208]		✓	✓	✓	✓
CVHO [209]		✓	✓	✓	✓
DPVHO [183]		✓	✓	✓	✓
GVHO-TW [197]		✓	✓	✓	✓
GVHO-PD [197]		✓	✓	✓	✓
NA-GVHO [197]		✓	✓	✓	✓
ePFMIPv6 [202]		✓	✓	✓	✓
AAMP [211]		✓	✓	✓	✓
INS [187]		✓	✓	✓	✓
HMM-KF [222]		✓	✓	✓	✓
QAH-SIP [223]		✓	✓	✓	✓
CAHP [184]		✓	✓	✓	✓
HO-CALB [185]		✓	✓	✓	✓
TOPSIS [188][189]		✓	✓	✓	✓
TFT [171]		✓	✓	✓	✓
TFT-ACW [66]		✓	✓	✓	✓
VHO-VCC [67]		✓	✓	✓	✓
GEO-MACHU [214]		✓	✓	✓	✓
SAW [188]		✓	✓	✓	✓
MEW [188]		✓	✓	✓	✓
GRA [192]		✓	✓	✓	✓
DIA [188]		✓	✓	✓	✓
WPM [195]		✓	✓	✓	✓
QICA-NS [196]		✓	✓	✓	✓
IAS-FNN [199]		✓	✓	✓	✓
FLB-VHO [219]		✓	✓	✓	✓
FMVHO [220]		✓	✓	✓	✓
HCA [217]	✓	✓	✓	✓	✓
VAH [218]		✓	✓	✓	✓

3.2.3.2 Mobility Management schemes for supporting 5G-VCC Communication Models

Each communication model could be applied to specific 5G-VCC architectures (Table 3.27). In general, V2V and V2P models can be applied in each 5G-VCC architecture, since the entire topologies can include both vehicular and pedestrian users. However, the V2I communication model requires a network infrastructure. Consequently, it cannot be applied to a VC architecture which is completely ad-hoc. On the other hand, V2I could be used in VuC and VuF topologies, since they provide access to network infrastructure through RSUs. Also, HVC could be applied to the entire topologies, since it combines multiple communication models.

Table 3.27 The Applicability of each Communication Model to each Architecture.

5G-VCC Architecture / Communication Model	**Vehicular Cloud (VC)**	**Vehicles using Cloud (VuC)**	**Vehicles using Fog (VuF)**	**Software Defined Vehicular Architectures (SDN-V)**	**Hybrid Vehicular Architectures (HVA)**
Vehicle to Vehicle (V2V)	✓	✓	✓	✓	✓
Vehicle to Infrastructure (V2I)		✓	✓	✓	✓
Vehicle to Pedestrian (V2P)	✓	✓	✓	✓	✓
Hybrid Vehicular Communication (HVC)	✓	✓	✓	✓	✓

Table 3.28 presents the applicability of each mobility management scheme to the available communication models. As could be observed the entire mobility management schemes support V2I communications, since these schemes could be applied to 5G-VCC topologies where an access network infrastructure exists. However, only the HCA [217] scheme supports V2V and V2P communications since it could also be applied to VC architectures where no access network infrastructure exists. Thus, the design of mobility management algorithms for supporting V2V and V2P communications could be considered as a scientific field for further future research, since these communications are necessary for supporting several vehicular services in smart cities environments [95][250].

Table 3.28 The Applicability of each Scheme to each Communication Model.

Scheme	Vehicle to Vehicle (V2V)	Vehicle to Infrastructure (V2I)	Vehicle to Pedestrian (V2P)	Hybrid Vehicular Communication (HVC)
VHOMP [225]		✓		
SSHVeT [180]		✓		
PHMVV [204]		✓		
MAH-SCE [205]		✓		
NASH [226]		✓		
MAH-UDVE [186]		✓		
RHVN [227]		✓		
S-VHO [207]		✓		
BFP-NEMO [200]		✓		
IINH [182]		✓		
IHVN [229]		✓		
VANBA [230]	✓	✓	✓	✓
iMAG-IDH [221]		✓		
VFMIPv6 [231]		✓		
MIH-PGI [208]		✓		
CVHO [209]		✓		
DPVHO [183]		✓		
GVHO-TW [197]		✓		
GVHO-PD [197]		✓		
NA-GVHO [197]		✓		
ePFMIPv6 [202]		✓		
AAMP [211]		✓		
INS [187]		✓		
HMM-KF [222]		✓		
QAH-SIP [223]		✓		
CAHP [184]		✓		
HO-CALB [185]		✓		
TOPSIS [188][189]		✓		
TFT [171]		✓		
TFT-ACW [66]		✓		
VHO-VCC [67]		✓		
GEO-MACHU [214]		✓		
SAW [188]		✓		
MEW [188]		✓		
GRA [192]		✓		
DIA [188]		✓		
WPM [195]		✓		
QICA-NS [196]		✓		
IAS-FNN [199]		✓		
FLB-VHO [219]		✓		
FMVHO [220]		✓		
HCA [217]	✓	✓	✓	✓
VAH [218]		✓		

Chapter 4

A Proposed Mobility Management Approach for 5G-VCC Systems

4.1 Mobility Management Requirements

This section describes the requirements that must be satisfied by a mobility management scheme. In a 5G-VCC system, vehicles move in several trajectories, while at the same time have different velocities. Also, each vehicle could serve multiple passengers with different services. Thus several requirements need to be addressed by HO schemes.

- *Seamless mobility* During the vehicles movement, their ability to remain connected while roaming across different access networks must be ensured, in order to avoid interruption of user's services.

- *Minimization of handover latency* Mobility management schemes should offer lightweight solutions to minimize the delay of the decision process as well as the signaling delays during the handover execution. Additionally, in urban environments multiple vehicles have similar trajectories requiring similar mobility management decisions and signaling-exchanges to be performed. For this reason, modern mobility management schemes cluster the vehicles with similar mobility and service requirements so that similar tasks are executed once for the entire cluster than for each vehicle.

- *Minimization of handovers count* Even in cases where the handover latency has been reduced enough, more handovers will always occur to higher total latencies and network signaling overhead. In the modern 5G network access environment, where multiple cells coexist in the same place, a vehicle could perform a large number of handovers reducing the perceived Quality of Service (QoS) of vehicular services.

- *Support of heterogeneous network access environments* Mobility management schemes for 5G networks should support the coexistence of multiple network access technologies. Thus, the utilization of the available spectrum will be maximized, since each technology operates to specific frequency bands, determined by its technical specifications.

- *Optimal network selection for satisfying QoS constraints of vehicular services* Connectivity to the most appropriate network supporting the constraints of vehicular services must be ensured. Accordingly, the available network alternatives must be continuously evaluated considering vehicular services requirements, as well as changes in the radio environment and operators policies.

4.2 System Architecture

The proposed HO management scheme uses some of the methods described in the previous section. Its design has been optimized to be applied in 5G network architectures where both Fog and Cloud infrastructures are available. The HO process includes the HO Initiation, the Velocity Monitoring, the Network Selection and the HO Execution subprocesses as presented in Figure 4.1.

Initially, the HO Initiation is executed in the Fog considering the Quality of Service (QoS) and the Signal to Noise plus Interference Ratio (SINR) that the vehicle perceives from its current network to evaluate the necessity to perform a handover. Both the Fog and the Cloud cooperate to accomplish the Velocity Monitoring process. Finally, the Cloud performs the Network Selection among the available networks depending on the vehicle's velocity. The vehicle is informed through the Fog infrastructure, to make a handover to the selected network.

The following subsections describe in depth each one of the aforementioned subprocesses.

4.2.1 VHO Initiation

During the HO initiation process the $S_{u,i}$ indicator is defined, determining the satisfaction grade of user u from his current network i. More specifically, the $S_{u,i}$ value is estimated considering as input the $SINR_{u,i}$ and the $Q_{u,i}$ parameters. The $SINR_{u,i}$ represents the Signal to Noice plus Interference, while the $Q_{u,i}$ represents the quality of the users' services offered from the current network. $Q_{u,i}$ is calculated using formula 4.1, where $th_{u,i,k}$, $d_{u,i,k}$, $j_{u,i,k}$ and $pl_{u,i,k}$ represent the throughput, the delay, the jitter and the packet loss ratio respectively, obtained by user u for service k. Additionally, $w_{th,k}$, $w_{d,k}$,$w_{j,k}$ and $w_{p,kl}$ represent the weights of the aforementioned parameters estimated using the PF-ANP method, while N represents the

number of the parameters considered and K the number of the available services.

$$Q_{u,i} = \left(\sum_{k=1}^{K} \left((w_{th,k} \cdot th_{u,i,k} + w_{d,k} \cdot \frac{1}{d_{u,i,k}} + w_{j,k} \cdot \frac{1}{j_{u,i,k}} + w_{pl,k} \cdot \frac{1}{pl_{u,i,k}}) / N \right) \right) / K \tag{4.1}$$

The user's equipment continuously monitors its perceived $SINR_{u,i}$ and $Q_{u,i}$ values. When either $SINR_{u,i}$ or $Q_{u,i}$ becomes less than a predefined threshold, the user equipment sends the obtained values to the Fog infrastructure. Subsequently, the Fog infrastructure uses the Mamdani satisfaction chart presented in Figure 4.2, in order to determine the $S_{u,i}$ satisfaction grade. If the satisfaction grade is less than a predefined S_{th} threshold value, then the network selection process is executed.

The satisfaction indicators chart presents the $S_{u,i}$ values obtained for each possible $SINR_{u,i}$ and $Q_{u,i}$ combination. Indicatively, when the $SINR_{u,i}$ and $Q_{u,i}$ values are too low, the produced $S_{u,i}$ value is too low as well. On the contrary, when the $SINR_{u,i}$ and $Q_{u,i}$ values are close to 1, the produced $S_{u,i}$ value is also high, indicating that the user is fully satisfied. Furthermore, when only one of the $SINR_{u,i}$ or the $Q_{u,i}$ values is close to 0, the user satisfaction is in quite low levels.

At this point, it has to be noted that since the user's satisfaction is obtained at the Fog by performing a lookup at the satisfaction indicators chart, the overhead introduced at the Fog is minimal. Also, the method does not impose any significant overhead at the user equipment due to the monitoring of the $SINR_{u,i}$ and $Q_{u,i}$ parameters.

4.2.1.1 Evaluation of the Satisfaction Indicators

The Mamdani satisfaction chart is evaluated once during the instantiation of the Fog services. Each satisfaction indicator $S_{u,i}$ of Figure 4.2 is obtained using the MPFIS method, considering the $SINR_{u,i}$ and the $Q_{u,i}$ as input parameters. Both $SINR_{u,i}$ and $Q_{u,i}$ are normalized in order to have values within the range [0, 1]. Also, the MF_{SINR}, MF_Q, MF_S membership functions (MF) are defined using the EUM method, indicating the linguistic terms and the corresponding Interval Valued Pentagonal Fuzzy Numbers (I-VPFN) for the fuzzy representation of the $SINR_{u,i}$, $Q_{u,i}$ and $S_{u,i}$ respectively. Thus, for each crisp value, two membership degrees are determined in the corresponding MF, one for the upper pentagon and one for the lower pentagon. Table 4.1 represents the linguistic terms and the corresponding interval-valued pentagonal fuzzy numbers of MF_{SINR}, MF_Q and MF_S membership functions, which are equally distributed inside the domain $[U_{min}, U_{max}]$ = [0, 1] as illustrated in Figures 4.3, 4.4 and 4.5, respectively. Table 4.2 shows the considered fuzzy rule base.

Table 4.1 Linguistic Terms and the corresponding Interval-Valued Pentagonal Fuzzy Numbers used for MF_{SINR}, MF_Q and MF_S.

MF_{SINR} **membership functions.**	
Linguistic term	**Interval-valued trapezoidal fuzzy number**
Absolute Bad (AB)	[(0.0, 0.0, 0.0, 0.062, 0.093, 0.8, 0.6, 0.6),(0.0, 0.0, 0.0, 0.083, 0.125, 1.0, 0.8, 0.8)]
Too Bad (TB)	[(0.072, 0.104, 0.166, 0.229, 0.26, 0.8, 0.6, 0.6),(0.041, 0.083, 0.166, 0.25, 0.291, 1.0, 0.8, 0.8)]
Bad (B)	[(0.239, 0.27, 0.333, 0.395, 0.427, 0.8, 0.6, 0.6),(0.208, 0.25, 0.333, 0.416, 0.458, 1.0, 0.8, 0.8)]
Enough (EN)	[(0.406, 0.437, 0.5, 0.562, 0.593, 0.8, 0.6, 0.6),(0.375, 0.416, 0.5, 0.583, 0.625, 1.0, 0.8, 0.8)]
More than Enough (ME)	[(0.572, 0.604, 0.667, 0.729, 0.76, 0.8, 0.6, 0.6),(0.541, 0.583, 0.667, 0.75, 0.791, 1.0, 0.8, 0.8)]
Almost Excellent (AE)	[(0.739, 0.77, 0.833, 0.895, 0.927, 0.8, 0.6, 0.6),(0.708, 0.75, 0.833, 0.916, 0.958, 1.0, 0.8, 0.8)]
Excellent (EX)	[(0.906, 0.937, 1.0, 1.0, 1.0, 0.8, 0.6, 0.6),(0.875, 0.916, 1.0, 1.0, 1.0, 1.0, 0.8, 0.8)]
MF_Q **membership functions.**	
Linguistic term	**Interval-valued trapezoidal fuzzy number**
Absolutely Poor (AP)	[(0.0, 0.0, 0.0, 0.046, 0.07, 0.8, 0.6, 0.6),(0.0, 0.0, 0.0, 0.062, 0.093, 1.0, 0.8, 0.8)]
Very Poor (VP)	[(0.054, 0.078, 0.125, 0.171, 0.195, 0.8, 0.6, 0.6),(0.031, 0.062, 0.125, 0.187, 0.218, 1.0, 0.8, 0.8)]
Poor (P)	[(0.179, 0.203, 0.25, 0.296, 0.32, 0.8, 0.6, 0.6),(0.156, 0.187, 0.25, 0.312, 0.343, 1.0, 0.8, 0.8)]
Medium Poor (MP)	[(0.304, 0.328, 0.375, 0.421, 0.445, 0.8, 0.6, 0.6),(0.281, 0.312, 0.375, 0.437, 0.468, 1.0, 0.8, 0.8)]
Medium (M)	[(0.429, 0.453, 0.5, 0.546, 0.57, 0.8, 0.6, 0.6),(0.406, 0.437, 0.5, 0.562, 0.593, 1.0, 0.8, 0.8)]
Medium Good (MG)	[(0.554, 0.578, 0.625, 0.671, 0.695, 0.8, 0.6, 0.6),(0.531, 0.562, 0.625, 0.687, 0.718, 1.0, 0.8, 0.8)]
Good (G)	[(0.679, 0.703, 0.75, 0.796, 0.82, 0.8, 0.6, 0.6),(0.656, 0.687, 0.75, 0.812, 0.843, 1.0, 0.8, 0.8)]
Very Good (VG)	[(0.804, 0.828, 0.875, 0.921, 0.945, 0.8, 0.6, 0.6),(0.781, 0.812, 0.875,0.937, 0.968, 1.0, 0.8, 0.8)]
Absolutely Good (AG)	[(0.929, 0.953, 1.0, 1.0, 1.0, 0.8, 0.6, 0.6),(0.906, 0.937, 1.0, 1.0, 1.0, 1.0, 0.8, 0.8)]
MF_S **membership functions.**	
Linguistic term	**Interval-valued trapezoidal fuzzy number**
Absolute Unsatisfactory (AU)	[(0.0, 0.0, 0.0, 0.034, 0.051, 0.8, 0.6, 0.6),(0.0, 0.0, 0.0, 0.045, 0.068, 1.0, 0.8, 0.8)]
Very Unsatisfactory (VU)	[(0.039, 0.056, 0.09, 0.125, 0.142, 0.8, 0.6, 0.6),(0.022, 0.045, 0.09, 0.136, 0.159, 1.0, 0.8, 0.8)]
Unsatisfactory (U)	[(0.13, 0.147, 0.181, 0.215, 0.232, 0.8, 0.6, 0.6),(0.113, 0.136, 0.181, 0.227, 0.25, 1.0, 0.8, 0.8)]
Slightly Unsatisfactory (SU)	[(0.221, 0.238, 0.272, 0.306, 0.323, 0.8, 0.6, 0.6),(0.204, 0.227, 0.272, 0.318, 0.34, 1.0, 0.8, 0.8)]
Less than Acceptable (LA)	[(0.312, 0.329, 0.363, 0.397, 0.414, 0.8, 0.6, 0.6),(0.295, 0.318, 0.363, 0.409, 0.431, 1.0, 0.8, 0.8)]
Slightly Acceptable (SA)	[(0.403, 0.42, 0.454, 0.488, 0.505, 0.8, 0.6, 0.6),(0.386, 0.409, 0.454, 0.5, 0.522, 1.0, 0.8, 0.8)]
Acceptable (A)	[(0.494, 0.511, 0.545, 0.579, 0.596, 0.8, 0.6, 0.6),(0.477, 0.5, 0.545, 0.59, 0.613, 1.0, 0.8, 0.8)]
More than Acceptable (MA)	[(0.585, 0.602, 0.636, 0.67, 0.687, 0.8, 0.6, 0.6),(0.568, 0.59, 0.636, 0.681, 0.704, 1.0, 0.8, 0.8)]
Slightly Satisfactory (SS)	[(0.676, 0.693, 0.727, 0.761, 0.778, 0.8, 0.6, 0.6),(0.659, 0.681, 0.727, 0.772, 0.795, 1.0, 0.8, 0.8)]
Satisfactory (S)	[(0.767, 0.784, 0.818, 0.852, 0.869, 0.8, 0.6, 0.6),(0.75, 0.772, 0.818, 0.863, 0.886, 1.0, 0.8, 0.8)]
Very Satisfactory (VS)	[(0.857, 0.875, 0.909, 0.943, 0.96, 0.8, 0.6, 0.6),(0.84, 0.863, 0.909, 0.954, 0.977, 1.0, 0.8, 0.8)]
Absolute Satisfactory (AS)	[(0.948, 0.965, 1.0, 1.0, 1.0, 0.8, 0.6, 0.6),(0.931, 0.954, 1.0, 1.0, 1.0, 1.0, 0.8, 0.8)]

4.2.2 Velocity Monitoring

During the entire vehicle movement, its velocity is monitored by the Fog-Cloud infrastructure. An enhanced version of the Mobility State Estimation (MSE) model defined in 3GPP LTE Release 11 [251] is used to estimate the vehicles' velocity. The MSE considers the number of handovers or reselections (N_{CR_u}) performed by a vehicle during a sliding time window (T_{CRmax}). The vehicle is categorized into one of three velocity states, namely the Normal, the Medium and the High, considering the $N_{CR_{Medium}}$ and $N_{CR_{High}}$ thresholds with $N_{CR_{Medium}} < N_{CR_{High}}$. The concept of this method is that the more handovers the vehicle performs during the T_{CRmax} period, the faster the vehicle is moving. In heterogeneous network environments that include both Macrocells and Femtocells, the default T_{CRmax} value is 120 seconds, while the default $N_{CR_{Medium}}$ and $N_{CR_{High}}$ values are equal to 10 and 16 handovers, respectively [251]. Furthermore, the estimated residence time $t_{u,i}^{residence}$ of vehicle u in each available cell i is estimated using

formula 4.2 defined in [252], where r_f is the radius of femtocell i and v_u is the velocity of the vehicle u.

$$t_{u,i}^{residence} = \frac{\pi \cdot r_i}{2 \cdot v_u} \tag{4.2}$$

Then, the vehicle velocity is obtained by formula 4.3 defined in [253].

$$v_u = \frac{\pi \cdot N_{CR_u}}{4 \cdot T_{CRmax} \cdot \sqrt{\lambda_u}} \tag{4.3}$$

The λ_u parameter, obtained by the SDN controller, denotes the cell's density in the location of vehicle u.

4.2.3 Network Selection

The mobility state of each vehicle is considered in order to select the set $A = \{A_1, A_2, \ldots, A_n\}$ of possible network alternatives based on the SINR perceived by each network. If the vehicle mobility state is Normal then the vehicle considers all the available networks as alternatives, including both Macrocells and Femtocells. On the contrary, if vehicle mobility state is Medium then the vehicle skips some Femtocells along its trajectory. In particular, the Femtocell i is considered as alternative if $t_{u,i}^{residence} \geqslant t_{u,mean}^{residence}$, where $t_{u,mean}^{residence}$ is the average residence time of vehicle u considering all the available Femtocells in its current location. Finally, if the vehicle mobility state is High then only Macrocells are considered as alternatives.

Thereafter the network selection is performed using the Pentagonal interval-valued Fuzzy TOPSIS (PFT), considering both QoS aware (throughput, delay, jitter and packet loss) and operator policies (service reliability, security and price) criteria. Since the list of network alternatives is constructed considering the vehicle's velocity and, then, the network selection is performed using QoS and policy related parameters, the ping pong effect is eliminated.

4.2.4 Handover Execution

During the handover execution, the vehicle is connected to the selected network. After each successfull handover of a vehicle, the number of handovers or reselections N_{CR_u} increases, in order the aforementioned handover to be considered for the estimation of the vehicle velocity.

4.2.5 Computational Complexity of the Proposed Approach

Regarding the computational complexity of the proposed approach the HO initiation subprocess requires a constant time to complete its tasks by performing simple checks against predefined thresholds, resulting in $O(1)$. Also, the network selection phase introduces an $O(n^2)$ complexity, due to the weighting and normalization of the $n \times m$ decision matrices. Similar complexities

are introduced by other handover algorithms proposed in the research literature. The novelty in our approach is that most of the computational complexity is performed at the Cloud/Fog infrastructure.

4.3 Simulation Setup

In our experiments, the Software Defined Vehicular Cloud topology presented in Figure 4.6 is considered. A mobility trace indicating the map of the city of Piraeus along with road traffic data has been created using the Open Street Map (OSM) software [176]. Then, the mobility trace has been used as input in the Simulator of Urban Mobility (SUMO) [177] allowing the production of a realistic mobility pattern for the simulated vehicles including 39807 vehicles in total, moving inside the Piraeus city in a 24 hours period. The average arrival rate of the vehicles into the map is equal to 0,460729167 vehicles per second, while their average departure rate is equal to 0,46 vehicles per second. Furthermore, the network topology is being built upon the map, using the Network Simulator 3 (NS3) [178]. It includes a Fog infrastructure and a Cloud infrastructure. The Fog infrastructure consists of 18 LTE Macrocell e-Node Bs (eNBs), 39 LTE Femtocell eNBs, 16 WiMAX Macrocell Base Stations (BSs), 26 WiMAX Femtocell BSs and 22 802.11p WAVE RSUs, equipped with additional computational and storage resources. The access networks have been located on the map, according to the Hellenic Telecommunications and Post Commission (EETT) [254] data about BSs' positions in the city of Piraeus. The positions and the spectrum of the BSs are presented in A1 to A3 tables (Appendix A), for the LTE, WiMAX and WAVE technologies, respectively. The SDN controller has a global view of the entire network environment. The Cloud infrastructure includes a set of Virtual Machines (VMs) providing services such as Navigation Assistance (NAV), Voice over IP (VoIP), Conversational Video (CV), Buffered Streaming (BS) and Web Browsing (WB). Furthermore, a Software Defined Network (SDN) controller provides centralized control for the entire system.

Each access network supports at least one of the aforementioned Cloud services, while four Service Level Agreements (SLAs) are defined. SLA1 has the higher service priority and SLA 4 has the lower service priority. SLA1 supports all the service types and provides the best values for QoS as well as policy decision criteria. SLA2 supports a smaller number of service types, by not providing support for the VoIP and NAV services. Additionally, it provides slightly worse decision criteria values than those offered by the SLA1. SLA3 supports only the BS and the WB services and satisfactory QoS characteristics and policies. Finally, SLA4 supports only the WB service while it provides acceptable decision criteria values.

Network specifications are expressed directly using linguistic terms (Appendix B). In particular, the crisp values of the network QoS characteristics are converted into linguistic terms which correspond to specific ranges of values per service type. Table 4.3 illustrates the mapping between ranges of network QoS characteristics values and the respective linguistic terms for the VoIP service. Table 4.4 summarizes the simulation parameters.

4.3.1 Study of a Simulation Snapshot

In this subsection, a snapshot of the simulation at time equal to 3600 seconds is considered. Specifically, the case where 10 of the vehicles are monitored is studied, while each vehicle needs to connect to a network which satisfies the requirements of its services and at the same time complies with its respective SLA agreements. Table 4.5 presents the available networks in the location of each vehicle.

4.3.1.1 VHO Initiation

During the HO initiation process, the user satisfaction $S_{u,i}$ is obtained using the MPFIS Satisfaction Chart, considering the estimated $Q_{u,i}$ and $SINR_{u,i}$ values. It should be noted that the services weights used for the $Q_{u,i}$ estimation are calculated using the PF-ANP method. The criteria used include throughput, delay, jitter and packet loss. Figure 4.7 depicts the estimated HO initiation weights for each service. Furthermore, the $S_{th,SLA}$ thresholds given in Table 4.6 are estimated considering the minimum acceptable Q_{SLA} and $SINR_{SLA}$ values per SLA. If the $S_{u,i}$ becomes less than the respective $S_{th,SLA}$ threshold then the vehicle should perform a handover to a new access network. The HO initiation results for each vehicle are presented in Table 4.7. As it can be observed, vehicle 8 will remain to its current network i, while the rest of the vehicles will procceed to handover.

4.3.1.2 Velocity Monitoring

For each one of the monitored vehicles, Table 4.8 presents its SLA, the services used, its geographical position and its estimated velocity.

4.3.1.3 Network Selection

During the network selection process the PF-ANP method is applied in order to estimate the weights of the network selection criteria per service type and SLA. Figure 4.8 depicts the PF-ANP network model. The criteria are classified into two groups, namely the Network QoS and the Network Policy characteristics. The Network QoS characteristics group contains

network performance related criteria including throughput, delay, jitter and packet loss. The Network Policy characteristics group contains operator defined rules such as price, security and service reliability. Pairwise comparison decision matrices are created based on relations among the eight selection criteria depicted in Figure 4.9. Then, these pairwise comparison decision matrices are used to evaluate the priority vectors of the criteria and to form the supermatrix per service type and SLA. Subsequently, the weighted supermatrices and, finally, the limited supermatrices are obtained. Indicatively, for the SLA1 NAV service, the initial, the weighted and the limited supermatrices are presented in Tables 4.9, 4.10 and 4.11 respectively.

The criteria weights per service and SLA obtained by the limit supermatrices are presented in Figures 4.10 - 4.13. As illustrated, the weights are proportional to the constraints of each service as well as to the agreements of each SLA. In particular, the weight of the price criterion is low for SLA1, in which the service reliability and the network QoS characteristics are considered as the most important factors. In SLA2 the price criterion is more important than in SLA1, thus the respective weight is greater than that of SLA1. Consequently, the weights of the service reliability and QoS characteristics criteria in SLA2 are lower compared to the relative weights of SLA1. In SLA3 the weights of price and service reliability criteria are balanced as they are almost of equivalent importance. Finally, in SLA4 the price is the most important criterion resulting in a high estimated weight value.

The PFT algorithm selects the best network for each vehicle considering the vehicle service requirements. Figure 4.14 compares the results of the proposed scheme with the ones obtained using VAH [218], FAT [255], FAS [255], FAM [255] and FAE [172]. In this Figure, for each vehicle the PFT ranking of the current network as well as of the target network connection estimated by each of the six schemes are presented. From the obtained results it is clear that the suggested algorithm outperforms the existing schemes since it selects as target networks for vehicles the ones with the best ranks. Also, in special cases where the velocity of the vehicles is high (eg. for vehicle 7) the proposed scheme considers only the wide coverage candidate networks as alternatives avoiding the handovers to femtocell networks.

Additionally, for a further evaluation of the proposed scheme, the user's satisfaction grade $S_{u,i}$ after the HO completion is considered. Figure 4.15 presents the estimated $S_{u,i}$ after the execution of each HO scheme. As it can be observed, the results are similar to the aforementioned PFT rankings, while the proposed approach achieves higher satisfaction grades than the existing schemes.

4.3.2 24 Hours Simulation Results

For the entire 24-hour simulation, Tables C1, C2 and C3 (Appendix C) present the number of vehicles that start their movement from each LTE, WiMAX and WAVE network, respectively, as well as their corresponding velocities.

Table C4 presents the vehicle count per service and SLA. The entire service combinations per SLA are considered, in order all the possible use cases to be studied during the simulation. The number of possible service combinations (S_c) is estimated using formula 4.4 [256] where S_n represents the number of the considered services. In this experiment, 5 services are considered, namely the Navigation Assistance (NAV), Voice over IP (VoIP), Conversational Video (CV), Buffered Streaming (BS) and Web Browsing (WB) and, thus, S_c is equal to 31. It should be noted that SLA 1 supports all the services, while SLA 2 supports only the CV, BS and WB services. Also, SLA 3 supports only the BS and WB services, while SLA 4 supports only the WB service.

$$S_c = 2^{S_n} - 1 \tag{4.4}$$

The average PFT rankings of each HO scheme are presented in Figure 4.16, where all the 39807 vehicles are considered. As it can be observed, the proposed scheme accomplishes higher ranking than the other schemes. On the contrary, the VAH scheme accomplishes the lower ranking, due to the fact that it does not consider neither QoS related parameters, nor operator policy related parameters. The other schemes accomplish intermediate results. The FAT results are slightly better than the ones achieved from the rest of the schemes. Also, Figure 4.17 presents the average satisfaction grade $S_{u,i}$ estimated for each HO scheme. The proposed approach accomplishes the highest average values, compared to the rest of the HO schemes. It should be noted that the number of HOs performed should be considered as a critical parameter for the evaluation of the proposed HO scheme efficiency, since a smaller number of HOs implies a lower network signaling overhead in both the user and the operator sides. Figure 4.18 presents the total number of HOs performed in each scheme, during the entire 24 hours simulation. As it is shown, the proposed scheme outperforms the other schemes, since it performs a smaller number of HOs. Also, the VAH scheme accomplishes an acceptable number of HOs, since it also considers the vehicle velocity for the handover process. However, it does not avoid useless HOs to femtocells providing worse results than the proposed scheme. The rest of the schemes accomplish similar HO numbers, since they are based on the perceived RSS per user for the HO initiation process.

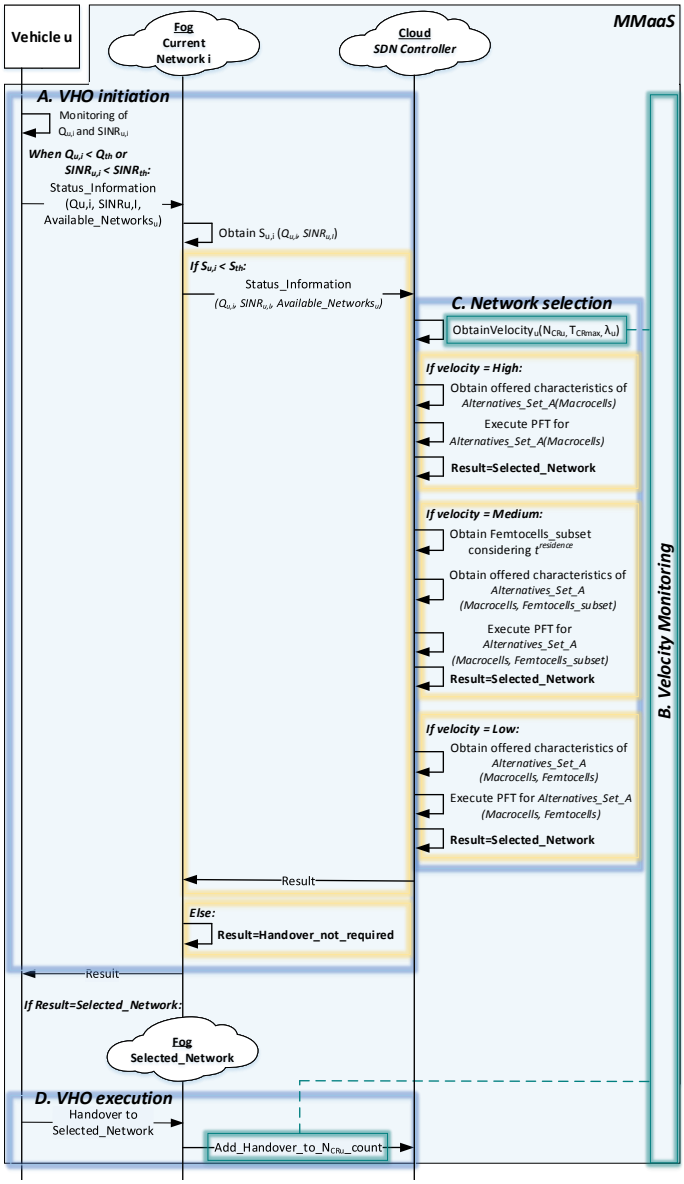

Figure 4.1 The Proposed Methodology.

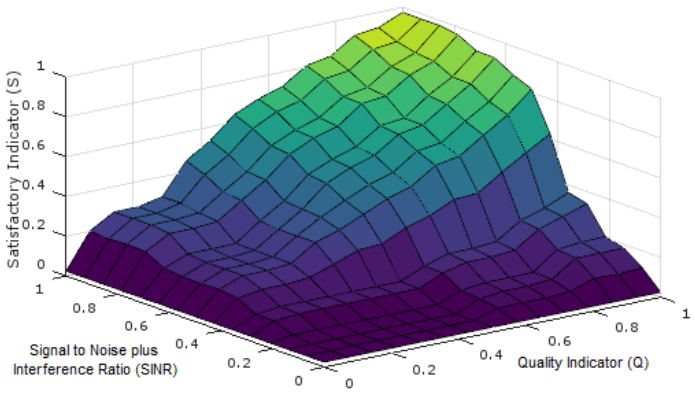

Figure 4.2 The S Values Range as obtained using the FIS.

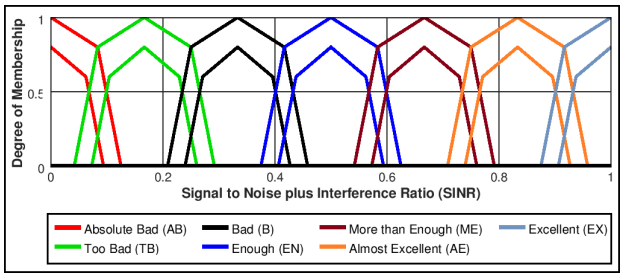

Figure 4.3 MF_{SINR} Membership Functions Balance.

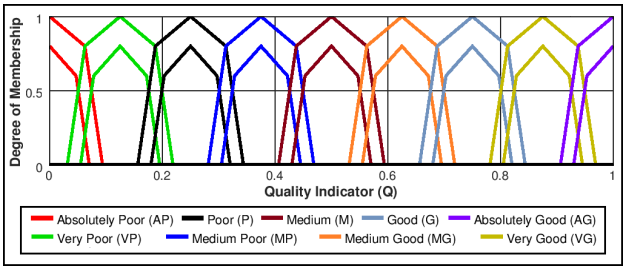

Figure 4.4 MF_Q Membership Functions Balance.

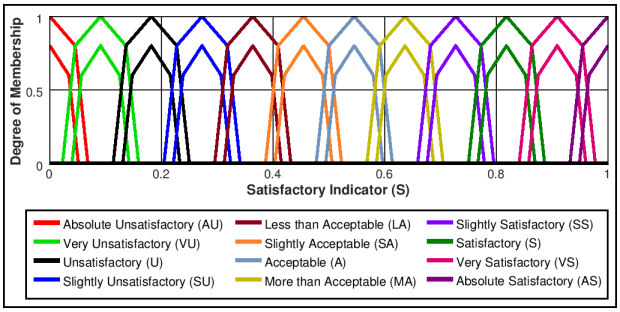

Figure 4.5 MF_S Membership Functions Balance.

Table 4.2 The Fuzzy Rule (or Knowledge) Base.

Rule	MF_{SINR}	**Operator**	MF_Q	MF_S
1	AB	or	AP	AU
2	TB	and	VP	AU
3	B	and	VP	VU
4	EN	and	VP	U
5	ME	and	VP	U
6	AE	and	VP	SU
7	EX	and	VP	SU
8	TB	and	P	AU
9	B	and	P	VU
10	EN	and	P	U
11	ME	and	P	U
12	AE	and	P	SU
13	EX	and	P	SU
14	TB	and	MP	AU
15	B	and	MP	VU
16	EN	and	MP	SU
17	ME	and	MP	SU
18	AE	and	MP	LA
19	EX	and	MP	SA
20	TB	and	M	AU
21	B	and	M	VU
22	EN	and	M	LA
23	ME	and	M	SA
24	AE	and	M	A
25	EX	and	M	MA
26	TB	and	MG	VU
27	B	and	MG	U
28	EN	and	MG	SA
29	ME	and	MG	A
30	AE	and	MG	MA
31	EX	and	MG	SS
32	TB	and	G	VU
33	B	and	G	U
34	EN	and	G	A
35	ME	and	G	MA
36	AE	and	G	SS
37	EX	and	G	S
38	TB	and	VG	U
39	B	and	VG	SU
40	EN	and	VG	MA
41	ME	and	VG	SS
42	AE	and	VG	S
43	EX	and	VG	VS
44	TB	and	AG	U
45	B	and	AG	LA
46	EN	and	AG	S
47	ME	and	AG	VS
48	AE	and	AG	AS
49	EX	and	AG	AS

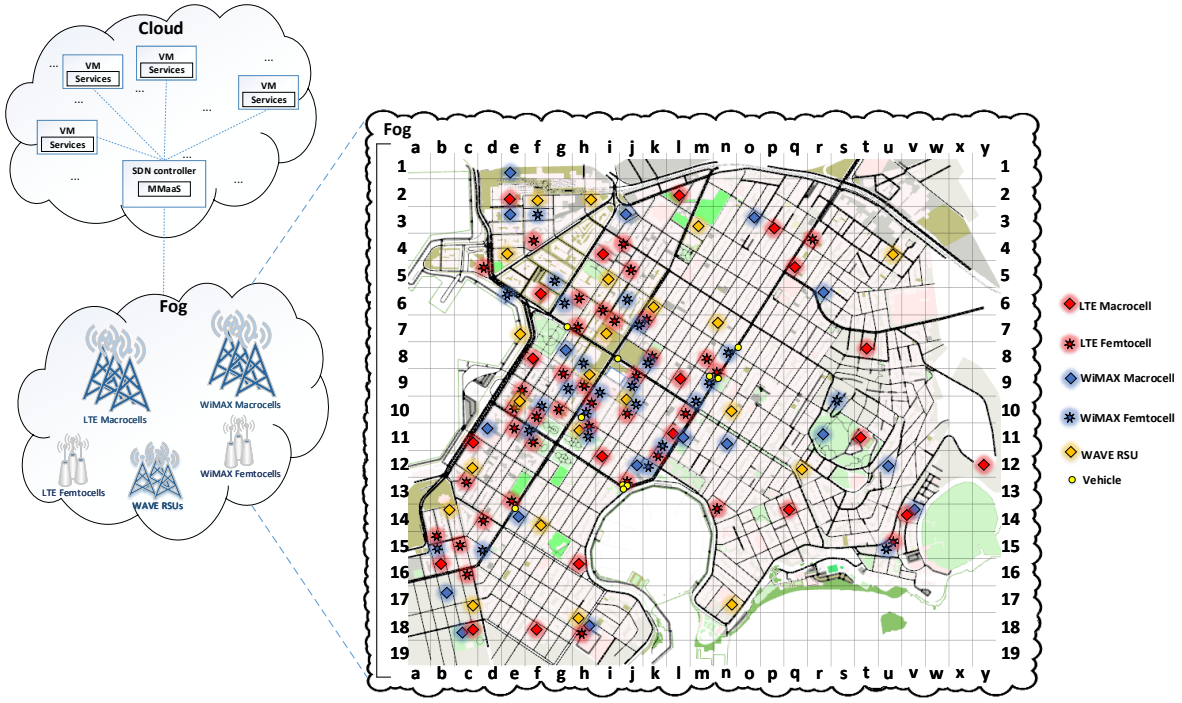

Figure 4.6 The Simulated Topology for the Evaluation of the proposed Mobility Management Scheme.

Table 4.3 Relation of the Network QoS Characteristics and Linguistic Terms for VoIP.

Linguistic term	Throughput range (Kbps)	Delay range (ms)	Jitter range (ms)	Packet loss range
AP	≤ 164	≥ 116	≥ 65	≥ 0.4
VP	165 - 174	111-115	55 - 64	≥ 0.2 - 0.4
P	175 - 184	106-110	45 - 54	$>10^{-1}$ - <0.2
MP	185 - 194	100 - 105	40 - 44	10^{-1}
M	195 - 204	95 - 99	35 - 49	10^{-2}
MG	205 - 214	86 - 94	30 - 34	10^{-3}
G	215 - 224	66 - 85	25 - 29	10^{-4}
VG	225 - 239	41 - 65	20 - 24	10^{-5}
AG	≥ 240	≤ 40	≤ 20	$\leq 10^{-6}$

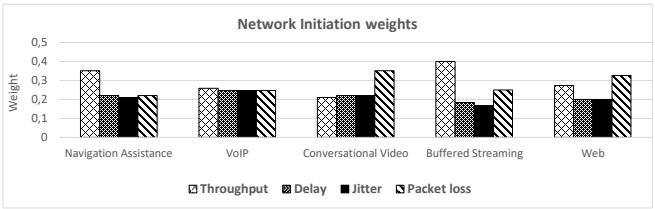

Figure 4.7 Criteria Weights per Service for the HO Initiation.

Table 4.4 The Simulation Parameters for the Evaluation of the proposed Mobility Management Scheme.

Parameter	Value
Simulation duration	86400 seconds (24 hours)
Networks count	LTE Macrocell BSs: 20 LTE Femtocell BSs: 37 WiMAX Macrocell BSs: 17 WiMAX Femtocell BSs: 25 WAVE RSUs: 22 Total: 121
Cells radius	LTE/WiMAX Macrocells: 400 meters LTE/WiMAX Femtocells: 30 meters WAVE RSUs: 150 meters
Networks positions	According to the Hellenic Telecommunications and Post Commission (EETT) [254] data (see Appendix A)
Networks frequencies	See Appendix A
Service Layer Agreements (SLA) count	4
Vehicles count	39807
Average vehicles arrival rate	0,460729167 vehicles per second
Average vehicles departure rate	0,46 vehicles per second
Vehicles per SLA	SLA 1: 9952 vehicles (25,00062803 %) SLA 2: 9952 vehicles (25,00062803 %) SLA 3: 9952 vehicles (25,00062803 %) SLA 4: 9951 vehicles (24,99811591 %)
Available networks per SLA	See Appendix B
Services	Navigation Assistance (NAV) Voice over IP (VoIP) Conversational Video (CV) Buffered Streaming (BS) Web Browsing (WB)
Distribution of services to vehicles	See Appendix C
Vehicles per velocity	Normal: 13348 (33.53 %) Medium: 13348 (33.53 %) High: 13111 (32.94 %)

Table 4.5 The available Networks for each Monitored Vehicle.

Vehicle	Available Networks in Current Location
1	LTE Macro 9, LTE Macro 11, LTE Femto 17, WiMAX Macro 8, WiMAX Macro 9, WiMAX Macro 11, WiMAX Femto 13, WAVE 14
2	LTE Macro 9, LTE Macro 11, LTE Femto 17, WiMAX Macro 8, WiMAX Macro 9, WiMAX Macro 11, WiMAX Femto 13, WAVE 14
3	LTE Macro 9, LTE Macro 11, LTE Macro 13, LTE Macro 18, LTE Femto 30, WiMAX Macro 8, WiMAX Macro 9, WiMAX Macro 11, WiMAX Macro 13
4	LTE Macro 4, LTE Macro 6, LTE Macro 7, LTE Macro 9, LTE Macro 11, LTE Macro 13, WiMAX Macro 6, WiMAX Macro 8, WiMAX Macro 11, WAVE 9, WAVE 11, WAVE 13
5	LTE Macro 4, LTE Macro 6, LTE Macro 7, WiMAX Macro 6, WAVE 9
6	LTE Macro 7, LTE Macro 9, LTE Macro 11, LTE Macro 13, LTE Femto 26, WiMAX Macro 6, WiMAX Macro 7, WiMAX Macro 8, WiMAX Macro 11, WiMAX Macro 13, WiMAX Femto 15, WAVE 11, WAVE 15
7	LTE Macro 10, LTE Macro 13, LTE Macro 17, LTE Macro 18, LTE Femto 29, WiMAX Macro 7, WiMAX Macro 13, WiMAX Macro 15, WAVE 19
8	LTE Macro 9, LTE Macro 11, LTE Macro 13, LTE Macro 18, LTE Femto 30, WiMAX Macro 8, WiMAX Macro 9, WiMAX Macro 11, WiMAX Macro 13
9	LTE Macro 3, LTE Macro 5, LTE Macro 9, WiMAX Macro 5, WiMAX Macro 8, WiMAX Macro 9
10	LTE Macro 9, LTE Macro 11, LTE Macro 13, LTE Macro 18, LTE Femto 30, WiMAX Macro 8, WiMAX Macro 9, WiMAX Macro 11, WiMAX Macro 13

Table 4.6 The Q_{SLA}, $SINR_{SLA}$ and $S_{th,SLA}$ thresholds per SLA.

SLA	Q_{SLA}	$SINR_{SLA}$	$S_{th,SLA}$
1	0.9	0.8	0.81675
2	0.8	0.7	0.70856
3	0.7	0.6	0.54440
4	0.6	0.5	0.42725

Table 4.7 The HO Initiation Results.

Vehicle	**Current Network i**	$Q_{u,i}$	$SINR_{u,i}$ ($SINR_{u,i}^{dB}$)	$S_{u,i}$	S_{th,SLA_u}	**Handover Required**
1	WAVE 14	0.871	0.14 (-5.1 dB)	0.18157	0.81843	Yes
2	LTE Macro 11	0.912	0.17 (-4.05 dB)	0.18212	0.81843	Yes
3	WiMAX Macro 8	0.948	0.29 (0.15 dB)	0.32523	0.81843	Yes
4	LTE Macro 7	0.644	0.23 (-1.95 dB)	0.12122	0.66980	Yes
5	WAVE 9	0.990	0.14 (-5.1 dB)	0.18156	0.66980	Yes
6	WAVE 11	0.827	0.04 (-8.6 dB)	0.02539	0.66980	Yes
7	WiMAX Macro 7	0.999	0.21 (-2.65 dB)	0.18965	0.57767	Yes
8	WiMAX Macro 11	0.704	0.71 (14.85 dB)	0.61247	0.57767	No
9	WiMAX Macro 5	0.988	0.25 (-1.25 dB)	0.27297	0.45457	Yes
10	LTE Macro 18	0.990	0.29 (0.15 dB)	0.35622	0.45457	Yes

Table 4.8 The Monitored Vehicles Status.

Vehicle	**SLA**	**Services**	**Current Position (Latitude, Longitude)**	**Velocity**
1	1	VoIP, CV, BS	9n (37.942128, 23.650937)	Medium
2	1	NAV, VoIP, WB	9m (37.942178, 23.650796)	Normal
3	1	NAV	13j (37.938831, 23.647276)	Medium
4	2	CV, BS	8i (37.942819, 23.647134)	Normal
5	2	BS	7g (37.943935, 23.645180)	High
6	2	CV, WB	10h (37.941048, 23.645664)	Normal
7	3	BS	14e (37.938048, 23.642797)	High
8	3	BS, WB	13j (37.988787, 23.647321)	Medium
9	4	WB	8o (37.943331, 23.652023)	High
10	4	WB	13j (37.938858, 23.647291)	Normal

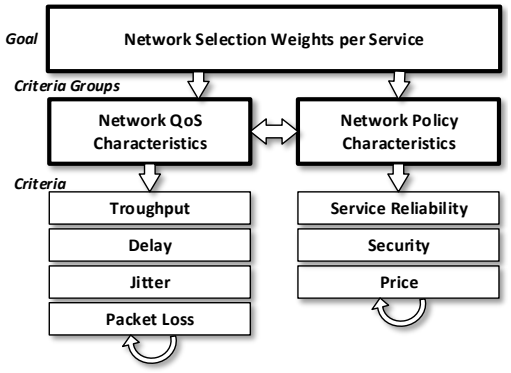

Figure 4.8 The PF-ANP Network Model.

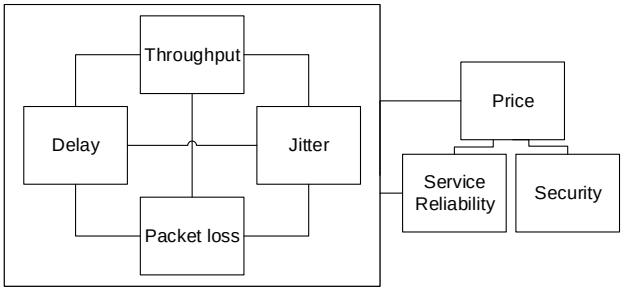

Figure 4.9 The Relations of the Criteria considered by the PF-ANP Network Model.

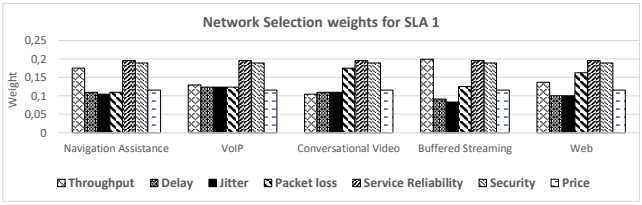

Figure 4.10 The Network Selection Weights per Service for SLA 1.

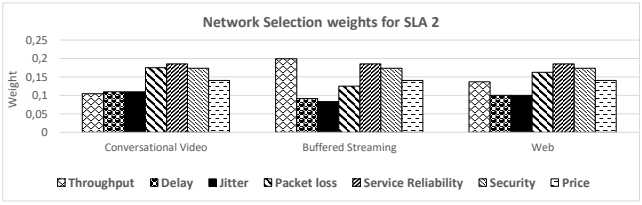

Figure 4.11 The Network Selection Weights per Service for SLA 2.

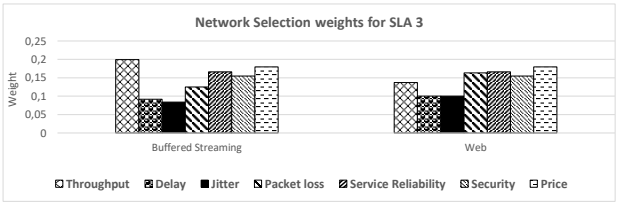

Figure 4.12 The Network Selection Weights per Service for SLA 3.

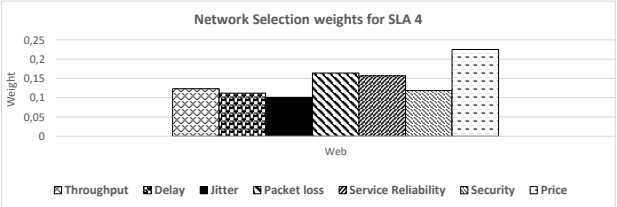

Figure 4.13 The Network Selection Weights per Service for SLA 4.

Table 4.9 The PF-ANP Initial Supermatrix for the SLA 1 NAV Service.

	Throughput	Delay	Jitter	Packet loss	Service Reliability	Security	Price
Throughput	[(0.37,0.36,0.34, 0.33,0.32,1,0.8,0.8), (0.36,0.36,0.34, 0.33,0.33,0.8,0.6,0.6)]	[(0.37,0.36,0.34, 0.33,0.32,1,0.8,0.8), (0.36,0.36,0.34, 0.33,0.33,0.8,0.6,0.6)]	[(0.37,0.36,0.34, 0.33,0.32,1,0.8,0.8), (0.36,0.36,0.34, 0.33,0.33,0.8,0.6,0.6)]	[(0.37,0.36,0.34, 0.33,0.32,1,0.8,0.8), (0.36,0.36,0.34, 0.33,0.33,0.8,0.6,0.6)]	[(0.37,0.36,0.349 0.33,0.32,1,0.8,0.8), (0.36,0.36,0.34, 0.33,0.33,0.8,0.6,0.6)]	[(0.37,0.36,0.34, 0.33,0.32,1,0.8,0.8), (0.36,0.36,0.34, 0.33,0.33,0.8,0.6,0.6)]	[(0.37,0.36,0.34, 0.33,0.32,1,0.8,0.8), (0.36,0.36,0.34, 0.33,0.33,0.8,0.6,0.6)]
Delay	[(0.23,0.21,0.21, 0.21,0.21,1,0.8,0.8), (0.21,0.21,0.21, 0.21,0.21,0.8,0.6,0.6)]	[(0.23,0.21,0.21 ,0.21,0.21,1,0.8,0.8), (0.21,0.21,0.21, 0.21,0.21,0.8,0.6,0.6)]	[(0.23,0.21,0.21, 0.21,0.21,1,0.8,0.8), (0.21,0.21,0.21, 0.21,0.21,0.8,0.6,0.6)]	[(0.23,0.21,0.21, 0.21,0.21,1,0.8,0.8), (0.21,0.21,0.21, 0.21,0.21,0.8,0.6,0.6)]	[(0.23,0.21,0.21, 0.21,0.21,1,0.8,0.8), (0.21,0.21,0.21, 0.21,0.21,0.8,0.6,0.6)]	[(0.23,0.21,0.21, 0.21,0.21,1,0.8,0.8), (0.21,0.21,0.21, 0.21,0.21,0.8,0.6,0.6)]	[(0.23,0.21,0.21, 0.21,0.21,1,0.8,0.8), (0.21,0.21,0.21, 0.21,0.21,0.8,0.6,0.6)]
Jitter	[(0.16,0.2,0.22, 0.23,0.24,1,0.8,0.8), (0.19,0.2,0.22, 0.23,0.23,0.8,0.6,0.6)]	[(0.16,0.2,0.22, 0.23,0.24,1,0.8,0.8), (0.19,0.2,0.22, 0.23,0.23,0.8,0.6,0.6)]	[(0.16,0.2,0.22, 0.23,0.24,1,0.8,0.8), (0.19,0.2,0.22, 0.23,0.23,0.8,0.6,0.6)]	[(0.16,0.2,0.22, 0.23,0.24,1,0.8,0.8), (0.19,0.2,0.22, 0.23,0.23,0.8,0.6,0.6)]	[(0.16,0.2,0.22, 0.23,0.24,1,0.8,0.8), (0.19,0.2,0.22, 0.23,0.23,0.8,0.6,0.6)]	[(0.16,0.2,0.22, 0.23,0.24,1,0.8,0.8), (0.19,0.2,0.22, 0.23,0.23,0.8,0.6,0.6)]	[(0.16,0.2,0.22, 0.23,0.24,1,0.8,0.8), (0.19,0.2,0.22, 0.23,0.23,0.8,0.6,0.6)]
Packet loss	[(0.23,0.21,0.21, 0.21,0.21,1,0.8,0.8), (0.21,0.21,0.21, 0.21,0.21,0.8,0.6)]	[(0.23,0.21,0.21, 0.21,0.21,1,0.8,0.8), (0.21,0.21,0.21, 0.21,0.21,0.8,0.6)]	[(0.23,0.21,0.21, 0.21,0.21,1,0.8,0.8), (0.21,0.21,0.21, 0.21,0.21,0.8,0.6)]	[(0.23,0.21,0.21, 0.21,0.21,1,0.8,0.8), (0.21,0.21,0.21, 0.21,0.21,0.8,0.6)]	[(0.23,0.21,0.21, 0.21,0.21,1,0.8,0.8), (0.21,0.21,0.21, 0.21,0.21,0.8,0.6)]	[(0.23,0.21,0.21, 0.21,0.21,1,0.8,0.8), (0.21,0.21,0.21, 0.21,0.21,0.8,0.6)]	[(0.23,0.21,0.21, 0.21,0.21,1,0.8,0.8), (0.21,0.21,0.21, 0.21,0.21,0.8,0.6)]
Service Reliability	[(0.52,0.47,0.42 ,0.4,0.4,1,0.8,0.8), (0.48,0.45,0.42, 0.41,0.4,0.8,0.6,0.6)]	[(0.52,0.47,0.42, 0.4,0.4,1,0.8,0.8), (0.48,0.45,0.42, 0.41,0.4,0.8,0.6,0.6)]	[(0.52,0.47,0.42, 0.4,0.4,1,0.8,0.8), (0.48,0.45,0.42, 0.41,0.4,0.8,0.6,0.6)]	[(0.52,0.47,0.42, 0.4,0.4,1,0.8,0.8), (0.48,0.45,0.42, 0.41,0.4,0.8,0.6,0.6)]	[(0.52,0.47,0.42, 0.4,0.4,1,0.8,0.8), (0.48,0.45,0.42, 0.41,0.4,0.8,0.6,0.6)]	[(0.52,0.47,0.42, 0.4,0.4,1,0.8,0.8), (0.48,0.45,0.42, 0.41,0.4,0.8,0.6,0.6)]	[(0.52,0.47,0.42, 0.4,0.4,1,0.8,0.8), (0.48,0.45,0.42, 0.41,0.4,0.8,0.6,0.6)]
Security	[(0.37,0.39,0.4, 0.4,0.4,1,0.8,0.8), (0.39,0.4,0.4, 0.4,0.4,0.8,0.6,0.6)]	[(0.37,0.39,0.4, 0.4,0.4,1,0.8,0.8), (0.39,0.4,0.4, 0.4,0.4,0.8,0.6,0.6)]	[(0.37,0.39,0.4, 0.4,0.4,1,0.8,0.8), (0.39,0.4,0.4, 0.405,0.4,0.8,0.6,0.6)]	[(0.37,0.39,0.4, 0.4,0.4,1,0.8,0.8), (0.39,0.4,0.4, 0.4,0.403,0.8,0.6,0.6)]	[(0.37,0.39,0.4, 0.4,0.4,1,0.8,0.8), (0.39,0.4,0.4, 0.4,0.4,0.8,0.6,0.6)]	[(0.37,0.39,0.4, 0.4,0.4,1,0.8,0.8), (0.39,0.4,0.4, 0.4,0.4,0.8,0.6,0.6)]	[(0.37,0.39,0.4, 0.4,0.4,1,0.8,0.8), (0.39,0.4,0.4, 0.4,0.4,0.8,0.6,0.6)]
Price	[(0.09,0.13,0.16, 0.18,0.19,1,0.8,0.8), (0.12,0.14,0.16, 0.18,0.18,0.8,0.6,0.6)]	[(0.09,0.13,0.16, 0.18,0.19,1,0.8,0.8), (0.12,0.14,0.16, 0.18,0.18,0.8,0.6,0.6)]	[(0.09,0.13,0.16, 0.18,0.19,1,0.8,0.8), (0.12,0.14,0.166, 0.18,0.18,0.8,0.6,0.6)]	[(0.09,0.13,0.16, 0.18,0.19,1,0.8,0.8), (0.12,0.14,0.16, 0.18,0.18,0.8,0.6,0.6)]	[(0.09,0.13,0.16, 0.18,0.19,1,0.8,0.8), (0.12,0.14,0.16, 0.18,0.18,0.8,0.6,0.6)]	[(0.09,0.13,0.16, 0.18,0.19,1,0.8,0.8), (0.12,0.14,0.16, 0.18,0.18,0.8,0.6,0.6)]	[(0.09,0.13,0.16, 0.18,0.19,1,0.8,0.8), (0.12,0.14,0.16, 0.18,0.18,0.8,0.6,0.6)]

Table 4.10 The PF-ANP Weighted Supermatrix for the SLA 1 NAV Service.

	Throughput	Delay	Jitter	Packet loss	Service Reliability	Security	Price
Throughput	[(0.18,0.18,0.17, 0.16,0.16,1,0.8,0.8), (0.18,0.18,0.17, 0.16,0.16,0.8,0.6,0.6)]	[(0.18,0.18,0.17, 0.16,0.16,1,0.8,0.8), (0.18,0.18,0.17, 0.16,0.16,0.8,0.6,0.6)]	[(0.18,0.18,0.17, 0.16,0.16,1,0.8,0.8), (0.18,0.18,0.17, 0.16,0.16,0.8,0.6,0.6)]	[(0.18,0.18,0.17, 0.16,0.16,1,0.8,0.8), (0.18,0.18,0.17, 0.16,0.16,0.8,0.6,0.6)]	[(0.18,0.18,0.17, 0.16,0.16,1,0.8,0.8), (0.18,0.18,0.17, 0.16,0.16,0.8,0.6,0.6)]	[(0.18,0.18,0.17, 0.16,0.16,1,0.8,0.8), (0.18,0.18,0.17, 0.16,0.16,0.8,0.6,0.6)]	[(0.18,0.18,0.17, 0.16,0.16,1,0.8,0.8), (0.18,0.18,0.17, 0.16,0.16,0.8,0.6,0.6)]
Delay	[(0.11,0.1,0.1, 0.1,0.1,1,0.8,0.8), (0.1,0.1,0.1, 0.1,0.1,0.8,0.6,0.6)]	[(0.11,0.1,0.1, 0.1,0.1,1,0.8,0.8), (0.1,0.1,0.1, 0.106,0.1,0.8,0.6,0.6)]	[(0.11,0.1,0.1, 0.1,0.1,1,0.8,0.8), (0.1,0.1,0.1, 0.1,0.1,0.8,0.6,0.6)]	[(0.11,0.1,0.1, 0.1,0.1,1,0.8,0.8), (0.1,0.1,0.1,0.1, 0.1,0.8,0.6,0.6)]	[(0.11,0.1,0.1, 0.1,0.1,1,0.8,0.8), (0.1,0.1,0.1, 0.1,0.1,0.8,0.6,0.6)]	[(0.11,0.1,0.1, 0.1,0.1,1,0.8,0.8), (0.1,0.1,0.1, 0.1,0.1,0.8,0.6,0.6)]	[(0.11,0.1,0.1, 0.1,0.1,1,0.8,0.8), (0.1,0.1,0.1, 0.1,0.1,0.8,0.6,0.6)]
Jitter	[(0.08,0.1,0.11, 0.11,0.12,1,0.8,0.8), (0.09,0.1,0.11, 0.11,0.11,0.8,0.6,0.6)]	[(0.08,0.1,0.11, 0.11,0.12,1,0.8,0.8), (0.09,0.1,0.11, 0.11,0.11,0.8,0.6,0.6)]	[(0.08,0.1,0.11, 0.11,0.12,1,0.8,0.8), (0.09,0.1,0.11, 0.11,0.11,0.8,0.6,0.6)]	[(0.08,0.1,0.11, 0.11,0.12,1,0.8,0.8), (0.09,0.1,0.11, 0.11,0.11,0.8,0.6,0.6)]	[(0.08,0.1,0.11, 0.11,0.12,1,0.8,0.8), (0.09,0.1,0.11, 0.11,0.11,0.8,0.6,0.6)]	[(0.08,0.1,0.11, 0.11,0.12,1,0.8,0.8), (0.09,0.1,0.11, 0.11,0.11,0.8,0.6,0.6)]	[(0.08,0.1,0.11, 0.11,0.12,1,0.8,0.8), (0.09,0.1,0.11, 0.11,0.11,0.8,0.6,0.6)]
Packet loss	[(0.11,0.1,0.1, 0.1,0.1,1,0.8,0.8), (0.1,0.1,0.1, 0.1,0.1,0.8,0.6,0.6)]	[(0.11,0.1,0.1, 0.1,0.1,1,0.8,0.8), (0.1,0.1,0.1, 0.106,0.1,0.8,0.6,0.6)]	[(0.11,0.1,0.1, 0.1,0.1,1,0.8,0.8), (0.1,0.1,0.1, 0.1,0.1,0.8,0.6,0.6)]	[(0.11,0.1,0.1, 0.1,0.10,1,0.8,0.8), (0.1,0.1,0.1, 0.1,0.1,0.8,0.6,0.6)]	[(0.11,0.1,0.1, 0.1,0.1,1,0.8,0.8), (0.1,0.1,0.1, 0.1,0.1,0.8,0.6,0.6)]	[(0.11,0.1,0.1, 0.1,0.1,1,0.8,0.8), (0.1,0.1,0.1, 0.1,0.1,0.8,0.6,0.6)]	[(0.11,0.1,0.1, 0.1,0.1,1,0.8,0.8), (0.1,0.1,0.1, 0.1,0.1,0.8,0.6,0.6)]
Service Reliability	[(0.26,0.23,0.21, 0.2,0.2,1,0.8,0.8), (0.24,0.22,0.21, 0.2,0.2,0.8,0.6,0.6)]	[(0.26,0.23,0.21, 0.2,0.2,1,0.8,0.8), (0.24,0.22,0.21, 0.2,0.2,0.8,0.6,0.6)]	[(0.26,0.23,0.21, 0.2,0.2,1,0.8,0.8), (0.24,0.22,0.21, 0.2,0.2,0.8,0.6,0.6)]	[(0.26,0.23,0.21, 0.2,0.2,1,0.8,0.8), (0.24,0.22,0.21, 0.2,0.2,0.8,0.6,0.6)]	[(0.26,0.23,0.21, 0.2,0.2,1,0.8,0.8), (0.24,0.22,0.21, 0.2,0.2,0.8,0.6,0.6)]	[(0.26,0.23,0.21, 0.2,0.2,1,0.8,0.8), (0.24,0.22,0.21, 0.2,0.2,0.8,0.6,0.6)]	[(0.26,0.23,0.21, 0.2,0.2,1,0.8,0.8), (0.24,0.2,0.21, 0.2,0.2,0.8,0.6,0.6)]
Security	[(0.18,0.19,0.2, 0.2,0.2,1,0.8,0.8), (0.19,0.2,0.2, 0.2,0.2,0.8,0.6,0.6)]	[(0.18,0.19,0.2, 0.2,0.2,1,0.8,0.8), (0.19,0.2,0.2, 0.2,0.2,0.8,0.6,0.6)]	[(0.18,0.19,0.2, 0.2,0.2,1,0.8,0.8), (0.19,0.2,0.2, 0.2,0.2,0.8,0.6,0.6)]	[(0.18,0.19,0.2, 0.2,0.2,1,0.8,0.8), (0.19,0.2,0.2, 0.2,0.2,0.8,0.6,0.6)]	[(0.18,0.19,0.2, 0.2,0.2,1,0.8,0.8), (0.19,0.2,0.2, 0.2,0.2,0.8,0.6,0.6)]	[(0.18,0.19,0.2, 0.2,0.2,1,0.8,0.8), (0.19,0.2,0.2, 0.2,0.2,0.8,0.6,0.6)]	[(0.18,0.19,0.2, 0.2,0.2,1,0.8,0.8), (0.19,0.2,0.2, 0.2,0.2,0.8,0.6,0.6)]
Price	[(0.04,0.06,0.08, 0.09,0.09,1,0.8,0.8), (0.06,0.07,0.08, 0.09,0.09,0.8,0.6,0.6)]	[(0.04,0.06,0.08, 0.09,0.09,1,0.8,0.8), (0.06,0.07,0.08, 0.09,0.09,0.8,0.6,0.6)]	[(0.04,0.06,0.08, 0.09,0.09,1,0.8,0.8), (0.06,0.07,0.08, 0.09,0.09,0.8,0.6,0.6)]	[(0.04,0.06,0.08, 0.09,0.09,1,0.8,0.8), (0.06,0.07,0.08, 0.09,0.09,0.8,0.6,0.6)]	[(0.04,0.06,0.08, 0.09,0.09,1,0.8,0.8), (0.06,0.07,0.08, 0.09,0.09,0.8,0.6,0.6)]	[(0.04,0.06,0.08, 0.09,0.09,1,0.8,0.8), (0.06,0.07,0.08, 0.09,0.09,0.8,0.6,0.6)]	[(0.04,0.06,0.08, 0.09,0.09,1,0.8,0.8), (0.06,0.07,0.08, 0.09,0.09,0.8,0.6,0.6)]

Table 4.11 The PF-ANP Limit Supermatrix for the SLA 1 NAV Service.

	Throughput	Delay	Jitter	Packet loss	Service Reliability	Security	Price
Throughput	0.175346	0.175346	0.175346	0.175346	0.175346	0.175346	0.175346
Delay	0.109943	0.109943	0.109943	0.109943	0.109943	0.109943	0.109943
Jitter	0.104768	0.104768	0.104768	0.104768	0.104768	0.104768	0.104768
Packet loss	0.109943	0.109943	0.109943	0.109943	0.109943	0.109943	0.109943
Service Reliability	0.195427	0.195427	0.195427	0.195427	0.195427	0.195427	0.195427
Security	0.188775	0.188775	0.188775	0.188775	0.188775	0.188775	0.188775
Price	0.115798	0.115798	0.115798	0.115798	0.115798	0.115798	0.115798

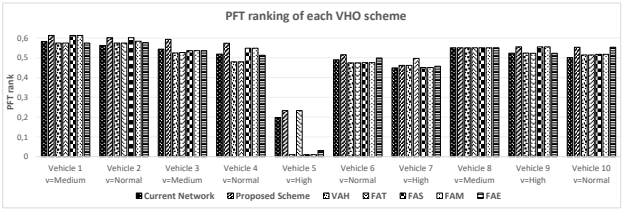

Figure 4.14 The PFT Ranking of each HO Scheme.

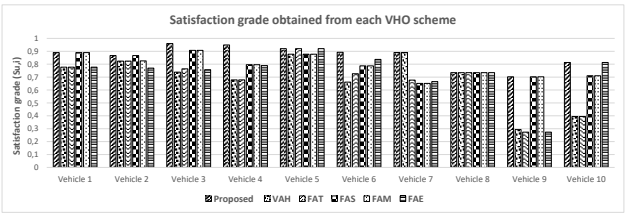

Figure 4.15 The Satisfaction Grade obtained from each HO Scheme.

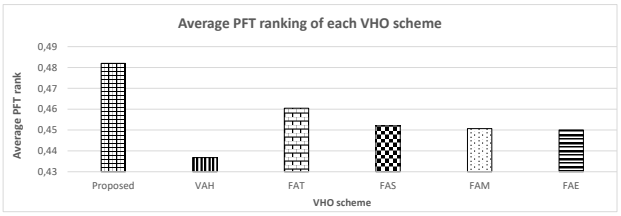

Figure 4.16 The Average PFT Ranking of each HO Scheme during the 24 Hours Simulation.

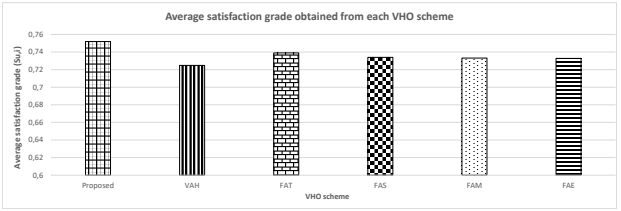

Figure 4.17 The Average Satisfaction Grade obtained from each HO Scheme during the 24 Hours Simulation.

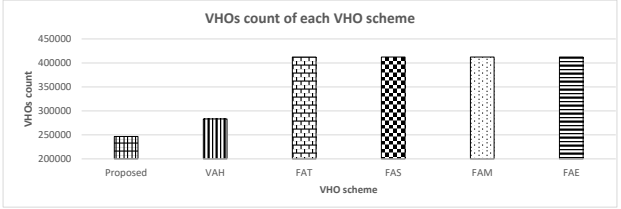

Figure 4.18 The Total HOs Count of each HO Scheme during the 24 Hours Simulation.

Chapter 5

Conclusion

In this doctoral thesis, two key aspects of the 5G-VCC systems were studied, namely the allocation of network resources and the handling of the vehicles' mobility.

Regarding the allocation of the network resources, an overview of the available MAC schemes for vehicular networks has been performed [257]. These schemes can be applied in 5G-VCC systems in order optimal manipulation of communication resources to be performed. Some schemes organize the vehicles into clusters, while GPS receivers are used in some cases in order the vehicles to be synchronized with each other. The discussed schemes apply either distributed or centralized control. In a 5G-VCC system the centralized control could be enhanced using an SDN controller, while the distributed control could be easily configured using a Fog computing infrastructure. Furthermore, V2V communication is supported from most schemes, while some schemes support V2I communication. Finally, during the medium access, CRN could be applied to take advantage of free white spaces into the available spectrum.

Subsequently, a QoS aware scheduler called FLSA [258][259] was proposed in order to improve the resource allocation for real time services in the LTE downlink. FLSA has been built on three distinct levels which cooperate with each other to allocate the network resources to users. In every TTI the upper level estimates the quota of the data that each real-time flow should transmit to satisfy its QoS constraints. Then, the middle level uses the M-LWDF algorithm to allocate RBs to real time flows in each TTI for transmitting their quota of data obtained by the upper level. Thereafter, if there are free RBs available in the current TTI, the lower level allocates them both to real time and to best effort flows, using the M-LWDF algorithm. The performance of FLSA for real time flows was compared against other scheduling algorithms in terms of PLR, attainable throughput and fairness. The simulation results showed that the FLSA scheduler outperforms the rest of the schemes by achieving better resource allocation for real time services.

Furthermore, FLSA-CC [260], QoS aware cross carrier downlink scheduler has also been proposed as an extended version of the FLSA. FLSA-CC operates in an LTE-A network with relay nodes in a CA mode. The proposed scheduler has been built upon three distinct levels which cooperate with each other to allocate the network resources to users in a manner that the requirements of strict real times services are satisfied while a starvation of the best effort traffic is avoided. The performance of FLSA-CC is compared against other scheduling algorithms in terms of PLR, throughput and fairness index, in a cloud assisted software defined architecture. The simulation results showed that the FLSA-CC scheduler outperforms the rest of the scheduling schemes by achieving better resource allocation for both real time and best effort services.

An overview of existing mobility management schemes has been made. These schemes can be applied to 5G-VCC systems in order an optimal manipulation of vehicles mobility to be performed. Each scheme implements one or more mobility management subprocesses, namely HO initiation, network selection and HO execution. The 5G-VCC topologies (e.g. VC, VuC, VuF, SDN-V and HVT) that each scheme supports were mentioned, while the communication models that could be applied in each scheme (V2V, V2I, V2P and HVC) were introduced. The control type of each scheme (vehicle or network controlled) was also described, while at the same time the OSI layer where each scheme was implemented indicate its mobility management capabilities. In addition, the supported message exchange mechanisms were considered, while the evaluation of each scheme considering the type of the implemented algorithms provided useful knowledge about its design.

Novel mobility management algorithms for 5G networks were proposed. Specifically, firstly, we described a network selection method that takes into account the network QoS characteristics policies, application requirements and different types of user SLAs to select the optimal network that will satisfy simultaneously all the applications' requirements and the users' preferences running on a mobile user's device [171]. The proposed method employed two MADM algorithms: the ANP for criteria weights calculation and the TFT for accomplishing the overall rating of the network technologies. ANP was selected to determine the relative importance and the dependence of the criteria. As selection criteria, we considered the network QoS parameters, service constraints, user requirements and provider policies. These criteria were represented by interval-valued trapezoidal fuzzy numbers. Then, the TFT algorithm was applied to calculate the overall rating of the available networks. The performance evaluation of TFT showed that when a user has only one service, it provides similar results to the original TOPSIS and FAE methods. However, when a user requires multiple services, TFT performs better by satisfying multiple groups of criteria per user since the original TOPSIS and FAE methods cannot support more than one services. Furthermore, according to the sensitivity

analysis of results it was shown that the described method doesn't suffer from the ranking abnormality problem, thus, the results are normally adjusted to the heterogeneous network environment changes.

Furthermore, we proposed a network selection scheme for supporting medical services in 5G-VCC systems [68][261]. The discussed scheme consists of the TF-ANP method to calculate the relative importance of the selection criteria and the TFT to accomplish the ranking of the candidate networks. The health status of each patient is considered, while the criteria used for network evaluation included throughput, delay, jitter, packet loss, service reliability, security and price. The performance evaluation showed that the proposed scheme outperforms existing network selection methods by satisfying multiple groups of criteria and medical services per user. Also, we proposed an improved version of this scheme [66]. In this case, the discussed scheme consists of two FMADM algorithms, namely the TF-AANP to calculate the relative importance of each service, as well as the weights of the selection criteria and the TFT-ACW to accomplish the ranking of the candidate networks. The health status of onboard patients and the SLA of each vehicle were considered, while the criteria used for network evaluation include throughput, delay, jitter, packet loss, service reliability, security and price. The performance evaluation showed that the proposed scheme outperforms existing network selection methods by satisfying the strict constraints of medical services, when the patient's health status becomes immediate and multiple types of non-medical services coexist with medical services to the vehicle.

Finally, we proposed a HO management scheme for 5G-VCC systems that takes into account the vehicle velocity, network's QoS and policy characteristics, the vehicular services' requirements and the various vehicle SLAs to select the optimal network that will satisfy simultaneously all the service requirements and onboard user preferences [67][262]. The HO management services are executed at the Cloud or the Fog infrastructure alleviating the vehicle's processing load and reducing HO latency. IVPFNs are used for the representation of both HO Initiation and Network Selection criteria values, while the PF-ANP algorithm is used for the estimation of the criteria weights for both HO Initiation and Network Selection. During the HO Initiation, MPFIS evaluates the necessity to perform a handover, while during the Network Selection, the PFT algorithm selects the most appropriate network considering the vehicle's velocity, the constraints of used vehicular services and the SLA of the vehicle. The performance evaluation showed that the Always Best Connected (ABC) principle is fully ensured, while at the same time the proposed scheme outperforms existing HO management algorithms in terms of the PFT ranks of the selected networks, the user satisfaction grade, as well as the VHOs count.

5.1 Directions for Future Work

This section discusses some open issues arising from the study of the existing resource allocation and mobility management schemes. Although several schemes have been proposed to the research literature, some issues need to be resolved in cases where they resource allocation and/or mobility management concerns a 5G-VCC system. Specifically, although many algorithms can perform resource allocation and/or mobility management in 5G-VCC systems, the support for relay vehicles is limited. Vehicular relaying could be used in order vehicles with no access to RSUs/BSs to obtain this access through vehicles that already have it and could be called as relay vehicles. In these cases, vehicular relaying increases the coverage area of the 5G-VCC system providing access to an increased number of vehicles. Furthermore, in these cases Vehicle to Vehicle (V2V) routing issues must be addressed, since a vehicle should obtain access to RSUs/BSs through more than one relaying vehicles. However, the existing resource allocation algorithms are not optimized for distributing the communication resources of relay vehicles. Also, mobility management schemes do not address relay vehicles selection or routing issues.

Furthermore, the resource allocation and/or mobility management functionalities of the 5G-VCC systems can be performed by a Cloud or a Fog infrastructure, as well as using SDN controllers, leading to solutions where both Host and Network control are combined. An open issue that arises from this situation is the need for the implementation of purely network controlled solutions, where components of the 5G-VCC infrastructure with fully knowledge about vehicles' network status as well as with a complete view of the entire system, will perform the resource allocation and/or the mobility management releasing the vehicular equipment from this task, freeing up its resources and reducing its energy requirements.

Publications

1. Emmanouil Skondras, Eirini Zoumi, Angelos Michalas, Dimitrios D. Vergados, "A Network Selection Algorithm for supporting Drone Services in 5G Network Architectures", Wireless Telecommunications Symposium (WTS), New York, USA, April 9-12, 2019

2. Konstantina Siountri, Emmanouil Skondras, Theodoros Mavroeidakos, Dimitrios D. Vergados, "The Convergence of Blockchain, Internet of Things (IoT) and Building Information Modeling (BIM): The smart museum case", Wireless Telecommunications Symposium (WTS), New York, USA, April 9-12, 2019

3. Emmanouil Skondras, Angelos Michalas, Dimitrios D. Vergados, "Mobility Management on 5G Vehicular Cloud Computing Systems", Vehicular Communications Journal, Elsevier, vol. 16, pp. 15-44, April 2019

4. Emmanouil Skondras, Konstantina Siountri, Angelos Michalas, Dimitrios D. Vergados, "Personalized Real-Time Virtual Tours in Places with Cultural Interest", International Journal of Computational Methods in Heritage Science (IJCMHS), IGI Global, vol. 3, issue 1, January 2019

5. Konstantina Siountri, Emmanouil Skondras, Dimitrios D. Vergados, Christos-Nikolaos Anagnostopoulos, "The Revival of Back-Filled Monuments through Augmented Reality (AR)", Visual Heritage Congress, Vienna, Austria, November 12-15, 2018

6. Konstantina Siountri, Emmanouil Skondras, Dimitrios D. Vergados, "A Delivery Model for Cultural Heritage Services in Smart Cities Environments", Euro-Mediterranean Conference (EUROMED), Springer, pp.279-288, Nicosia, Cyprus, October 29-November 3, 2018

7. Emmanouil Skondras, Angelos Michalas, Dimitrios D. Vergados, "A Survey on Medium Access Control Schemes for 5G Vehicular Cloud Computing Systems", Global Information Infrastructure and Networking Symposium (GIIS), Thessaloniki, Greece, October 23-25, 2018

8. Emmanouil Skondras, Konstantina Siountri, Angelos Michalas, Dimitrios D. Vergados, "A Route Selection Scheme for supporting Virtual Tours in Sites with Cultural Interest using Drones", International Conference on Information, Intelligence, Systems and Applications (IISA), Zakynthos, Greece, July 23-25, 2018

9. Emmanouil Skondras, Angelos Michalas, Nikolaos Tsolis, Dimitrios D. Vergados, "A Network Selection Scheme with Adaptive Criteria Weights for 5G Vehicular Systems", International Conference on Information, Intelligence, Systems and Applications (IISA), Zakynthos, Greece, July 23-25, 2018

10. Emmanouil Skondras, Angelos Michalas, Nikolaos Tsolis, Dimitrios D. Vergados, "A VHO Scheme for supporting Healthcare Services in 5G Vehicular Cloud Computing Systems", Wireless Telecommunications Symposium (WTS), Phoenix, Arizona, USA, April 18-20, 2018

11. Emmanouil Skondras, Angelos Michalas, Nikolaos Tsolis, Aggeliki Sgora, Dimitrios D. Vergados, "A Network Selection Scheme for Healthcare Vehicular Cloud Computing Systems", International Conference on Information, Intelligence, Systems and Applications (IISA), Larnaka, Cyprus, August 28-30, 2017

12. Emmanouil Skondras, Angelos Michalas, Aggeliki Sgora, Dimitrios D. Vergados, "A Vertical Handover management scheme for VANET Cloud Computing systems", IEEE Symposium on Computers and Communications (ISCC), Heraklion, Crete, Greece, July 3-6, 2017

13. Emmanouil Skondras, Angelos Michalas, Aggeliki Sgora, Dimitrios D. Vergados, "QoS-aware scheduling in LTE-A networks with SDN control", International Conference on Information, Intelligence, Systems and Applications (IISA), Chalkidiki, Greece, July 13-15, 2016

14. Emmanouil Skondras, Angelos Michalas, Aggeliki Sgora, Dimitrios D. Vergados, "A downlink scheduler supporting real time services in LTE cellular networks", International Conference on Information, Intelligence, Systems and Applications (IISA), Ionian University, Corfu, Greece, July 6-8, 2015

15. Emmanouil Skondras, Angelos Michalas, Aggeliki Sgora, Dimitrios D. Vergados, "A QoS Aware Three Level Scheduler for the LTE Downlink", Wireless Telecommunications Symposium (WTS), Poster Paper, New York, USA, April 15-17, 2015

16. Emmanouil Skondras, Aggeliki Sgora, Angelos Michalas, Dimitrios D. Vergados, “An analytic network process and trapezoidal interval-valued fuzzy technique for order preference by similarity to ideal solution network access selection method”, International Journal of Communication Systems (IJCS), Wiley, September 2014

17. Emmanouil Skondras, Angelos Michalas, Malamati Louta, George Kouzas, “Personalized Multimedia Web Services in Peer to Peer Networks Using MPEG-7 and MPEG-21 Standards”, Studies in Computational Intelligence – Semantic Hyper/Multimedia Adaptation, Volume 418/2013 (book chapter), pp. 361-383, Springer-Verlag Berlin Heidelberg, 2013

Bibliography

[1] Ricard Vilalta, Victor Lopez, Alessio Giorgetti, Shuping Peng, Vittorio Orsini, Luis Velasco, Rene Serral-Gracia, Donal Morris, Silvia De Fina, Filippo Cugini, et al. Telcofog: A unified flexible fog and cloud computing architecture for 5g networks. *IEEE Communications Magazine*, 55(8):36–43, 2017.

[2] Faqir Zarrar Yousaf, Michael Bredel, Sibylle Schaller, and Fabian Schneider. Nfv and sdn-key technology enablers for 5g networks. *IEEE Journal on Selected Areas in Communications*, 2017.

[3] Hojjat Salehinejad, Hossein Nezamabadi-pour, Saeid Saryazdi, and Fereydoun Farrahi-Moghaddam. Combined a*-ants algorithm: a new multi-parameter vehicle navigation scheme. *arXiv preprint arXiv:1504.07329*, 2015.

[4] Pietro Edoardo Carnelli, Joy Yeh, Mahesh Sooriyabandara, and Aftab Khan. Parkus: A novel vehicle parking detection system. In *AAAI*, pages 4650–4656, 2017.

[5] Yang Li, Xiaoming Tao, and Jianhua Lu. Hybrid model-and-object-based real-time conversational video coding. *Signal Processing: Image Communication*, 35:9–19, 2015.

[6] Toon De Pessemier, Isabelle Stevens, Lieven De Marez, Luc Martens, and Wout Joseph. Quality assessment and usage behavior of a mobile voice-over-ip service. *Telecommunication Systems*, 61(3):417–432, 2016.

[7] Henrik Klessig and Gerhard Fettweis. Impact of inter-cell interference on buffered video streaming startup delays. In *Vehicular Technology Conference (VTC Fall), 2015 IEEE 82nd*, pages 1–2. IEEE, 2015.

[8] Verdes Pedras, Marco Sousa, Pedro Vieira, Maria-Paula Queluz, and Antonio Rodrigues. A no-reference user centric qoe model for voice and web browsing based on 3g/4g radio measurements. In *Wireless Communications and Networking Conference (WCNC), 2018 IEEE*, pages 1–6. IEEE, 2018.

[9] Zinonas C Antoniou, Andreas S Panayides, Marios Pantziaris, Anthony G Constantinides, Constantinos S Pattichis, and Marios S Pattichis. Dynamic network adaptation for real-time medical video communication. In *XIV Mediterranean Conference on Medical and Biological Engineering and Computing 2016*, pages 1099–1104. Springer, 2016.

[10] Luís FR Lucas, Nuno MM Rodrigues, Luis A da Silva Cruz, and Sérgio MM de Faria. Lossless compression of medical images using 3-d predictors. *IEEE transactions on medical imaging*, 36(11):2250–2260, 2017.

[11] Gopi Krishna Garge, Chitra Balakrishna, and Soumya Kanti Datta. Consumer health care: Current trends in consumer health monitoring. *IEEE Consumer Electronics Magazine*, 7(1):38–46, 2018.

[12] Qinghan Xue and Mooi Choo Chuah. Incentivising high quality crowdsourcing medical data for disease diagnose & survival prediction. *Smart Health*, 2017.

[13] Tugce Bilen, Berk Canberk, and Kaushik R Chowdhury. Handover management in software-defined ultra-dense 5g networks. *IEEE Network*, 31(4):49–55, 2017.

[14] TS 36.213 version 14.2.0: Evolved Universal Terrestrial Radio Access Network (E-UTRAN) (Release 14). *Technical Specification, 3GPP*, 2017.

[15] P802.16/d4 - ieee draft standard for air interface for broadband wireless access systems (revision of ieee std 802.16-2012). *IEEE Standard*, 2017.

[16] 1609.12-2016 - ieee standard for wireless access in vehicular environments (wave) – networking services. *IEEE Standard*, 2016.

[17] Hucheng Wang, Shanzhi Chen, Ming Ai, and Hui Xu. Localized mobility management for 5g ultra dense network. *IEEE Transactions on Vehicular Technology*, 66(9):8535–8552, 2017.

[18] Daniel Calabuig, Sokratis Barmpounakis, Sonia Gimenez, Apostolos Kousaridas, Tilak R Lakshmana, Javier Lorca, Petteri Lunden, Zhe Ren, Pawel Sroka, Emmanuel Ternon, et al. Resource and mobility management in the network layer of 5g cellular ultra-dense networks. *IEEE Communications Magazine*, 55(6):162–169, 2017.

[19] Tarik Taleb, Adlen Ksentini, and Riku Jantti. " anything as a service" for 5g mobile systems. *IEEE Network*, 30(6):84–91, 2016.

[20] Rakibul Islam Rony, Akshay Jain, Elena Lopez-Aguilera, Eduard Garcia-Villegas, and Ilker Demirkol. Joint access-backhaul perspective on mobility management in 5g networks. In *Standards for Communications and Networking (CSCN), 2017 IEEE Conference on*, pages 115–120. IEEE, 2017.

[21] Akshay Jain, Elena Lopez-Aguilera, and Ilker Demirkol. Mobility management as a service for 5g networks. *arXiv preprint arXiv:1705.09101*, 2017.

[22] Ke Zhang, Yuming Mao, Supeng Leng, Yejun He, and Yan Zhang. Mobile-edge computing for vehicular networks: A promising network paradigm with predictive off-loading. *IEEE Vehicular Technology Magazine*, 12(2):36–44, 2017.

[23] Binxu Yang, Wei Koong Chai, Zichuan Xu, Konstantinos V Katsaros, and George Pavlou. Cost-efficient nfv-enabled mobile edge-cloud for low latency mobile applications. *IEEE Transactions on Network and Service Management*, 2018.

[24] Xumin Huang, Rong Yu, Jiawen Kang, Yejun He, and Yan Zhang. Exploring mobile edge computing for 5g-enabled software defined vehicular networks. *IEEE Wireless Communications*, 24(6):55–63, 2017.

[25] Mehdi Sookhak, F Richard Yu, Ying He, Hamid Talebian, Nader Sohrabi Safa, Nan Zhao, Muhammad Khurram Khan, and Neeraj Kumar. Fog vehicular computing: Augmentation of fog computing using vehicular cloud computing. *IEEE Vehicular Technology Magazine*, 12(3):55–64, 2017.

[26] Cheng Huang, Rongxing Lu, and Kim-Kwang Raymond Choo. Vehicular fog computing: architecture, use case, and security and forensic challenges. *IEEE Communications Magazine*, 55(11):105–111, 2017.

[27] Jiafu Wan, Daqiang Zhang, Shengjie Zhao, Laurence T Yang, and Jaime Lloret. Context-aware vehicular cyber-physical systems with cloud support: architecture, challenges, and solutions. *IEEE Communications Magazine*, 52(8):106–113, 2014.

[28] A.R. Deepti G.Sasikala. Real time services for future cloud computing enabled vehicle networks. In *IOSR Journal of Computer Engineering (IOSR-JCE)*, volume 11, pages 8–14, 2013.

[29] Dipal Vashi Priyank Sharma, Sandip Vaniya. Communication as a service based cloud computing. *IEEE International Conference on Emerging Technology Trends (ICETECT), Nagercoil, India*, pages 15–17, 2011.

[30] Quang Hieu Vu, Tran-Vu Pham, Hong-Linh Truong, Schahram Dustdar, and Rasool Asal. Demods: A description model for data-as-a-service. In *2012 IEEE 26th International Conference on Advanced Information Networking and Applications*, pages 605–612. IEEE, 2012.

[31] Fekri M Abduljalil. Video capture service in the intelligent transportation system based on cloud computing. *International Journal of Computer Applications*, 97(5), 2014.

[32] Rasheed Hussain, Fizza Abbas, Junggab Son, and Heekuck Oh. Tiaas: Secure cloud-assisted traffic information dissemination in vehicular ad hoc networks. In *Cluster, Cloud and Grid Computing (CCGrid), 2013 13th IEEE/ACM International Symposium on*, pages 178–179. IEEE, 2013.

[33] Mario Gerla, Jui-Ting Weng, and Giovanni Pau. Pics-on-wheels: Photo surveillance in the vehicular cloud. In *Computing, Networking and Communications (ICNC), 2013 International Conference on*, pages 1123–1127. IEEE, 2013.

[34] Stefano Ferretti and Gabriele D'Angelo. Smart shires: The revenge of countrysides. In *Computers and Communication (ISCC), 2016 IEEE Symposium on*, pages 756–759. IEEE, 2016.

[35] Rasheed Hussain and Heekuck Oh. Cooperation-aware vanet clouds: Providing secure cloud services to vehicular ad hoc networks. *JIPS*, 10(1):103–118, 2014.

[36] Moustafa AbdelBaky, Manish Parashar, Kirk Jordan, Hyunjoo Kim, Hani Jamjoom, Zon-Yin Shae, Gergina Pencheva, Vipin Sachdeva, James Sexton, Mary Wheeler, et al. Enabling high-performance computing as a service. *Computer*, 45(10):72–80, 2012.

[37] Steffen Kächele, Christian Spann, Franz J Hauck, and Jörg Domaschka. Beyond iaas and paas: An extended cloud taxonomy for computation, storage and networking. In *Proceedings of the 2013 IEEE/ACM 6th International Conference on Utility and Cloud Computing*, pages 75–82. IEEE Computer Society, 2013.

[38] Khaleel Mershad and Hassan Artail. Finding a star in a vehicular cloud. *IEEE Intelligent transportation systems magazine*, 5(2):55–68, 2013.

[39] Rasheed Hussain, Junggab Son, Hasoo Eun, Sangjin Kim, and Heekuck Oh. Rethinking vehicular communications: Merging vanet with cloud computing. In *Cloud Computing Technology and Science (CloudCom), 2012 IEEE 4th International Conference on*, pages 606–609. IEEE, 2012.

[40] Alexander Stanik, Matthias Hovestadt, and Odej Kao. Hardware as a service (haas): Physical and virtual hardware on demand. In *Cloud Computing Technology and Science (CloudCom), 2012 IEEE 4th International Conference on*, pages 149–154. IEEE, 2012.

[41] Monica Mandal, Chaitrali Landge, Pramila Gaikwad, Uma Nagaraj, and Ashwini Abhale. Implementing storage as a service in vanet using cloud environment. *International Journal of Advance Foundation and Research in Computer (IJAFRC)*, 1, 2014.

[42] Mario Gerla, Eun-Kyu Lee, Giovanni Pau, and Uichin Lee. Internet of vehicles: From intelligent grid to autonomous cars and vehicular clouds. In *Internet of Things (WF-IoT), 2014 IEEE World Forum on*, pages 241–246. IEEE, 2014.

[43] Peyman Talebifard and Victor CM Leung. Towards a content-centric approach to crowd-sensing in vehicular clouds. *Journal of Systems Architecture*, 59(10):976–984, 2013.

[44] Hajar Mousannif, Ismail Khalil, and Hassan Al Moatassime. Cooperation as a service in vanets. *J. UCS*, 17(8):1202–1218, 2011.

[45] K Rajbhojsupriya and Pankaj R Ch. Implementation of enhanced security on vehicular cloud computing. *International Journal of Computer Science and Information Technologies (IJCSIT)*, 5:1315–1318, 2014.

[46] Jithrendra H. N. Jyoti Metan, Narasimha K. N. Murthy. Moving vanet to vehicular cloud. *International Journal of Innovative Research in Computer and Communication Engineering (IJIRCCE)*, 2, 2014.

[47] Mehmet Ali Ertürk, Muhammed Ali Aydin, Luca Vollero, and Roberto Setola. Ieee 802.11 s mesh network analysis for post disaster communication. In *International Telecommunications Conference*, pages 53–59. Springer, 2019.

[48] Mehdi Sookhak, F Richard Yu, and Helen Tang. Secure data sharing for vehicular ad-hoc networks using cloud computing. In *Ad Hoc Networks*, pages 306–315. Springer, 2017.

[49] Md Whaiduzzaman, Mehdi Sookhak, Abdullah Gani, and Rajkumar Buyya. A survey on vehicular cloud computing. *Journal of Network and Computer Applications*, 40:325–344, 2014.

[50] Stephan Olariu, Tihomir Hristov, and Gongjun Yan. The next paradigm shift: from vehicular networks to vehicular clouds, 2013.

[51] Benjamin Baron, Miguel Campista, Prométhée Spathis, Luís Henrique MK Costa, Marcelo Dias de Amorim, Otto Carlos MB Duarte, Guy Pujolle, and Yannis Viniotis. Virtualizing vehicular node resources: Feasibility study of virtual machine migration. *Vehicular Communications*, 4:39–46, 2016.

[52] Tarek K Refaat, Burak Kantarci, and Hussein T Mouftah. Virtual machine migration and management for vehicular clouds. *Vehicular Communications*, 4:47–56, 2016.

[53] Salim Bitam, Abdelhamid Mellouk, and Sherali Zeadally. Vanet-cloud: a generic cloud computing model for vehicular ad hoc networks. *IEEE Wireless Communications*, 22(1):96–102, 2015.

[54] Neeraj Kumar, Rahat Iqbal, Sudip Misra, and Joel JPC Rodrigues. Bayesian coalition game for contention-aware reliable data forwarding in vehicular mobile cloud. *Future Generation Computer Systems*, 48:60–72, 2015.

[55] Yen-Wen Lin, Jie-Min Shen, and Hao-Chun Weng. Gateway discovery in vanet cloud. In *High Performance Computing and Communications (HPCC), 2011 IEEE 13th International Conference on*, pages 951–954. IEEE, 2011.

[56] Yen-Wen Lin, Jie-Min Shen, and Hao-Jun Weng. Cloud-assisted gateway discovery for vehicular ad hoc networks. In *Information Science and Service Science (NISS), 2011 5th International Conference on New Trends in*, volume 2, pages 237–240. IEEE, 2011.

[57] Rasheed Hussain, Zeinab Rezaeifar, Yong-Hwan Lee, and Heekuck Oh. Secure and privacy-aware traffic information as a service in vanet-based clouds. *Pervasive and Mobile Computing*, 24:194–209, 2015.

[58] Priya. V. Cloud service for best gateway in vanet. *International Journal of Advanced Research in Computer Science and Software Engineering*, 4, 2014.

[59] Ms Madhuri H Badole and Mr Pritam Nikam. Performance evaluation of an efficient cloud-assisted gateway discovery for vehicular ad hoc network. *Performance Evaluation*, 1(7), 2014.

[60] C Shravanthi and HS Guruprasad. Vanet using cloud [vuc]. 2:1–7, 2014.

[61] China Mobile. C-ran: the road towards green ran. *White Paper, ver*, 2, 2011.

[62] Diego Kreutz, Fernando MV Ramos, Paulo Esteves Verissimo, Christian Esteve Rothenberg, Siamak Azodolmolky, and Steve Uhlig. Software-defined networking: A comprehensive survey. *Proceedings of the IEEE*, 103(1):14–76, 2015.

[63] Ievgen Volvach and Larysa Globa. Mobile networks disaster recovery using sdn-nfv. In *Radio Electronics & Info Communications (UkrMiCo), 2016 International Conference*, pages 1–3. IEEE, 2016.

[64] Rashid Mijumbi, Joan Serrat, Juan-Luis Gorricho, Niels Bouten, Filip De Turck, and Raouf Boutaba. Network function virtualization: State-of-the-art and research challenges. *IEEE Communications Surveys & Tutorials*, 18(1):236–262, 2015.

[65] Sherif Abdelwahab, Bechir Hamdaoui, Mohsen Guizani, and Taieb Znati. Network function virtualization in 5g. *IEEE Communications Magazine*, 54(4):84–91, 2016.

[66] Emmanouil Skondras, Angelos Michalas, Nikolaos Tsolis, and Dimitrios D Vergados. A network selection scheme with adaptive criteria weights for 5g vehicular systems. In *Information, Intelligence, Systems & Applications (IISA), 2018 9th International Conference on*. IEEE, 2018.

[67] Emmanouil Skondras, Angelos Michalas, Aggeliki Sgora, and Dimitrios D Vergados. A vertical handover management scheme for vanet cloud computing systems. In *Computers and Communications (ISCC), 2017 IEEE Symposium on*, pages 371–376. IEEE, 2017.

[68] Emmanouil Skondras, Angelos Michalas, Nikolaos Tsolis, and Dimitrios D Vergados. A vho scheme for supporting healthcare services in 5g vehicular cloud computing systems. In *Wireless Telecommunications Symposium (WTS), 2018*, pages 1–6. IEEE, 2018.

[69] Mohammad A Salahuddin, Ala Al-Fuqaha, Mohsen Guizani, and Soumaya Cherkaoui. Rsu cloud and its resource management in support of enhanced vehicular applications. In *2014 IEEE Globecom Workshops (GC Wkshps)*, pages 127–132. IEEE, 2014.

[70] Mohammad Ali Salahuddin. Opportunistic service differentiation and cloud resource management in support of enhanced vehicular applications. *Thesis at Western Michigan University*, 2014.

[71] Md Faizul Bari, Arup Raton Roy, Shihabur Rahman Chowdhury, Qi Zhang, Mohamed Faten Zhani, Reaz Ahmed, and Raouf Boutaba. Dynamic controller provisioning in software defined networks. In *Proceedings of the 9th International Conference on Network and Service Management (CNSM 2013)*, pages 18–25. IEEE, 2013.

[72] Nguyen B Truong, Gyu Myoung Lee, and Yacine Ghamri-Doudane. Software defined networking-based vehicular adhoc network with fog computing. In *2015 IFIP/IEEE International Symposium on Integrated Network Management (IM)*, pages 1202–1207. IEEE, 2015.

[73] Nicola Cordeschi, Danilo Amendola, Mohammad Shojafar, and Enzo Baccarelli. Distributed and adaptive resource management in cloud-assisted cognitive radio vehicular networks with hard reliability guarantees. *Vehicular Communications*, 2(1):1–12, 2015.

[74] Joy Eze, Sijing Zhang, Enjie Liu, and Elias Eze. Cognitive radio-enabled internet of vehicles: a cooperative spectrum sensing and allocation for vehicular communication. *IET Networks*, 2018.

[75] Rong Yu, Yan Zhang, Stein Gjessing, Wenlong Xia, and Kun Yang. Toward cloud-based vehicular networks with efficient resource management. *IEEE Network*, 27(5):48–55, 2013.

[76] Md Ali Al Mamun, Khairul Anam, Md Fakhrul Alam Onik, and AM Esfar-E-Alam. Deployment of cloud computing into vanet to create ad hoc cloud network architecture. In *Proceedings of the World Congress on Engineering and Computer Science*, volume 1, pages 24–26, 2012.

[77] Carl Bergenhem, Erik Coelingh, Rolf Johansson, and Ali Tehrani. V2v communication quality: measurements in a cooperative automotive platooning application. *SAE International Journal of Passenger Cars-Electronic and Electrical Systems*, 7(2014-01-0302):462–470, 2014.

[78] Mohammed Abdulhakim Al-Absi, Ahmed Abdulhakim Al-Absi, Young-Jin Kang, and Hoon Jae Lee. Obstacles effects on signal attenuation in line of sight for different environments in v2v communication. In *2018 20th International Conference on Advanced Communication Technology (ICACT)*, pages 17–20. IEEE, 2018.

[79] Juinn-Horng Deng, Su-Hua Chen, Chia-Fang Lee, Chorng-Ren Sheu, Hua-Lung Tsai, Shubhranshu Singh, and Jen-Shun Yang. Joint time-frequency dmrs design for high mobility lte-a v2v communication systems. In *Microwaves, Antennas, Communications and Electronic Systems (COMCAS), 2017 IEEE International Conference on*, pages 1–6. IEEE, 2017.

[80] Hazem M Fahmy, Gerd Baumann, Mohamed A Abd El Ghany, and Hassan Mostafa. V2v-based vehicle risk assessment and control for lane-keeping and collision avoidance. In *Microelectronics (ICM), 2017 29th International Conference on*, pages 1–5. IEEE, 2017.

[81] Wanlu Sun, Erik G Ström, Fredrik Brännström, Yutao Sui, and Kin Cheong Sou. D2d-based v2v communications with latency and reliability constraints. In *2014 IEEE Globecom Workshops (GC Wkshps)*, pages 1414–1419. IEEE, 2014.

[82] Hao Ye and Geoffrey Ye Li. Deep reinforcement learning for resource allocation in v2v communications. In *2018 IEEE International Conference on Communications (ICC)*, pages 1–6. IEEE, 2018.

[83] Yanbing Liu, Yuhang Wang, and Guanghui Chang. Efficient privacy-preserving dual authentication and key agreement scheme for secure v2v communications in an iov paradigm. *IEEE Transactions on Intelligent Transportation Systems*, 18(10):2740–2749, 2017.

[84] Arindam Ghosh, Vishnu Vardhan Paranthaman, Glenford Mapp, Orhan Gemikonakli, and Jonathan Loo. Enabling seamless v2i communications: toward developing cooperative automotive applications in vanet systems. *IEEE Communications Magazine*, 53(12):80–86, 2015.

[85] Yuanguo Bi, Haibo Zhou, Weihua Zhuang, and Hai Zhao. Safety message dissemination in v2i communication networks. In *Safety Message Broadcast in Vehicular Networks*, pages 83–101. Springer, 2017.

[86] Xiao-Feng Xie and Zun-Jing Wang. Siv-dss: Smart in-vehicle decision support system for driving at signalized intersections with v2i communication. *Transportation Research Part C: Emerging Technologies*, 90:181–197, 2018.

[87] Michał Hoeft and Jacek Rak. How to provide fair service for v2i communications in vanets? *Ad Hoc Networks*, 37:283–294, 2016.

[88] Gerard Aguilar Ubiergo and Wen-Long Jin. Mobility and environment improvement of signalized networks through vehicle-to-infrastructure (v2i) communications. *Transportation Research Part C: Emerging Technologies*, 68:70–82, 2016.

[89] Ribal Atallah, Maurice Khabbaz, and Chadi Assi. Multihop v2i communications: A feasibility study, modeling, and performance analysis. *IEEE Transactions on Vehicular Technology*, 66(3):2801–2810, 2017.

[90] Otilia Popescu, Sarwar Sha-Mohammad, Hussein Abdel-Wahab, Dimitrie C Popescu, and Samy El-Tawab. Automatic incident detection in intelligent transportation systems using aggregation of traffic parameters collected through v2i communications. *IEEE Intelligent Transportation Systems Magazine*, 9(2):64–75, 2017.

[91] I Rashdan, F de Ponte Muller, Wei Wang, M Schmidhammer, and S Sand. Vehicle-to-pedestrian channel characterization: Wideband measurement campaign and first results. 2018.

[92] Pooya Rahimian, Elizabeth E O'Neal, Shiwen Zhou, Junghum Paul Yon, Luke Franzen, Jodie M Plumert, and Joseph K Kearney. Vehicle-to-pedestrian (v2p) communications technology: Do cell phone warnings improve road-crossing safety for texting pedestrians? *AND30 Standing Committee on Simulation and Measurement of Vehicle and Operator Performance*, 2018.

[93] José Javier Anaya, Pierre Merdrignac, Oyunchimeg Shagdar, Fawzi Nashashibi, and José E Naranjo. Vehicle to pedestrian communications for protection of vulnerable road users. In *Intelligent Vehicles Symposium Proceedings, 2014 IEEE*, pages 1037–1042. IEEE, 2014.

[94] Pooya Rahimian, Elizabeth E O'Neal, Shiwen Zhou, Jodie M Plumert, and Joseph K Kearney. Harnessing vehicle-to-pedestrian (v2p) communication technology: Sending traffic warnings to texting pedestrians. *Human Factors*, 2018.

[95] Pierre Merdrignac, Oyunchimeg Shagdar, and Fawzi Nashashibi. Fusion of perception and v2p communication systems for the safety of vulnerable road users. *IEEE Transactions on Intelligent Transportation Systems*, 18(7):1740–1751, 2017.

[96] Ahmed Hussein, Fernando García, José María Armingol, and Cristina Olaverri-Monreal. P2v and v2p communication for pedestrian warning on the basis of autonomous vehicles. In *Intelligent Transportation Systems (ITSC), 2016 IEEE 19th International Conference on*, pages 2034–2039. IEEE, 2016.

[97] Mehrdad Bagheri, Matti Siekkinen, and Jukka K Nurminen. Cellular-based vehicle to pedestrian (v2p) adaptive communication for collision avoidance. In *Connected Vehicles and Expo (ICCVE), 2014 International Conference on*, pages 450–456. IEEE, 2014.

[98] Kai Liu, Joseph KY Ng, Victor CS Lee, Sang H Son, and Ivan Stojmenovic. Cooperative data scheduling in hybrid vehicular ad hoc networks: Vanet as a software defined network. 2015.

[99] Yuanzhi Ni, Jianping He, Lin Cai, and Yuming Bo. Data uploading in hybrid v2v/v2i vehicular networks: Modeling and cooperative strategy. *IEEE Transactions on Vehicular Technology*, 67(5):4602–4614, 2018.

[100] Norbert Bissmeyer, Jan-Felix van Dam, Christian Zimmermann, and Kurt Eckert. Security in hybrid vehicular communication based on its-g5, lte-v, and mobile edge computing. In *AmE 2018-Automotive meets Electronics; 9th GMM-Symposium*, pages 1–6. VDE, 2018.

[101] Susumu Ishihara, Vince Rabsatt, and Mario Gerla. Secure autonomous platooning with hybrid vehicular communication. *ACM HotMobile*, 2015.

[102] Kai Liu, Joseph KY Ng, Victor Lee, Sang H Son, and Ivan Stojmenovic. Cooperative data scheduling in hybrid vehicular ad hoc networks: Vanet as a software defined network. *IEEE/ACM Transactions on Networking (TON)*, 24(3):1759–1773, 2016.

[103] Nils Dreyer, Andreas Moller, Zeeshan Hameed Mir, Fethi Filali, and Thomas Kurner. A data traffic steering algorithm for ieee 802.11 p/lte hybrid vehicular networks. In *Vehicular Technology Conference (VTC-Fall), 2016 IEEE 84th*, pages 1–6. IEEE, 2016.

[104] Nils Dreyer, Andreas Moeller, Johannes Baumgarten, Zeeshan Hameed Mir, Thomas Kuerner, and Fethi Filali. On building realistic reference scenarios for ieee 802.11 p/lte-based vehicular network evaluations. In *2018 IEEE 87th Vehicular Technology Conference (VTC Spring)*, pages 1–7. IEEE, 2018.

[105] Wei-dong YANG, LI Pan, Hong-song ZHU, et al. Adaptive tdma slot assignment protocol for vehicular ad-hoc networks. *The Journal of China Universities of Posts and Telecommunications*, 20(1):11–25, 2013.

[106] Tsang-Ling Sheu and Yu-Hung Lin. A cluster-based tdma system for inter-vehicle communications. *J. Inf. Sci. Eng.*, 30(1):213–231, 2014.

[107] Kazi Atiqur Rahman and Kemal E Tepe. Towards a cross-layer based mac for smooth v2v and v2i communications for safety applications in dsrc/wave based systems. In *2014 IEEE Intelligent Vehicles Symposium Proceedings*, pages 969–973. IEEE, 2014.

[108] Rui Zou, Zishan Liu, Lin Zhang, and Muhammad Kamil. A near collision free reservation based mac protocol for vanets. In *2014 IEEE Wireless Communications and Networking Conference (WCNC)*, pages 1538–1543. IEEE, 2014.

[109] Hassan Aboubakr Omar, Weihua Zhuang, and Li Li. Vemac: A tdma-based mac protocol for reliable broadcast in vanets. *IEEE Transactions on Mobile Computing*, 12(9):1724–1736, 2013.

[110] VanDung Nguyen, Duc Ngoc Minh Dang, Sungman Jang, and Choong Seon Hong. e-vemac: an enhanced vehicular mac protocol to mitigate the exposed terminal problem. In *Network Operations and Management Symposium (APNOMS), 2014 16th Asia-Pacific*, pages 1–4. IEEE, 2014.

[111] Nurullah Shahin and Young-Tak Kim. An enhanced tdma cluster-based mac (etcm) for multichannel vehicular networks. In *Selected Topics in Mobile & Wireless Networking (MoWNeT), 2016 International Conference on*, pages 1–8. IEEE, 2016.

[112] Xiaoxiao Jiang and David Du. Ptmac: A prediction-based tdma mac protocol for reducing packet collisions in vanet. 2015.

[113] Rongqing Zhang, Xiang Cheng, Liuqing Yang, Xia Shen, and Bingli Jiao. A novel centralized tdma-based scheduling protocol for vehicular networks. *IEEE Transactions on Intelligent Transportation Systems*, 16(1):411–416, 2015.

[114] Sailesh Bharati and Weihua Zhuang. Cah-mac: Cooperative adhoc mac for vehicular networks. *IEEE Journal on Selected Areas in Communications*, 31(9):470–479, 2013.

[115] Lili Zheng, Yi Wu, Zhexin Xu, and Xiao Lin. A novel mac protocol for vanet based on improved generalized prime sequence. In *Advanced Infocomm Technology (ICAIT), 2014 IEEE 7th International Conference on*, pages 1–7. IEEE, 2014.

[116] Hang Yu, Zhiqiang He, and Kai Niu. Stdma for vehicle-to-vehicle communication in a highway scenario. In *Microwave, Antenna, Propagation and EMC Technologies for Wireless Communications (MAPE), 2013 IEEE 5th International Symposium on*, pages 133–138. IEEE, 2013.

[117] Mohammad S Almalag, Stephan Olariu, and Michele C Weigle. Tdma cluster-based mac for vanets (tc-mac). In *World of Wireless, Mobile and Multimedia Networks (WoWMoM), 2012 IEEE International Symposium on a*, pages 1–6. IEEE, 2012.

[118] Shanqiang Yi, Wuwen Lai, Di Tang, and Hua Wang. A context-aware mac protocol in vanet based on bayesian networks. In *Communications and Networking in China (CHINACOM), 2014 9th International Conference on*, pages 191–196. IEEE, 2014.

[119] Xin Zhou, Changwen Zheng, Xiaoxin He, et al. Adaptive contention window tuning for ieee 802.11. In *22nd International Conference on Telecommunications: ICT 2015*, page 74. Engineers Australia, 2015.

[120] Peppino Fazio, Floriano De Rango, and Cesare Sottile. A predictive cross-layered interference management in a multichannel mac with reactive routing in vanet. 2015.

[121] Hikmat El Ajaltouni, Richard W Pazzi, and Azzedine Boukerche. An efficient qos mac for ieee 802.11p over cognitive multichannel vehicular networks. In *2012 IEEE International Conference on Communications (ICC)*, pages 413–417. IEEE, 2012.

[122] Celimuge Wu, Satoshi Ohzahata, Yusheng Ji, and Toshihiko Kato. A mac protocol for delay-sensitive vanet applications with self-learning contention scheme. In *2014 IEEE 11th Consumer Communications and Networking Conference (CCNC)*, pages 438–443. IEEE, 2014.

[123] Weijie Guo, Liusheng Huang, Long Chen, Hongli Xu, and Jietao Xie. An adaptive collision-free mac protocol based on tdma for inter-vehicular communication. In *Wireless Communications & Signal Processing (WCSP), 2012 International Conference on*, pages 1–6. IEEE, 2012.

[124] Rongqing Zhang, Jinsung Lee, Xia Shen, Xiang Cheng, Liuqing Yang, and Bingli Jiao. A unified tdma-based scheduling protocol for vehicle-to-infrastructure communications. In *Wireless Communications & Signal Processing (WCSP), 2013 International Conference on*, pages 1–6. IEEE, 2013.

[125] Duc Ngoc Minh Dang, Hanh Ngoc Dang, Vandung Nguyen, Zaw Htike, and Choong Seon Hong. Her-mac: A hybrid efficient and reliable mac for vehicular ad hoc networks. In *2014 IEEE 28th International Conference on Advanced Information Networking and Applications*, pages 186–193. IEEE, 2014.

[126] Weijie Guo, Liusheng Huang, Long Chen, Hongli Xu, and Chenglin Miao. R-mac: Risk-aware dynamic mac protocol for vehicular cooperative collision avoidance system. *International Journal of Distributed Sensor Networks*, 2013, 2013.

[127] Lin Zhang, Zishan Liu, Rui Zou, Jinjie Guo, and Yu Liu. A scalable csma and self-organizing tdma mac for ieee 802.11 p/1609. x in vanets. *Wireless Personal Communications*, 74(4):1197–1212, 2014.

[128] Alessandro Bazzi, Alberto Zanella, and Barbara Maví Masini. An ofdma-based mac protocol for next-generation vanets. *IEEE Transactions on Vehicular Technology*, 64(9):4088–4100, 2015.

[129] Baozhu Li, Xuhui Zhao, Shiyuan Han, and Zhenxiang Chen. New sdn-based architecture for integrated vehicular cloud computing networking. In *2018 International Conference on Selected Topics in Mobile and Wireless Networking (MoWNeT)*, pages 1–4. IEEE, 2018.

[130] Redowan Mahmud, Ramamohanarao Kotagiri, and Rajkumar Buyya. Fog computing: A taxonomy, survey and future directions. In *Internet of everything*, pages 103–130. Springer, 2018.

[131] Behnam Khodapanah, Ahmad Awada, Ingo Viering, David Oehmann, Meryem Simsek, and Gerhard P Fettweis. Fulfillment of service level agreements via slice-aware radio resource management in 5g networks. In *2018 IEEE 87th Vehicular Technology Conference (VTC Spring)*, pages 1–6. IEEE, 2018.

[132] Dizhi Zhou, Nicola Baldo, and Marco Miozzo. Implementation and Validation of LTE Downlink Schedulers for ns-3. In *Simulation Tools and Techniques (SimuTools '13), 6th International ICST Conference on*, pages 211–218, 2013.

[133] F. Capozzi, G. Piro, L. A. Grieco, G. Boggia, and P. Camarda. Downlink packet scheduling in LTE cellular networks: Key design issues and a survey. *Communications Surveys and Tutorials, IEEE*, 99, 2012.

[134] Akhilesh Pokhariyal, Klaus I Pedersen, Guillaume Monghal, Istvan Z Kovacs, Claudio Rosa, Troels E Kolding, and Preben E Mogensen. HARQ aware frequency domain packet scheduler with different degrees of fairness for the UTRAN long term evolution. In *Vehicular Technology Conference, 2007. VTC2007-Spring. IEEE 65th*, pages 2761–2765. IEEE, 2007.

[135] Dizhi Zhou, Wei Song, Nicola Baldo, and Marco Miozzo. Evaluation of TCP performance with LTE downlink schedulers in a vehicular environment. In *Wireless Communications and Mobile Computing Conference (IWCMC), 2013 9th International*, pages 1064–1069. IEEE, 2013.

[136] Huda Adibah Mohd Ramli, Kumbesan Sandrasegaran, Riyaj Basukala, Rachod Patachaianand, and Toyoba Sohana Afrin. Video Streaming Performance Under Well-Known Packet Scheduling Algorithms. *International Journal of Wireless & Mobile Networks (IJWMN)l*, 3:25–38, 2011.

[137] Yasir Zaki, Thushara Weerawardane, Carmelita Gorg, and Andreas Timm-Giel. Multi-QoS-aware fair scheduling for LTE. In *Vehicular technology conference (VTC spring), 2011 IEEE 73rd*, pages 1–5. IEEE, 2011.

[138] Li Chen, Bin Wang, Xiaohang Chen, Xin Zhang, and Dacheng Yang. Utility-based resource allocation for mixed traffic in wireless networks. In *Computer Communications Workshops (INFOCOM WKSHPS), 2011 IEEE Conference on*, pages 91–96. IEEE, 2011.

[139] M Andrews, K. Kumaran, K. Ramanan, A. Stolyar, P. Whiting, and R. Vijayakumar. Providing quality of service over a shared wireless link. *Communications Magazine, IEEE*, 39(2):150–154, 2001.

[140] K. Sandrasegaran R. Basukala, H. Mohd Ramli. Performance analysis of EXP/PF and M-LWDF in downlink 3GPP LTE system. In *AH-ICI 2009. 1st Asian Himalayas International Conference on Internet*, pages 1–5. IEEE, 2009.

[141] Bilal Sadiq, Ritesh Madan, and Ashwin Sampath. Downlink scheduling for multiclass traffic in LTE. *EURASIP Journal on Wireless Communications and Networking*, 2009(14), 2009.

[142] Giuseppe Piro, Luigi Alfredo Grieco, Gennaro Boggia, Rossella Fortuna, and Pietro Camarda. Two-level downlink scheduling for real-time multimedia services in LTE networks. *Multimedia, IEEE Transactions on*, 13(5):1052–1065, 2011.

[143] Huda Adibah Mohd Ramli, Riyaj Basukala, Kumbesan Sandrasegaran, and Rachod Patachaianand. Performance of well known packet scheduling algorithms in the downlink 3GPP LTE system. In *Communications (MICC), 2009 IEEE 9th Malaysia International Conference on*, pages 815–820. IEEE, 2009.

[144] Sadiq Bilal, Madan Ritesh, and Sampath Ashwin. Downlink scheduling for multiclass traffic in LTE. *EURASIP Journal on Wireless Communications and Networking*, 2009, 2009.

[145] Giuseppe Piro, Luigi Alfredo Grieco, Gennaro Boggia, Francesco Capozzi, and Pietro Camarda. Simulating LTE cellular systems: An open-source framework. *Vehicular Technology, IEEE Transactions on*, 60(2):498–513, 2011.

[146] TS 36.322 (V8.8.0): Evolved Universal Terrestrial Radio Access (E-UTRA), Radio Link Control (RLC) protocol specification(Release 8). *Technical Specification, 3GPP*, 2010.

[147] Mohamed Hadi Habaebi Mohammed Abdul Jawad M. Al-Shibly and Md. Rafiqul Islam. Radio resource scheduling in LTE-Advanced system with Carrier Aggregation. *ARPN Journal of Engineering and Applied Sciences*, 10(22):17281–17285, 2015.

[148] Sangchul Oh, JeeHyeon Na, and Dongseung Kwon. Performance Analysis of Cross Component Carrier Scheduling in LTE Small Cell Access Point System. In *The Second International Conference on Electrical, Electronics, Computer Engineering and their Applications (EECEA2015)*, page 146, 2015.

[149] Alberto Núñez, Jose L Vázquez-Poletti, Agustin C Caminero, Gabriel G Castañé, Jesus Carretero, and Ignacio M Llorente. iCanCloud: A flexible and scalable cloud infrastructure simulator. *Journal of Grid Computing*, 10(1):185–209, 2012.

[150] Dominik Klein and Michael Jarschel. An OpenFlow extension for the OMNeT++ INET framework. In *Proceedings of the 6th International ICST Conference on Simulation Tools and Techniques*, pages 322–329. ICST (Institute for Computer Sciences, Social-Informatics and Telecommunications Engineering), 2013.

[151] András Varga and Rudolf Hornig. An overview of the OMNeT++ simulation environment. In *Proceedings of the 1st international conference on Simulation tools and techniques for communications, networks and systems & workshops*, page 60. ICST (Institute for Computer Sciences, Social-Informatics and Telecommunications Engineering), 2008.

[152] TR 36.814 (V9.0.0): Further advancements for E-UTRA physical layer aspects (Release 9). *Technical Specification Group Radio Access Network, 3GPP*, 2010.

[153] TR 36.942 (V10.2.0): Radio Frequency (RF) system scenarios (Release 10). *Technical Specification, 3GPP*, 2011.

[154] Lotfi Asker Zadeh. Fuzzy sets. *Information and control*, 8(3):338–353, 1965.

[155] Roland Sambuc. *Fonctions and floues: application a l'aide au diagnostic en pathologie thyroidienne*. Faculté de Médecine de Marseille, 1975.

[156] Peide Liu and Fang Jin. A multi-attribute group decision-making method based on weighted geometric aggregation operators of interval-valued trapezoidal fuzzy numbers. *Applied Mathematical Modelling*, 36(6):2498–2509, 2012.

[157] Chris Cornelis, Glad Deschrijver, and EE Kerre. Advances and challenges in interval-valued fuzzy logic. *Fuzzy sets and systems*, 157(5):622–627, 2006.

[158] Behzad Ashtiani, Farzad Haghighirad, Ahmad Makui, et al. Extension of fuzzy topsis method based on interval-valued fuzzy sets. *Applied Soft Computing*, 9(2):457–461, 2009.

[159] Shih-Hua Wei and Shyi-Ming Chen. Fuzzy risk analysis based on interval-valued fuzzy numbers. *Expert Systems with Applications*, 36(2):2285–2299, 2009.

[160] Apurba Panda and Madhumangal Pal. A study on pentagonal fuzzy number and its corresponding matrices. *Pacific Science Review B: Humanities and Social Sciences, Elsevier*, 1(3):131–139, 2015.

[161] Mu-Song Chen and Shinn-Wen Wang. Fuzzy clustering analysis for optimizing fuzzy membership functions. *Fuzzy sets and systems, Elsevier*, 103(2):239–254, 1999.

[162] Marcos E Cintra, Heloisa A Camargo, and Maria Carolina Monard. Genetic generation of fuzzy systems with rule extraction using formal concept analysis. *Information Sciences, Elsevier*, 349:199–215, 2016.

[163] Jin-Shyan Lee and Chih-Lin Teng. An enhanced hierarchical clustering approach for mobile sensor networks using fuzzy inference systems. *IEEE Internet of Things Journal*, 4(4):1095–1103, 2017.

[164] Javier Andreu-Perez, Fan Cao, Hani Hagras, and Guang-Zhong Yang. A self-adaptive online brain machine interface of a humanoid robot through a general type-2 fuzzy inference system. *IEEE Transactions on Fuzzy Systems*, 2016.

[165] Chengdong Li, Junlong Gao, Jianqiang Yi, and Guiqing Zhang. Analysis and design of functionally weighted single-input-rule-modules connected fuzzy inference systems. *IEEE Transactions on Fuzzy Systems*, 2016.

[166] Thomas L Saaty. Decision making with dependence and feedback: The analytic network process. 1996.

[167] İhsan Yüksel and Metin Dagdeviren. Using the analytic network process (anp) in a swot analysis–a case study for a textile firm. *Information Sciences*, 177(16):3364–3382, 2007.

[168] Thomas L Saaty and Luis G Vargas. Diagnosis with dependent symptoms: Bayes theorem and the analytic hierarchy process. *Operations Research*, 46(4):491–502, 1998.

[169] Tong Wu, Xin-Wang Liu, and Shu-Li Liu. A fuzzy anp with interval type-2 fuzzy sets approach to evaluate enterprise technological innovation ability. In *Fuzzy Systems (FUZZ-IEEE), 2015 IEEE International Conference on*, pages 1–8. IEEE, 2015.

[170] Ching-Lai Hwang and Kwangsun Yoon. *Multiple attribute decision making*. Springer, 1981.

[171] Emmanouil Skondras, Aggeliki Sgora, Angelos Michalas, and Dimitrios D Vergados. An analytic network process and trapezoidal interval-valued fuzzy technique for order preference by similarity to ideal solution network access selection method. *International Journal of Communication Systems*, 29(2):307–329, 2016.

[172] Dimitris E Charilas, Ourania I Markaki, John Psarras, and Philip Constantinou. Application of fuzzy ahp and electre to network selection. In *Mobile Lightweight Wireless Systems*, pages 63–73. Springer, 2009.

[173] Thereza Raquel Machado Azeredo, Helisamara Mota Guedes, Ricardo Alexandre Rebelo de Almeida, Tânia Couto Machado Chianca, and José Carlos Amado Martins. Efficacy of the manchester triage system: a systematic review. *International emergency nursing, Elsevier*, 23(2):47–52, 2015.

[174] Hoe Tung Yew, Eko Supriyanto, Muhammad H Satria, and YW Hau. Adaptive network selection mechanism for telecardiology system in developing countries. In *Biomedical and Health Informatics (BHI), 2016 IEEE-EMBS International Conference on*, pages 94–97. IEEE, 2016.

[175] Driss Aboutajdine Maroua Drissi, Mohammed Oumsis. A fuzzy ahp approach to network selection improvement in heterogeneous wireless networks. *Networked Systems*, pages 169–182.

[176] Open street map (osm). https://www.openstreetmap.org, 2018. Accessed: 2018.

[177] Michael Behrisch, Laura Bieker, Jakob Erdmann, and Daniel Krajzewicz. Sumo–simulation of urban mobility: an overview. In *Proceedings of SIMUL 2011, The Third International Conference on Advances in System Simulation*. ThinkMind, 2011.

[178] Network simulator 3 (ns3). https://www.nsnam.org/, 2018. Accessed: 2018.

[179] E Roszkowska and D Kacprzak. The fuzzy saw and fuzzy topsis procedures based on ordered fuzzy numbers. *Information Sciences*, 369:564–584, 2016.

[180] Zhe Ren, Peter Fertl, Qi Liao, Federico Penna, and Slawomir Stanczak. Street-specific handover optimization for vehicular terminals in future cellular networks. In *Vehicular Technology Conference (VTC Spring), 2013 IEEE 77th*, pages 1–5. IEEE, 2013.

[181] David González, Mario García-Lozano, Silvia Ruiz, and Dong Seop Lee. A metaheuristic-based downlink power allocation for lte/lte-a cellular deployments. *Wireless Networks*, 20(6):1369–1386, 2014.

[182] Soumaya Cherkaoui, Tarik Taleb, and Eugene David Ngangue Ndih. Improved internetwork handover for highly mobile users and vehicular networks. In *Vehicular Technology Conference (VTC Spring), 2011 IEEE 73rd*, pages 1–5. IEEE, 2011.

[183] Suganthi Evangeline and Vinoth Babu Kumaravelu. Decision process for vertical handover in vehicular adhoc networks. In *Microelectronic Devices, Circuits and Systems (ICMDCS), 2017 International conference on*, pages 1–5. IEEE, 2017.

[184] Francesco Guidolin, Irene Pappalardo, Andrea Zanella, and Michele Zorzi. Context-aware handover policies in hetnets. *IEEE Transactions on Wireless Communications*, 15(3):1895–1906, 2016.

[185] Abhijit Sarma, Sandip Chakraborty, and Sukumar Nandi. Deciding handover points based on context-aware load balancing in a wifi-wimax heterogeneous network environment. *IEEE Transactions on Vehicular Technology*, 65(1):348–357, 2016.

[186] Shipra Kapoor, David Grace, and Tim Clarke. A base station selection scheme for handover in a mobility-aware ultra-dense small cell urban vehicular environment. In *Personal, Indoor, and Mobile Radio Communications (PIMRC), 2017 IEEE 28th Annual International Symposium on*, pages 1–5. IEEE, 2017.

[187] Ali Safa Sadiq, Kamalrulnizam Abu Bakar, Kayhan Zrar Ghafoor, Jaime Lloret, and Rashid Khokhar. An intelligent vertical handover scheme for audio and video streaming in heterogeneous vehicular networks. *Mobile Networks and Applications*, 18(6):879–895, 2013.

[188] Mohamed Lahby, Cherkaoui Leghris, and Abdellah Adib. New multi access selection method based on mahalanobis distance. *Applied Mathematical Sciences*, 6(53-56):2745–2760, 2012.

[189] Vishal Gupta. Network selection in 3g-wlan interworking environment using topsis. In *Industrial and Information Systems (ICIIS), 2016 11th International Conference on*, pages 512–517. IEEE, 2016.

[190] Werner Toth and Harald Vacik. A comprehensive uncertainty analysis of the analytic hierarchy process methodology applied in the context of environmental decision making. *Journal of Multi-Criteria Decision Analysis*, 2018.

[191] Mohamed Lahby, Cherkaoui Leghris, and Abdellah Adib. New multi access selection method using differentiated weight of access interface. In *Communications and Information Technology (ICCIT), 2012 International Conference on*, pages 237–242. IEEE, 2012.

[192] KSS Anupama, S Sri Gowri, and B Prabakara Rao. Application of grey relational analysis to network selection: A case study. 2017.

[193] Abudukeremu Kadier, Peyman Abdeshahian, Yibadatihan Simayi, Manal Ismail, Aidil Abdul Hamid, and Mohd Sahaid Kalil. Grey relational analysis for comparative assessment of different cathode materials in microbial electrolysis cells. *Energy*, 90:1556–1562, 2015.

[194] Wei-Yu Chiu, Gary G Yen, and Teng-Kuei Juan. Minimum manhattan distance approach to multiple criteria decision making in multiobjective optimization problems. *IEEE Transactions on Evolutionary Computation*, 20(6):972–985, 2016.

[195] Novi Sofia Fitriasari, Syifa Afifah Fitriani, and Rosa Ariani Sukamto. Comparison of weighted product method and technique for order preference by similarity to ideal solution method: Complexity and accuracy. In *Science in Information Technology (ICSITech), 2017 3rd International Conference on*, pages 453–458. IEEE, 2017.

[196] Xingwei Wang, Dapeng Qu, Keqin Li, Hui Cheng, Sajal K Das, Min Huang, Renzheng Wang, and Shuliu Chen. A flexible and generalized framework for access network selection in heterogeneous wireless networks. *Pervasive and Mobile Computing*, 40:556–576, 2017.

[197] Lei Sun, Hui Tian, and Ping Zhang. Decision-making models for group vertical handover in vehicular communications. *Telecommunication Systems*, 50(4):257–266, 2012.

[198] B Farhadinia. Sensitivity analysis in interval-valued trapezoidal fuzzy number linear programming problems. *Applied Mathematical Modelling*, 38(1):50–62, 2014.

[199] Huiqiang Wang, Zhendong Wang, Guangsheng Feng, Hongwu LV, Xiaoming Chen, and Qiang Zhu. Intelligent access selection in cognitive networks: A fuzzy neural network approach. *Journal of Computational Information Systems*, 8(21):8877–8884, 2012.

[200] Mun-Suk Kim and SuKyoung Lee. Group-based fast handover for pmipv6-based network mobility in vehicular networks. In *Computer Communications Workshops (INFOCOM WKSHPS), 2015 IEEE Conference on*, pages 113–114. IEEE, 2015.

[201] Jonathan Prados-Garzon, Juan J Ramos-Munoz, Pablo Ameigeiras, Pilar Andres-Maldonado, and Juan M Lopez-Soler. Modeling and dimensioning of a virtualized mme for 5g mobile networks. *IEEE Transactions on Vehicular Technology*, 66(5):4383–4395, 2017.

[202] Mun-Suk Kim, SuKyoung Lee, and Nada Golmie. Enhanced fast handover for proxy mobile ipv6 in vehicular networks. *Wireless Networks*, 18(4):401–411, 2012.

[203] Mun-Suk Kim, Sukyoung Lee, David Cypher, and Nada Golmie. Performance analysis of fast handover for proxy mobile ipv6. *Information Sciences*, 219:208–224, 2013.

[204] Emna Bouzid Smida, Sonia Gaied Fantar, and Habib Youssef. Predictive handoff mechanism for video streaming in a cloud-based urban vanet. In *Computer Systems and Applications (AICCSA), 2017 IEEE/ACS 14th International Conference on*, pages 1170–1177. IEEE, 2017.

[205] Massimo Dalla Cia, Federico Mason, Davide Peron, Federico Chiariotti, Michele Polese, Toktam Mahmoodi, Michele Zorzi, and Andrea Zanella. Mobility-aware handover strategies in smart cities. In *Wireless Communication Systems (ISWCS), 2017 International Symposium on*, pages 438–443. IEEE, 2017.

[206] Ammar Gharaibeh, Mohammad A Salahuddin, Sayed Jahed Hussini, Abdallah Khreishah, Issa Khalil, Mohsen Guizani, and Ala Al-Fuqaha. Smart cities: A survey on data management, security, and enabling technologies. *IEEE Communications Surveys & Tutorials*, 19(4):2456–2501, 2017.

[207] Flavio Esposito, Anna Maria Vegni, Ibrahim Matta, and Alessandro Neri. On modeling speed-based vertical handovers in vehicular networks:“dad, slow down, i am watching the movie”. In *GLOBECOM Workshops (GC Wkshps), 2010 IEEE*, pages 11–15. IEEE, 2010.

[208] Chi Ma, Enda Fallon, Yuansong Qiao, and Brian Lee. Optimizing media independent handover using predictive geographical information for vehicular based systems. In *UKSim Fourth European Modelling Symposium on Computer Modelling and Simulation*, pages 420–425. IEEE, 2010.

[209] Sourav Dhar, Amitava Ray, and Rabindranath Bera. Cognitive vertical handover engine for vehicular communication. *Peer-to-Peer Networking and Applications*, 6(3):305–324, 2013.

[210] Gul Muhammad Khan. Artificial neural network (anns). In *Evolution of Artificial Neural Development*, pages 39–55. Springer, 2018.

[211] Guoxia Zhang and Fuqiang Liu. An auction approach to group handover with mobility prediction in heterogeneous vehicular networks. In *ITS Telecommunications (ITST), 2011 11th International Conference on*, pages 584–589. IEEE, 2011.

[212] Rahul Garg and Sanjiv Kapoor. Auction algorithms for market equilibrium. *Mathematics of Operations Research*, 31(4):714–729, 2006.

[213] Faisal Riaz, Rehana Asif, Hina Sajid, and Muaz A Niazi. Augmenting autonomous vehicular communication using the appreciation emotion: A mamdani fuzzy inference system model. In *Frontiers of Information Technology (FIT), 13th International Conference on*, pages 178–184. IEEE, 2015.

[214] Johann Marquez-Barja, Carlos T Calafate, Juan-Carlos Cano, and Pietro Manzoni. A geolocation-based vertical handover decision algorithm for vehicular networks. In *Local Computer Networks (LCN), 2012 IEEE 37th Conference on*, pages 360–367. IEEE, 2012.

[215] Johann M Marquez-Barja, Hamed Ahmadi, Sergio M Tornell, Carlos T Calafate, Juan-Carlos Cano, Pietro Manzoni, and Luiz A DaSilva. Breaking the vehicular wireless communications barriers: Vertical handover techniques for heterogeneous networks. *IEEE Transactions on Vehicular Technology*, 64(12):5878–5890, 2015.

[216] Wei-Kuo Chiang and Shih-Chieh Chien. Deploying the media independent information service at the edge of next-generation network. In *Electronics Information and Emergency Communication (ICEIEC), 2015 5th International Conference on*, pages 182–185. IEEE, 2015.

[217] Mohamed Ben Brahim, Zeeshan Hameed Mir, Wassim Znaidi, Fethi Filali, and Noureddine Hamdi. Qos-aware video transmission over hybrid wireless network for connected vehicles. *IEEE Access*, 5:8313–8323, 2017.

[218] Rabe Arshad, Hesham ElSawy, Sameh Sorour, Tareq Y Al-Naffouri, and Mohamed-Slim Alouini. Velocity-aware handover management in two-tier cellular networks. *IEEE Transactions on Wireless Communications*, 16(3):1851–1867, 2017.

[219] Lu Zhang, Lu Ge, Xin Su, and Jie Zeng. Fuzzy logic based vertical handover algorithm for trunking system. In *Wireless and Optical Communication Conference (WOCC), 2017 26th*, pages 1–5. IEEE, 2017.

[220] Aymen Ben Zineb, Mohamed Ayadi, and Sami Tabbane. Fuzzy madm based vertical handover algorithm for enhancing network performances. In *Software, Telecommunications and Computer Networks (SoftCOM), 2015 23rd International Conference on*, pages 153–159. IEEE, 2015.

[221] Kang-Won Lee, Won-Kyeong Seo, You-Ze Cho, Jong-Woo Kim, Jin-Soo Park, and Byoung-Sub Moon. Inter-domain handover scheme using an intermediate mobile access gateway for seamless service in vehicular networks. *International Journal of Communication Systems*, 23(9-10):1127–1144, 2010.

[222] Alexander Magnano, Xin Fei, Azzedine Boukerche, and Antonio AF Loureiro. A novel predictive handover protocol for mobile ip in vehicular networks. *IEEE Transactions on Vehicular Technology*, 65(10):8476–8495, 2016.

[223] Bayrem Triki, Slim Rekhis, and Noureddine Boudriga. Secure and qos-aware sip handover for voip communication in vehicular adhoc networks. In *Wireless Communications and Mobile Computing Conference (IWCMC), 2011 7th International*, pages 695–700. IEEE, 2011.

[224] Ashraf A Ali and Khalid Al-Begain. Ip multimedia subsystem and sip signaling performance metrics. In *Multimedia Services and Applications in Mission Critical Communication Systems*, pages 19–35. IGI Global, 2017.

[225] U Kumaran and RS Shaji. Vertical handover in vehicular ad-hoc network using multiple parameters. In *Control, Instrumentation, Communication and Computational Technologies (ICCICCT), 2014 International Conference on*, pages 1059–1064. IEEE, 2014.

[226] Ming-Chin Chuang and Meng Chang Chen. Nash: Navigation-assisted seamless handover scheme for smart car in ultradense networks. *IEEE Transactions on Vehicular Technology*, 67(2):1649–1659, 2018.

[227] Hayoung Oh and Chong-kwon Kim. A robust handover under analysis of unexpected vehicle behaviors in vehicular ad-hoc network. In *Vehicular Technology Conference (VTC 2010-Spring), 2010 IEEE 71st*, pages 1–7. IEEE, 2010.

[228] Hayoung Oh. Mobility-aware video streaming in mimo-capable heterogeneous wireless networks. *Mathematical Problems in Engineering*, 2016, 2016.

[229] André Almeida, Nuno Lopes, and Alexandre Santos. Intelligent handover for vehicular networks. In *Software, Telecommunications and Computer Networks (SoftCOM), 2014 22nd International Conference on*, pages 298–304. IEEE, 2014.

[230] José Antonio Olivera, Ismael Cortázar, Carolina Pinart, Alberto Los Santos, and Iván Lequerica. Vanba: a simple handover mechanism for transparent, always-on v2v communications. In *Vehicular Technology Conference, 2009. VTC Spring 2009. IEEE 69th*, pages 1–5. IEEE, 2009.

[231] Laurence Banda, Mjumo Mzyece, and Guillaume Nóel. Fast handover management in ip-based vehicular networks. In *Industrial Technology (ICIT), 2013 IEEE International Conference on*, pages 1279–1284. IEEE, 2013.

[232] Jasmine P Valera and Sunguk Lee. Security measures in overcoming mobile ipv6 security issues. *International Journal of Database Theory and Application*, 9(7):297–304, 2016.

[233] H. Takahashi and T. Minohara. Enhancing location privacy in mobile ipv6 by using redundant home agents. In *2012 IEEE International Conference on Pervasive Computing and Communications Workshops*, pages 451–454, March 2012.

[234] Yuqing Zhu, Weili Wu, and Deying Li. Efficient client assignment for client-server systems. *IEEE Transactions on Network and Service Management*, 13(4):835–847, 2016.

[235] Luis Diego Briceno, Howard Jay Siegel, Anthony A Maciejewski, Ye Hong, Brad Lock, Charles Panaccione, Fadi Wedyan, Mohammad Nayeem Teli, and Chen Zhang. Resource allocation in a client/server system for massive multi-player online games. *IEEE Transactions on Computers*, 63(12):3127–3142, 2014.

[236] Hiroshi Nishida and Thinh Nguyen. Optimal client-server assignment for internet distributed systems. *IEEE Transactions on Parallel and Distributed Systems*, 24(3):565–575, 2013.

[237] Farkhana Muchtar, Abdul Hanan Abdullah, Suhaidi Hassan, and Farhan Masud. Energy conservation strategies in host centric networking based manet: A review. *Journal of Network and Computer Applications*, 2018.

[238] Christian Dannewitz, Dirk Kutscher, BöRje Ohlman, Stephen Farrell, Bengt Ahlgren, and Holger Karl. Network of information (netinf)–an information-centric networking architecture. *Computer Communications, Elsevier*, 36(7):721–735, 2013.

[239] Hongbin Luo, Hongke Zhang, Moshe Zukerman, and Chunming Qiao. An incrementally deployable network architecture to support both data-centric and host-centric services. *IEEE Network*, 28(4):58–65, 2014.

[240] Bengt Ahlgren, Christian Dannewitz, Claudio Imbrenda, Dirk Kutscher, and Borje Ohlman. A survey of information-centric networking. *IEEE Communications Magazine*, 50(7), 2012.

[241] Haolin Guo, Dewan Tanvir Ahmed, and Abdulmotaleb El Saddik. Web services for vanet: a service oriented architecturefor infotainment system based on mashup using open apis. In *Proceedings of the third ACM international symposium on Design and analysis of intelligent vehicular networks and applications*, pages 61–68. ACM, 2013.

[242] Wei-Tek Tsai, Xin Sun, and Janaka Balasooriya. Service-oriented cloud computing architecture. In *Information Technology: New Generations (ITNG), 2010 Seventh International Conference on*, pages 684–689. IEEE, 2010.

[243] Xiang Sun and Nirwan Ansari. Dynamic resource caching in the iot application layer for smart cities. *IEEE Internet of Things Journal*, 5(2):606–613, 2018.

[244] Jyoti Deogirikar and Amarsinh Vidhate. An improved publish-subscribe method in application layer protocol for iot. In *2017 International Conference On Smart Technologies For Smart Nation (SmartTechCon)*, pages 1070–1075. IEEE, 2017.

[245] Zubaida Alazawi, Saleh Altowaijri, Rashid Mehmood, and Mohmmad B Abdljabar. Intelligent disaster management system based on cloud-enabled vehicular networks. In *ITS Telecommunications (ITST), 2011 11th International Conference on*, pages 361–368. IEEE, 2011.

[246] Weijing Qi, Qingyang Song, Xiaojie Wang, Lei Guo, and Zhaolong Ning. Sdn-enabled social-aware clustering in 5g-vanet systems. *IEEE Access*, 6:28213–28224, 2018.

[247] Hamada Alshaer. An overview of network virtualization and cloud network as a service. *International Journal of Network Management*, 25(1):1–30, 2015.

[248] Navid Nikaein, Raymond Knopp, Lionel Gauthier, Eryk Schiller, Torsten Braun, Dominique Pichon, Christian Bonnet, Florian Kaltenberger, and Dominique Nussbaum. Closer to cloud-ran: Ran as a service. In *Proceedings of the 21st Annual International Conference on Mobile Computing and Networking*, pages 193–195. ACM, 2015.

[249] Rastin Pries, Hans-Jochen Morper, Nandor Galambosi, and Michael Jarschel. Network as a service-a demo on 5g network slicing. In *Teletraffic Congress (ITC 28), 2016 28th International*, volume 1, pages 209–211. IEEE, 2016.

[250] Hiroki Nishiyama, Thuan Ngo, Shoki Oiyama, and Nei Kato. Relay by smart device: Innovative communications for efficient information sharing among vehicles and pedestrians. *IEEE Vehicular Technology Magazine*, 10(4):54–62, 2015.

[251] TS 36.839 version 11.1.0: Mobility enhancements in heterogeneous networks (Release 11). *Technical Specification, 3GPP*, 2012.

[252] Jae-Wook Lee and Sang-Jo Yoo. Probabilistic path and data capacity based handover decision for hierarchical macro-and femtocell networks. *Mobile Information Systems*, 2016, 2016.

[253] Arvind Merwaday and Ismail Güvenç. Handover count based velocity estimation and mobility state detection in dense hetnets. *IEEE Transactions on Wireless Communications*, 15(7):4673–4688, 2016.

[254] Hellenic telecommunications and post commission (eett). http://keraies.eett.gr/, 2018. Accessed: 2018.

[255] Raman Kumar Goyal, Sakshi Kaushal, and Arun Kumar Sangaiah. The utility based non-linear fuzzy ahp optimization model for network selection in heterogeneous wireless networks. *Applied Soft Computing*, 2017.

[256] John Riordan. *Introduction to combinatorial analysis*. Courier Corporation, 2012.

[257] Emmanouil Skondras, Angelos Michalas, and Dimitrios D Vergados. A survey on medium access control schemes for 5g vehicular cloud computing systems. In *2018 Global Information Infrastructure and Networking Symposium (GIIS)*, pages 1–5. IEEE, 2018.

[258] Emmanouil Skondras, Angelos Michalas, Aggeliki Sgora, and Dimitrios D Vergados. A downlink scheduler supporting real time services in lte cellular networks. In *2015 6th International Conference on Information, Intelligence, Systems and Applications (IISA)*, pages 1–6. IEEE, 2015.

[259] Emmanouil Skondras, Angelos Michalas, Angeliki Sgora, and Dimitrios D Vergados. A qos aware three level scheduler for the lte downlink. In *2015 Wireless Telecommunications Symposium (WTS), Poster Session*, pages 1–2. IEEE, 2015.

[260] Emmanouil Skondras, Angelos Michalas, Aggeliki Sgora, and Dimitrios D Vergados. Qos-aware scheduling in lte-a networks with sdn control. In *2016 7th International Conference on Information, Intelligence, Systems & Applications (IISA)*, pages 1–6. IEEE, 2016.

[261] Emmanouil Skondras, Angelos Michalas, Nikolaos Tsolis, Aggeliki Sgora, and Dimitrios D Vergados. A network selection scheme for healthcare vehicular cloud computing systems. In *2017 8th International Conference on Information, Intelligence, Systems & Applications (IISA)*, pages 1–6. IEEE, 2017.

[262] Emmanouil Skondras, Angelos Michalas, and Dimitrios D Vergados. Mobility management on 5g vehicular cloud computing systems. *Vehicular Communications*, 16:15–44, 2019.

Appendix A

The positions of the available networks

In this appendix the positions and the spectrum of the available access networks are presented.

Table A1 The positions of the available LTE Access Networks.

Network	Position	Geographic Latitude	Geographic Longitude	Downlink & Uplink Spectrum in MHz (LTE Band)
LTE Macro 1	2e	37.948056	23.643056	1805-1825 & 1710-1730 (3)
LTE Macro 2	2l	37.947500	23.650278	2150-2170 & 1960-1980 (1)
LTE Macro 3	3p	37.946667	23.653611	2130-2150 & 1940-1960 (1)
LTE Macro 4	4i	37.946111	23.646389	2110-2130 & 1920-1940 (1)
LTE Macro 5	5q	37.945556	23.654167	1805-1825 & 1710-1730 (3)
LTE Macro 6	6f	37.945000	23.644444	1825-1845 & 1730-1750 (3)
LTE Macro 7	8f	37.942778	23.643611	1845-1865 & 1750-1770 (3)
LTE Macro 8	8t	37.942778	23.656944	1825-1845 & 1730-1750 (3)
LTE Macro 9	9l	37.941944	23.649444	925-945 & 880-900 (8)
LTE Macro 10	11c	37.940000	23.641111	1805-1825 & 1710-1730 (3)
LTE Macro 11	11l	37.939722	23.648611	778-798 & 723-743 (28)
LTE Macro 12	11t	37.939722	23.656111	2150-2170 & 1960-1980 (1)
LTE Macro 13	12i	37.939722	23.645833	758-778 & 703-723 (28)
LTE Macro 14	12y	37.938333	23.661389	1845-1865 & 1750-1770 (3)
LTE Macro 15	14q	37.938056	23.653889	2110-2130 & 1920-1940 (1)
LTE Macro 16	14v	37.937222	23.658333	2130-2150 & 1940-1960 (1)
LTE Macro 17	16b	37.936667	23.640000	2110-2130 & 1920-1940 (1)
LTE Macro 18	16h	37.936667	23.645556	1825-1845 & 1730-1750 (3)
LTE Macro 19	18c	37.934722	23.640833	2130-2150 & 1940-1960 (1)
LTE Macro 20	18f	37.934444	23.643889	2150-2170 & 1960-1980 (1)
LTE Femto 1	4f	37.946944	23.644444	925-945 & 880-900 (8)
LTE Femto 2	4j	37.946111	23.647222	758-778 & 703-723 (28)
LTE Femto 3	4r	37.946389	23.655000	925-945 & 880-900 (8)
LTE Femto 4	5d	37.945833	23.641944	758-778 & 703-723 (28)
LTE Femto 5	5j	37.945556	23.647500	778-798 & 723-743 (28)
LTE Femto 6	6h	37.944444	23.645833	2180-2200 & 2000-2020 (23)
LTE Femto 7	6i	37.944444	23.646667	1475.9-1495.9 & 1427.9-1447.9 (11)
LTE Femto 8	7h	37.944167	23.645833	860-875 & 815-830 (18)
LTE Femto 9	7i	37.943889	23.647222	2130-2150 & 1940-1960 (1)
LTE Femto 10	7k	37.943889	23.648056	2180-2200 & 2000-2020 (23)
LTE Femto 11	8k	37.942778	23.648611	1475.9-1495.9 & 1427.9-1447.9 (11)
LTE Femto 12	8m	37.942500	23.650556	2180-2200 & 2000-2020 (23)
LTE Femto 13	9e	37.941667	23.643333	860-875 & 815-830 (18)
LTE Femto 14	9g	37.942222	23.645000	2180-2200 & 2000-2020 (23)
LTE Femto 15	9h	37.941944	23.645833	860-875 & 815-830 (18)
LTE Femto 16	9j	37.942222	23.647778	2180-2200 & 2000-2020 (23)
LTE Femto 17	9n	37.942222	23.651111	1475.9-1495.9 & 1427.9-1447.9 (11)
LTE Femto 18	10e	37.941944	23.643333	2130-2150 & 1940-1960 (1)
LTE Femto 19	10f	37.941389	23.644167	2180-2200 & 2000-2020 (23)
LTE Femto 20	10g	37.941111	23.644444	860-875 & 815-830 (18)
LTE Femto 21	10h	37.941389	23.645833	2180-2200 & 2000-2020 (23)
LTE Femto 22	10j	37.941389	23.647500	860-875 & 815-830 (18)
LTE Femto 23	10l	37.941111	23.649722	1475.9-1495.9 & 1427.9-1447.9 (11)
LTE Femto 24	11e	37.940556	23.643056	1475.9-1495.9 & 1427.9-1447.9 (11)
LTE Femto 25	11f	37.940278	23.643611	860-875 & 815-830 (18)
LTE Femto 26	11h	37.940833	23.645833	1475.9-1495.9 & 1427.9-1447.9 (11)
LTE Femto 27	12k	37.940000	23.648889	1180-2200 & 2000-2020 (23)
LTE Femto 28	13c	37.939444	23.641111	1475.9-1495.9 & 1427.9-1447.9 (11)
LTE Femto 29	13e	37.938333	23.642778	925-945 & 880-900 (8)
LTE Femto 30	13j	37.939444	23.648333	1175.9-1495.9 & 1427.9-1447.9 (11)
LTE Femto 31	14d	37.938333	23.642222	1180-2200 & 2000-2020 (23)
LTE Femto 32	14n	37.938333	23.650556	1805-1825 & 1710-1730 (3)
LTE Femto 33	15b	37.937222	23.639722	925-945 & 880-900 (8)
LTE Femto 34	15c	37.937222	23.640833	778-798 & 723-743 (28)
LTE Femto 35	15u	37.936944	23.657778	925-945 & 880-900 (8)
LTE Femto 36	16c	37.936389	23.641111	860-875 & 815-830 (18)
LTE Femto 37	18h	37.934444	23.645278	925-945 & 880-900 (8)

Table A2 The positions of the available WiMAX Access Networks.

Network	Position	Geographic Latitude	Geographic Longitude	Downlink & Uplink Spectrum in MHz (WiMAX 2 Band)
WiMAX Macro 1	1e	37.949444	23.642500	3500-3510 & 3400-3410 (5L)
WiMAX Macro 2	3e	37.947778	23.643333	3510-3520 & 3410-3420 (5L)
WiMAX Macro 3	3j	37.947222	23.647500	3530-3540 & 3430-3440 (5L)
WiMAX Macro 4	3o	37.947222	23.652778	3540-3550 & 3440-3450 (5L)
WiMAX Macro 5	6r	37.944722	23.655000	3590-3600 & 3490-3600 (5L)
WiMAX Macro 6	8g	37.943333	23.645278	3590-3600 & 3490-3600 (5L)
WiMAX Macro 7	11d	37.940833	23.641944	3500-3510 & 3400-3410 (5L)
WiMAX Macro 8	11l	37.940556	23.649722	3530-3540 & 3430-3440 (5L)
WiMAX Macro 9	11n	37.940000	23.651389	3540-3550 & 3440-3450 (5L)
WiMAX Macro 10	11r	37.940278	23.655278	3550-3560 & 3450-3460 (5L)
WiMAX Macro 11	12j	37.939494	23.648333	3510-3520 & 3410-3420 (5L)
WiMAX Macro 12	12u	37.939444	23.657778	3500-3510 & 3400-3410 (5L)
WiMAX Macro 13	14e	37.938056	23.643333	3580-3590 & 3480-3490 (5L)
WiMAX Macro 14	14v	37.937222	23.658611	3510-3520 & 3410-3420 (5L)
WiMAX Macro 15	17b	37.935833	23.639722	3540-3550 & 3440-3450 (5L)
WiMAX Macro 16	18c	37.934722	23.640833	3530-3540 & 3430-3440 (5L)
WiMAX Macro 17	18i	37.934444	23.645278	2305-2315 & 2345-2355 (2)
WiMAX Femto 1	3f	37.947500	23.644444	3520-3530 & 3420-3430 (5L)
WiMAX Femto 2	5g	37.945278	23.644167	3550-3560 & 3450-3460 (5L)
WiMAX Femto 3	6e	37.945000	23.642222	3560-3570 & 3460-3470 (5L)
WiMAX Femto 4	6g	37.944444	23.645278	3570-3580 & 3470-3480 (5L)
WiMAX Femto 5	6j	37.944444	23.647222	3580-3500 & 3480-3490 (5L)
WiMAX Femto 6	7j	37.943889	23.647778	3520-3530 & 3420-3430 (5L)
WiMAX Femto 7	8h	37.942222	23.646111	2305-2315 & 2345-2355 (2)
WiMAX Femto 8	8k	37.942500	23.648056	3550-3560 & 3450-3460 (5L)
WiMAX Femto 9	8n	37.942778	23.651389	3520-3530 & 3420-3430 (5L)
WiMAX Femto 10	9g	37.942222	23.645278	2305-2315 & 2345-2355 (2)
WiMAX Femto 11	9i	37.941667	23.646389	3550-3560 & 3450-3460 (5L)
WiMAX Femto 12	9j	37.941944	23.647500	2305-2315 & 2345-2355 (2)
WiMAX Femto 13	9m	37.942222	23.651111	2305-2315 & 2345-2355 (2)
WiMAX Femto 14	10f	37.941389	23.644167	3520-3530 & 3420-3430 (5L)
WiMAX Femto 15	10h	37.941389	23.645833	3520-3530 & 3420-3430 (5L)
WiMAX Femto 16	10j	37.941389	23.647500	3550-3560 & 3450-3460 (5L)
WiMAX Femto 17	10m	37.941389	23.650000	3520-3530 & 3420-3430 (5L)
WiMAX Femto 18	10s	37.941389	23.655556	3520-3530 & 3420-3430 (5L)
WiMAX Femto 19	11f	37.940278	23.643333	2305-2315 & 2345-2355 (2)
WiMAX Femto 20	11h	37.940556	23.645556	2305-2315 & 2345-2355 (2)
WiMAX Femto 21	11k	37.939722	23.648611	2305-2315 & 2345-2355 (2)
WiMAX Femto 22	12k	37.929167	23.648056	3520-3530 & 3420-3430 (5L)
WiMAX Femto 23	15b	37.937222	23.640000	2305-2315 & 2345-2355 (2)
WiMAX Femto 24	15d	37.936944	23.641667	3520-3530 & 3420-3430 (5L)
WiMAX Femto 25	15u	37.936944	23.657778	2305-2315 & 2345-2355 (2)

Table A3 The positions of the available WAVE Access Networks.

Network	Position	Geographic Latitude	Geographic Longitude	Spectrum in MHz (DSRC Europe Band)
WAVE 1	2f	37.948056	23.644444	5915-5925 (SCH4)
WAVE 2	2h	37.947500	23.646389	5905-5915 (SCH3)
WAVE 3	3m	37.946667	23.650278	5895-5905 (SCH2)
WAVE 4	4e	37.946111	23.642500	5895-5905 (SCH2)
WAVE 5	4u	37.945556	23.658056	5875-5885 (SCH1)
WAVE 6	5i	37.945000	23.646944	5915-5925 (SCH4)
WAVE 7	6k	37.944167	23.648056	5905-5915 (SCH3)
WAVE 8	7e	37.943056	23.643333	5875-5885 (SCH1)
WAVE 9	7i	37.943889	23.646667	5895-5905 (SCH2)
WAVE 10	7n	34.943889	23.651111	5875-5885 (SCH1)
WAVE 11	9h	37.942222	23.646389	5915-5925 (SCH4)
WAVE 12	10e	37.941667	23.643333	5895-5905 (SCH2)
WAVE 13	10j	37.941667	23.647500	5875-5885 (SCH1)
WAVE 14	10n	37.941111	23.651667	5905-5915 (SCH3)
WAVE 15	11h	37.940556	23.645556	5905-5915 (SCH3)
WAVE 16	12c	37.939444	23.641389	5875-5885 (SCH1)
WAVE 17	12q	37.938889	23.654444	5875-5885 (SCH1)
WAVE 18	14b	37.938056	23.640556	5915-5925 (SCH4)
WAVE 19	14f	37.937778	23.644167	5905-5915 (SCH3)
WAVE 20	17c	37.935000	23.641389	5895-5905 (SCH2)
WAVE 21	17n	37.935278	23.651389	5895-5905 (SCH2)
WAVE 22	18i	37.934722	23.645278	5875-5885 (SCH1)

Appendix B

The available networks per SLA

In this appendix the available networks per SLA are presented.

Table B1 The available LTE networks of SLA 1.

Network	SLA 1																																		
	NAV							VoIP							CV							BS							Web						
	Throughput	Delay	Jitter	Packet Loss	Service Reliability	Security	Price	Throughput	Delay	Jitter	Packet Loss	Service Reliability	Security	Price	Throughput	Delay	Jitter	Packet Loss	Service Reliability	Security	Price	Throughput	Delay	Jitter	Packet Loss	Service Reliability	Security	Price	Throughput	Delay	Jitter	Packet Loss	Service Reliability	Security	Price
LTE Macro 1	AG	AG	G	VG	MG	G	AP	AG	AG	G	VG	G	VG	VP	G	VG	G	MG	MG	M	AP	M	MG	AG	M	G	AG	P	AG	AG	G	VG	VG	AG	AP
LTE Macro 2	VG	AG	G	G	AG	AG	AP	M	MG	MG	M	G	M	P	AG	AG	M	VG	M	MG	AP	MG	G	MG	M	MG	AG	VP	VG	AG	G	G	G	AG	P
LTE Macro 3	VG	AG	M	G	M	G	VP	M	MG	MG	M	MG	VG	VP	MG	G	G	M	VG	MG	VP	G	VG	MG	MG	VG	M	P	VG	AG	G	G	M	AG	VP
LTE Macro 4	M	MG	M	M	VG	AG	P	M	MG	MG	M	G	G	P	VG	AG	AG	G	VG	AG	P	AG	AG	M	VG	MG	G	P	MG	G	MG	M	G	G	VP
LTE Macro 5	AG	AG	VG	VG	VG	AG	VP	AG	AG	VG	VG	M	VG	AP	G	VG	AG	MG	AG	M	AP	MG	G	VG	MG	AG	G	VP	G	VG	AG	MG	M	G	VP
LTE Macro 6	M	MG	G	M	VG	G	P	MG	G	MG	M	VG	MG	AP	VG	AG	AG	G	G	MG	VP	G	G	VG	MG	VG	VG	P	AG	AG	VG	VG	VG	AG	VP
LTE Macro 7	MG	G	MG	M	AG	G	VP	MG	G	G	M	M	VG	VP	MG	G	G	M	M	MG	P	VG	AG	AG	G	G	MG	P	AG	AG	G	VG	G	VG	P
LTE Macro 8	MG	G	AG	MG	AG	M	P	AG	AG	G	VG	AG	AG	AP	AG	AG	AG	VG	AG	G	P	G	G	M	MG	AG	AG	P	G	VG	MG	MG	VG	AG	AP
LTE Macro 9	M	MG	VG	M	AG	M	VP	M	MG	AG	M	MG	M	AP	G	VG	G	MG	MG	VG	P	VG	AG	VG	G	VG	VG	P	M	MG	VG	M	AG	AG	P
LTE Macro 10	MG	G	AG	MG	MG	MG	AP	AG	AG	M	VG	VG	M	P	G	VG	G	MG	M	AG	VP	G	VG	G	MG	AG	AG	P	G	VG	MG	MG	G	G	VP
LTE Macro 11	M	MG	VG	M	VG	MG	VP	M	MG	MG	M	AG	MG	VP	G	VG	G	MG	M	VG	AP	M	MG	MG	M	G	G	P	G	G	MG	MG	G	VG	AP
LTE Macro 12	M	MG	M	M	VG	G	AP	VG	AG	AG	G	G	MG	AP	VG	AG	G	G	AG	G	VP	AG	AG	MG	VG	G	VG	AP	AG	AG	VG	VG	MG	MG	P
LTE Macro 13	VG	AG	MG	G	G	MG	AP	M	MG	M	M	MG	MG	P	AG	AG	VG	VG	G	M	P	AG	AG	VG	VG	MG	G	AP	VG	AG	VG	G	VG	AG	AP
LTE Macro 14	VG	AG	AG	G	MG	M	AP	AG	AG	VG	VG	VG	G	P	VG	AG	G	G	G	AG	VP	VG	AG	G	G	G	M	AP	G	VG	G	MG	G	AG	AP
LTE Macro 15	M	MG	MG	M	G	VG	P	AG	AG	G	VG	G	M	P	M	MG	G	M	VG	VG	AP	M	MG	AG	M	VG	AG	VP	AG	AG	M	VG	VG	G	AP
LTE Macro 16	AG	AG	MG	VG	AG	VG	VP	VG	AG	VG	G	MG	MG	P	VG	AG	AG	G	AG	MG	VP	G	G	MG	MG	AG	M	P	G	VG	MG	MG	G	VG	P
LTE Macro 17	G	VG	MG	MG	MG	M	VP	AG	AG	AG	VG	AG	M	P	G	VG	VG	MG	MG	AG	P	G	VG	VG	MG	G	AG	AP	VG	AG	VG	G	G	MG	AP
LTE Macro 18	MG	G	MG	M	G	G	VP	VG	AG	G	G	VG	VG	VP	G	VG	G	MG	AG	MG	AP	MG	G	MG	M	VG	MG	AP	M	MG	AG	M	G	G	VP
LTE Macro 19	AG	AG	MG	VG	AG	VG	VP	MG	G	MG	M	G	M	VP	G	VG	AG	MG	G	G	P	G	VG	M	MG	VG	MG	AP	VG	AG	VG	G	VG	VG	P
LTE Macro 20	M	MG	MG	M	AG	AG	VP	MG	G	G	M	M	G	P	MG	G	G	M	AG	MG	VP	G	VG	G	MG	MG	M	AP	MG	G	AG	M	VG	VG	P
LTE Femto 1	MG	G	AG	M	MG	M	P	VG	AG	M	G	VG	M	VP	MG	G	VG	M	VG	AG	AP	VG	AG	M	G	G	VG	VP	G	VG	MG	MG	AG	G	VP
LTE Femto 2	VG	AG	M	G	M	M	AP	AG	AG	G	VG	M	M	AP	MG	G	M	M	VG	MG	AP	MG	G	M	M	VG	MG	P	G	VG	MG	MG	G	MG	P
LTE Femto 3	AG	AG	MG	VG	VG	MG	P	AG	AG	G	VG	AG	VG	VP	G	VG	G	MG	VG	G	P	AG	AG	VG	VG	G	G	VP	VG	AG	MG	G	MG	VG	AP
LTE Femto 4	MG	G	AG	M	VG	AG	VP	G	VG	VG	MG	VG	AG	VP	G	VG	G	MG	AG	MG	VP	MG	G	G	M	M	AG	AP	AG	AG	G	VG	MG	G	VP
LTE Femto 5	MG	G	M	M	G	G	VP	M	MG	MG	M	AG	M	P	VG	AG	AG	G	VG	AG	AP	VG	AG	AG	G	G	VG	P	G	VG	VG	MG	AG	VG	P
LTE Femto 6	AG	AG	M	VG	VG	VG	AP	AG	AG	AG	VG	MG	M	P	M	MG	AG	M	G	VG	AP	M	MG	MG	M	VG	AG	AP	MG	G	G	M	MG	AG	P
LTE Femto 7	MG	G	M	M	M	MG	AP	VG	AG	VG	G	VG	M	VP	AG	AG	G	VG	MG	MG	AP	MG	G	MG	M	VG	VG	P	AG	AG	G	VG	AG	G	P
LTE Femto 8	M	MG	AG	M	MG	M	VP	AG	AG	M	VG	M	M	VP	AG	AG	AG	VG	G	AG	P	G	VG	G	MG	MG	M	P	AG	AG	AG	VG	VG	G	AP
LTE Femto 9	G	VG	M	MG	AG	VG	VP	MG	G	G	M	M	MG	AP	G	VG	MG	MG	MG	MG	AP	MG	G	G	M	MG	AG	P	M	MG	MG	M	MG	AG	AP
LTE Femto 10	VG	AG	AG	G	G	M	AP	VG	AG	VG	G	VG	VG	VP	AG	AG	VG	VG	MG	AG	AP	VG	AG	M	G	AG	MG	AP	VG	AG	VG	G	G	AG	AP
LTE Femto 11	AG	AG	G	VG	VG	AG	P	AG	AG	G	VG	M	MG	AP	G	G	M	MG	M	M	P	AG	AG	G	VG	MG	M	P	AG	AG	G	VG	MG	VG	VP
LTE Femto 12	MG	G	M	M	VG	MG	P	M	MG	VG	M	VG	AG	AP	MG	G	AG	M	G	G	AP	AG	AG	MG	VG	G	G	AP	M	MG	G	M	VG	VG	P
LTE Femto 13	MG	G	MG	M	M	M	P	VG	AG	M	G	M	M	VP	AG	AG	M	VG	AG	G	VP	MG	G	AG	M	G	MG	VP	AG	AG	G	VG	G	MG	AP
LTE Femto 14	G	VG	M	MG	M	AG	VP	MG	G	G	M	AG	G	VP	VG	AG	VG	G	VG	MG	VP	AG	AG	M	VG	MG	G	VP	G	VG	MG	MG	G	AG	AP
LTE Femto 15	MG	G	G	M	G	G	AP	MG	G	G	M	AG	MG	P	M	MG	AG	M	AG	M	VP	MG	G	MG	M	G	AG	AP	VG	AG	MG	G	MG	MG	VP
LTE Femto 16	VG	AG	M	G	VG	MG	VP	AG	AG	M	VG	AG	G	VP	G	VG	MG	MG	G	MG	P	G	G	MG	G	AG	VG	VP	AG	AG	M	VG	M	AG	AP
LTE Femto 17	VG	AG	M	G	AG	VG	P	VG	AG	AG	G	VG	MG	VP	MG	G	AG	M	VG	VG	P	AG	AG	VG	VG	G	M	AP	G	G	MG	MG	G	VG	AP
LTE Femto 18	MG	G	M	M	VG	G	P	G	VG	M	MG	MG	G	VP	VG	AG	MG	G	AG	MG	P	G	VG	MG	MG	VG	MG	AP	G	VG	VG	MG	VG	AG	VP
LTE Femto 19	VG	AG	G	G	AG	M	P	VG	AG	AG	G	G	AG	AP	AG	AG	M	VG	VG	M	AP	VG	AG	G	G	G	G	P	VG	AG	MG	G	MG	G	P
LTE Femto 20	G	VG	G	MG	MG	AG	AP	M	MG	MG	M	MG	M	VP	VG	AG	AG	G	MG	MG	AP	VG	AG	VG	G	G	G	VP	MG	G	G	M	G	MG	VP
LTE Femto 21	M	MG	G	M	VG	AG	VP	M	MG	M	M	MG	AG	AP	G	VG	G	MG	MG	VG	AP	M	MG	G	M	MG	M	AP	VG	AG	MG	G	VG	MG	P
LTE Femto 22	AG	AG	MG	VG	VG	AG	VP	G	VG	MG	MG	AG	VG	VP	AG	AG	AG	VG	VG	AG	P	M	MG	VG	M	G	G	P	MG	G	VG	M	M	M	VP
LTE Femto 23	M	MG	G	M	M	AG	P	AG	AG	M	VG	MG	AG	AP	AG	AG	MG	VG	G	MG	P	G	VG	AG	MG	VG	G	AP	M	MG	M	M	AG	G	P
LTE Femto 24	MG	G	MG	M	AG	AG	AP	AG	AG	MG	VG	M	M	VP	MG	G	MG	M	G	G	AP	M	MG	VG	M	M	G	P	VG	AG	MG	G	AG	G	P
LTE Femto 25	G	VG	AG	MG	G	MG	AP	G	VG	G	MG	MG	MG	VP	AG	AG	AG	VG	VG	VG	P	VG	AG	AG	G	G	G	AP	AG	AG	AG	VG	VG	AG	VP
LTE Femto 26	G	VG	G	MG	M	G	VP	MG	G	AG	M	G	G	VP	AG	AG	M	VG	G	G	VP	G	VG	G	MG	VG	G	VP	M	MG	VG	M	G	VG	AP
LTE Femto 27	MG	G	G	M	G	M	AP	VG	AG	G	G	VG	AG	P	MG	G	G	MG	AG	AG	VP	G	VG	AG	MG	G	VG	P	AG	AG	AG	VG	VG	G	AP
LTE Femto 28	M	MG	G	M	MG	G	VP	MG	G	G	M	G	G	VP	MG	G	AG	M	G	G	AP	G	G	VG	MG	G	MG	VP	G	VG	VG	MG	G	MG	P
LTE Femto 29	VG	AG	M	G	M	MG	AP	AG	AG	VG	VG	VG	AG	P	G	VG	MG	MG	MG	M	VP	AG	AG	AG	VG	MG	MG	VP	M	MG	VG	M	MG	G	AP
LTE Femto 30	AG	AG	AG	VG	M	AG	VP	G	VG	M	MG	MG	MG	AP	MG	G	G	M	G	G	VP	AG	AG	G	VG	G	AG	P	M	MG	M	M	G	G	VP
LTE Femto 31	VG	AG	AG	G	AG	MG	P	AG	AG	VG	VG	VG	AG	AP	MG	G	G	M	G	M	AP	M	MG	MG	M	MG	M	AP	AG	AG	G	VG	AG	G	AP
LTE Femto 32	VG	AG	AG	G	VG	MG	AP	G	VG	M	MG	G	MG	VP	VG	AG	VG	G	M	MG	VP	MG	G	M	M	MG	G	AP	M	MG	M	M	VG	MG	VP
LTE Femto 33	AG	AG	MG	VG	AG	MG	P	G	VG	M	MG	M	VG	VP	VG	AG	AG	G	G	AG	P	VG	AG	G	G	VG	VG	VP	G	VG	VG	MG	G	VG	P
LTE Femto 34	AG	AG	G	VG	MG	MG	VP	VG	AG	MG	G	MG	MG	P	VG	AG	M	G	G	MG	VP	M	MG	VG	M	AG	AG	VP	MG	G	VG	M	G	M	P
LTE Femto 35	VG	AG	G	G	MG	M	VP	G	VG	M	MG	AG	VG	P	VG	AG	VG	G	MG	MG	P	VG	AG	G	G	MG	AG	P	G	VG	G	MG	VG	M	P
LTE Femto 36	G	VG	M	MG	MG	G	AP	MG	G	VG	M	MG	AG	VP	VG	AG	G	G	AG	MG	AP	MG	G	VG	M	AG	MG	P	G	VG	MG	MG	M	G	AP
LTE Femto 37	G	VG	AG	MG	M	MG	P	AG	AG	VG	VG	VG	AG	AP	AG	AG	VG	VG	M	G	AP	AG	AG	AG	VG	MG	MG	AP	G	VG	VG	MG	VG	MG	P

Table B2 The available WiMAX and WAVE networks of SLA 1.

Network	SLA 1																																		
	NAV							VoIP							CV							BS							Web						
	Throughput	Delay	Jitter	Packet Loss	Service Reliability	Security	Price	Throughput	Delay	Jitter	Packet Loss	Service Reliability	Security	Price	Throughput	Delay	Jitter	Packet Loss	Service Reliability	Security	Price	Throughput	Delay	Jitter	Packet Loss	Service Reliability	Security	Price	Throughput	Delay	Jitter	Packet Loss	Service Reliability	Security	Price
WiMAX Macro 1	MG	G	G	M	G	VG	P	G	VG	VG	MG	VG	G	P	M	MG	M	M	VG	M	P	G	G	VG	MG	G	MG	AP	MG	G	M	M	AG	G	AP
WiMAX Macro 2	MG	G	M	M	MG	G	P	MG	G	VG	M	MG	G	P	AG	AG	G	VG	AG	MG	AP	AG	AG	VG	VG	MG	M	AP	G	VG	AG	MG	AG	M	P
WiMAX Macro 3	G	VG	MG	MG	G	G	VP	MG	G	M	M	VG	M	P	VG	AG	MG	G	G	M	P	M	MG	G	M	MG	M	VP	VG	AG	MG	G	AG	M	VP
WiMAX Macro 4	MG	G	M	M	AG	VG	VP	MG	G	M	M	AG	MG	AP	VG	AG	MG	G	VG	M	VP	AG	AG	AG	VG	MG	G	P	G	VG	M	MG	G	AG	AP
WiMAX Macro 5	AG	AG	AG	VG	MG	M	VP	VG	AG	G	G	MG	AG	P	VG	AG	M	G	AG	M	AP	MG	G	VG	M	G	G	P	AG	AG	G	VG	M	G	VP
WiMAX Macro 6	M	MG	MG	M	G	M	P	MG	G	VG	M	VG	VG	AP	VG	AG	G	G	VG	M	P	G	VG	MG	MG	VG	VG	AP	G	VG	G	MG	VG	VG	VP
WiMAX Macro 7	AG	AG	G	VG	M	VG	AP	AG	AG	MG	VG	VG	G	P	G	VG	MG	MG	VG	M	AP	G	VG	M	MG	AG	G	AP	MG	G	M	M	AG	G	AP
WiMAX Macro 8	M	MG	VG	M	AG	MG	VP	VG	AG	MG	G	MG	VG	AP	M	MG	VG	M	G	G	VP	MG	G	G	M	G	AG	VP	G	VG	MG	MG	M	MG	P
WiMAX Macro 9	AG	AG	M	VG	M	MG	P	M	MG	M	M	AG	VG	AP	AG	AG	G	VG	G	M	VP	MG	G	MG	M	G	M	AP	M	MG	MG	M	AG	G	VP
WiMAX Macro 10	MG	G	M	M	VG	G	P	AG	AG	AG	VG	MG	G	VP	AG	AG	G	VG	G	MG	VP	G	VG	M	MG	M	VG	AP	VG	AG	AG	G	G	VG	VP
WiMAX Macro 11	M	MG	G	M	VG	MG	AP	MG	G	AG	M	G	MG	P	G	VG	M	MG	G	M	AP	G	VG	VG	MG	VG	G	P	M	MG	VG	M	VG	G	VP
WiMAX Macro 12	G	VG	AG	MG	G	M	P	AG	AG	VG	VG	G	G	P	VG	AG	M	G	G	AG	AP	VG	AG	G	G	G	MG	P	VG	AG	G	G	M	MG	P
WiMAX Macro 13	G	VG	MG	MG	AG	M	VP	M	MG	VG	M	M	G	P	AG	AG	VG	VG	VG	G	VP	M	MG	AG	M	AG	G	AP	G	VG	G	MG	AG	AG	VP
WiMAX Macro 14	AG	AG	AG	VG	G	M	P	M	MG	M	M	M	VG	P	VG	AG	G	G	AG	VG	P	MG	G	G	M	M	VG	AP	MG	G	MG	M	G	MG	VP
WiMAX Macro 15	VG	AG	VG	G	MG	G	AP	AG	AG	G	VG	G	M	VP	MG	G	VG	M	VG	MG	P	M	MG	M	M	AG	G	P	G	VG	G	MG	VG	MG	AP
WiMAX Macro 16	M	MG	M	M	VG	MG	AP	VG	AG	MG	G	M	VG	AP	M	MG	M	M	MG	MG	AP	G	G	VG	MG	VG	G	P	AG	AG	AG	VG	G	AG	AP
WiMAX Macro 17	M	MG	G	M	G	AG	AP	M	MG	MG	M	AG	AG	VP	MG	G	G	M	AG	VG	VP	AG	AG	VG	VG	G	MG	AP	VG	AG	VG	G	VG	MG	VP
WiMAX Femto 1	VG	AG	AG	G	G	MG	AP	M	MG	M	M	VG	MG	P	MG	G	MG	M	G	MG	AP	VG	AG	G	G	AG	G	AP	G	VG	VG	MG	VG	G	P
WiMAX Femto 2	M	MG	G	M	MG	AG	VP	G	VG	AG	MG	AG	AG	P	M	MG	MG	M	VG	VG	VP	G	VG	M	MG	M	VG	VP	MG	G	VG	M	G	VG	P
WiMAX Femto 3	M	MG	G	M	AG	G	AP	M	MG	AG	M	G	M	AP	VG	AG	VG	G	G	G	AP	MG	G	VG	M	M	AG	VP	M	MG	MG	M	AG	AG	AP
WiMAX Femto 4	MG	G	VG	M	MG	VG	P	AG	AG	AG	VG	VG	MG	P	G	VG	G	MG	MG	MG	VP	M	MG	M	M	M	MG	P	G	G	G	MG	G	M	AP
WiMAX Femto 5	AG	AG	G	VG	G	M	VP	VG	AG	MG	G	MG	AG	VP	VG	AG	AG	G	AG	VG	VP	VG	AG	M	G	VG	VG	P	MG	G	M	M	MG	M	AP
WiMAX Femto 6	M	MG	MG	M	G	VG	AP	MG	G	AG	M	M	MG	P	VG	AG	G	G	MG	M	AP	MG	G	VG	M	G	G	VP	AG	AG	G	VG	VG	VG	VP
WiMAX Femto 7	MG	G	G	M	MG	M	VP	M	MG	M	M	VG	VG	P	G	VG	VG	MG	G	VG	P	M	MG	G	M	G	VG	P	AG	AG	VG	VG	G	AG	P
WiMAX Femto 8	G	VG	G	MG	G	MG	AP	VG	AG	M	G	G	VG	P	AG	AG	MG	VG	AG	G	P	VG	AG	AG	G	MG	AG	VP	AG	AG	VG	VG	VG	MG	AP
WiMAX Femto 9	MG	G	MG	M	VG	M	P	M	MG	M	M	AG	G	AP	MG	G	G	M	G	MG	VP	M	MG	VG	M	AG	M	AP	MG	G	MG	M	G	G	AP
WiMAX Femto 10	AG	AG	AG	VG	M	AG	AP	G	VG	AG	MG	M	MG	AP	G	VG	M	MG	G	AG	VP	VG	AG	G	G	VG	G	P	AG	AG	AG	VG	MG	MG	P
WiMAX Femto 11	MG	G	G	M	G	AG	P	VG	AG	AG	G	VG	G	P	AG	AG	AG	VG	MG	G	P	AG	AG	VG	VG	G	VG	AP	AG	AG	AG	VG	VG	AG	VP
WiMAX Femto 12	G	VG	G	MG	AG	VG	P	M	MG	MG	M	M	MG	AP	MG	G	MG	M	VG	G	P	G	VG	G	MG	VG	AG	VP	G	VG	MG	MG	G	M	P
WiMAX Femto 13	AG	AG	MG	VG	VG	VG	VP	M	MG	AG	M	G	M	AP	G	VG	VG	MG	G	VG	P	AG	AG	VG	VG	G	VG	VP	VG	AG	MG	G	MG	M	AP
WiMAX Femto 14	AG	AG	VG	VG	M	G	AP	AG	AG	M	VG	M	M	AP	VG	AG	MG	G	MG	G	VP	AG	AG	VG	VG	VG	G	AP	MG	G	G	M	VG	G	AP
WiMAX Femto 15	AG	AG	G	VG	G	MG	VP	MG	G	VG	M	G	MG	VP	G	G	MG	MG	G	AG	AP	AG	AG	M	VG	MG	G	P	G	VG	M	MG	MG	MG	P
WiMAX Femto 16	M	MG	M	M	MG	M	VP	G	VG	M	MG	G	M	AP	VG	G	MG	G	G	AG	P	VG	AG	MG	G	AG	VG	P	AG	AG	AG	VG	AG	G	P
WiMAX Femto 17	M	MG	G	M	MG	M	AP	G	VG	VG	MG	M	M	AP	G	VG	AG	MG	AG	VG	P	MG	G	VG	M	VG	AG	VP	VG	AG	AG	G	AG	MG	P
WiMAX Femto 18	G	VG	AG	MG	M	VG	VP	AG	AG	VG	VG	VG	M	VP	VG	AG	G	G	MG	G	P	M	MG	AG	M	G	VG	P	VG	AG	VG	G	AG	M	VP
WiMAX Femto 19	M	MG	M	M	G	M	VP	AG	AG	M	VG	AG	M	VP	AG	AG	G	VG	G	M	AP	G	VG	MG	MG	G	MG	AP	VG	AG	M	G	G	VG	P
WiMAX Femto 20	G	VG	AG	MG	G	AG	VP	M	MG	M	M	M	MG	AP	G	VG	MG	MG	M	AG	P	MG	G	G	M	VG	G	P	M	MG	AG	M	VG	VG	AP
WiMAX Femto 21	MG	G	M	M	MG	AG	P	M	MG	M	M	M	AG	P	M	MG	AG	M	M	AG	P	G	VG	M	MG	VG	G	AP	VG	AG	G	G	G	G	AP
WiMAX Femto 22	VG	AG	AG	G	MG	M	AP	G	VG	M	MG	M	AG	VP	G	VG	G	MG	VG	M	AP	M	MG	VG	M	M	VG	VP	MG	G	M	M	G	MG	AP
WiMAX Femto 23	MG	G	G	M	MG	M	AP	VG	AG	AG	G	AG	M	VP	MG	G	MG	M	G	MG	AP	MG	G	G	M	G	AG	AP	VG	AG	G	G	VG	AG	VP
WiMAX Femto 24	G	VG	M	MG	VG	G	VP	AG	AG	AG	VG	MG	MG	AP	G	VG	MG	MG	MG	M	VP	G	VG	AG	MG	G	MG	AP	VG	AG	VG	G	G	G	P
WiMAX Femto 25	MG	G	VG	M	MG	VG	AP	VG	AG	G	G	VG	G	P	MG	G	G	M	AG	MG	P	VG	AG	AG	G	MG	MG	AP	MG	G	AG	M	VG	MG	AP
WAVE 1	AG	AG	G	VG	VG	VG	VP	G	VG	VG	MG	AG	AG	P	MG	G	M	M	VG	G	P	MG	G	G	M	VG	AG	P	VG	AG	G	G	AG	M	VP
WAVE 2	VG	AG	MG	G	AG	MG	VP	MG	G	MG	M	G	M	P	VG	AG	AG	G	G	M	VP	M	MG	VG	M	G	VG	AP	M	MG	VG	M	VG	MG	P
WAVE 3	VG	AG	M	G	M	VG	AP	M	MG	G	M	VG	VG	VP	AG	AG	MG	VG	VG	MG	VP	MG	G	M	M	VG	G	P	MG	G	G	G	M	VG	VP
WAVE 4	AG	AG	AG	VG	AG	AG	P	G	VG	M	MG	MG	MG	VP	G	G	M	MG	AG	G	VP	AG	AG	G	VG	AG	MG	VP	G	VG	MG	MG	G	VG	AP
WAVE 5	M	MG	M	M	AG	VG	AP	MG	G	VG	M	VG	AG	AP	G	VG	VG	MG	MG	MG	AP	AG	AG	G	VG	MG	MG	P	M	MG	AG	M	M	G	AP
WAVE 6	M	MG	VG	MG	MG	M	VP	G	VG	AG	MG	AG	VG	AP	M	MG	G	M	MG	G	VP	AG	AG	M	VG	G	VG	AP	MG	G	G	M	G	MG	AP
WAVE 7	M	MG	AG	M	MG	VG	VP	VG	AG	MG	G	M	G	P	VG	AG	VG	G	AG	G	VP	AG	AG	VG	VG	G	G	P	VG	AG	G	G	AG	VG	AP
WAVE 8	MG	G	G	MG	MG	MG	VP	M	MG	M	M	AG	MG	P	VG	AG	AG	G	M	MG	AP	AG	AG	G	VG	M	MG	P	VG	AG	AG	G	G	VG	AP
WAVE 9	MG	G	G	MG	G	M	P	M	MG	M	M	VG	MG	VP	M	MG	M	M	VG	VG	P	AG	AG	M	VG	VG	G	AP	M	MG	G	M	AG	G	P
WAVE 10	MG	G	G	M	AG	VG	P	M	MG	VG	M	AG	M	VP	AG	AG	M	VG	MG	G	VP	M	MG	G	M	MG	G	VP	MG	G	VG	M	G	AG	AP
WAVE 11	M	MG	G	M	G	AG	AP	VG	AG	G	G	M	M	VP	G	VG	G	MG	MG	MG	VP	AG	AG	G	VG	AG	MG	VP	VG	AG	G	G	VG	M	P
WAVE 12	AG	AG	MG	VG	M	VG	VP	AG	AG	VG	VG	VG	G	VP	M	MG	VG	M	G	VG	VP	VG	AG	MG	G	MG	VG	AP	AG	AG	M	VG	G	AG	AP
WAVE 13	M	MG	G	M	G	M	VP	MG	G	VG	M	VG	MG	P	AG	AG	G	VG	VG	G	VP	VG	AG	MG	G	AG	G	AP	AG	AG	VG	VG	VG	VG	P
WAVE 14	AG	AG	AG	VG	G	VG	AP	G	VG	VG	MG	G	M	AP	G	G	G	MG	VG	AG	P	M	MG	G	M	G	MG	P	MG	G	MG	M	AG	G	VP
WAVE 15	G	VG	G	MG	M	MG	VP	AG	AG	VG	VG	G	MG	AP	AG	AG	G	VG	AG	M	VP	M	MG	VG	M	G	MG	P	MG	G	G	M	G	AG	VP
WAVE 16	VG	AG	MG	M	VG	G	VP	G	VG	MG	MG	VG	AG	VP	G	VG	AG	MG	G	G	AP	VG	AG	AG	G	MG	G	AP	G	VG	G	MG	AG	G	AP
WAVE 17	M	MG	VG	M	VG	VG	P	VG	AG	AG	G	M	MG	VP	M	MG	G	M	AG	MG	VP	VG	AG	MG	G	MG	M	AP	VG	AG	G	G	AG	VG	P
WAVE 18	G	VG	G	MG	MG	AG	AP	MG	G	M	M	VG	VG	AP	MG	G	M	M	VG	G	VP	AG	AG	G	VG	AG	G	P	M	MG	AG	M	VG	G	P
WAVE 19	VG	AG	MG	G	MG	M	P	G	VG	AG	MG	VG	G	AP	VG	AG	G	G	AG	G	P	MG	G	AG	M	MG	VG	AP	AG	AG	AG	VG	M	AG	AP
WAVE 20	M	MG	M	M	G	G	AP	MG	G	AG	M	G	MG	VP	VG	AG	MG	G	AG	AG	AP	M	MG	MG	M	VG	AG	P	M	MG	VG	M	AG	AG	VP
WAVE 21	M	MG	VG	M	VG	AG	P	G	VG	AG	MG	MG	G	AP	G	VG	M	MG	MG	MG	P	G	VG	G	MG	AG	VG	VP	G	VG	M	MG	MG	G	P
WAVE 22	MG	G	G	MG	MG	G	VP	MG	G	G	M	G	AG	AP	AG	AG	MG	VG	MG	AG	VP	VG	AG	G	G	G	MG	VP	AG	AG	G	VG	G	AG	AP

Table B3 The available LTE networks of SLA 2, SLA 3 and SLA 4.

Network	SLA 2															SLA 3														SLA 4						
	CV							BS							Web							BS							Web							Web						
	Throughput	Delay	Jitter	Packet Loss	Service Reliability	Secutiy	Price	Throughput	Delay	Jitter	Packet Loss	Service Reliability	Security	Price	Throughput	Delay	Jitter	Packet Loss	Service Reliability	Security	Price	Throughput	Delay	Jitter	Packet Loss	Service Reliability	Security	Price	Throughput	Delay	Jitter	Packet Loss	Service Reliability	Security	Price	Throughput	Delay	Jitter	Packet Loss	Service Reliability	Security	Price
LTE Macro 1	G	G	G	MG	MG	P	P	MP	M	MG	P	G	MP	P	G	G	G	MG	G	MP	P	MP	M	MG	P	M	MP	M	P	MP	MG	P	MG	MP	M	VP	P	VP	AP	VP	P	VG
LTE Macro 2	M	MG	P	MP	M	MP	M	MG	G	M	M	P	MG	M	G	G	MP	MG	MP	MG	P	P	MP	MP	P	P	MP	M	M	MG	MP	MP	MP	MG	MG	M	M	AP	MP	MP	P	G
LTE Macro 3	MG	G	G	M	G	MG	MP	P	MP	M	P	P	P	M	MG	G	P	M	M	P	M	P	MP	P	P	P	P	M	MG	MG	P	M	M	P	G	AP	VP	VP	AP	M	VP	AG
LTE Macro 4	M	MG	P	MP	P	MP	MP	G	G	P	MG	P	G	P	MG	G	M	M	G	M	P	MP	M	P	P	P	P	M	MG	MG	MP	M	MG	P	M	M	M	MP	MP	VP	P	AG
LTE Macro 5	MP	M	M	P	P	M	M	MG	G	G	M	MG	G	M	MG	G	P	M	M	G	M	MG	MG	MG	M	P	MP	M	M	MG	P	MP	M	MP	M	AP	VP	P	AP	AP	P	AG
LTE Macro 6	MP	M	MP	P	G	MG	M	G	G	G	MG	MP	G	M	M	MG	G	MP	MG	MP	MP	MG	MG	MP	M	MP	P	M	M	MG	MP	MP	MP	P	G	P	MP	MP	VP	VP	P	G
LTE Macro 7	MG	G	G	M	P	M	P	M	MG	MG	MP	M	P	M	M	MG	P	MP	G	M	P	MP	M	P	P	MP	P	MG	MP	M	P	P	P	P	M	AP	VP	VP	AP	AP	VP	VG
LTE Macro 8	G	G	P	MG	P	MP	M	G	G	P	MG	MG	G	MP	M	MG	M	MP	G	M	P	P	MP	P	MP	P	M	G	M	MG	P	MP	MP	MP	M	P	MP	AP	VP	VP	MP	AG
LTE Macro 9	MG	G	P	M	M	G	MP	MP	M	MG	P	G	MP	P	M	MG	MG	MP	MG	MG	P	P	MP	MP	VP	M	P	G	P	MP	M	VP	P	MP	G	P	MP	P	VP	P	VP	AG
LTE Macro 10	G	G	G	MG	M	M	M	MG	G	G	M	MP	MG	M	P	MP	P	P	G	M	MP	MP	M	P	MP	P	G	P	MP	P	P	M	MP	MG	P	MP	VP	P	AP	MP	VG
LTE Macro 11	M	MG	MP	MP	P	MG	MP	P	MP	MG	P	G	P	M	G	G	P	MG	G	G	M	P	MP	MG	P	P	P	MG	M	MG	P	MP	MP	P	G	P	MP	VP	VP	MP	P	AG
LTE Macro 12	MP	M	G	P	MP	G	M	MP	M	MG	P	M	MG	MP	MP	M	P	P	MG	MG	P	MP	M	MG	P	M	MP	MG	MP	M	P	P	MP	M	M	MP	M	VP	P	VP	AP	VG
LTE Macro 13	G	G	G	MG	G	MP	MP	P	MP	MG	P	MG	G	M	P	MP	P	MP	P	P	MP	P	MP	M	M	P	MP	P	VP	P	P	G	P	MP	P	VP	P	VP	AP	VP	VG
LTE Macro 14	M	MG	MG	MP	G	P	M	G	G	G	MG	P	M	MP	P	MP	G	P	G	G	P	M	MG	M	MP	P	MP	M	P	MP	MG	P	MP	P	G	P	MP	M	VP	MP	AP	G
LTE Macro 15	M	MG	MG	MP	G	MP	P	P	MP	M	P	MG	MP	MP	MG	G	P	M	P	P	P	P	MP	M	P	P	P	M	MP	M	P	P	P	VP	G	MP	M	P	P	P	VP	VG
LTE Macro 16	MG	G	MP	M	P	MG	P	G	G	MG	MG	MG	P	M	M	MG	MG	MP	M	MP	M	P	MP	M	P	P	P	M	M	MG	P	MP	M	P	M	M	M	P	MP	MP	P	G
LTE Macro 17	MP	M	P	P	P	G	M	P	MP	P	P	P	MG	P	M	MG	P	MP	MP	MG	P	P	MP	P	P	P	M	G	P	MP	P	P	MP	M	MG	P	MP	AP	VP	VP	VP	G
LTE Macro 18	MG	G	M	M	MP	M	MP	MG	G	MG	M	P	MP	M	M	MG	G	MP	M	G	P	P	MP	P	P	P	MP	G	P	MP	P	VP	MP	P	G	AP	VP	P	AP	P	AP	VG
LTE Macro 19	MP	M	MP	P	M	P	M	G	G	MP	MG	MG	P	M	MP	M	MG	P	MP	MG	M	MP	M	MP	MP	P	M	MP	M	MP	MP	P	MP	MP	G	MP	M	P	P	P	MP	AG
LTE Macro 20	MG	G	MG	M	M	MG	M	M	MG	G	MP	MG	M	MP	MG	G	G	M	G	M	M	MP	M	P	P	P	M	G	MP	M	M	P	P	M	MG	P	MP	AP	P	AP	AP	AG
LTE Femto 1	P	MP	G	P	G	M	MP	G	G	M	MG	MG	P	P	MP	M	P	P	M	P	P	P	MP	P	P	MG	P	MG	MP	M	P	P	M	P	M	MP	M	VP	P	AP	VP	G
LTE Femto 2	P	MP	MP	P	M	MG	MP	M	MG	P	MP	P	MG	MP	MP	M	P	MP	G	M	M	M	MG	P	MP	P	MP	G	P	MP	P	VP	P	P	G	P	MP	AP	VP	AP	VP	G
LTE Femto 3	G	G	MG	MG	M	G	M	MG	G	G	M	MP	P	P	MP	M	MP	P	P	M	M	P	MP	P	P	MG	MP	M	MP	P	P	P	M	VP	P	MP	AP	P	AP	VG
LTE Femto 4	G	G	P	MG	G	M	P	MG	G	MG	M	P	MP	P	MG	G	M	M	P	G	MP	MP	M	MG	P	P	P	G	MP	M	MP	P	P	P	G	MP	M	MP	P	VP	P	VG
LTE Femto 5	G	G	M	MG	P	MP	M	MG	G	MG	M	MG	P	M	P	MP	G	P	G	M	P	P	MP	P	P	MP	P	G	P	MP	MP	P	MG	P	G	P	MP	MP	VP	P	VP	VG
LTE Femto 6	P	MP	M	P	G	P	P	P	MP	MG	P	M	G	MP	MP	M	G	P	P	M	MP	P	MP	MG	P	P	P	MG	MP	M	MG	P	P	MP	MG	M	AP	P	VP	MP	G
LTE Femto 7	M	MG	P	MP	M	M	MP	MG	G	MG	M	MP	P	P	MG	G	G	M	MP	M	M	M	MG	MP	MP	P	P	M	P	MP	P	P	P	P	G	P	MP	P	VP	VP	P	VG
LTE Femto 8	G	G	MP	MG	MP	M	P	P	MP	G	P	MG	MP	P	G	G	MP	MG	G	M	P	P	MP	P	P	MP	P	G	MG	MG	MP	M	P	P	G	M	M	P	MP	P	VP	VG
LTE Femto 9	MG	G	M	M	MG	M	P	MG	G	M	M	MG	MP	M	M	MG	M	MP	MP	MG	M	P	MP	MP	G	M	MG	M	MP	MP	M	G	MP	M	MP	P	MP	MP	G	MP	G
LTE Femto 10	P	MP	MG	P	MP	MG	M	G	G	P	MG	MP	MP	MP	MP	M	G	P	G	G	P	MP	M	P	P	MP	MP	M	MP	M	P	P	M	MG	G	P	MP	P	P	P	P	AG
LTE Femto 11	G	G	P	MG	P	MP	M	MP	M	G	P	MG	M	P	MG	G	M	M	M	MG	P	MP	M	M	P	MP	M	P	P	P	MG	P	P	P	P	VP	VP	AG
LTE Femto 12	P	MP	M	P	MP	P	MP	MP	M	MG	P	G	P	MP	MP	M	G	P	MG	M	M	P	MP	M	P	M	P	MG	P	MP	P	VP	MP	MP	M	P	MP	VP	VP	VP	MP	G
LTE Femto 13	M	MG	P	MP	MP	M	MP	MG	G	G	M	MP	P	MP	MP	M	MG	P	G	MG	P	MG	MG	MG	M	MP	P	G	MP	M	M	P	MG	MP	M	P	MP	VP	VP	VP	VG
LTE Femto 14	MG	G	G	M	MG	MP	MP	MG	G	P	M	MG	M	P	P	MP	MP	P	MP	G	P	P	MP	G	M	MP	G	P	MP	MP	P	MP	MP	M	VP	P	VP	P	VP	MP	VG
LTE Femto 15	P	MP	G	P	G	P	MP	MG	G	M	M	MG	M	P	MG	G	MG	M	MP	M	M	MG	MG	P	M	MP	MP	MG	P	MP	MP	P	MP	M	M	P	MP	VP	VP	VP	M	VG
LTE Femto 16	M	MG	P	MP	G	MG	P	MG	G	MG	M	M	G	M	G	G	M	MG	MP	M	P	P	MP	MP	P	P	P	M	MG	MG	MP	M	MP	MP	M	MP	M	P	MP	AP	VG
LTE Femto 17	MG	G	MG	M	G	MG	M	MG	G	P	M	MG	MG	P	P	MP	P	P	M	G	MP	MG	MG	P	M	MG	MP	MG	P	MP	P	VP	MP	MG	G	P	MP	AP	VP	MP	M	G
LTE Femto 18	MP	M	P	P	G	MG	M	P	MP	MG	P	MG	MP	M	MG	G	M	M	MG	M	M	P	MP	MP	P	M	MP	G	MG	MG	M	M	MG	P	MG	M	M	AP	MP	M	VP	AG
LTE Femto 19	G	G	M	MG	G	P	MP	MP	M	MP	P	G	MG	MP	G	G	M	MG	P	MG	MP	MP	M	P	P	M	MG	MG	MG	MG	M	M	P	MP	M	M	M	MP	AP	MP	AG
LTE Femto 20	M	MG	M	MP	MG	P	MP	MP	M	M	P	G	MP	MP	MG	G	MG	M	MG	MG	M	MP	M	P	P	MP	G	P	MP	M	P	M	P	M	VP	P	AP	AP	M	VP	G
LTE Femto 21	P	MP	P	P	P	M	P	P	MP	G	P	MG	MP	MP	MG	G	M	M	G	M	M	P	MP	MP	VP	MP	MP	MG	MG	MG	M	M	M	M	M	M	MP	MP	P	AP	G
LTE Femto 22	MG	G	G	M	MP	MG	P	P	MP	MG	P	G	MP	MP	MG	G	G	M	M	M	MP	P	MP	MP	P	P	P	MG	MG	MG	M	M	M	M	G	AP	VP	M	AP	AP	P	AG
LTE Femto 23	MG	G	M	M	M	M	MP	MG	G	G	M	M	M	M	M	G	MG	M	MP	G	P	P	MP	M	P	G	M	MG	P	MP	M	P	MG	MP	M	VP	P	P	P	AG
LTE Femto 24	M	MG	M	MP	G	G	M	MP	M	M	P	P	MG	M	MG	G	P	M	MP	P	M	MP	M	M	P	P	P	G	M	MG	P	MP	P	P	M	M	M	VP	MP	P	VP	G
LTE Femto 25	G	G	G	MG	G	MG	MP	P	MP	MG	P	MG	MG	MP	M	MG	MG	MP	G	G	P	P	MP	MP	VP	MG	P	G	M	MG	M	MP	MP	MG	M	P	MP	M	VP	VP	VP	VG
LTE Femto 26	MG	G	M	M	MG	P	M	MG	G	MG	M	MP	MP	MP	G	G	MP	MG	M	M	M	P	MP	MG	P	P	MP	M	M	MG	M	MP	P	MP	G	M	M	MP	P	P	G
LTE Femto 27	MG	G	G	M	G	G	MP	P	MP	P	P	MG	P	MP	G	G	M	MG	P	P	M	VP	P	P	VP	M	P	M	M	MG	M	MP	P	P	MG	MP	M	AP	P	VP	VP	AG
LTE Femto 28	P	MP	MP	P	M	P	P	G	G	MP	MG	MP	P	MP	M	MG	P	MP	MG	M	MP	MG	MG	P	M	P	P	M	M	MG	P	MP	P	M	M	P	MP	AP	VP	AP	AP	G
LTE Femto 29	G	G	P	MG	P	P	MP	G	G	G	MG	M	MP	MP	MP	M	P	P	M	M	MP	MG	M	M	MG	M	M	MP	M	P	P	M	M	M	MP	M	P	P	P	VP	AG
LTE Femto 30	G	G	M	MG	MG	P	P	P	MP	M	P	MG	M	M	P	MP	G	P	M	MP	M	MP	MG	MG	MG	MP	MP	MP	MG	M	MG	MG	MP	MP	MG	MP	M	M	P	MP	MP	VG
LTE Femto 31	M	MG	G	MP	G	P	P	M	MG	P	MP	P	MP	MP	MP	M	G	P	MP	MP	P	MP	M	P	P	P	MP	MG	MP	M	P	P	MP	P	M	VP	P	AP	VP	VP	P	G
LTE Femto 32	M	MG	G	MP	MP	MG	M	MP	M	MP	P	P	MG	MP	M	MG	MP	MP	MG	P	P	MP	M	P	P	M	P	G	P	MP	AP	VP	MP	AP	AG
LTE Femto 33	MG	G	P	M	MP	MP	P	M	MG	P	MP	MG	P	M	MP	M	G	P	M	G	MP	MP	P	M	MP	M	M	P	M	M	G	MP	M	M	P	VP	M	AG
LTE Femto 34	P	MP	P	P	P	M	MP	M	MG	G	MP	M	MP	MP	MP	M	MG	P	G	MP	MP	MP	M	P	MG	P	MP	P	VP	M	MP	G	VP	P	P	AP	M	P	VG
LTE Femto 35	P	MP	P	P	MP	MP	P	G	G	G	MG	P	MP	P	MG	G	G	M	G	MP	M	P	MP	MG	MP	P	MP	MP	P	MP	P	G	P	MP	MP	VP	MP	P	AG
LTE Femto 36	M	MG	G	MP	MG	P	P	M	MG	MP	MP	M	P	M	P	MP	MP	MP	P	G	M	P	MP	P	P	M	P	M	VP	P	P	MP	P	M	M	VP	P	VP	P	P	AP	VG
LTE Femto 37	P	MP	G	P	M	M	P	MG	G	MP	M	M	MG	P	P	MP	MP	P	MP	MG	M	M	MG	G	P	MP	MP	P	MP	M	MG	P	MP	VP	P	AP	VP	VG

Table B4 The available WiMAX and WAVE networks of SLA 2, SLA 3 and SLA 4.

Network	SLA 2 CV Throughput	SLA 2 CV Delay	SLA 2 CV Jitter	SLA 2 CV Packet Loss	SLA 2 CV Service Reliability	SLA 2 CV Secutiy	SLA 2 CV Price	SLA 2 BS Throughput	SLA 2 BS Delay	SLA 2 BS Jitter	SLA 2 BS Packet Loss	SLA 2 BS Service Reliability	SLA 2 BS Security	SLA 2 BS Price	SLA 2 Web Throughput	SLA 2 Web Delay	SLA 2 Web Jitter	SLA 2 Web Packet Loss	SLA 2 Web Service Reliability	SLA 2 Web Security	SLA 2 Web Price
WiMAX Macro 1	MP	M	M	P	P	P	P	G	G	G	MG	G	M	P	M	MG	MP	MP	MG	MG	P
WiMAX Macro 2	G	G	MG	MG	G	MG	P	P	MP	P	P	M	MP	P	M	MG	MP	MP	M	P	MP
WiMAX Macro 3	MG	G	MG	M	G	MP	P	P	MP	P	P	P	P	M	P	MP	P	P	M	M	M
WiMAX Macro 4	M	MG	P	MP	P	P	MP	MP	M	MG	P	MG	G	MP	MG	G	MP	M	MP	G	MP
WiMAX Macro 5	MP	M	MP	P	G	P	MP	MP	M	P	P	MG	G	MP	MG	G	M	M	M	MP	P
WiMAX Macro 6	MP	M	G	P	G	M	M	G	G	M	MG	P	MP	M	M	MG	MP	MP	MG	P	MP
WiMAX Macro 7	M	MG	MG	MP	MG	MP	P	MG	G	M	M	MG	MG	MP	MP	M	P	P	M	G	MP
WiMAX Macro 8	M	MG	M	MP	G	MP	MP	M	MG	G	MP	M	P	MP	MP	M	MP	P	P	MG	P
WiMAX Macro 9	M	MG	M	MP	G	M	M	MP	M	P	P	MP	P	P	MP	M	MP	P	MP	G	P
WiMAX Macro 10	P	MP	MG	P	MG	M	MP	MP	M	M	P	MP	MP	P	P	MP	MG	P	G	MP	MP
WiMAX Macro 11	MP	M	P	P	G	M	MP	P	MP	G	P	G	MP	M	M	MG	MG	MP	P	MG	MP
WiMAX Macro 12	MG	G	M	M	P	MG	M	P	MP	G	P	G	MG	P	P	MP	G	P	P	MP	M
WiMAX Macro 13	MP	M	MP	P	G	M	P	M	MG	G	MP	P	MG	P	MP	M	MP	P	G	MG	M
WiMAX Macro 14	MP	M	MG	P	M	G	M	P	MP	G	P	M	G	MP	MG	G	MP	M	G	MP	M
WiMAX Macro 15	MG	G	P	M	P	P	M	P	MP	P	P	MG	M	MP	P	MP	G	P	M	MP	MP
WiMAX Macro 16	MP	M	P	P	MG	MG	MP	G	G	MP	MG	G	G	M	MG	G	M	M	MP	M	MP
WiMAX Macro 17	MG	G	MP	M	P	MP	M	G	G	MG	MG	M	MP	MP	M	MG	MG	MP	MG	MG	MP
WiMAX Femto 1	MP	M	MG	P	G	MG	P	M	MG	M	MP	MG	MG	MP	G	G	M	MG	G	MG	P
WiMAX Femto 2	M	MG	MP	MP	M	P	MP	MG	G	M	M	MP	MP	MP	MG	G	P	M	P	MG	P
WiMAX Femto 3	P	MP	MP	P	G	M	M	MG	G	M	M	P	MP	MP	MP	M	M	P	M	M	MP
WiMAX Femto 4	G	G	P	MG	MP	P	MP	P	MP	MP	P	P	MG	P	G	G	G	MG	P	MP	P
WiMAX Femto 5	G	G	MP	MG	M	G	M	M	MG	P	MP	MP	P	P	MP	M	MP	P	P	M	MP
WiMAX Femto 6	M	MG	M	MP	MP	M	P	M	MG	MG	MP	P	MG	M	MP	M	G	P	M	MP	M
WiMAX Femto 7	M	MG	MG	MP	MG	M	M	P	MP	P	P	MG	P	M	MG	G	MP	M	MG	M	M
WiMAX Femto 8	G	G	M	MG	P	MP	MP	MG	G	M	M	MP	G	MP	P	MP	M	P	MP	M	MP
WiMAX Femto 9	MG	G	G	M	P	MP	P	MP	M	MG	P	MG	P	P	P	MP	M	P	G	G	P
WiMAX Femto 10	MG	G	MP	M	MP	MP	M	MP	M	G	P	M	MP	MP	P	MP	P	P	MG	MG	M
WiMAX Femto 11	M	MG	M	MP	M	G	MP	G	G	P	MG	MP	MP	P	MP	M	M	P	M	MP	MP
WiMAX Femto 12	MP	M	MG	P	G	G	P	M	MG	G	MP	G	MG	P	MP	M	M	P	M	MP	MP
WiMAX Femto 13	G	G	MG	MG	G	P	MP	G	G	P	MG	G	MG	P	MP	M	MG	P	MP	MP	P
WiMAX Femto 14	MP	M	P	P	M	G	P	M	MG	MP	MP	MP	G	MP	MP	M	M	P	P	G	P
WiMAX Femto 15	G	G	M	MG	MP	MP	M	MP	M	P	P	MG	MP	P	G	G	MP	MG	MG	P	M
WiMAX Femto 16	G	G	MG	MG	G	MG	MP	P	MP	M	P	MG	P	P	M	MG	MG	MP	M	MP	M
WiMAX Femto 17	MG	G	P	M	G	MP	P	MP	M	P	P	P	P	MP	G	G	MP	MG	MP	P	M
WiMAX Femto 18	G	G	G	MG	P	MP	P	M	MG	MP	MP	P	MP	M	G	G	MG	MG	M	M	MP
WiMAX Femto 19	MG	G	MP	M	MG	M	P	P	MP	MG	P	M	MP	M	MP	M	MP	P	G	MP	M
WiMAX Femto 20	MG	G	MG	M	M	MG	P	MP	M	MP	P	G	P	MP	MP	M	P	P	P	MP	MP
WiMAX Femto 21	P	MP	P	P	M	P	M	G	G	M	MG	P	M	P	M	MG	MP	MP	M	G	MP
WiMAX Femto 22	P	MP	P	P	G	P	M	P	MP	G	P	P	G	MP	M	MG	P	MP	P	P	MP
WiMAX Femto 23	MG	G	MG	M	G	MG	P	MG	G	MP	M	M	M	P	MG	G	M	M	MG	MG	M
WiMAX Femto 24	MG	G	MP	M	M	MP	M	MP	M	MG	P	P	P	M	M	MG	P	MP	G	M	M
WiMAX Femto 25	MG	G	M	M	G	P	MP	MG	G	M	M	MG	MG	P	MP	M	M	P	G	MG	M
WAVE 1	MG	G	MP	M	MG	G	MP	P	MP	MP	P	MP	M	P	MP	M	M	P	MG	P	M
WAVE 2	M	MG	P	MP	P	M	M	P	MP	G	P	G	G	P	M	MG	MG	MP	P	MP	MP
WAVE 3	M	MG	MP	MP	G	MP	MP	MP	M	M	P	MG	G	P	MP	M	G	P	MP	MG	P
WAVE 4	G	G	M	MG	M	MG	P	MP	M	G	P	G	P	MP	M	MG	M	MP	G	G	P
WAVE 5	MG	G	MP	M	MG	P	P	P	MP	G	P	MP	MG	M	MP	M	MG	P	M	P	P
WAVE 6	M	MG	G	MP	M	G	P	M	MG	M	MP	MG	G	MP	P	MP	G	P	MP	P	M
WAVE 7	P	MP	MG	P	P	MP	P	MG	G	MG	M	M	MP	MP	MP	M	MG	P	MG	MP	P
WAVE 8	G	G	P	MG	P	M	MP	MG	G	M	M	P	M	MP	G	G	G	MG	P	MP	MP
WAVE 9	MP	M	P	P	MP	M	M	G	G	P	MG	MP	G	P	P	MP	MP	P	P	MG	M
WAVE 10	G	G	MP	MG	MG	MP	M	MP	M	MP	P	MG	G	P	P	MP	G	P	G	MP	P
WAVE 11	MP	M	P	P	MP	MG	M	MP	M	MG	P	M	P	M	G	G	M	MG	G	M	P
WAVE 12	M	MG	MG	MP	G	P	MP	M	MG	MG	MP	MG	G	P	MG	G	MP	M	G	G	M
WAVE 13	G	G	G	MG	MP	G	P	G	G	MG	MG	MG	G	P	G	G	M	MG	MG	MP	P
WAVE 14	G	G	MP	MG	M	MG	MP	P	MP	G	P	G	P	P	M	MG	MP	MP	P	G	M
WAVE 15	P	MP	G	P	M	P	M	MP	M	G	P	P	MP	MP	P	MP	MG	P	G	MP	MP
WAVE 16	G	G	P	MG	MG	MG	M	MP	M	M	P	MG	P	P	M	MG	MP	MP	P	G	M
WAVE 17	P	MP	P	P	MG	M	M	M	MG	MG	MP	M	MP	M	MG	G	MG	M	MP	MP	MP
WAVE 18	MG	G	MP	M	G	G	MP	MG	G	MG	M	MP	MP	M	P	MP	M	P	MP	G	M
WAVE 19	M	MG	M	MP	MG	MP	M	MP	M	MP	P	M	P	P	MG	G	G	M	P	MP	P
WAVE 20	M	MG	P	MP	MP	P	P	MP	M	P	P	G	M	MP	M	MG	G	MP	G	MP	P
WAVE 21	G	G	M	MG	MP	MG	MP	M	MG	P	MP	G	G	P	MP	M	P	P	M	M	M
WAVE 22	G	G	M	MG	MG	MG	M	MG	G	G	M	G	M	M	MP	M	MG	P	G	MG	P

Network	SLA 3 BS Throughput	SLA 3 BS Delay	SLA 3 BS Jitter	SLA 3 BS Packet Loss	SLA 3 BS Service Reliability	SLA 3 BS Security	SLA 3 BS Price	SLA 3 Web Throughput	SLA 3 Web Delay	SLA 3 Web Jitter	SLA 3 Web Packet Loss	SLA 3 Web Service Reliability	SLA 3 Web Security	SLA 3 Web Price	SLA 4 Web Throughput	SLA 4 Web Delay	SLA 4 Web Jitter	SLA 4 Web Packet Loss	SLA 4 Web Service Reliability	SLA 4 Web Security	SLA 4 Web Price
WiMAX Macro 1	M	MG	MG	MP	P	MP	G	M	MG	MP	MP	M	P	G	AP	VP	AP	AP	M	VP	G
WiMAX Macro 2	P	MP	P	P	P	MP	M	M	MG	MP	MP	M	P	M	M	M	AP	MP	P	P	AG
WiMAX Macro 3	P	MP	P	P	P	P	MG	P	MP	P	P	MP	M	G	VP	P	VP	AP	AP	MP	G
WiMAX Macro 4	MP	M	MG	P	MP	M	M	MG	MG	MP	M	P	M	G	AP	VP	VP	AP	P	MP	G
WiMAX Macro 5	MP	M	P	P	MP	MP	MG	P	MP	M	P	MP	P	M	AP	VP	P	AP	AP	VP	AG
WiMAX Macro 6	MG	M	M	M	P	MP	MG	M	MG	MP	MP	P	P	M	VP	P	MP	AP	P	AP	VG
WiMAX Macro 7	MP	M	P	P	MP	MP	M	MP	M	P	P	P	P	MG	P	MP	AP	VP	MP	AP	AG
WiMAX Macro 8	M	M	M	MP	MP	P	M	MP	M	MP	P	P	P	MG	P	MP	MP	VP	P	VP	AG
WiMAX Macro 9	MP	M	P	P	MP	P	G	MP	M	P	P	P	MP	MG	MP	M	VP	P	AP	AP	VG
WiMAX Macro 10	MP	M	M	P	MP	MP	M	P	MP	MG	P	P	P	MG	P	MP	AP	VP	P	P	G
WiMAX Macro 11	M	MG	M	MP	MP	MP	G	P	MP	MP	P	MP	P	M	VP	P	VP	AP	MP	P	AG
WiMAX Macro 12	P	MP	MP	P	M	P	MG	VP	P	P	P	P	MP	M	AP	VP	P	AP	AP	VP	G
WiMAX Macro 13	P	MP	M	P	P	MG	G	P	MP	MP	P	M	P	MG	P	MP	MP	VP	M	VP	VG
WiMAX Macro 14	VP	P	MG	P	M	P	M	M	MG	P	MP	MP	MP	MG	P	MP	VP	VP	MP	AP	G
WiMAX Macro 15	P	MP	P	P	P	MP	G	P	MP	M	P	P	MP	G	VP	P	VP	AP	P	AP	AG
WiMAX Macro 16	M	MG	MP	MP	MP	MP	M	MG	MG	M	M	P	M	G	P	MP	AP	VP	P	MP	VG
WiMAX Macro 17	M	MG	MP	MP	M	MP	G	P	MP	P	VP	MG	MG	MG	P	MP	AP	VP	P	VP	G
WiMAX Femto 1	M	MG	MP	MP	P	MG	M	MP	M	M	P	MP	MP	MG	AP	VP	M	AP	VP	P	AG
WiMAX Femto 2	P	MP	MP	P	MP	MP	M	MP	M	P	P	P	P	G	MP	M	AP	P	VP	AP	VG
WiMAX Femto 3	P	MP	MP	P	P	P	G	MP	M	M	P	M	M	M	VP	P	P	AP	AP	P	AG
WiMAX Femto 4	P	MP	P	P	P	MP	M	M	MG	MP	MP	P	MP	M	MP	M	P	P	AP	P	VG
WiMAX Femto 5	M	MG	P	MP	P	P	M	MP	M	MP	P	P	M	G	P	MP	AP	P	AP	VP	G
WiMAX Femto 6	M	MG	MP	MP	P	M	MG	MP	M	MP	P	M	P	G	AP	VP	VP	AP	MP	P	VG
WiMAX Femto 7	P	MP	P	P	P	P	G	MP	M	MP	P	M	M	G	VP	P	MP	AP	P	VP	VG
WiMAX Femto 8	P	MP	P	P	MP	P	M	P	MP	P	P	MP	M	MG	P	MP	VP	VP	MP	P	AG
WiMAX Femto 9	MP	M	P	P	MP	P	G	P	MP	M	VP	MG	P	M	AP	VP	M	AP	MP	VP	G
WiMAX Femto 10	MP	M	M	P	M	MP	G	P	MP	P	P	MG	M	M	VP	P	AP	AP	P	P	AG
WiMAX Femto 11	MG	MG	P	M	MP	MP	MG	MP	M	M	P	MP	MP	G	AP	VP	M	AP	VP	VP	AG
WiMAX Femto 12	MP	M	P	P	MP	MG	G	MP	M	M	P	MP	P	M	AP	VP	MP	AP	MP	P	AG
WiMAX Femto 13	M	MG	P	MP	P	MG	G	MP	M	P	P	MP	MP	M	P	MP	P	VP	MP	AP	VG
WiMAX Femto 14	M	MG	MP	MP	P	MG	MG	P	MP	M	P	P	P	M	VP	P	AP	VP	AP	AP	AG
WiMAX Femto 15	MP	M	P	P	MG	MP	G	M	MG	MP	MP	MP	P	G	M	M	MP	MP	MP	VP	G
WiMAX Femto 16	P	MP	M	P	P	P	M	M	MG	MG	MP	M	MP	MG	VP	P	MP	AP	AP	AP	VG
WiMAX Femto 17	MP	M	P	P	VP	P	G	P	MP	MP	P	MP	P	M	VP	P	AP	AP	P	VP	G
WiMAX Femto 18	P	MP	VP	P	P	P	M	P	MP	MP	P	M	P	MG	P	MP	VP	P	VP	P	AG
WiMAX Femto 19	P	MP	MG	P	M	MP	M	P	MP	P	P	P	P	M	P	MP	P	VP	P	P	VG
WiMAX Femto 20	MP	M	MP	P	MG	P	M	P	MP	P	P	P	MP	MG	P	MP	P	P	VP	AP	G
WiMAX Femto 21	MG	MG	P	M	P	MP	G	M	MG	MP	MP	MP	M	M	M	M	VP	MP	MP	P	AG
WiMAX Femto 22	P	MP	M	P	P	MG	MG	P	MP	P	P	P	P	MG	P	MP	AP	VP	VP	AP	AG
WiMAX Femto 23	M	MG	MP	MP	M	P	MG	M	MG	MP	MP	M	MG	MG	P	MP	P	VP	AP	AP	VG
WiMAX Femto 24	MP	M	MG	P	P	P	MG	MP	M	P	P	MG	M	G	MP	M	P	P	AP	MP	AG
WiMAX Femto 25	MG	M	P	M	MG	MP	M	P	MP	M	P	MG	M	MG	VP	P	P	AP	AP	MP	AG
WAVE 1	P	MP	MP	P	MP	M	MG	P	MP	M	VP	MP	P	G	P	MP	M	VP	VP	P	G
WAVE 2	P	MP	MP	VP	MP	MP	G	MP	M	M	P	P	MP	MG	VP	P	MP	AP	AP	MP	AG
WAVE 3	MP	M	MP	P	MP	M	MG	MP	M	M	P	P	MG	M	AP	VP	M	AP	VP	P	AG
WAVE 4	MP	MP	M	P	P	P	M	P	MP	M	P	MP	MP	M	VP	P	M	AP	AP	AP	AG
WAVE 5	P	MP	MP	P	MP	P	G	MP	M	M	P	P	P	G	VP	P	P	AP	P	AP	VG
WAVE 6	MP	M	P	P	MG	M	G	P	MP	MG	P	MP	P	G	P	MP	P	VP	VP	VP	AG
WAVE 7	M	MG	MG	MP	P	MP	G	P	MP	P	VP	MG	MP	M	VP	P	VP	VP	MP	MP	G
WAVE 8	M	M	MP	MP	P	M	G	P	MP	M	VP	P	MP	G	P	MP	P	VP	AP	MP	G
WAVE 9	MG	M	P	M	MP	M	M	P	MP	MP	P	P	P	G	VP	P	AP	P	VP	P	AG
WAVE 10	MP	M	MP	P	MG	MP	G	P	MP	MP	P	P	MP	MG	P	MP	VP	VP	P	AP	VG
WAVE 11	MP	M	M	P	P	P	MG	MG	MG	M	M	MP	MP	G	M	M	M	MP	P	VP	G
WAVE 12	M	M	MP	MP	M	MG	G	M	MG	MP	MP	MG	MP	M	M	M	MP	MP	VP	MP	VG
WAVE 13	MG	MG	P	M	MG	MP	G	P	MP	M	P	MP	P	M	VP	P	M	AP	MP	P	AG
WAVE 14	P	MP	P	P	MG	P	MG	MP	M	MP	P	P	P	MG	VP	P	VP	AP	AP	VP	AG
WAVE 15	MP	M	M	P	P	MP	MG	P	MP	P	P	MP	MP	M	P	MP	VP	VP	AP	VP	AG
WAVE 16	MP	M	P	P	MG	P	G	MP	M	MP	P	P	M	M	MP	M	VP	P	AP	VP	G
WAVE 17	MP	M	MP	P	M	MP	MG	MP	M	M	P	MP	MP	G	P	MP	P	VP	AP	AP	AG
WAVE 18	P	MP	MG	P	P	MP	M	P	MP	P	P	MP	MP	M	AP	VP	P	AP	AP	MP	AG
WAVE 19	MP	M	P	P	MP	P	M	MP	M	MP	P	P	MP	MG	AP	VP	MP	AP	AP	VP	G
WAVE 20	P	MP	P	P	MG	MP	MG	M	MG	P	MP	MP	MP	M	P	MP	AP	VP	VP	P	AG
WAVE 21	P	P	P	P	M	M	M	MP	M	P	P	M	M	G	MP	M	VP	P	VP	P	VG
WAVE 22	P	MP	P	P	MG	MP	M	MP	M	M	P	M	M	MG	VP	P	AP	AP	P	M	VG

Appendix C

The distribution of vehicles during the 24 hours simulation

In this appendix the distribution of vehicles across velocity categories, access networks, services and SLAs, during the 24 hours simulation is presented.

Table C1 Number of vehicles that start from each LTE network and their corresponding velocities.

Network	Number of vehicles (%)	Normal velocity	Medium velocity	High velocity
LTE Macro 1	329 (0,82648%)	109 (0,27382%)	111 (0,27884%)	109 (0,27382%)
LTE Macro 2	329 (0,82648%)	109 (0,27382%)	111 (0,27884%)	109 (0,27382%)
LTE Macro 3	329 (0,82648%)	109 (0,27382%)	111 (0,27884%)	109 (0,27382%)
LTE Macro 4	329 (0,82648%)	109 (0,27382%)	111 (0,27884%)	109 (0,27382%)
LTE Macro 5	329 (0,82648%)	109 (0,27382%)	111 (0,27884%)	109 (0,27382%)
LTE Macro 6	329 (0,82648%)	109 (0,27382%)	111 (0,27884%)	109 (0,27382%)
LTE Macro 7	329 (0,82648%)	109 (0,27382%)	111 (0,27884%)	109 (0,27382%)
LTE Macro 8	329 (0,82648%)	109 (0,27382%)	111 (0,27884%)	109 (0,27382%)
LTE Macro 9	329 (0,82648%)	109 (0,27382%)	111 (0,27884%)	109 (0,27382%)
LTE Macro 10	329 (0,82648%)	109 (0,27382%)	111 (0,27884%)	109 (0,27382%)
LTE Macro 11	329 (0,82648%)	109 (0,27382%)	111 (0,27884%)	109 (0,27382%)
LTE Macro 12	329 (0,82648%)	109 (0,27382%)	111 (0,27884%)	109 (0,27382%)
LTE Macro 13	329 (0,82648%)	109 (0,27382%)	111 (0,27884%)	109 (0,27382%)
LTE Macro 14	329 (0,82648%)	109 (0,27382%)	111 (0,27884%)	109 (0,27382%)
LTE Macro 15	329 (0,82648%)	109 (0,27382%)	111 (0,27884%)	109 (0,27382%)
LTE Macro 16	329 (0,82648%)	109 (0,27382%)	111 (0,27884%)	109 (0,27382%)
LTE Macro 17	329 (0,82648%)	109 (0,27382%)	111 (0,27884%)	109 (0,27382%)
LTE Macro 18	329 (0,82648%)	109 (0,27382%)	111 (0,27884%)	109 (0,27382%)
LTE Macro 19	329 (0,82648%)	109 (0,27382%)	111 (0,27884%)	109 (0,27382%)
LTE Macro 20	329 (0,82648%)	109 (0,27382%)	111 (0,27884%)	109 (0,27382%)
LTE Femto 1	329 (0,82648%)	109 (0,27382%)	111 (0,27884%)	109 (0,27382%)
LTE Femto 2	329 (0,82648%)	109 (0,27382%)	111 (0,27884%)	109 (0,27382%)
LTE Femto 3	329 (0,82648%)	109 (0,27382%)	111 (0,27884%)	109 (0,27382%)
LTE Femto 4	329 (0,82648%)	109 (0,27382%)	111 (0,27884%)	109 (0,27382%)
LTE Femto 5	329 (0,82648%)	109 (0,27382%)	111 (0,27884%)	109 (0,27382%)
LTE Femto 6	329 (0,82648%)	109 (0,27382%)	111 (0,27884%)	109 (0,27382%)
LTE Femto 7	329 (0,82648%)	109 (0,27382%)	111 (0,27884%)	109 (0,27382%)
LTE Femto 8	329 (0,82648%)	109 (0,27382%)	111 (0,27884%)	109 (0,27382%)
LTE Femto 9	329 (0,82648%)	109 (0,27382%)	111 (0,27884%)	109 (0,27382%)
LTE Femto 10	329 (0,82648%)	109 (0,27382%)	111 (0,27884%)	109 (0,27382%)
LTE Femto 11	329 (0,82648%)	109 (0,27382%)	111 (0,27884%)	109 (0,27382%)
LTE Femto 12	329 (0,82648%)	109 (0,27382%)	111 (0,27884%)	109 (0,27382%)
LTE Femto 13	329 (0,82648%)	109 (0,27382%)	111 (0,27884%)	109 (0,27382%)
LTE Femto 14	329 (0,82648%)	109 (0,27382%)	111 (0,27884%)	109 (0,27382%)
LTE Femto 15	329 (0,82648%)	109 (0,27382%)	111 (0,27884%)	109 (0,27382%)
LTE Femto 16	329 (0,82648%)	109 (0,27382%)	111 (0,27884%)	109 (0,27382%)
LTE Femto 17	329 (0,82648%)	109 (0,27382%)	111 (0,27884%)	109 (0,27382%)
LTE Femto 18	329 (0,82648%)	109 (0,27382%)	111 (0,27884%)	109 (0,27382%)
LTE Femto 19	329 (0,82648%)	109 (0,27382%)	111 (0,27884%)	109 (0,27382%)
LTE Femto 20	329 (0,82648%)	109 (0,27382%)	111 (0,27884%)	109 (0,27382%)
LTE Femto 21	329 (0,82648%)	110 (0,27633%)	110 (0,27633%)	109 (0,27382%)
LTE Femto 22	329 (0,82648%)	110 (0,27633%)	110 (0,27633%)	109 (0,27382%)
LTE Femto 23	329 (0,82648%)	110 (0,27633%)	110 (0,27633%)	109 (0,27382%)
LTE Femto 24	329 (0,82648%)	111 (0,27884%)	110 (0,27633%)	108 (0,27130%)
LTE Femto 25	329 (0,82648%)	111 (0,27884%)	110 (0,27633%)	108 (0,27130%)
LTE Femto 26	329 (0,82648%)	111 (0,27884%)	110 (0,27633%)	108 (0,27130%)
LTE Femto 27	329 (0,82648%)	111 (0,27884%)	110 (0,27633%)	108 (0,27130%)
LTE Femto 28	329 (0,82648%)	111 (0,27884%)	110 (0,27633%)	108 (0,27130%)
LTE Femto 29	329 (0,82648%)	111 (0,27884%)	110 (0,27633%)	108 (0,27130%)
LTE Femto 30	329 (0,82648%)	111 (0,27884%)	110 (0,27633%)	108 (0,27130%)
LTE Femto 31	329 (0,82648%)	111 (0,27884%)	110 (0,27633%)	108 (0,27130%)
LTE Femto 32	329 (0,82648%)	111 (0,27884%)	110 (0,27633%)	108 (0,27130%)
LTE Femto 33	329 (0,82648%)	111 (0,27884%)	110 (0,27633%)	108 (0,27130%)
LTE Femto 34	329 (0,82648%)	111 (0,27884%)	110 (0,27633%)	108 (0,27130%)
LTE Femto 35	329 (0,82648%)	111 (0,27884%)	110 (0,27633%)	108 (0,27130%)
LTE Femto 36	329 (0,82648%)	111 (0,27884%)	110 (0,27633%)	108 (0,27130%)
LTE Femto 37	329 (0,82648%)	111 (0,27884%)	110 (0,27633%)	108 (0,27130%)

Table C2 Number of vehicles that start from each WiMAX network and their corresponding velocities.

Network	Number of vehicles (%)	Normal velocity	Medium velocity	High velocity
WiMAX Macro 1	329 (0,82648%)	111 (0,27884%)	110 (0,27633%)	108 (0,27130%)
WiMAX Macro 2	329 (0,82648%)	111 (0,27884%)	110 (0,27633%)	108 (0,27130%)
WiMAX Macro 3	329 (0,82648%)	111 (0,27884%)	110 (0,27633%)	108 (0,27130%)
WiMAX Macro 4	329 (0,82648%)	111 (0,27884%)	110 (0,27633%)	108 (0,27130%)
WiMAX Macro 5	329 (0,82648%)	111 (0,27884%)	110 (0,27633%)	108 (0,27130%)
WiMAX Macro 6	329 (0,82648%)	111 (0,27884%)	110 (0,27633%)	108 (0,27130%)
WiMAX Macro 7	329 (0,82648%)	111 (0,27884%)	110 (0,27633%)	108 (0,27130%)
WiMAX Macro 8	329 (0,82648%)	111 (0,27884%)	110 (0,27633%)	108 (0,27130%)
WiMAX Macro 9	329 (0,82648%)	111 (0,27884%)	110 (0,27633%)	108 (0,27130%)
WiMAX Macro 10	329 (0,82648%)	111 (0,27884%)	110 (0,27633%)	108 (0,27130%)
WiMAX Macro 11	329 (0,82648%)	111 (0,27884%)	110 (0,27633%)	108 (0,27130%)
WiMAX Macro 12	329 (0,82648%)	111 (0,27884%)	110 (0,27633%)	108 (0,27130%)
WiMAX Macro 13	329 (0,82648%)	111 (0,27884%)	110 (0,27633%)	108 (0,27130%)
WiMAX Macro 14	329 (0,82648%)	111 (0,27884%)	110 (0,27633%)	108 (0,27130%)
WiMAX Macro 15	329 (0,82648%)	111 (0,27884%)	110 (0,27633%)	108 (0,27130%)
WiMAX Macro 16	329 (0,82648%)	111 (0,27884%)	110 (0,27633%)	108 (0,27130%)
WiMAX Macro 17	329 (0,82648%)	111 (0,27884%)	110 (0,27633%)	108 (0,27130%)
WiMAX Femto 1	329 (0,82648%)	111 (0,27884%)	110 (0,27633%)	108 (0,27130%)
WiMAX Femto 2	329 (0,82648%)	111 (0,27884%)	110 (0,27633%)	108 (0,27130%)
WiMAX Femto 3	329 (0,82648%)	111 (0,27884%)	110 (0,27633%)	108 (0,27130%)
WiMAX Femto 4	329 (0,82648%)	111 (0,27884%)	110 (0,27633%)	108 (0,27130%)
WiMAX Femto 5	329 (0,82648%)	111 (0,27884%)	110 (0,27633%)	108 (0,27130%)
WiMAX Femto 6	329 (0,82648%)	111 (0,27884%)	110 (0,27633%)	108 (0,27130%)
WiMAX Femto 7	329 (0,82648%)	111 (0,27884%)	110 (0,27633%)	108 (0,27130%)
WiMAX Femto 8	329 (0,82648%)	111 (0,27884%)	110 (0,27633%)	108 (0,27130%)
WiMAX Femto 9	329 (0,82648%)	111 (0,27884%)	110 (0,27633%)	108 (0,27130%)
WiMAX Femto 10	329 (0,82648%)	111 (0,27884%)	110 (0,27633%)	108 (0,27130%)
WiMAX Femto 11	329 (0,82648%)	111 (0,27884%)	110 (0,27633%)	108 (0,27130%)
WiMAX Femto 12	329 (0,82648%)	111 (0,27884%)	110 (0,27633%)	108 (0,27130%)
WiMAX Femto 13	329 (0,82648%)	111 (0,27884%)	110 (0,27633%)	108 (0,27130%)
WiMAX Femto 14	329 (0,82648%)	111 (0,27884%)	110 (0,27633%)	108 (0,27130%)
WiMAX Femto 15	329 (0,82648%)	111 (0,27884%)	110 (0,27633%)	108 (0,27130%)
WiMAX Femto 16	329 (0,82648%)	111 (0,27884%)	110 (0,27633%)	108 (0,27130%)
WiMAX Femto 17	329 (0,82648%)	111 (0,27884%)	110 (0,27633%)	108 (0,27130%)
WiMAX Femto 18	329 (0,82648%)	111 (0,27884%)	110 (0,27633%)	108 (0,27130%)
WiMAX Femto 19	329 (0,82648%)	111 (0,27884%)	110 (0,27633%)	108 (0,27130%)
WiMAX Femto 20	329 (0,82648%)	111 (0,27884%)	110 (0,27633%)	108 (0,27130%)
WiMAX Femto 21	329 (0,82648%)	111 (0,27884%)	110 (0,27633%)	108 (0,27130%)
WiMAX Femto 22	329 (0,82648%)	111 (0,27884%)	110 (0,27633%)	108 (0,27130%)
WiMAX Femto 23	329 (0,82648%)	111 (0,27884%)	110 (0,27633%)	108 (0,27130%)
WiMAX Femto 24	329 (0,82648%)	111 (0,27884%)	110 (0,27633%)	108 (0,27130%)
WiMAX Femto 25	329 (0,82648%)	111 (0,27884%)	110 (0,27633%)	108 (0,27130%)

Table C3 Number of vehicles that start from each WAVE network and their corresponding velocities.

Network	Number of vehicles (%)	Normal velocity	Medium velocity	High velocity
WAVE 1	329 (0,82648%)	111 (0,27884%)	110 (0,27633%)	108 (0,27130%)
WAVE 2	329 (0,82648%)	111 (0,27884%)	110 (0,27633%)	108 (0,27130%)
WAVE 3	329 (0,82648%)	111 (0,27884%)	110 (0,27633%)	108 (0,27130%)
WAVE 4	329 (0,82648%)	111 (0,27884%)	110 (0,27633%)	108 (0,27130%)
WAVE 5	329 (0,82648%)	111 (0,27884%)	110 (0,27633%)	108 (0,27130%)
WAVE 6	329 (0,82648%)	111 (0,27884%)	110 (0,27633%)	108 (0,27130%)
WAVE 7	329 (0,82648%)	111 (0,27884%)	110 (0,27633%)	108 (0,27130%)
WAVE 8	329 (0,82648%)	111 (0,27884%)	110 (0,27633%)	108 (0,27130%)
WAVE 9	329 (0,82648%)	111 (0,27884%)	110 (0,27633%)	108 (0,27130%)
WAVE 10	329 (0,82648%)	111 (0,27884%)	110 (0,27633%)	108 (0,27130%)
WAVE 11	329 (0,82648%)	111 (0,27884%)	110 (0,27633%)	108 (0,27130%)
WAVE 12	329 (0,82648%)	111 (0,27884%)	110 (0,27633%)	108 (0,27130%)
WAVE 13	329 (0,82648%)	111 (0,27884%)	110 (0,27633%)	108 (0,27130%)
WAVE 14	329 (0,82648%)	111 (0,27884%)	110 (0,27633%)	108 (0,27130%)
WAVE 15	329 (0,82648%)	111 (0,27884%)	110 (0,27633%)	108 (0,27130%)
WAVE 16	329 (0,82648%)	111 (0,27884%)	110 (0,27633%)	108 (0,27130%)
WAVE 17	329 (0,82648%)	111 (0,27884%)	110 (0,27633%)	108 (0,27130%)
WAVE 18	329 (0,82648%)	111 (0,27884%)	110 (0,27633%)	108 (0,27130%)
WAVE 19	329 (0,82648%)	111 (0,27884%)	110 (0,27633%)	108 (0,27130%)
WAVE 20	329 (0,82648%)	111 (0,27884%)	110 (0,27633%)	108 (0,27130%)
WAVE 21	328 (0,82397%)	111 (0,27884%)	109 (0,27382%)	108 (0,27130%)
WAVE 22	328 (0,82397%)	111 (0,27884%)	109 (0,27382%)	108 (0,27130%)

Table C4 Vehicles count per service and SLA.

Services	SLA 1 vehicles (%)	SLA 2 vehicles (%)	SLA 3 vehicles (%)	SLA 4 vehicles (%)	Sum
NAV	322 (0,808902%)	-	-	-	322 (0,808902%)
VoIP	321 (0,806390%)	-	-	-	321 (0,806390%)
CV	321 (0,806390%)	1422 (3,572236%)	-	-	1743 (4,378626%)
BS	321 (0,806390%)	1422 (3,572236%)	3318 (8,335217%)	-	5061 (12,71384%)
WB	321 (0,806390%)	1422 (3,572236%)	3317 (8,332705%)	9951 (24,99811%)	15011 (37,70944%)
NAV, VoIP	321 (0,806390%)	-	-	-	321 (0,806390%)
NAV, CV	321 (0,806390%)	-	-	-	321 (0,806390%)
NAV, BS	321 (0,806390%)	-	-	-	321 (0,806390%)
NAV, WB	321 (0,806390%)	-	-	-	321 (0,806390%)
VoIP, CV	321 (0,806390%)	-	-	-	321 (0,806390%)
VoIP, BS	321 (0,806390%)	-	-	-	321 (0,806390%)
VoIP, WB	321 (0,806390%)	-	-	-	321 (0,806390%)
CV, BS	321 (0,806390%)	1422 (3,572236%)	-	-	1743 (4,378626%)
CV, WB	321 (0,806390%)	1422 (3,572236%)	-	-	1743 (4,378626%)
BS, WB	321 (0,806390%)	1421 (3,569723%)	3317 (8,332705%)	-	5059 (12,7088%)
NAV, VoIP, CV	321 (0,806390%)	-	-	-	321 (0,806390%)
NAV, VoIP, BS	321 (0,806390%)	-	-	-	321 (0,806390%)
NAV, VoIP, WB	321 (0,806390%)	-	-	-	321 (0,806390%)
NAV, CV, BS	321 (0,806390%)	-	-	-	321 (0,806390%)
NAV, CV, WB	321 (0,806390%)	-	-	-	321 (0,806390%)
NAV, BS, WB	321 (0,806390%)	-	-	-	321 (0,806390%)
VoIP, CV, BS	321 (0,806390%)	-	-	-	321 (0,806390%)
VoIP, CV, WB	321 (0,806390%)	-	-	-	321 (0,806390%)
VoIP, BS, WB	321 (0,806390%)	-	-	-	321 (0,806390%)
CV, BS, WB	321 (0,806390%)	1421 (3,569723%)	-	-	1742 (4,376114%)
NAV, VoIP, CV, BS	321 (0,806390%)	-	-	-	321 (0,806390%)
NAV, VoIP, CV, WB	321 (0,806390%)	-	-	-	321 (0,806390%)
NAV, VoIP, BS, WB	321 (0,806390%)	-	-	-	321 (0,806390%)
NAV, CV, BS, WB	321 (0,806390%)	-	-	-	321 (0,806390%)
VoIP, CV, BS, WB	321 (0,806390%)	-	-	-	321 (0,806390%)
NAV, VoIP, CV, BS, WB	321 (0,806390%)	-	-	-	321 (0,806390%)
Sum:	9952 (25,00062%)	9952 (25,00062%)	9952 (25,00062%)	9951 (24,99811%)	39807 (100%)